UNIVERSITY OF
CALGARY

THE UNIVERSITY OF CALGARY

Mechanistic Studies of $B(C_6F_5)_3$-Catalyzed Reactions of Si and Sn Reagents.

by

James Munro Blackwell

A DISSERTATION
SUBMITTED TO THE FACULTY OF GRADUATE STUDIES
IN PARTIAL FULFILLMENT OF THE REQUIREMENTS FOR THE
DEGREE OF DOCTOR OF PHILOSOPHY

DEPARTMENT OF CHEMISTRY

CALGARY, ALBERTA
DECEMBER, 2001

Abstract

$B(C_6F_5)_3$-catalyzed organic transformations have been studied both from synthetic development and mechanistic perspectives. This highly electrophilic borane Lewis acid is shown herein to catalyze many important organic reactions such as carbonyl hydrosilation, enone hydrosilation, silyl enol ether hydrosilation, alcohol silation, imine hydrosilation, allylstannane isomerization and carbonyl allylstannation. Mechanisms are proposed for these reactions based on extensive NMR spectroscopic studies. The ability of $B(C_6F_5)_3$ to form stable, anionic borates is fundamental to the success of this Lewis acid as an efficient catalyst. Adducts of $B(C_6F_5)_3$ and aldehydes and imines were also studied by X-ray crystallography.

Acknowledgments

First and foremost, I acknowledge my Ph. D. supervisor, Professor Warren Piers, for his outstanding mentorship throughout my doctoral studies at the University of Calgary. The other members of my Ph. D. supervisory committee, Dr. Brian Keay, Dr. Tom Ziegler, Dr. Leland Jackson, Dr. Andrei Yudin, Dr. Tristram Chivers and Dr. Rupert Spence are also gratefully acknowledged.

The Alberta Heritage Foundation (Steinhauer Award), the Sir Isaak Walton Killam Foundation (Killam predoctoral awards) and the Natural Sciences and Engineering Research Council (NSERC PGS-B award) are thanked for financial support throughout my studies.

I would also like to personally thank the technical and support staff in the Department of Chemistry especially Qiao Wu, Dorothy Fox, Dr. Raghav Yamdagni, Dr. Masood Parvez, Greta Prihodko and Bonnie King.

The members of the Piers group, past and present, must also be thanked especially Dr. Dan Parks. Also, Kevin Cook, Bryon Carpenter, Preston Chase, Lisa Knight, Paul Hayes, Lee Henderson, Patricio Romero and Darryl Morrison are thanked both for their help in the lab and their friendship outside. I also thank Dr. Geoff Irvine, Dr. Cliff Williams, Dr. Suobo Zhang, Dr. David Emslie and Dr. Roland Roesler for their help and camaraderie. I also had the opportunity to co-supervise four undergratuate researchers, Katie Foster, Vickie Beck, Eric Sonmor and Tiziana Scocitti during my stay here, all of whom made contributions to this dissertation. Other friends and colleagues from the department especially Dr. Neal Anderson, Steve Lau, Kristine Muller, Dr. Naomi Kruhlak, Dr. Justin Brask and Mark Krahn are thanked for their friendship during my stay at the University of Calgary.

Finally, I express my sincere gratitude to my parents, Shirley and Munro Blackwell, my siblings, Jody, Tracy, Ted, Kristy and Kelly, any my best friend, Sue Oldham, for their never-ending support throughout my graduate career.

Table of Contents

List of Abbreviations

Å	Ångstroms
anal.	analytical
Ar	aromatic
Ar_f	fluorinated aromatic
Bn	benzyl
br.	broad
Bu	butyl
Calcd	calculated
cm^{-1}	wavenumbers
Cp*	pentamethylcyclopentadienyl
d	doublet
dd	doublet of doublets
DEPT	distortionless enhancement by polarization transfer
DMSO	dimethylsulfoxide
eq.	equivalents
GC-MS	gas chromatography - mass spectrometry
h	hours
HETCOR	heteronuclear chemical shift correlation
HMPA	hexamethylphosphoramide
HMQC	heteronuclear correlation through multiple quantum coherence
HRMS	high resolution mass spectrometry
Hz	Hertz
IR	infrared
J	symbol for coupling constant
LA	Lewis acid
m	multiplet
Mes	mesityl; (2, 4, 6-trimethylphenyl)
MHz	megahertz
min	minutes

mmol	millimole
NMR	nuclear magnetic resonance
nOe	nuclear Overhauser effect
OTf	triflate, trifluoromethanesulfonate
ppm	parts per million
q	quartet
t	triplet
TBS	*tert*-butyldimethylsilyl
TLC	thin layer chromatography
TMS	trimethylsilyl (Me_3Si)
TPFPB	*tetrakis*-pentafluorophenylborate; ($B(C_6F_5)_4^-$)
Trityl	triphenylmethyl (Ph_3C)
UV	ultraviolet
w	weak
WCA	weakly coordinating anion

Chapter 1

General Introduction

1.1.1 Lewis Acids in Organic Synthesis

Lewis acids have been used by synthetic chemists to promote a number of important organic reactions.[1] Typically, Lewis acids are comprised of a main group element or transition metal with electron-withdrawing substituents. Some common Lewis acids used routinely in organic synthesis are BF_3, $TiCl_4$, $SnCl_4$, TMSOTf, $ZnCl_2$ and $AlCl_3$. The Lewis acidic metal center accepts electron density through coordination of a Lewis base such as carbonyls, alcohols, ethers, imines, amines, nitriles, sulfides, halides, alkenes, alkynes, etc. Coordination of a Lewis base to a Lewis acid leads to polarization of a bond thus promoting reaction with a nucleophile. For example, coordination of a carbonyl function to a Lewis acid leads to positive charge build-up at the carbon as in resonance forms **A/A'**.[2,3] In many instances the nucleophilic component is an organometallic reagent such as an organosilane, -stannane, -borane or -alane.[4] Lewis acids have been used successfully in Diels-Alder reactions, aldol reactions, allylmetallations, cyanometallations, epoxidations, aziridinations, cyclizations etc. Furthermore, chiral Lewis acids promote several efficient enantioselective reactions.[5]

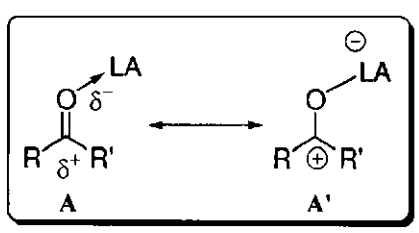

1.1.2 Coordination Chemistry of Common Lewis Acids with Carbonyl Functions

The formation of crystalline complexes between BF_3 and aromatic aldehydes was reported in 1878.[6] The advantages of using Lewis acids to activate carbonyl functions, however, only started to become fully appreciated in the past 40-50 years. Yates and

Eaton at the University of Toronto discovered that $AlCl_3$ promoted the Diels-Alder reaction between anthracene and maleic anhydride.[7] In the presence of $AlCl_3$, the cycloaddition reaction occurs in 90 seconds at room temperature as opposed to an estimated 4800 hours for the uncatalyzed reaction. Coordination of a C=O bond in maleic anhydride to $AlCl_3$ leading to a polar, more reactive intermediate, **B**, causes this dramatic effect. Similar rate accelerations as observed in this example have since been observed in a wide range of processes involving carbonyl groups as electrophiles.

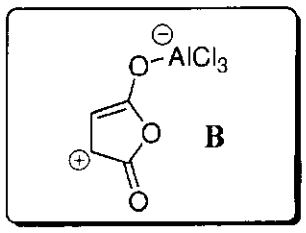

B

Figure 1.1: Coordination Modes of Lewis Acids to Aldehydes.

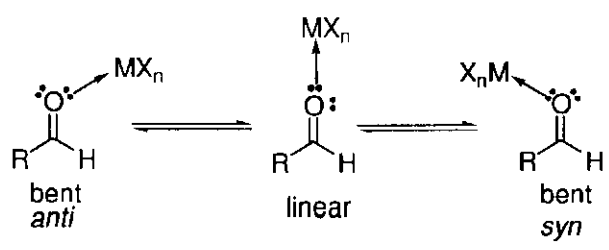

Although carbonyls can coordinate to Lewis acids through the π-electrons (η^2-coordination), most carbonyl Lewis bases are believed to coordinate via a lone pair of electrons to form a σ-bond.[2] Either linear or bent geometries at the C-O-M bond can occur, Figure 1.1. Theoretical studies have indicated that generally, cationic Lewis acids with a second vacant orbital prefer linear binding since this allows a significant amount of π-bonding from the second lone pair to occur.[8] Neutral Lewis acids, however, prefer a bent coordination mode in plane with the C=O bond. The difference in energies between these two bonding modes can be small and thus subtle factors (*eg.* size of carbonyl substituents) can determine which mode predominates.[9] Isomerization between *syn*- and

anti-bent coordination modes is speculated to occur via a linear transition state or intermediate.

Experimental work has largely corroborated early calculations. UV and IR spectroscopic studies of BF_3 and aromatic aldehydes indicated formation of a σ-complex with a lengthened C=O bond and a highly delocalized π-system.[10] NMR spectroscopic studies of BF_3/methyl ketone complexes established that BF_3 exchange between ketones is rapid at room temperature.[11] However, at -90 °C, signals for free and bound ketone are discernible in the ^1H NMR spectrum. Furthermore, for pentan-3-one:BF_3, two sets of methylene signals (*syn*- and *anti*- to BF_3) are observed at -125 °C, confirming a bent coordination mode.[12] The signals coalesced at -111 °C representing a small 8 kcal mol^{-1} barrier to *syn/anti* isomerization.[13] In 1986, Reetz and co-workers characterized benzaldehyde:BF_3 by X-ray crystallography where the Lewis acid was indeed shown to be coordinated *syn* to the aldehydic hydrogen.[14] Recently, the equilibrium constants between BF_3 (introduced in its most common form as $BF_3{\bullet}OEt_2$) with a variety of carbonyl compounds have been reported.[15]

Borane Lewis acids such as BF_3 are generally considered to be capable of accepting only one Lewis base. Although claims have been made in the recent past suggesting the intervention of hypercoordinate borane intermediates,[16] no experimental evidence exists for these species. BF_3 is thus considered the quintessential Lewis acid for *avoiding* chelation by a bifunctional base.[17] Larger Lewis acids such as $TiCl_4$ and $SnCl_4$ have been shown however, to readily accommodate two basic groups (either two carbonyl groups or one chelating, bifunctional Lewis base). For example, Denmark has

isolated and characterized by X-ray crystallography the complex (4-^{t}BuC$_6$H$_4$CHO)$_2$SnCl$_4$ where the two aldehyde substituents bind in *cis* positions (< O-Sn-O = 78.9°).[18]

Since it was first proposed, the Cram chelation-control model has been used to rationalize stereoselectivity in a organic reactions catalyzed by Lewis acids.[19,20] However, it was not until the 1980's that evidence for chelated Lewis acid/carbonyl complexes began to appear. For example, Reetz used NMR spectroscopy to characterize the two chelated complexes **C** and **D** formed between MeTiCl$_3$ and 2-benzyloxy-3-pentanone.[21,22] Crystal structures of chelates of TiCl$_4$[23] (eg. **E**) and SnCl$_4$[24] (eg. **F**) have also been obtained.

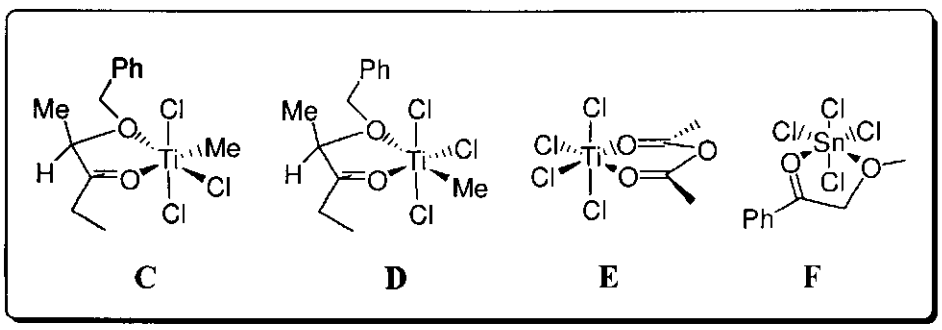

C **D** **E** **F**

1.2 Perfluorinated Aryl Boranes and Borates in Synthesis

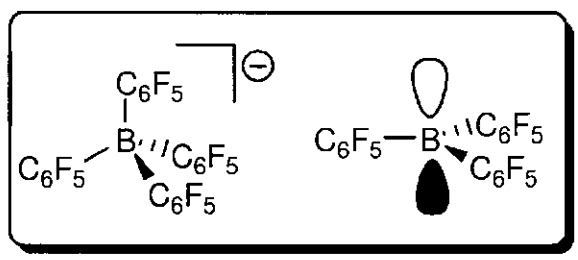

In the past fifteen years, a demand has arisen for weaker coordinating anions in the field of olefin polymerization and in synthetic efforts to synthesize highly reactive cationic species. Reclassification of anions previously considered non-coordinating such

as BF_4^-, SbF_6^-, PF_6^- etc. has taken place as chemists have realized basicity and nucleophilicity are relative terms. Not surprisingly, it has been discovered that syntheses of extreme electrophiles require so-called "super-anions" resistant to degradation by the cation. Furthermore, to prepare so-called naked cations, the anions had to be considerably less basic than those available. One class of anion that has been effectively utilized are based on *tetrakis*-perfluoroaryl borate anions such as $[B(C_6F_5)_4]^-$. The neutral *tris*-pentafluorophenyborane, $B(C_6F_5)_3$, **1**, has subsequently been reevaluated by organometallic and organic chemists as a Lewis acid.

1.2.1 $B(C_6F_5)_3$ in Organometallic Chemistry

Tris-pentafluorophenylborane was first prepared by Massey, Park and Stone in 1963.[25,26] This Lewis acid was largely ignored throughout the 1970's and 1980's but in the past ten years has experienced a renaissance.[27] Marks[28] and Ewen[29] independently introduced this reagent into the field of olefin polymerization as a neutral activator for early transition metal catalysts.

Scheme 1.1: Activation of Metal Alkyl Precatalysts by $B(C_6F_5)_3$.

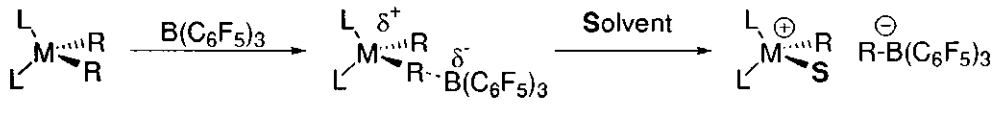

The role of **1** in these reactions is to abstract an alkide (most commonly methide) group. Electrophilic attack by the Lewis acidic boron atom of **1** occurs at moderately basic alkyl groups of metal alkyls, Scheme 1.1. Depending on the reaction conditions and the nature of the catalyst, either partial or full alkide abstraction can occur leading to weakly coordinated ion-pairs (coordinated alkylborate anion, $[R\text{-}B(C_6F_5)_3]^-$) or solvent

separated ion-pairs (discrete alkylborate anion) respectively. In both cases, the Lewis acidity of the metal center has been greatly increased. Coordination of olefin to either species is much more facile than to the non-activated pre-catalysts enabling polymerization to proceed. Although initially, little importance was ascribed to the weakly coordinating anion (WCA) during the polymerization process, this thinking is now being questioned.[30]

Some of the characteristics of **1** (and the alkylborate anions derived from reaction of **1** with metal alkyls) that have led to its effectiveness as a co-catalyst in olefin polymerization are the following. First, **1** is a strong Lewis acid; a recent estimate using the Child's method[31] resulted in the following order of decreasing Lewis acidity; BCl_3 (1.0) > BF_3 (0.77) > 1 (0.72) > $SnCl_4$ (0.50). Compared to haloborane Lewis acids, **1** is much more thermally robust, stable to oxygen and only slowly hydrolyzed by H_2O (a stable trihydrate can be isolated[32,33]). Alkylborate anions are also more well behaved than those derived from BF_3; specifically, the $-C_6F_5$ groups are much more resistant to ligand redistribution reactions which are well documented for $[R\text{-}BF_3]^-$ anions.[34] Third, the basicity of anionic borates derived from **1** is low leading to ion-pairs coordinated only weakly through the alkyl group. The basicity of the fluorine lone pairs is substantially suppressed by electron delocalization into the aromatic system precluding neutralizing F^- abstraction reactions by the electrophilic metal center. Finally, $[R\text{-}B(C_6F_5)_3]^-$ anions are also strongly resistant to oxidation reactions by electrophilic cations. A number of variations on **1** have been prepared and studied as co-catalysts in the past ten years as summarized in a recent review on activator technology.[35]

Other applications of **1** in organometallic chemistry have appeared recently including formation of interesting early transition metal zwitterions,[36] reactions with phosphorus ylides,[31] coordination of a carbene,[37] coordination of Cp*Al(I),[38] and one-electron reduction chemistry.[39]

1.2.2 Perfluoroarylborates in Organometallic Chemistry

Prior to the development of neutral activators, ionic activators had been used. Typically these activators are comprised of a WCA such as $[B(C_6F_5)_4]^-$ in conjunction with a trityl (triphenylmethyl)[40] or ammonium cation.[41] It should be noted that the trityl cation and **1** are isoelectronic. During the activation process (alkide abstraction or protonolysis), the WCA is transferred to the newly formed metal cation. The poorly coordinating nature of the anion dissipates the electrophilicity of the metal cation only moderately. The main difference then between neutral and ionic activators is the nature of the anion produced, $[R\text{-}B(C_6F_5)_3]^-$ vs $[B(C_6F_5)_4]^-$. Generally alkylborates have been found to be more strongly coordinating than the *tetrakis*-perfluorinated arylborates. Although the more coordinating alkylborates can diminish the reactivity of the metal cation, they can also be advantageous since the ion-pairs are generally more stable. Other WCA's have also been investigated in olefin polymerization.[35, 42]

Perfluoroaryl borate anions and WCA's in general have also found considerable utility particularly as non-coordinating counterions for highly reactive "naked" cations. Some recent examples of compounds possessing WCA's include protonated arene salts,[43] diaryliodonium salts,[44] a hypervalent tellurium cation $Ph_5Te(VI)^+$,[45] trisilylsubstituted sulfur(IV) cations,[46] cationic aluminum and gallium complexes,[47] and protonated

fullerene.[48] WCA's have been used effectively in the quest for tricoordinate Group IV cations and will be discussed specifically in Sections 1.3 and 1.4.

1.2.3 $B(C_6F_5)_3$ in Organic Synthesis

Figure 1.2: Representative Reactions Catalyzed or Promoted by $B(C_6F_5)_3$.

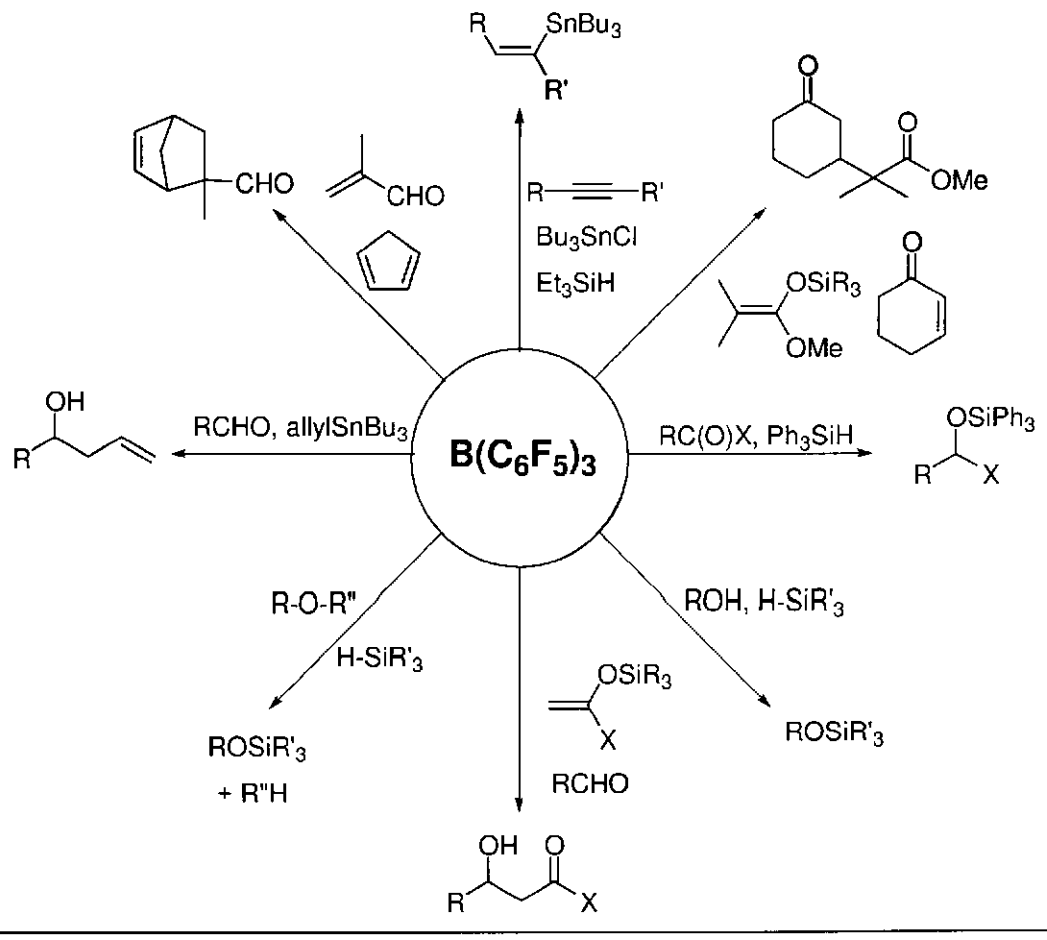

Over the past ten years, a number of uses of **1** as a Lewis acid catalyst for organic transformations have been reported, Figure 1.2.[49] These include the Mukaiyama aldol reaction between ketene silyl acetals or silyl enol ethers and aldehydes or imines,[50,51] the vinylogous Mukaiyama aldol reaction,[52] Sakurai-Hosomi allylation,[51] Diels-Alder reactions,[51] epoxide rearrangement reactions,[53] allylstannation of carbonyls,[54]

hydrostannation of alkynes,[55] reductive alcohol and ether cleavage reactions,[56] and allylation of benzyl acetates.[57] The Piers research group has investigated the hydrosilation of carbonyls,[58] silation of alcohols,[59] hydrosilation of imines,[60] and, reported herein for the first time, the 1,4-hydrosilation of enones and the novel hydrosilation of silyl enol ethers. Very little mechanistic work has been carried out on these reactions. In most cases, the authors ascribe a conventional role to **1** where the Lewis acid activates a base (carbonyl, imine etc.) to attack by a nucleophile (silane, allylstannane, etc.).

Scheme 1.2:The Parks/Piers Mechanism for $B(C_6F_5)_3$-Catalyzed Hydrosilation.

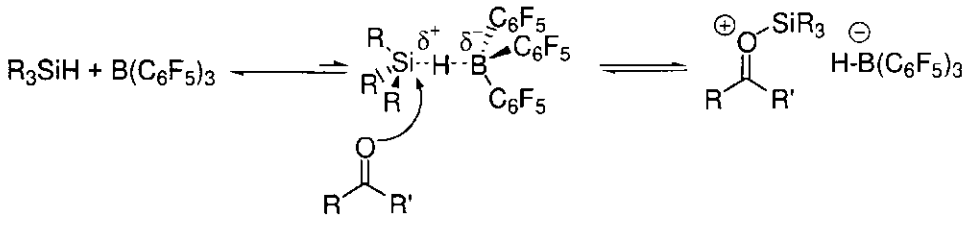

Studies by Parks and Piers however, have established that the hydrosilation of carbonyls proceeds via a mechanism involving activation of the Si-H bond by **1**, Scheme 1.2. The details of this reaction mechanism will be discussed in Chapter 2. One of the major objectives of the work presented in this dissertation was to determine the relevance of this type of mechanism to some of the other reactions catalyzed by **1**. Gaining such an understanding would be valuable in attaining future goals such as developing asymmetric reactions.

1.2.4 Applications of $[M]^+[B(C_6F_5)_4]^-$ in Organic Synthesis

Both $[Ph_3C]^+[B(C_6F_5)_4]^-$ and "$LiB(C_6F_5)_4$" have found recent application as catalysts for a number of organic reactions. The WCA increases the reactivity of the

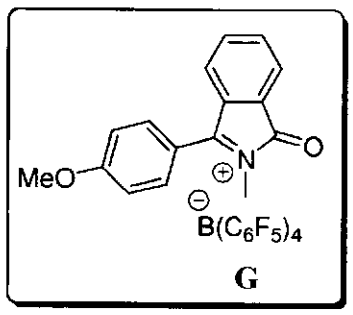

G

cation not observed with triflate or tetrafluoroborate derivatives. For example, $[Ph_3C]^+[B(C_6F_5)_4]^-$ has been used to catalyze the aldol reaction between silyl enol ethers and acetals or aldehydes[61] and an intramolecular hydrosilation of an alkyne.[62] "$LiB(C_6F_5)_4$" has been used as a catalyst for effecting Friedel-Crafts benzylation reactions[63] and benzylation of alcohols.[64] Mukaiyama and co-workers have also shown that the acyliminium salt, **G**, can be used as a catalyst for aldol reactions.[65] Mori, Sonoda and co-workers have used a related lithium perfluoroarylborate ion-pair to catalyze Diels-Alder reactions.[66]

1.2.5 NMR Spectroscopic Characterization of Derivatives of $B(C_6F_5)_3$

^{19}F NMR spectroscopy has become extremely useful in analyzing reactions involving neutral and anionic base complexes of **1**. The donating properties of a base (R)

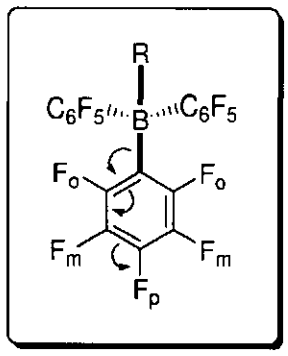

affects the extent of electron delocalization into the C_6F_5 rings and thus will affect the ^{19}F NMR chemical shifts. In non-coordinating solvents, $\Delta\delta_{p,m}$ (the chemical shift difference between the *para* and *meta* fluorines) for the parent compound **1** is approximately 18 ppm. Coordination of a neutral base can lower this value considerably. For weakly coordinating molecules this effect can be slight whereas for donors such as those listed in Table 1.1, coordination can cause a large change. Anionic donors lead to an even greater contraction, generally the value for $\Delta\delta_{p,m}$ being less than 6 ppm. Horton and de With have suggested that for methyl- and benzylborate anions, the extent of coordination of the corresponding cation can be judged based on this value.[67] In short, if the cation is strongly associated, the value is >3.5 ppm

whereas if the cation is not associated (ion separated) the value $\Delta\delta_{p,m}$ is typically less than 3 ppm. Although these are empirical trends, they have become a useful diagnostic tool in analyzing reaction products derived from **1**. Some ^{19}F NMR shifts of some neutral and anionic derivatives of **1** are included in Table 1.1.[68]

Table 1.1: ^{19}FNMR Chemical Shifts of Some Representative Complexes.

R	^{19}F NMR Shifts (*o*, *p*, *m*, ppm)	$\Delta\delta_{p,m}$
CH_3CN[a]	-134.7, -154.8, -163.2	8.4 ppm
^{t}BuNC[a]	-134.8, -155.3, -162.9	7.6 ppm
PPh_3[a]	-134.8, -157.3, -164.4	7.1 ppm
Cp*Al(I)[b]	-127.2, -154.9, -159.8	4.9 ppm
PhC(O)H[c]	-133.9, -154.3, -162.5	8.2 ppm
C_6F_5[d]	-133.1, -163.7, -167.3	3.6 ppm
CH_3[e]	-135.3, -160.8, -166.1	5.3 ppm
CH_3[f]	-133.2, -165.2, -167.8	2.6 ppm
$PhCH_2$[g]	-132.2, -161.7, -165.7	4.0 ppm
$PhCH_2$[h]	-130.4, -163.7, -166.5	2.8 ppm

[a] see ref. 68a.
[b] see ref. 38.
[c] see ref. 68b.
[d] $[Ph_5Te][B(C_6F_5)_4]$ see ref. 45.
[e] $[(1,2\text{-}Me_2Cp)_2ZrMe]^+$ countercation (strongly associated), see ref. 28.
[f] non-coordinating Bu_4N^+ countercation, see ref. 68c.
[g] strongly associated to cation, see ref. 67.
[h] ion-pair separated, see ref. 68d.

1.3 "Silylium" Cations

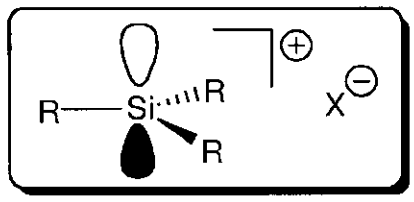

Over the past twenty years, a number of groups have been involved in attempts to prepare the first stable, tricoordinate silicon cation. These studies have been fraught with

controversy as interpretations of which criteria constitute a legitimate "silylium" ion have not been consistent. A definite learning curve was established as chemists rediscovered that "silicon is not carbon" [69] and that different considerations than those used to isolate carbocations would have to be applied. This work has culminated in the isolation of "Mes_3Si^+" (Mes = mesityl) by Lambert and co-workers which is generally regarded as the closest example to a free tricoordinate silicon cation so far achieved.[70]

1.3.1 The Race for the First Silicon Cation

In the mid-1980's, Lambert reported evidence for silylium ions in solution (CH_3CN, sulfolane, chlorocarbons) possessing perchlorate counteranions.[71] Conductivity measurements established the presence of ion-pairs in the polar media. However, Olah and Prakash disputed these results and based on ^{37}Cl NMR line broadening experiments determined that the perchlorate anions were actually covalently bound (through O) to the silicon.[72] Other groups established that the observation of conductivity was likely a result of formation of solvated ion-pairs in equilibrium with covalently bound silyl perchlorates, equation 1.1.

$$R_3Si\text{-}OClO_3 \rightleftharpoons [R_3Si(solvent)]^{\oplus}\ {}^{\ominus}[ClO_4] \quad (1.1)$$

Subsequently, Boudjouk[73] and Reed[74] extensively characterized nitrile-solvated silylium cations while the groups of Kira[75] and Olah[76] characterized silyloxonium cations. Cremer and co-workers[77] have also contributed through an extensive tandem NMR/theoretical study on solvated triorganosilicon compounds. In spite of the supposedly non-nucleophilic nature of these solvents, extremely electrophilic silylium cations are readily solvated. The description of perchlorate and other anions as being

non-coordinating was also found to be inappropriate in reference to silylium cations. New strategies would thus be necessary to isolate a tricoordinate silicon cation.

While different strategies were being explored, further research by the Northwestern group created yet more controversy. Lambert and co-workers were able to isolate and characterize crystallographically what they termed a "Et_3Si^+" cation, **2a**.[78] Weak ("distant") coordination of a toluene molecule was present in the X-ray structure (C-Si = 2.18 Å); however, "covalent bonding was weak or absent". In order to isolate this compound, Lambert took advantage of the beneficial properties of the WCA, $[B(C_6F_5)_4]^-$. The complete formulation of this compound then is $[Et_3Si(toluene)]^+[B(C_6F_5)_4]^-$. However, a subsequent onslaught of research from other groups led to a reinterpretation of Lambert's work once again.

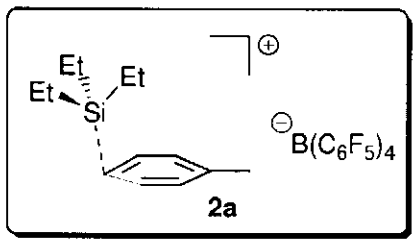

2a

The groups of Reed,[79] Schleyer,[80] Olah,[81] Cremer[82] and Linus Pauling[83] quickly provided evidence that the bonding between Si and the toluene had a considerable covalent component to it. Furthermore, the ^{29}Si NMR shift observed for this species was 82 ppm, far short of a theoretical value of 350 ppm calculated using the IGLO method. Although this species came closest to the ultimate goal of preparing a silicon cation, it too did not completely satisfy the necessary criteria. This ion is more aptly described as a silylated toluenium cation, **2b**. Nonetheless, using WCA's and preventing solvent coordination would be an absolute necessity to successfully produce a tricoordinate silicon cation.

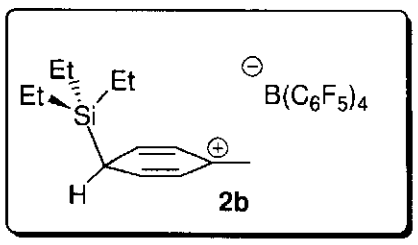

2b

Reed and co-workers have championed the use of hexahalocarborane anions ($CB_{11}H_6Cl_6$) in preparing highly reactive cations[43] and have shown them to be even less coordinating than perfluorinated arylborate anions. Indeed, this group characterized $[^iPr_3Si(CH_3CN)]^+[CB_{11}H_6Br_6]^-$ from CH_3CN and $[^iPr_3Si]^+[CB_{11}H_6Br_6]^-$ from toluene by X-ray crystallography. Although, in the latter case, toluene does not coordinate in the solid state, one of the bromines of the hexabromocarborane is weakly coordinated.

Reed and co-workers also characterized $[^iPr_3Si]^+[CB_{11}H_6Cl_6]^-$ by X-ray crystallography.[84] The steric bulk of the isopropyl groups prevents solvent coordination. Although again this species approaches a legitimate tricoordinate cation, weak coordination of one of the chlorines of the hexachlorocarborane is observed. This weak bonding has the effect of slightly pyramidalizing the trialkylsilyl moiety from the idealized 120° to 117.3° leading to Reed's estimate of this species being 60% ionized. Evidence for hyperconjugative stabilization of the silylium center by a C-H bond is observed in the solid state for $[^iPr_3Si]^+[CB_{11}H_6Cl_6]^-$. Interestingly, this group did attempt to prepare species of the form $[^tBu_3Si]^+[X]^-$, but they did not ionize efficiently.

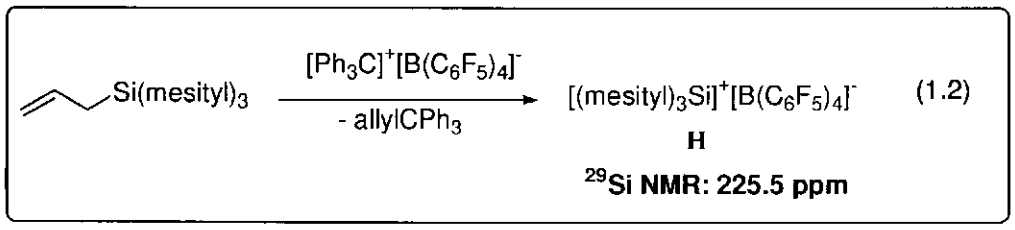

Soon thereafter, Lambert reported his results using a similar strategy of bulking up the silyl substituents, but instead of using trialkylsilyl derivative, he used a triarylsilane. Lambert reacted allylSiMes_3 and $[Ph_3C]^+[B(C_6F_5)_4]^-$ in toluene leading to the formation of $[Mes_3Si]^+[B(C_6F_5)_4]^-$, **H**, and allyl$CPh_3$. Although this compound was not characterized by X-ray crystallography, a ^{29}Si NMR shift of 225.5 in C_6D_6 does

indicate that solvent is not coordinated. This NMR shift is consistent with calculated values taking into consideration the use of aryl groups instead of alkyl groups and the still significant effect of non-coordinated solvent on the ^{29}Si chemical shift.[69] Thus **H** most closely approaches a free, tricoordinate silylium ion.

1.3.2 The Chemistry of Coordinated Silylium Cations

As mentioned in the previous section, a number of solvent coordinated trialkylsilylium cations have been characterized both in solution and the solid state. Even aromatic solvents have been shown to coordinate these highly electrophilic species. ^{29}Si NMR spectroscopic studies on these species indicate little difference between them and other four-coordinate silanes and thus they are best described as silylated solvent ions (eg. silylnitrilium, silylpyridinium, silyloxonium etc.).

Bahr and Boudjouk studied the chemistry of silylnitrilium ions of the form $[R_3Si(C_3H_7CN)]^+[B(3,5\text{-}(CF_3)_2C_6H_3)_4]^-$.[73a] However, when exposed to nucleophiles (H_2O, MeOH, BuOH, F^-), reactions occurred at the electrophilic Si center; that is, these species react as silylium ions. Solvent coordination stabilizes these otherwise reactive compounds. Rapid nitrile exchange was observed at the Si, the authors favoring a facile associative transition state (five-coordinate siliconium cation).

Cremer and co-workers carried out an elaborate study involving a range of

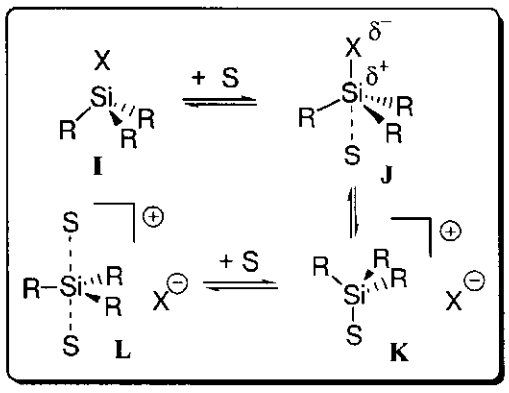

solvents (CH_2Cl_2, DMPU, DMSO, sulfolane, HMPA, acetonitrile, pyridine, N-methylimidazole and Et_3N) that showed that weakly covalent bonds between Si and solvent existed in each case, precluding any real

silylium cation character in the ions.[77] Trialkylsilylium cations ("R_3Si^+") are stabilized by formation of tetracoordinate species (**K**). Pentacoordination only occurs in the transition state for solvent exchange (**L**) or anion displacement (**J**). For R_2HSi^+, RH_2Si^+ and H_3Si^+, pentacoordination is possible both because of lesser steric demands and because of decreased electronic stabilization of the H substituent versus alkyl substituent (hyperconjugation). Unsolvated, tricoordinate silicon cations are never formed.

Mishima and co-workers[85] have carried out experimental and theoretical studies to determine the relative gas-phase basicities (GB) of a number of nucleophiles to the "Me_3Si^+" cation. GB("Me_3Si^+") was found to increase in the order aniline < benzaldehyde < acetophenone < N,N-dimethylaniline < pyridine while GB(H^+) increases in the order benzaldehyde < acetophenone < aniline < pyridine < N,N-dimethylaniline. Binding interactions have a pronounced covalent character leading again to the conclusion, that these coordinated species do not possess substantial silylium character.

1.3.3 Applications of Silylium Ions

In addition to the academic pursuit of tricoordinate silicon cations, species possessing silylium character have found other applications. Trialkylsilyl triflates (eg. TMSOTf, ^{t}BuMe$_2$SiOTf), trimethylsilyl perchlorate (TMSClO$_4$) and trimethylsilyl iodide (TMSI) have been used for many years now as relatively stable, powerful Lewis acids for catalyzing/promoting a number of useful organic reactions[86,87] which undoubtedly

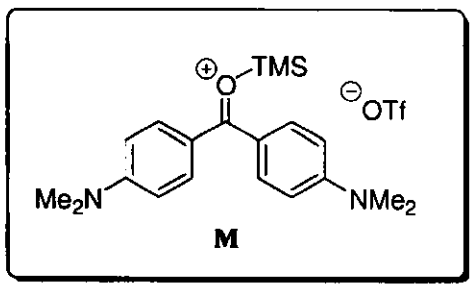

M

involve ionic intermediates. Bassindale and Stout have found that TMSOTf forms conducting solutions in nucleophilic solvents through formation of tetracoordinate salts of the form

$[Me_3Si(S)]^+OTf^-$.[88] Simchen and co-workers have observed by UV spectroscopy the trimethylsilylcarboxonium triflate ion-pair, **M**, prepared from reaction of 4,4'-dimethylaminobenzophenone with TMSOTf.[89] Species such as this have been implicated in silyl enol ether isomerization chemistry. Silation reactions between silyl triflates or halides (R_3Si-X) and alcohols or ketones which are catalyzed by bases such as Et_3N and imidazole proceed via silylammonium intermediates $[R_3Si(Et_3N)]^+[X]^-$.[90] The crystal structures of 1:1 adducts of pyridine with each of TMSI and TMSBr have been reported where the halide anions are completely dissociated.[91] Aldol reactions,[92] carbosilations, cyanosilation,[93] Diels-Alder reactions, hydrosilation,[94] epoxide opening,[95] ionization reactions[96] additions to imines, [97] have all been catalyzed by silyl triflates. Recently, trimethsilyl methanesulfonate (TMSOMs) has been introduced as a convenient alternative to TMSOTf.[98]

Carreira[99] and Bosnich[100] have demonstrated that silicon catalysis can occur under conditions where a discrete silicon Lewis acid catalyst is not introduced externally. Carreira's mechanistic study of the Mukaiyama aldol reaction of silyl enol ethers catalyzed by a number of Lewis acids such as $Yb(OTf)_3$, $Sn(OTf)_2$, $LiClO_4$ and $Zn(OTf)_2$ were shown to proceed primarily via Lewis acidic silicon species. The metal salts act as initiators, producing the active silicon Lewis acid from the silyl enol ether. An extensive study by Bosnich emphasizes the difficulty of distinguishing between metal versus silyl catalysis in the Mukaiyama aldol and Sakurai allylation reactions. Denmark showed that silyl triflate formation occurs during the Mukaiyama aldol reaction catalyzed by triarylcarbenium ions.[101] However, deactivation of the silyl triflate was shown to occur competitively over subsequent silyl catalysis.

In 1992, Davis and Jaspars reported the use of a new "supersilylating reagent", $[Me_3Si]^+[B(OTf)_4]^-$ (formed *in situ* from TMSOTf and $B(OTf)_3$) for catalyzing the allylsilation of aldehydes.[102] In general, TMSOTf[103] and TMSI[104] had been found to be ineffective for allylsilation reactions. Although $[Me_3Si]^+[B(OTf)_4]^-$ is still considered to be a covalent compound, the less strongly associating $B(OTf)_4^-$ anion enables "Me_3Si^+" to be unleashed via coordination of an aldehyde molecule. This Lewis acid was also used to catalyze the Mukaiyama aldol reaction with high Cram selectivity.[105] Davis has also reported that "supersilylating reagents" are formed from the reaction of silyl chlorides and $B(OTf)_3$.[106]

Jørgensen and co-workers have sought further to increase the electrophilicity of a silicon-based Lewis acid by adopting the strategy of using weakly coordinating perfluorinated aryl borates (*tetrakis*-pentafluorophenylborate (TPFPB) and *tetrakis*-(3,5-$CF_3C_6H_3$)borate (TFPB)).[107] The unfortunately misnamed[108] silylium cations **N** and **O**

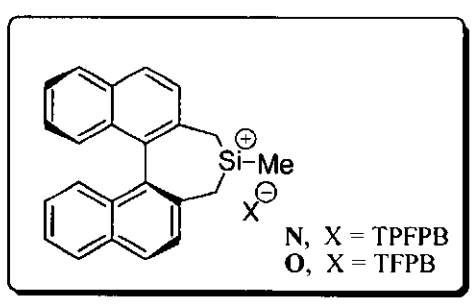

were prepared by trityl abstraction of the appropriate silyl hydride in CH_3CN and used to catalyze Diels-Alder reactions (albeit with little enantioselectivity). Olah and co-workers noted that these species were certainly silynitrilium ions. Nonetheless, this was a notable application of a masked "R_3Si^+" cation possessing the new breed of WCA's toward organic synthesis.

Yamamoto has developed a clever strategy for preparing *in situ* trialkylsilylium species with a WCA starting from commercially available silyl triflates.[109] When silyl triflates are mixed with strong aluminum Lewis acids such as methylaluminum *bis*-(2,6-

di-*tert*-butyl-4-methylphenoxide), (MAD), silicon "super Lewis acids" are formed. This strategy has been used to effect aldol reactions[109a] and to polymerize silyl vinyl ethers.[109b]

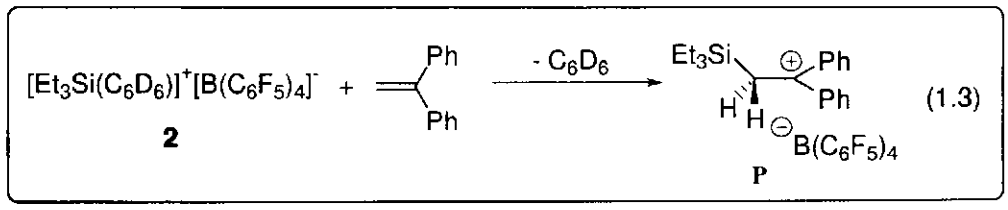

Lambert and co-workers have used $[Et_3Si(benzene)]^+[B(C_6F_5)_4]^-$, **2**, as a reagent to prepare the β-silyl carbocation, **P**, *in situ*, equation 1.3.[110] The low nucleophilicity of the borate counterion was crucial to the success of this approach; other attempts to observe these important intermediates[111] had failed due to unwanted nucleophilic attack of the anion with the positive silicon center.[112] Reaction with Et_3SiH leads to formation of $Et_3SiCH_2CHPh_2$ presumably via the intermediacy of **P**. ^{13}C and ^{29}Si NMR indicate only a small percentage of silylium character remaining at the Si.

The advance in silylium ion chemistry has been accompanied by the design and synthesis of fundamentally interesting compounds such as the 2-silanorbornyl cation,[113] a homocyclotrisilylenium cation,[114] and a silylium cation intramolecularly solvated by a Si-H bond (3-center Si-H-Si bond).[115]

1.4 Stannylium Cations

Interest in solvated triorganotin cations dates back over 40 years. In particular, the fungicidal properties of triorganyl compounds prompted research on preparing water soluble *bis*-aquated triorganyltin cations. In the past ten years, developments in the synthesis of tricoordinate silicon cations has encouraged similar research toward tricoordinate tin cations.

1.4.1 Preparation of Solvated Tin Cations

Figure 1.3: Examples of Base-Stabilized Tin Cations.

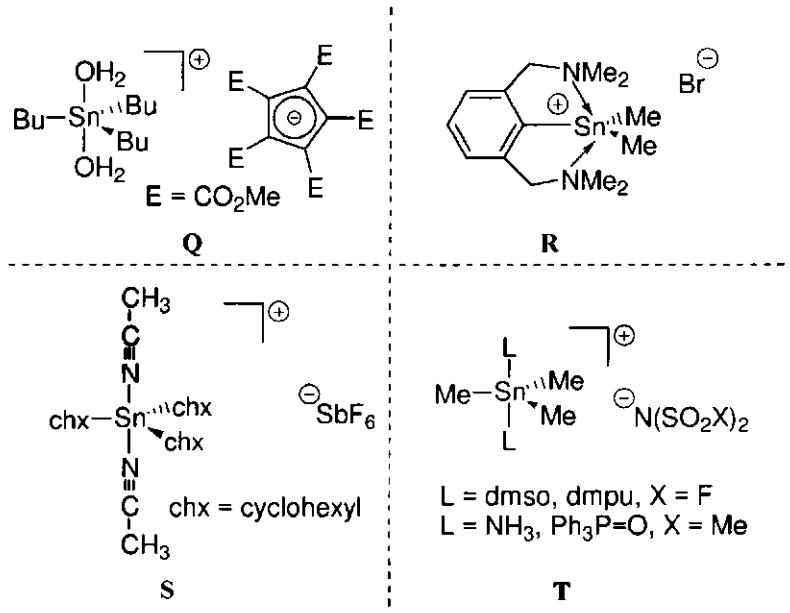

Evidence for *bis*-aquated triorganyltin cations was first presented in the early 1960's.[116] Wada and Okawara isolated and characterized $[Me_3Sn(OH_2)_2]^+[BPh_4]^-$ by IR spectroscopy and elemental analysis.[117] Clark prepared and characterized by IR spectroscopy compounds of the form $[Me_3Sn(NH_3)_2]^+[X]^-$.[118] Since this early work, a number of compounds of general formula $[R_3Sn(L)_2]^+[X]^-$ have been described and characterized by NMR spectroscopy and/or X-ray crystallography. Notable examples include those by Das,[119] Davies,[120] **Q**, van Koten,[121] **R**, Nugent,[122] **S**, and Blaschette and Jones[123] **T**, Figure 1.3.

In all cases, the two donor groups are co-axially arranged around a planar triorganyltin atom. Interestingly, no examples of four-coordinate tin ion-pairs have been described[124,125] although compounds of the general form $R_3Sn(L)X$ possessing a trigonal bipyramidal tin center have been characterized.[126,127] In the solid state, compounds such as Me_3SnF[128] and Me_3SnClO_4[129] exist as polymeric arrays where the tin atom is five-coordinate. Studies of Me_3SnBF_4, Me_3SnPF_6 and Me_3SnSbF_6 confirm the preponderance of pentacoordination even in solution.[130]

1.4.2 NMR studies of Solvated Triorganostannyl Cations

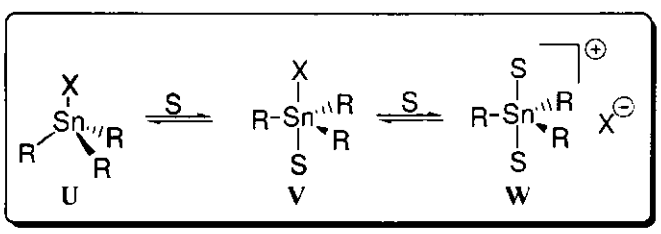

Edlund and co-workers have carried out extensive NMR investigations on the ionization behaviour of triorganotin compounds, R_3Sn-X, in a number of solvents, S.[131] Their results support the existence of an equilibrium between a tetrahedral structure, **U**, and two solvated trigonal bipyramidal structures, **V** and **W**, similar to those proposed by Cremer for solvated silicon cations. Equilibrium positions are dependent on the properties of R (Bu vs Ph), X (Cl^-, ClO_4^- or BF_4^-) and S (CH_2Cl_2, sulfolane, CH_3CN, pyridine, DMPU, DMSO, HMPA). Strongly ionizing solvents such as HMPA favor structure **W**. The observation of large values for $^1J_{C\text{-}Sn}$ (> 400 Hz for Bu_3Sn derivatives) was used to confirm species of the ilk **V/W** since s-orbital contribution to Sn-C equatorial bonds in trigonal bipyramidal complexes had previously been established.[132]

A theoretical study by Edlund and co-workers used *ab initio* IGLO calculations to estimate the "expected" value for a non-solvated trimethyltin cation to be >1000.[133] An

empirical correlation graph between known ^{29}Si and ^{119}Sn NMR shifts and the calculated value for "Me_3Si^+" (356 ppm) supported this estimate and could be used to approximate % tin cation character in known complexes.

1.4.3 Toward Non-solvated Triorganotin Cations

The groups of Birchall, Kira and Lambert have been actively involved in attempting to prepare non-solvated tricoordinate tin cations in solution. Birchall reported in 1985 that $[Me_3Sn]^+[FSO_3]^-$ possessed a ^{119}Sn NMR shift of 322 ppm.[134] Using the WCA $[(3,5\text{-}(CF_3)_2C_6H_3)_4B]^-$ (TFPB), Kira prepared and characterized $[Bu_3Sn]^+[TFPB]^-$ from the reaction of Bu_3SnH with $[Ph_3C]^+[TFPB]^-$ in CD_2Cl_2.[125] This compound exhibits a ^{119}Sn NMR shift of 356 ppm at -20 °C. Although, these values suggest considerable cationic character for the two compounds, it is far below the theoretical value >1000 ppm expected from Edlund's studies.

Scheme 1.3: Early Strategies Toward Free Tin Cations.

(a) $R_3Sn\text{-}H + Ph_3ClO_4 \xrightarrow{-\ Ph_3CH} R_3Sn\text{-}OClO_3$

(b) $R_3Sn\text{-}Cl + AgClO_4 \xrightarrow{-\ AgCl} R_3Sn\text{-}OClO_3$

(c) $R_3Sn\text{-}H + B(C_6F_5)_3 \longrightarrow [R_3Sn]^+[H\text{-}B(C_6F_5)_3]^-$

Lambert's first attempts involved preparing stannyl perchlorates via hydride abstraction, Scheme 1.3a or chloride abstraction, Scheme 1.3b. Although these stannyl perchlorates were more conducting (more ionogenic) than the silyl perchlorates, ^{119}Sn NMR supports only moderate tin cation character. A novel approach inspired by olefin polymerization technology involved the use of **1** with Bu_3SnH to form a species

formulated by Lambert as $[Bu_3Sn]^+[H\text{-}B(C_6F_5)_3]^-$, Scheme 1.6c. The ^{119}Sn NMR shift of this compound was measured to be 360 ppm indicating substantial stannylium character, but still well below the theoretical value for a naked tin cation. NMR and theoretical studies by Edlund and co-workers firmly established that neither Kira nor Lambert were observing free tricoordinate tin cations in solution.

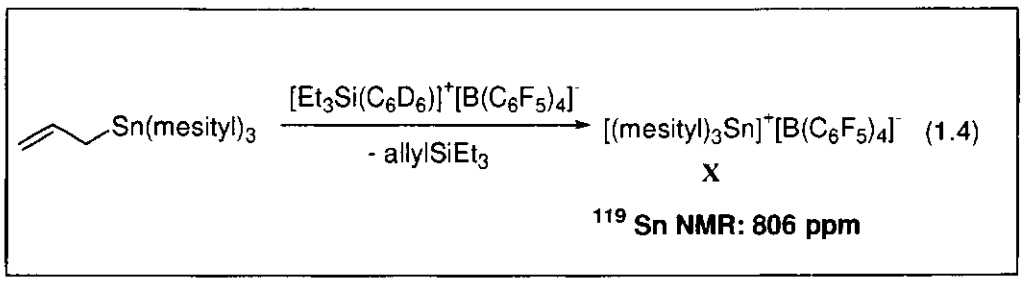

(1.4)

In 1999, Lambert prepared $[Mes_3Sn]^+[B(C_6F_5)_4]^-$, **X**, in C_6D_6 from the reaction of $[Et_3Si(C_6D_6)]^+[B(C_6F_5)_4]^-$ and allyltrimesitylstannane.[135] This compound possesses a ^{119}Sn NMR shift of 806 ppm, significantly downfield of any triorganotin compound so far generated. Using Edlund's $^{29}Si/^{119}Sn$ NMR correlation technique, this species is calculated to be 75% of the extreme expected for tricoordinate tin. This value is based on a strictly linear relationship between ^{29}Si and ^{119}Sn NMR shifts and therefore could either over- or underestimate the true extent of tricoordination. Weak coordination of a fluorine atom from the anion could be present.[136] Regardless, this compound represents the extreme in tricoordinate tin. $[Bu_3Sn]^+[B(C_6F_5)_4]^-$ has also been prepared.[137] The reported ^{119}Sn NMR shift of 263 ppm suggests 33% stannylium character. Work presented in this dissertation corrects this value as 434.2 ppm, but the upfield-shifted value relative to the trimesityltin species indicates that either stronger association of the anion occurs or more likely, that arene solvent can coordinate weakly as observed for $[Et_3Si(arene)]^+[B(C_6F_5)_4]^-$.

1.4.4 Applications of Triorganotin Cations

Applications of triorganotin compounds in organic synthesis lags far behind those of silicon,[138] although, triorganotin alkanesulfonates have been shown to be readily ionized by Lewis bases such as H_2O.[139] Bu_3SnClO_4, $Bu_2Sn(ClO_4)_2$ and $Bu_2Sn(OTf)_2$ have been used to catalyze Mukaiyama aldol reactions.[140] Nugent recognized the potential of triorganotin cations as Lewis acids for promoting sluggish Diels-Alder reactions.[122a] Compounds such as $[(cyclohexyl)_3Sn(CH_3CN)_2]^+[SbF_6]^-$ were generated *in situ* and used to effect the cycloaddition of furan with alkenes such as methyl methacrylate. McKinney and Nugent have also this strategy for generating tin Lewis acids to be used in conjunction with Ni catalysts in the industrially important adiponitrile process.[124b] Finally, Blaschette and Jones have demonstrated that triorganotin dimesylamides ($[R_3Sn]^+[(MeSO_2)_2N]^-$) are readily ionized in the presence of strong bases.[141] A diverse series of structures was obtained from these versatile starting materials.

1.5 Outline for Thesis

This introductory chapter has attempted to illustrated some of the diverse applications and techniques for the characterization of perfluoroaryl borane, silylium and stannylium Lewis acids. All three of these types of Lewis acids play a prominent role in the original research presented in this dissertation. Chapter 2 documents synthetic and mechanistic studies directed toward reactions of hydrosilanes with carbonyl compounds or alcohols catalyzed by **1**. In Chapter 3, the hydrosilation of imines catalyzed by **1** and the coordination chemistry of imines with **1** is studied. In both these chapters, silylium Lewis acids are important. Chapter 4 describes a study aimed at elucidating the

mechanism of allylstannation of aldehydes catalyzed by **1**. In this case, the intermediacy of reactive stannylium species is revealed.

---

[1] (a) Santelli, M.; Pons, J. -M. *Lewis Acids and Selectivity in Organic Synthesis* CRC Press, New York, 1996. (b) *Lewis Acids in Organic Synthesis Vols. I-II* Yamamoto, H. ed.; Wiley-VCH: Toronto, 2000.

[2] Shambayati, S.; Schreiber, S. L. in *Comprehensive Organic Synthesis* Trost, B. M.; Fleming, I., Eds.; Pergamon Press: New York, 1991; Vol. 8, p.283.

[3] Yamamoto, Y.; Shida, N. in *Advances in Detailed Reaction Mechanisms*, **1994**, *3*, 1.

[4] Yamaguchi, M. in *Comprehensive Organic Synthesis* Trost, B. M.; Fleming, I., Eds.; Pergamon Press: New York, 1991; Vol. 8, p.325.

[5] *Comprehensive Asymmetric Catalysis Vols. I-III* Jacobsen, E. N.; Pfaltz, A.; Yamamoto, H. eds.; Springer-Verlag: New York, 1999.

[6] Landolf, M. C. R. *Hebd. Seances Acad. Sci.* **1878**, *86*, 671.

[7] Yates, P.; Eaton, P. E. *J. Am. Chem. Soc.* **1960**, *82*, 4436.

[8] Photoelectron spectroscopy studies have shown that carbonyls possess two non-equivalent lone pairs, one in an *sp*-hybridized orbital, the other in a *p*-type orbital, see Raber, D. J.; Raber, N. K.; Chandrasekhar, J.; Schleyer, P. v. R. *Inorg. Chem.* **1984**, *23*, 4076.

[9] (a) Nelson, D. J. *J. Org. Chem.* **1986**, *51*, 3185. (b) Loncharich, R. J.; Schwartz, T. R.; Houk, K. N. *J. Am. Chem. Soc.* **1987**, *109*, 14.

[10] Lappert, M. F.; Smith, J. K. *J. Chem. Soc.* **1965**, 7102.

[11] Gillespie, R. J.; Hartman, J. S. *Can. J. Chem.* **1968**, *46*, 2147.

[12] Henriksson, U.; Forsen, S. *J. Chem. Soc. (D)* **1970**, 1229.

[13] See also (a) Hartman, J. S.; Stilbs, P.; Forsen, S. *Tetrahedron Lett.* **1975**, 3497. (b) Stilbs, P.; Forsen, S. *Tetrahedron Lett.* **1974**, 3185. (c) Fratiello, A.; Kubo, R.; Chow, S. *J. Chem. Soc.; Perkin Trans. 2* **1975**, *2*, 1205.

[14] Reetz, M. T.; Hullmann, M.; Massa, W.; Berger, S.; Rademacher, P.; Heymanns, P. *J. Am. Chem. Soc.* **1986**, *108*, 2405.

[15] Gajewski, J. J.; Ngermeesri, P. *Org. Lett.* **2000**, *2*, 2813.

[16] For example, see Yamamoto, Y.; Yatagai, H.; Ishihara, Y.; Maeda, N.; Maruyama, K. *Tetrahedron*, **1984**, *40*, 2239.

[17] A theoretical study has shown that the 2:1 adduct of NH_3 and BH_3 exists only as a transition state, see Czerw, M.; Goldman, A. S.; Krogh-Jespersen, K. *Inorg. Chem.* **2000**, *39*, 363.

[18] Denmark, S. E.; Henke, B. R.; Weber, E. *J. Am. Chem. Soc.* **1987**, *109*, 2512.

[19] Cram, D. J.; Elhafez, F. A. A. *J. Am. Chem. Soc.* **1952**, *74*, 5828.

[20] Reetz, M. T. *Acc. Chem. Res.* **1993**, *26*, 462.

[21] (a) Reetz, M. T.; Kesseler, K.; Schmidtberger, S.; Wenderoth, B.; Steinbach, R. *Angew. Chem. Int. Ed. Engl.* **1983**, *22*, 989. (b) Reetz, M. T.; Kesseler, K.; Schmidtberger, S.; Wenderoth, B.; Steinbach, R. *Angew. Chem. Suppl.* **1983**, 1511. (c) Reetz, M. T.; Hüllmann, M.; Seitz, T. *Angew. Chem. Int. Ed. Engl.* **1987**, *26*, 477.

[22] Keck, G. E.; Castellino, S. *J. Am. Chem. Soc.* **1986**, *108*, 3847.

[23] (a) Poll, T.; Metter, J. O.; Helmchen, G. *Angew. Chem. Int. Ed. Engl.* **1985**, *24*, 112. (b) Viard, B.; Poulain, M.; Grandjean, D.; Anandrut, J. *J. Chem. Res. (S)* **1983**, 850. (c) Maier, G.; Siepp, U. *Tetrahedron Lett.* **1987**, *28*, 4515. (d) Utka, J.; Sobota, P.; Lis, T. *J. Organomet. Chem.* **1982**, *334*, 341.

[24] (a) Reetz, M. T.; Harms, K.; Reif, W. *Tetrahedron Lett.* **1988**, *29*, 5881.

[25] (a) Massey, A. G.; Park, A. J.; Stone, F. G. A. *Proc. Chem. Soc.***1963**, 212. (b) Massey, A. G.; Park, A. J. *J. Organomet. Chem.* **1964**, *2*, 245. (c) Massey, A. G.; Park, A. J. *J. Organomet. Chem.* **1966**, *5*, 218.

[26] For reviews, see (a) Chambers, R. D.; Chivers, T. *Organomet. Chem. Rev.*, **1966**, *1*, 279. (b) Cohen, S. C.; Massey, A. G. *Adv. Fluorine Chem.* **1970**, *6*, 149.

[27] Piers, W. E.; Chivers, T. *Chem. Soc. Rev.* **1997**, *26*, 345.

[28] Yang, X.; Stern, C. L.; Marks, T. J. *J. Am. Chem. Soc.* **1991**, *113*, 3623.

[29] Ewen, J. A.; Edler, M. J. *Chem. Abstr.*, **1991**, *115*, 136998g; 256895t.

[30] (a) Vanka, K.; Chan, M. S. W.; Pye, C. C.; Ziegler, T. *Organometallics*, **2000**, *19*, 1841. (b) Lanza, G.; Fragala, I. L.; Marks, T. J. *J. Am. Chem. Soc.* **1998**, *120*, 8257. (c) Lanza, G.; Fragala, I. L.; Marks, T. J. *J. Am. Chem. Soc.* **2000**, *122*, 12764.

[31] Döring, S.; Erker, G.; Frölich, R.; Meyer, O.; Bergander, K. *Organometallics*, **1998**, *17*, 2183 and references therein.

[32] Siedle, A. R.; Newmark, R. A.; Lamanna, W. M. *Organometallics* **1993**, *12*, 1491.

[33] Bergquist, C.; Bridgewater, B. M.; Harlan, C. J.; Norton, J. R.; Friesner, R. A.; Parkin, G. *J. Am. Chem. Soc.* **2000**, *122*, 10581.

[34] For examples see, (a) Davies, J. -E.; Raithby, P. R.; Snaith, R.; Wheatley, A. E. H. *J. Chem. Soc., Chem. Commun.* **1997**, 1797. (b) Barr, D.; Hutton, K. B.; Morris, J. H.; Mulvey, R. E.; Reed, D.; Snaith, R. *J. Chem. Soc., Chem. Commun.* **1986**, 127. (c) Brown, H. C.; Racherla, U. S.; Singh, S. M. *Tetrahedron Lett.* **1984**, *25*, 2411. (d) Aubrecht, K. A.; Winemiller, M. D.; Collum, D. B. *J. Am. Chem. Soc.* **2000**, *122*, 11084.

[35] Chen, E. Y. -X.; Marks, T. J. *Chem. Rev.* **2000**, *100*, 1391.

[36] Piers, W. E. *Chem. Eur. J.* **1998**, 13 and references therein.

[37] Metzler, N.; Denk, M. *Chem. Commun.* **1996**, 2657.

[38] Gorden, J. D.; Voigt, A.; MacDonald, C. L. B.; Silverman, J. S.; Cowley, A. H. *J. Am. Chem. Soc.* **2000**, *122*, 950.

[39] Harlan, C. J.; Hascall, T.; Fujita, E.; Norton, J. R. *J. Am. Chem. Soc.* **1999**, *121*, 7274.

[40] (a) Chien, J. C. W.; Tsai, W. -M.; Rausch, M. D. *J. Am. Chem. Soc.* **1991**, *113*, 8570. (b) Ewen, J. A.; Elder, M. J. Eur. Pat, Appl. 0,426,637, **1991**.

[41] (a) Hlatky, G. G.; Upton, D. J.; Turner, H. W. PCT Int. Appl. WO 91/09882 **1991**. (b) Turner, H. W. Eur. Pat. Appl. EP 0 277 004 A1, **1988**. (c) Yang. X.; Stern, C. L.; Marks, T. J. *Organometallics*, **1991**, *10*, 840.

[42] Strauss, S. H. *Chem. Rev.* **1993**, *93*, 927.

[43] Reed, C. A.; Fackler, N. L. P.; Kim, K. -C.; Stasko, D.; Evans, D. R.; Boyd, P. D. W.; Rickard, C. E. F. *J. Am. Chem. Soc.* **1999**, *121*, 6314.

[44] Gu, H.; Ren, K.; Grinevich, O.; Malpert, J. H.; Neckers, D. C. *J. Org. Chem.* **2001**, *66*, 4161.

[45] Minoura, M.; Mukuda. T.; Sagami, T.; Akiba, K. *J. Am. Chem. Soc.* **1999**, *121*, 10852.

[46] Prakash, G. K. S.; Bae, C.; Wang, Q.; Rasul, G.; Olah, G. A. *J. Org. Chem.* **2000**, *65*, 7646.

[47] Dagorne, S.; Guzei, I. A.; Coles, M. P.; Jordan, R. F. *J. Am. Chem. Soc.* **2000**, *122*, 274.

[48] Bolskar, R. D.; Mathur, R. S.; Reed, C. A. *J. Am. Chem. Soc.* **1996**, *118*, 13093.

[49] Ishihara, K.; Yamamoto, H. *Eur. J. Org. Chem.* **1999**, 527.

[50] (a) Ishihara, K.; Hanaki, N.; Yamamoto, H. *Synlett*, **1993**, 577. (b) Ishihara, K.; Funahashi, M.; Hanaki, N.; Miyata, M.; Yamamoto, H. *Synlett*, **1994**, 963.

[51] Ishihara, K.; Hanaki, N.; Funahashi, M.; Miyata, M.; Yamamoto, H. *Bull. Chem. Soc. Jpn.* **1995**, *68*, 1721.

[52] Hassfield, J.; Christmann, M.; Kalesse, M. *Org. Lett.* **2001**, *3*, 3561.

[53] Ishihara, K.; Hanaki, N.; Yamamoto, H. *Synlett*, **1995**, 721.

[54] (a) Ooi, T.; Uraguchi, D.; Kagoshima, N.; Maruoka, K. *J. Am. Chem. Soc.* **1998**, *120*, 5327. (b) Blackwell, J. M.; Piers, W. E. *Org. Lett.* **2000**, *2*, 695.

[55] Gevorgyan, V.; Li, J. -X.; Yamamoto, Y. *J. Chem. Soc. Chem. Commun.* **1997**, 37.

[56] (a) Gevorgyan, V.; Liu, J. -X.; Rubin, M.; Benson, S.; Yamamoto, Y. *Tetrahedron Lett.* **1999**, *40*, 8919. (b) Gevorgyan, V.; Rubin, M.; Benson, S.; Liu, J. -X.; Yamamoto, Y. *J. Org. Chem.* **2000**, *65*, 6179.

[57] Rubin, M.; Gevorgyan, V. *Org. Lett.* **2001**, *3*, 2705.

[58] (a) Parks, D. J.; Piers, W. E. *J. Am. Chem. Soc.* **1996**, *118*, 9440. (b) Parks, D. J.; Blackwell, J. M.; Piers, W. E. *J. Org. Chem.* **2000**, *65*, 3090.

[59] Blackwell, J. M.; Foster, K. L.; Beck, V. H.; Piers, W. E. *J. Org. Chem.* **1999**, *64*, 4887.

[60] Blackwell, J. M.; Sonmor, E. R.; Scoccitti, T.; Piers, W. E. *Org. Lett.* **2000**, *2*, 3921.

[61] Mukaiyama, T.; Nakano, M.; Kikuchi, W.; Matsuo, J. -I. *Chem. Lett.* **2000**, 606.

[62] Müller, T.; Meyer, R.; Lennartz, D.; Siehl, H. -U. *Angew. Chem. Int. Ed. Engl.* **2000**, *39*, 17.

[63] Mukaiyama, T.; Nakano, M.; Kikuchi, W.; Matsuo, J. -I. *Chem. Lett.* **2000**, 1010.

[64] Nakano, M.; Matsuo, J. -I.; Mukaiyama, T. *Chem. Lett.* **2000**, 1352.

[65] Mukaiyama, T.; Yanagisawa, M.; Iida, D.; Hachiya, I. *Chem. Lett.* **2000**, 606.

[66] Fujiki, K.; Ikeda, S.; Kobayashi, H.; Mori, A.; Nagira, A.; Nie, J.; Sonoda, T.; Yagupolskii, Y. *Chem. Lett.* **2000**, 62.

[67] (a) Horton, A. D.; de With, J.; van der Linden, A. J.; van de Wig, H. *Organometallics*, **1996**, *15*, 2672. (b) Horton, A. D.; de With, J. *Organometallics*, **1997**, *16*, 5424.

[68] (a) Jacobsen, H.; Berke, H.; Döring, S.; Kehr, G.; Erker, G.; Fröhlich, R.; Meyer, O. *Organometallics*, **1999**, *18*, 1724. (b) Parks, D. J.; Piers, W. E.; Parvez, M.; Atencio, R.; Zaworotko, M. J. *Organometallics*, **1998**, *17*, 1369. (c) Chase, P. A.; Piers, W. E. unpublished results. (d) Amor, F.; Butt, A.; du Plooy, K. E.; Spaniol, T. P.; Okuda, J. *Organometallics*, **1998**, *17*, 5836.

[69] Reed, C. A. *Acc. Chem. Res.* **1998**, *31*, 325.

[70] Lambert, J. B.; Zhao, Y. *Angew. Chem. Int. Ed. Engl.* **1997**, *36*, 400.

[71] (a) Lambert, J.B.; McConnell, J. A.; Shulz Jr., W. J. J. *J. Am. Chem. Soc.* **1986**, *108*, 2482. (b) Lambert, J.B.; McConnell, J. A.; Schilf, W.; Shulz Jr., W. J. J. *J. Chem. Soc., Chem. Commun.* **1988**, 455.

[72] Prakash, G. K. S.; Keyanian, S.; Aniszfeld, R.; Heileger, L.; Olah, G. A.; Stevens, R.C.; Choi, H.K.; Bau, R. *J. Am. Chem. Soc.* **1987**, *109*, 5123.

[73] (a) Bahr, S. R.; Boudjouk, P. *J. Am. Chem. Soc.* **1993**, *115*, 4514. (b) see also Ichinohe, M.; Fukui, H.; Sekiguchi, A. *Chem. Lett.* **2000**, 600.

[74] Xie, Z.; Liston, D. J.; Jelinek, T.; Mitro, V.; Bau, R.; Reed, C. A. *J. Chem. Soc., Chem. Commun.* **1993**, 384.

[75] Kira, M.; Hino, T.; Sakurai, H. *Chem. Lett.* **1993**, 153.

[76] Olah, G. A.; Li, X. -Y.; Wang, Q.; Rasul, G.; Prakash, G. K. S. *J. Am. Chem. Soc.* **1995**, *117*, 8962.

[77] Arshadi, M.; Johnels, D.; Edlund, U.; Ottosson, C. -H.; Cremer, D. *J. Am. Chem. Soc.* **1996**, *118*, 5120.

[78] (a) Lambert, J. B.; Zhang, S, *Science*, **1993**, *260*, 1917. (b) Lambert, J. B.; Zhang, S.; Ciro, S. M. *Organometallics* **1994**, *13*, 2430.

[79] Reed, C. A.; Xie, Z.; Bau, R.; Benesi, A. *Science*, **1993**, *262*, 402.

[80] Schleyer, P. v. R.; Buzek, P.; Müller, T.; Apeliog, Y.; Siehl, H. U. *Angew. Chem. Int. Ed. Engl.* **1993**, *32*, 1471.

[81] Olah, G. A.; Rasul, G.; Li, X. -Y.; Buchholz, H. A.; Sanford, G.; Prakash, G. K. S. *Science*, **1994**, *263*, 983.

[82] Olsson, L.; Cremer, D. *Chem. Phys. Lett.* **1993**, *215*, 433.

[83] Pauling, L. *Science*, **1994**, *263*, 983.

[84] Xie, Z.; Manning, J.; Reed, R. W.; Mathur, R.; Boyd, P. D. W.; Benesi, A.; Reed, C. A. *J. Am. Chem. Soc.* **1996**, *118*, 2922.

[85] Mustanir, K. S.; Ohta, F.; Mishima, M. *Bull. Chem. Soc. Jpn.* **2000**, *73*, 1845.

[86] Emde, H.; Domsch, D.; Feger, H.; Frick, U.; Götz, A.; Hergott, H. H.; Hofmann, K.; Kober, W.; Krägeloh, K.; Oesterle, T.; Steppan, W.; West, W.; Simchen, G. *Synthesis*, **1982**, 1.

[87] Oishi, M. in Reference 1b, Vol. 1, p355.

[88] Bassindale, A. R.; Stout, T. *Tetrahedron Lett.* **1985**, *26*, 3403.

[89] Emde, H.; Götz, A.; Hofmann, K.; Simchen, G. *Justus Liebigs Ann. Chem.* **1981**, 1643.

[90] (a) Brook, M. A. *Silicon in Organic, Organometallic and Polymer Chemistry*, John Wiley & Sons, Toronto, 2000. (b) Bassindale, A. R.; Glynn, S. J.; Taylor, P. G. in *The Chemistry of Organic Silicon Compounds* John Wiley & Sons, Toronto, 1998, Vol.2 Part 1, p. 495.

[91] Hensen, K.; Zengerly, T.; Pickel, P.; Klebe, G. *Angew. Chem. Int. Ed. Engl.* **1983**, *22*, 725.

[92] Murata, S.; Suzuki, M.; Noyori, R. *J. Am. Chem. Soc.* **1980**, *102*, 3248.

[93] Kaur, H.; Kaur, G.; Trehan, S. *Synth. Commun.* **1996**, *26*, 1925.

[94] Tsunoda, T.; Suzuki, M.; Noyori, R. *Tetrahedron Lett.* **1979**, *20*, 4679.

[95] Murata, S.; Suzuki, M.; Noyori, R. *J. Am. Chem. Soc.* **1979**, *101*, 2738.

[96] Ishikawa, T.; Okano, M.; Aikawa, T.; Saito, S. *J. Org. Chem.* **2001**, *66*, 4635.

[97] Jahangir; MacLean, D. B.; Brook, M. A.; Holland, H. L. *J. Chem. Soc. Chem. Commun.* **1986**, 1608.

[98] (a) Jun, J. -G.; Ha, T. H.; Kim, D. -W. *Tetrahedron Lett.* **1994**, *35*, 1735. (b) Wang, M. W.; Chen, Y. J.; Wang, D. *Synthesis*, **2000**, 385.

[99] Carreira, E. M.; Singer, R. A. *Tetrahedron Lett.* **1994**, *35*, 4323.

[100] Hollis, T. K.; Bosnich, B. *J. Am. Chem. Soc.* **1995**, *117*, 4570.

[101] Denmark, S. E.; Chen, C. -T. *Tetrahedron Lett.* **1994**, *35*, 4327.

[102] Davis, A. P.; Jaspars, M. *Angew. Chem. Int. Ed. Engl.* **1992**, *31*, 470.

[103] (a) Tsunoda, T.; Suzuki, M.; Noyori, R. *Tetrahedron Lett.* **1980**, *21*, 71. (b) Sakurai, H.; Sasaki, K.; Hosomi, A. *Tetrahedron Lett.* **1981**, *22*, 745.

[104] Mekhalfia, A.; Markó, I. E. *Tetrahedron Lett.* **1991**, *32*, 4779.

[105] Davis, A. P.; Plunkett, S. J. *J. Chem. Soc. Chem. Commun.* **1995**, 2173.

[106] Davis, A. P.; Muir, J. E.; Plunkett, S. J. *Tetrahedron Lett.* **1996**, *37*, 9401.

[107] Johannsen, M.; Jørgensen, K. A.; Helmchen, G. *J. Am. Chem. Soc.* **1998**, *120*, 7637.

[108] Olah, G. A.; Rasul, G.; Prakash, G. K. S. *J. Am. Chem. Soc.* **1999**, *121*, 9615.

[109] (a) Oishi, M.; Aratake, S.; Yamamoto, H. *J. Am. Chem. Soc.* **1998**, *120*, 8271. (b) Oishi, M.; Yamamoto, H. *Macromolecules* **2001** *34*, 3512.

[110] Lambert, J. B.; Zhao, Y.; Wu. H. *J. Org. Chem.* **1999**, *64*, 2729.

[111] Lambert, J. B.; *Tetrahedron* **1990**, *46*, 2677.

[112] Olah, G. A.; Berrier, A. L.; Field, L. D.; Prakash, G. K. S. *J. Am. Chem. Soc.* **1999**, *64*, 2729.

[113] (a) Steinberger, H. -U.; Müller, T.; Auner, N.; Maerker, C.; Schleyer, P. v. R. *Angew. Chem. Int. Ed. Engl.* **1997**, *36*, 626. (b) Schuppan, J.; Herrschaft, B.; Müller *Organometallics*, **2001**, *20*, 4584.

[114] Sekiguchi, A.; Matsuno, T.; Ichinohe, M. *J. Am. Chem. Soc.* **2000**, *122*, 11250.

[115] Müller, T. *Angew. Chem. Int. Ed. Engl.* **2001**, *40*, 3033 and references therein.

[116] Okawara, R.; Rochow, E. G. *J. Am. Chem. Soc.* **1960**, *82*, 3285.

[117] Wada, M.; Okawara, R. *J. Organomet. Chem.* **1965**, *4*, 487.

[118] Clark, H. C.; O'Brien, R. J. *Inorg. Chem.* **1963**, *2*, 1020.

[119] Das, V. G. K. *J. Inorg. Nucl. Chem.* **1976**, 1241.

[120] (a) Davies, A. G.; Goddard, J. P.; Hursthouse, M. B.; Walker, N. P. C. *J. Chem. Soc., Chem. Commun.* **1983**, 597. (b) Davies, A. G.; Goddard, J. P.; Hursthouse, M. B.; Walker, N. P. C. *J. Chem. Soc. Dalton Trans.* **1986**, 1873.

[121] van Koten, G.; Jastrzebski, J. T. B. H.; Noltes, J. G.; Spek, A. L.; Schoone, J. C. *J. Organomet. Chem.* **1978**, *148*, 233.

[122] (a) Nugent, W. A.; McKinney, R. J.; Harlow, R. L *Organometallics*, **1984**, *3*, 1315. (b) McKinney, R. J.; Nugent, W. A. *Organometallics*, **1989**, *8*, 2871.

[123] (a) Lange, I.; Krahl, J.; Jones, P. G.; Blaschette, A. *J. Organomet. Chem.* **1994**, *474*, 97. (b) Hiemisch, O.; Henschel, D.; Blaschette, A.; Jones, P. G. *Z. Anorg. Allg. Chem.* **1999**, *625*, 1391.

[124] Sekiguchi reported the synthesis of $[^tBu_3Sn(CH_3CN)]^+[TFPB]^-$ from the reaction of $[Ph_3C]^+[TFPB]^-$ and $^tBu_3Sn\text{-}Sn^tBu_3$ in CH_3CN, see reference 114. No spectral data was included. Based on Boudjouk's and Cremer's studies, the characterization of this species as being a *mono*-acetonitrile complex is unlikely.

[125] Kira has reported the synthesis of $[Bu_3Sn(OEt_2)]^-[TFPB]^-$, but based on ^{119}Sn NMR shift of 164.6 ppm, this ion-pair is likely the *bis*-ether complex, see Kira, M.; Oyamada, T.; Sakurai, H. *J. Organomet. Chem.* **1994**, *471*, C4.

[126] The X-ray structure of Me_3SnCl:pyridine has been reported where the Cl^- and pyridine are situated co-axially, see Hulme, R. *J. Chem. Soc.* **1963**, 1524.

[127] For ^{119}Sn NMR studies on base complexes of triorganotin halides, see Colton, R.; Dakternieks, D. *Inorg. Chim. Acta* **1988**, *148*, 31.

[128] Clark, H. C.; O'Brien, R. J.; Trotter, J. *Proc. Chem. Soc.* **1963**, 85.

[129] (a) Clark, H. C.; O'Brien, R. J. *Inorg. Chem.* **1963**, *2*, 740. (b) Okawara, R.; Hathaway, B. J.; Webster, D. E. *Proc. Chem. Soc.* **1963**, 13.

[130] (a) Hathaway, J. B.; Webster, D. E. *Proc. Chem. Soc.* **1963**, 14. (b) Clark, H. C.; O'Brien, R. J. *Inorg. Chem.* **1963**, *2*, 1020.

[131] Edlund, U.; Arshadi, M.; Johnels, D. *J. Organomet. Chem.* **1993**, *456*, 57.

[132] (a) Holeček, J.; Nádvornik, M.; Handlíř, K.; Lyčka, A. *J. Organomet. Chem.* **1983**, *241*, 1476. (b) Nádvornik, M.; Holeček, J.; Handlíř, K.; Lyčka, A. *J. Organomet. Chem.* **1984**, *275*, 43.

[133] Arshadi, M.; Johnels, D.; Edlund, U. *Chem. Commun.* **1996**, 1279.

[134] Birchall, T.; Manivannan, V. *J. Chem. Soc., Dalton Trans.* **1985**, 2671.

[135] Lambert, J. B.; Zhao, Y.; Wu, H.; Tse, W. C.; Kuhlmann, B. *J. Am. Chem. Soc.* **1999**, *121*, 5001.

[136] Yang, X.; Stern, C. L.; Marks, T. J. *Organometallics*, **1991**, *10*, 840.

[137] Lambert, J. B.; Zhao, Y, Wu, H. *J. Org. Chem.* **1999**, *64*, 2729.

[138] Ishihara, K. in reference 1b, Vol. 1, p.395.

[139] Blunden, S. J.; Hill, R. *Inorg. Chim. Acta* **1984**, *87*, 83.

[140] (a) Otera, J.; Chen, J. *Synlett* **1996**, 321. (b) Chen, J.; Sakamoto, K.; Orita, A.; Otera, J. *Synlett* **1996**, 877. (c) Chen, J.; Otera, J. *Tetrahedron* **1997**, *54*, 14275. (d) Chen, J.; Otera, J. *Synlett*, **1997**, 29.

Chapter 2

$B(C_6F_5)_3$-Catalyzed Reactions of Hydrosilanes with Carbonyls and Alcohols

2.1 Hydrosilanes in Organic Synthesis

Table 1.1 Commercial Availability of Hydrosilanes.[2]

Silane	Cost ($/mmol)	Cost of Si-Cl
$PhMe_2SiH$	0.33	0.65
Ph_2MeSiH	0.35	0.42
Me_2ClSiH	0.077	0.0055
Ph_3SiH	0.94	0.81
$^tBuMe_2SiH$	0.94	0.41
$^iPr_3SiH$	0.36	1.02
Ph_2SiH_2	0.73	0.13
$PhSiH_3$	0.74	0.19
Et_3SiH	0.11	0.82

Hydrosilanes, R_3Si-H, are extremely useful reagents in organic synthesis.[1] A number of silanes are commercially available, oftentimes cheaper than the corresponding chlorosilane, Table 2.1.[2] Much of the synthetic utility of silanes in organic synthesis stems from their ability to participate in the following three general reaction modes: (1) as reducing agents especially of carbonyl, alkene and alkyne functions, Scheme 2.1a; (2) as co-reactants in dehydrocoupling reactions with a variety of acidic partners, Scheme 2.1b; and (3) as co-reactants in metathesis reactions with another main group or transition metal compounds M-X, Scheme 2.1c. These reactivity patterns all originate from the polar nature of the $Si^{\delta+}$-$H^{\delta-}$ bond which imparts modest hydridicity. Based on the Allred-Rochow scale, Si has an electronegativity of 1.74 compared to H which has value of 2.20.[3]

Scheme 2.1: Reactivity of Hydrosilanes.

(a) Hydrosilation of Unsaturated Functional Groups.

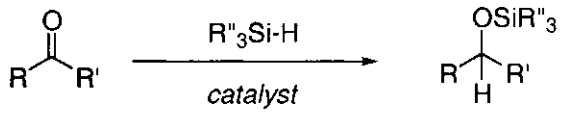

(b) Dehydrocoupling with Acidic Functional Groups.

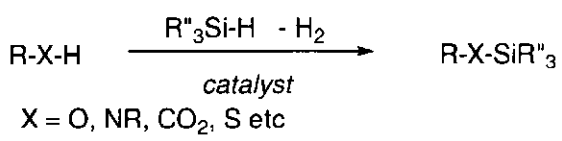

(c) α-Bond Metathesis with Organometallic Compounds.

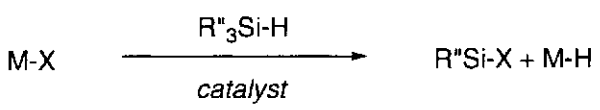

2.1.1 Reduction of Aldehydes/Ketones

Although not as popular as methods using alkali main group hydrides such as $LiAlH_4$ or $NaBH_4$, hydrosilanes have been applied effectively in the reduction of carbonyls, particularly ketones and aldehydes.[4,5] In contrast to other methods that typically produce the free alcohol after work-up procedures, hydrosilation chemistry often leads beneficially to stable silyl ether products (*i.e.* protected alcohols). If necessary, the silyl ether can be readily cleaved to give the alcohol. Brønsted acid,[6] Lewis acid and transition metal catalysts have been employed to promote hydrosilation reactions. Fluoride and other anions promote hydrosilation reactions as well.[7,8]

Brønsted Acid Catalysis: Brønsted acid catalysis or ionic hydrogenation has long been used in conjunction with hydrosilanes to effect carbonyl reduction.[9] The most common acids used are trifluoroacetic acid (TFA) and sulfuric acid. Protonation of the carbonyl

gives a carboxylium species susceptible to attack by the silane. Disadvantages with this approach are (1) that large excesses of strong acid are required (often as solvent) (2) that acid sensitive groups are therefore incompatible and (3) that side reactions often occur.

Lewis Acid Catalysis: Common Lewis acid catalysts such as $BF_3{\cdot}OEt_2$,[10] BF_3,[11] and TMSOTf[12] have been used in conjunction with hydrosilanes to effect reduction of carbonyls and/or acetals to alcohols or silyl ether products. The mechanistic consensus

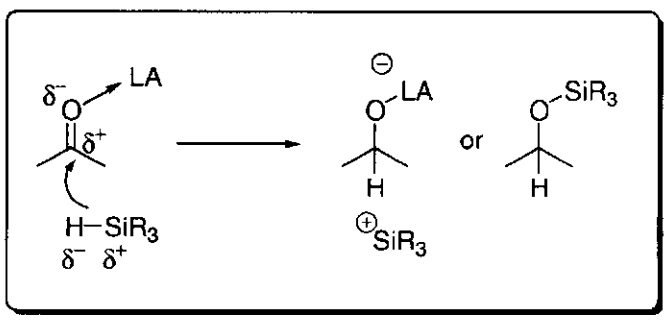

attributes a carbonyl-activating role to the Lewis acid. The polarized C=O bond is thus rendered more electrophilic to the relatively non-nucleophilic hydrosilane. In many cases employing main group Lewis acids, greater than catalytic quantities are required to effect the reduction since halosilyl byproducts are often formed, destroying the initial Lewis acid. For example, Doyle found that 1/3 equivalents of $BF_3{\cdot}OEt_2$ was required since the main products formed were $ROBF_2$ and R'_3SiF.[10] Other side reactions such as deoxygenation (over-reduction) or coupling reactions can compete in certain cases as well although methods have been developed to suppress or favor these secondary reactions. Fry and co-workers used gaseous BF_3 with excess Et_3SiH to effect complete reduction of ketones and aldehydes to alkanes.[11] In 1979, Noyori circumvented many of these problems using TMSOTf to catalyze the reduction of dimethyl acetals to provide methyl ethers in high yields.[12] Mukaiyama has also reported similar success using trityl perchlorate as a catalyst in tandem with silanes toward the reduction of carbonyls.[13]

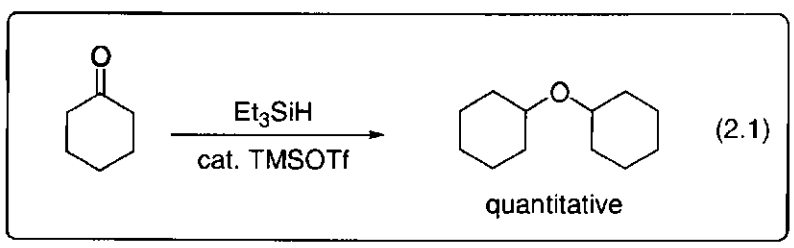

Olah has reported that TMSOTf and TMSI catalyze the reductive coupling of carbonyl groups in the presence of Et_3SiH, equation 2.1.[14] Similar to mechanisms proposed by Doyle for acid catalyzed reductive coupling, silylcarboxonium and silyloxonium intermediates are presumably involved, Scheme 2.2. Selective cross-coupling reactions between carbonyls and silyl ethers were also achieved using TMSI. Subsequently, Komatsu and co-workers reported that $BiBr_3$ (1-3 mol%) catalyzed reductive coupling reactions; the methodology was applied to a novel crownophane synthesis.[15]

Transition Metal Catalysis:

Scheme 2.2: General Mechanisms for Metal-Catalyzed Hydrosilation of Carbonyl Compounds

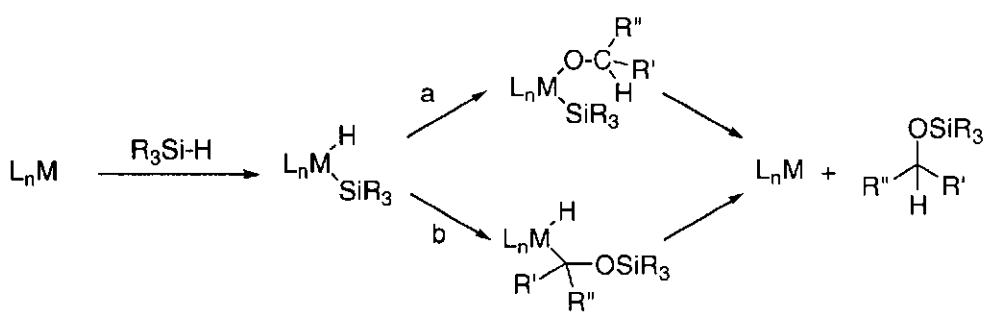

Although some transition metal catalysis undoubtedly involves Lewis acid activation of the carbonyl similar to the examples above, most transition metals owe their success as hydrosilation catalysts to their ability to oxidatively add Si-H bonds, Scheme

2.2. Insertion of the C=O bond into either the M-H (path a) or M-Si (path b) bond can then occur followed by reductive elimination of silyl ether (O-Si or C-H) thus regenerating the active catalyst. Since 1972 when Ojima used Wilkinson's catalyst, $RhCl(PPh_3)_3$ to hydrosilate aldehydes and ketones, several other late transition metal catalysts have been shown to catalyze this important transformation.[4] Asymmetric hydrosilations can be accomplished using chiral ligands.[16,17] Examples of early transtion metal catalyzed hydrosilation have also recently been reported.[18]

Anionic Activation: Anions such as fluoride and alkoxides can also catalyze

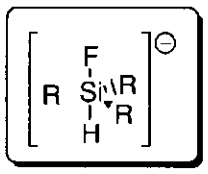

hydrosilation chemistry by forming activated pentacoordinate silane intermediates.[19] Hypercoordination renders the Si-H bond more hydridic and thus more reactive.

2.1.2 1,4-Hydrosilation of α,β-Unsaturated Ketones and Aldehydes

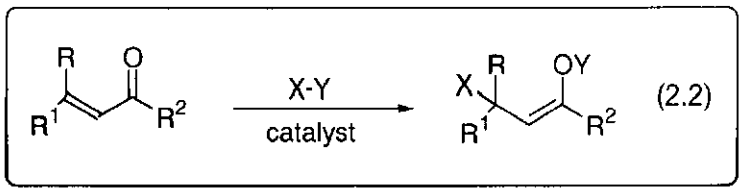

(2.2)

Many methods for the selective addition of a variety of nucleophiles, X-Y, to the β-carbon (4-position) of conjugated enones and enals have been developed including methods for hydride delivery (X = H), equation 2.2.[20] Common methods to effect conjugate reduction include dissolving metal reductions, reductions with low valent transition metals, electrochemical reduction, radical reactions with tin hydrides and the use of boron and aluminum hydrides. The selectivity of 1,4- versus 1,2-reduction can be highly dependent on the reaction conditions and the enone/enal substrate.

Hydrosilanes have also been used in conjugate reduction chemistry. For example, selective 1,4-addition can be achieved under ionic hydrogenation conditions using CF_3CO_2H in conjunction with silanes such as Et_3SiH.[6] Lewis acid activation with $TiCl_4$ for the conjugate reduction of enones and dienones has been reported.[21] Other transition metal catalyst precursors that have been used include $(PPh_3)_3RhCl$,[22] $RhCl_3$,[23] $(PPh_3)_4RhH$,[24] and Karstedt's Pt catalyst.[25]

Lipshutz and co-wokers have used Stryker's reagent, $[CuH(PPh_3)]_6$, with hydrosilanes such as $PhMe_2SiH$ to effect the the selective reduction of a number of enones to the corresponding silyl enol ethers.[26] The silyl enol ethers could then be reacted *in situ* via addition of an aldehyde and Lewis acid to give the aldol products, equation 2.3. The reactivity of silyl enol ethers with electrophiles has been extensively developed leading to a number of important C-C and C-X bond-forming reactions.[27]

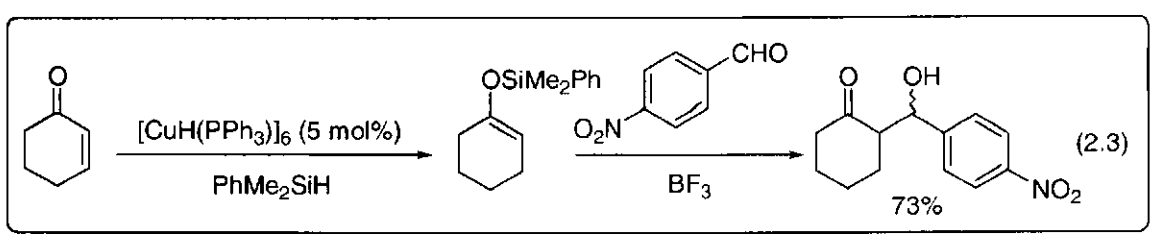

2.1.3 Other Reduction Chemistry

Alkenes and alkynes can also be hydrosilated providing alkyl and vinyl silanes respectively.[28] Although Lewis acid catalysis[29,30,31,32,33] and anionic activation have both been demonstrated, transition metal catalysis is much more common.[34] Hydrosilation of enamines[35] and enamides[36] have both been reported. Cutler has shown that the acetyl group of manganese and iron acetyl compounds can be hydrosilated by various monohydrosilanes.[37] Carbon monoxide has been hydrosilated in the presence of Rh[38] and

Ru[39] catalysts. Hydrosilanes have also found use in the silylcarbonylation reaction of epoxides catalyzed by $Co_2(CO)_8$.[40]

2.1.4 Dehydrocoupling Chemistry

Metal-catalyzed dehydrocoupling of silanes leading to polysilanes has become an important method in polymer synthesis.[41] In spite of the propensity of silanes to react with themselves, synthetically useful dehydrocoupling reactions of silanes with suitable protic partners have been successfully applied. Several protocols using Lewis acid, transition metal and fluoride catalysts have been reported for the silation of H_2O,[42] alcohols,[43] carboxylic acids,[44] amines,[45] alkenes[46] and alkynes.[47] One of the key advantages to this dehydrogenative strategy is that the sole byproduct is H_2; protocols using silyl chlorides and triflates require a stoichiometric equivalent of a base to neutralize HCl or HOTf that is formed.[48] This section will focus on synthetic and mechanistic aspects of alcohol silation.

A number of transition metal complexes serve as precatalysts for alcohol silation. These include early transition metal catalyst systems such as Cp_2TiPh_2[49] and $Cp_2TiCl_2/^nBuLi$.[50] However, middle and late transition metal catalysts are much more common including $[Ph_3PCuH]_6$,[51] $Re_2(CO)_{10}$,[52] $Rh_2(pfb)_4$,[53] $[IrH_2(thf)_2(PPh_3)_2]SbF_6$,[54] $Ru(PMe_3)_2(CO)_2Cl_2$,[55] $Co_2(CO)_8$,[56] $(CO)_4MnBr$,[57] and $(PMe_3)_4RuH_2$.[58]

Anionic activation of hydrosilanes has also been applied to alcohol silation. For example, Corriu has shown that KF and CsF promote silane alcoholysis with primary and secondary silanes.[59] As a homogeneous alternative, TBAF was shown to catalyze (0.02 eq.) the silation of a number of alcohols using hydrosilanes such as $^tBuMe_2SiH$, Et_3SiH

and $PhMe_2SiH$ and disilanes leading to high yields of silyl ethers.[60] The combination of KOH and 18-crown-6 also catalyzes the silation of alcohols with $PhSiH_3$.[61]

Main group Lewis acid catalysts for alcohol silation are much less common. However, Fry and co-workers have used gaseous BF_3 and excess Et_3SiH to effect the deoxygenative transformation, alcohol to alkane.[62] The use of bifunctional silanes ($R_2Si(H)$-linker-$Si(H)R_2$) in tandem with H_2O or diols has been adapted to the synthesis of siloxane polymers. For example, a variety of late transition metal precatalysts (*eg.* $Pd_2(dba)_3$, Pd/C, $Pt(PPh_3)_4$, $RhCl(PPh_3)_3$) were used to form polymers of general form **Y** via a double silation reaction of H_2O.[63] The same authors also reacted diols with 1,4-bis(dimethylsilyl)benzene.[64] Other applications of this technology have been made in the controlled preparation of complex silsequioxane derivatives.[65]

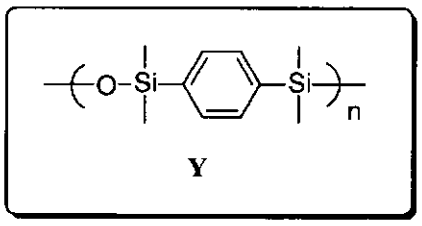

Y

Scheme 2.3: General Mechanism for Metal-Catalyzed Silation of Alcohols.

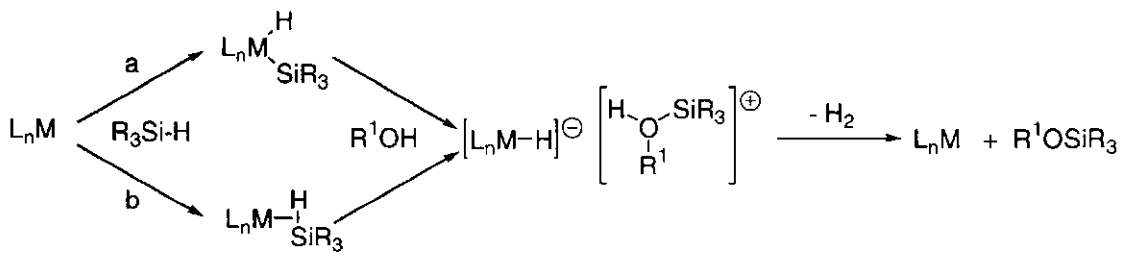

Two general mechanistic pathways can be considered for metal-catalyzed alcohol silation, Scheme 2.3. Mechanistic pathways (a) and (b) both involve activation of the silane by the metal. In pathway (a), full oxidative addition of the Si-H bond by the metal center occurs. In pathway (b), the Si-H bond coordinates to the electrophilic metal (σ-complex formation) activating the silicon to nucleophilic attack by the alcohol. This type

of activation has been proposed to occur with the precatalysts $[IrH_2(thf)_2(PPh_3)_2]SbF_6$, $Rh_2(pfb)_4$ and $Re_2(CO)_{10}$. These two mechanisms share intermediates of the form $[L_nM\text{-}H]^-[RO(H)SiR_3]^+$ in common thus making it potentially difficult to distinguish between

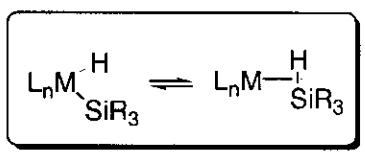

the two. Indeed, as with the dihydrogen ligand, subtle factors can determine whether oxidative addition or σ-complex formation occurs with hydrosilanes and a particular metal complex and the two extremes can be in rapid equilibrium.[66] Often, inverse rate dependences on [ROH] have been observed which has been interpreted to result from competitive coordination of the alcohol at the metal preventing silane activation by the metal center.

A third mechanistic pathway involves the formation of silyl metal species, which react via σ-bond metathesis with alcohols to provide a silyl ether and a metal hydride. The metal hydride then reacts with hydrosilane to regenerate the active silyl metal species and H_2 (either via σ-bond metathesis or oxidative addition/reductive elimination).

A fourth type of mechanism that has not been widely proposed involves coordination of the alcohol to the Lewis acidic center followed by reaction with silane. Coordination should lead to an increase in the Brønsted acidity of the alcohol function potentially enabling deprotonation by mildly basic hydrosilanes.

2.2 $B(C_6F_5)_3$-Catalyzed Hydrosilation of Carbonyl Functions

In 1996, Parks and Piers reported that $B(C_6F_5)_3$ catalyzes the hydrosilation of various carbonyl functional groups.[67] A mechanistic proposal was advanced for the first stage of the reaction, the Lewis acid activation step; however, the second stage, hydride delivery, was not studied. Since designing an asymmetric hydrosilation reaction was an important ultimate objective of the research programme, understanding the details of this

second stage of the reaction was considered to be of fundamental importance. In Section 2.2.1, the majority of the results presented are those of Dr. Dan Parks. Sections 2.2.2 and 2.2.3 are new results most of which have been published.[68]

2.2.1 Lewis Acid Activation

Scheme 2.4: Proposed Mechanism for the Lewis Acid Activation Step in the Hydrosilation of Carbonyl Compounds.

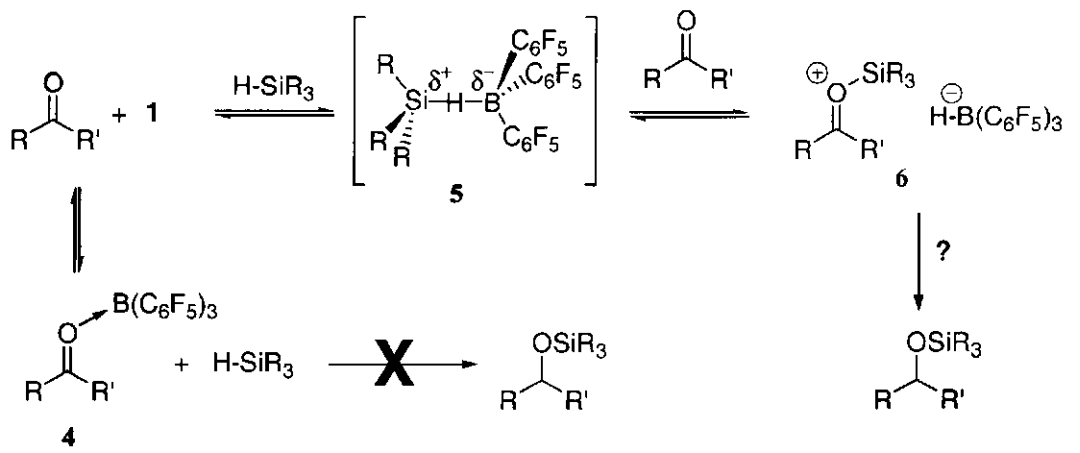

An unusual mechanism has been proposed for the hydrosilation of carbonyls in which **1** activates the silane (as complex **5**) to nucleophilic attack by the carbonyl, Scheme 2.4. A silylcarboxonium species with a hydridoborate counterion, **6**, is proposed as an intermediate although convincing spectroscopic evidence was not obtained.[69] This unconventional mechanism was proposed based on a number of observations.

First, it was found that the rate of hydrosilation was inversely dependent on the concentration of carbonyl. An inverse rate dependence would not be expected for simple hydride addition to a carbonyl complexed by **1**. Secondly, the following order of reactivity of different carbonyl functions was found, ester > ketone > aldehyde. This trend was opposite to the order of Lewis basicity toward **1** found for these groups.

Parks has shown however that **1** does form stable adducts, **4**, with a variety of carbonyls.[70] When hydrosilation reactions were monitored by ^{1}H and ^{19}F NMR under conditions where reaction does ensue, the only borane-containing species observed were the carbonyl adducts of **1**. Thus, in order for hydrosilation to take place, the carbonyl borane adduct, **4**, must dissociate freeing **1** to activate silane.

Although direct observation of silane coordinated to **1** has not been made, experiments have confirmed that interaction of these two species can occur. First, ^{1}H NMR analysis of a mixture of Et_3SiH and catalytic **1** indicates that degenerate scrambling of Si-H bonds occurs. Initially, ^{1}H NMR analyis shows no change in the Et_3SiH signals; however, over time, the septet observed for the Si-H hydrogen becomes a broad singlet and the CH_2 resonances from the ethyl groups lose their coupling to the silane hydrogen. This behaviour has been attributed to a rapid scrambling process involving activation of a Si-H bond by **1** to hydride attack from another silane, Scheme 2.5. Scrambling between Ph_3SiD and Et_3SiH to give Ph_3SiH and Et_3SiD was also observed. Furthermore, when Et_3SiH and $B(C_6F_5)_3$ are heated for several days, formation of $H\text{-}B(C_6F_5)_2$ and $Et_3SiC_6F_5$ occurs.

Scheme 2.5: Proposed Mechanism for Silane Scrambling.

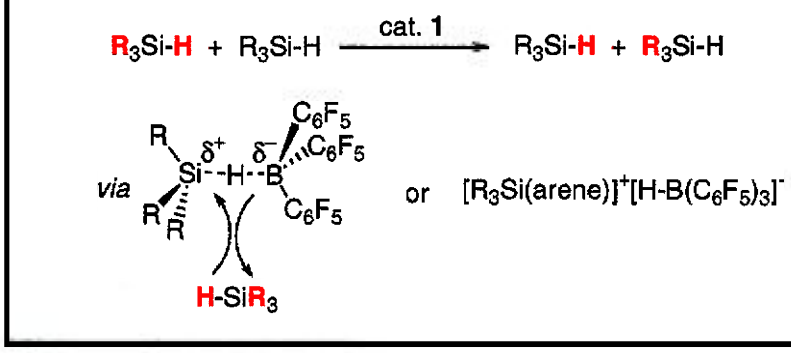

2.2.2 Hydride Delivery

Although the Parks' experiments clearly implicate silylcarboxonium intermediates, **6**, specific details of the C-H bond formation step were not established. In particular, it was unclear whether hydride delivery occurred from the displaced hydridoborate anion or an additional equivalent of silane. In the former case, **1** would be directly regenerated which could activate an additional equivalent of silane to carbonyl attack, Scheme 2.6, path a. By this route, the hydride and trialkylsilyl group from the same molecule of silane end up in the same product. Alternatively, silane delivery could lead to regeneration of **5** which could perpetuate catalysis by coordination of carbonyl to the silicon to once again give **6**, Scheme 2.6, path b. Collapse of **5** to silane and **1** could also occur at this stage, necessitating activation of another equivalent of silane by **1**. For both of these versions of path b, the hydride and trialkylsilyl group from two independent molecules of silane end up in the product.

Scheme 2.6: Mechanistic Possibilities for Hydride Delivery.

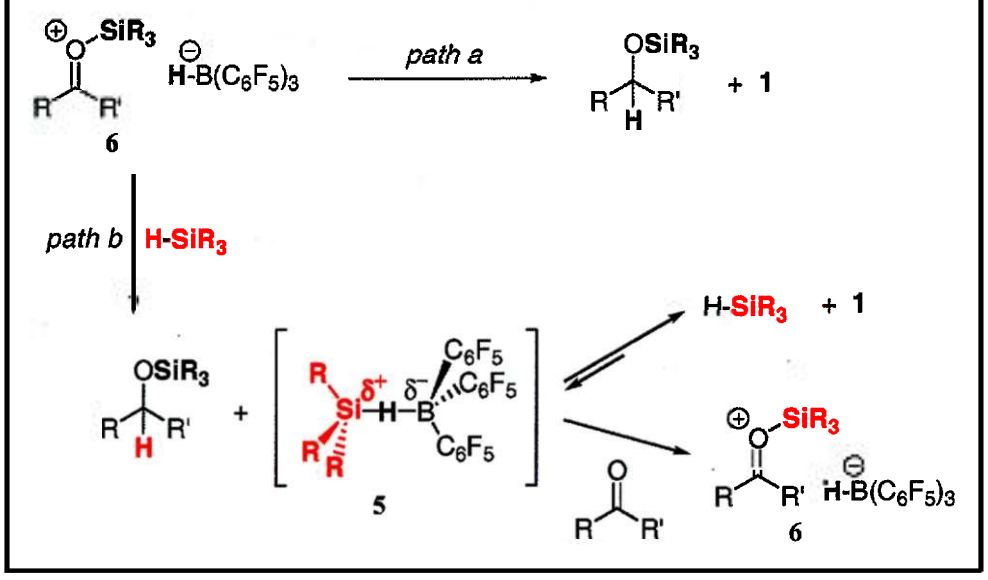

To determine the species responsible for hydride delivery ($[H\text{-}B(C_6F_5)_3]^-$ vs H-SiR_3), two cross-over experiments were designed and carried out, Scheme 2.7. First, a 1:1 mixture of Ph_3SiD and (*para*-tolyl)$_3$SiH were added to excess acetophenone and catalytic **1**. Product analysis of the silyl ethers showed that only **7** and **8** were formed. These findings support pathway (a) being responsible for hydride delivery; that is hydridoborate delivers the hydride to the silylcarboxonium cation. If hydride is delivered via path (b), cross-over products **9** and **10** would be formed since little discrimination between Ph_3Si-D and (*para*-tolyl)$_3$SiH should occur during C-H bond formation. The experiment was carried out using excess acetophenone to minimize scrambling between the silanes since scrambling occurs via the same intermediate, **5**.

Scheme 2.7: Cross-over Experiments to Determine Nature of Hydride Delivery.

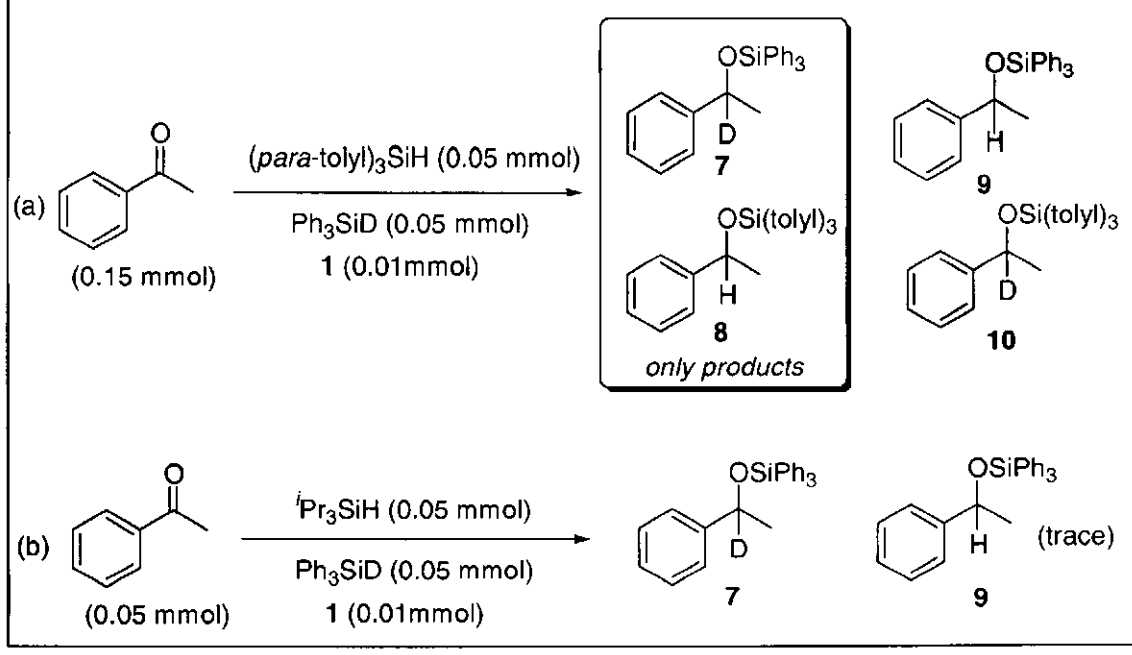

Secondly, the hydrosilation of acetophenone was carried out using Ph_3SiD and $^iPr_3SiH$. $^iPr_3SiH$ was shown to be incapable of hydrosilating benzaldehyde in the presence of **1** presumably because borane activation of silane to a silylcarboxonium

intermediate is sterically disfavored. However, $^{i}Pr_3SiH$ has been shown to possess superior reducing ability compared to Ph_3SiH in additions to diarylcarbenium ions.[71] Furthermore, a tri-(isopropyl)silylcarboxonium intermediate, **11**, was shown to be reactive to hydride attack by reacting $^{i}Pr_3SiH$ with acetophenone catalyzed by $[^{i}Pr_3Si]^{+}[B(C_6F_5)_4]^{-}$, Scheme 2.8.

Scheme 2.8: $^{i}Pr_3SiH$ as a Hydride Delivery Agent.

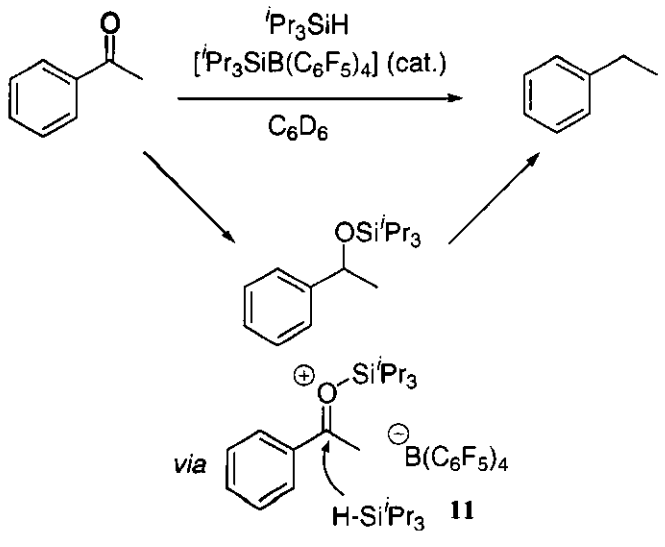

Since Ph_3SiH readily hydrosilates benzaldehyde, it was reasoned that initiation would necessarilly occur via activation of Ph_3SiD by **1** leading to silylcarboxonium **12'**. Intermediate **13** could not be formed directly by activation of $^{i}Pr_3SiH$ by **1**. At this stage hydride delivery to **12'** could occur either by Ph_3SiD (leading to **7**) or by the stronger reducing agent $^{i}Pr_3SiH$ (leading to **9**). Silyl ether **7** was the predominant compound formed under these conditions implying that silane delivery was not occurring since

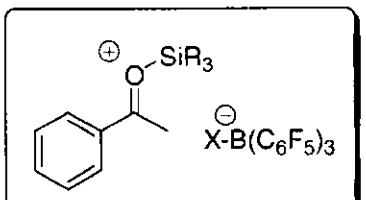

12 R = Ph, X = H
12' R = Ph, X = D
13 R = ^{i}Pr, X = H
13' R = ^{i}Pr, X = D

$^{i}Pr_3SiH$ is the superior nucleophile.[i]

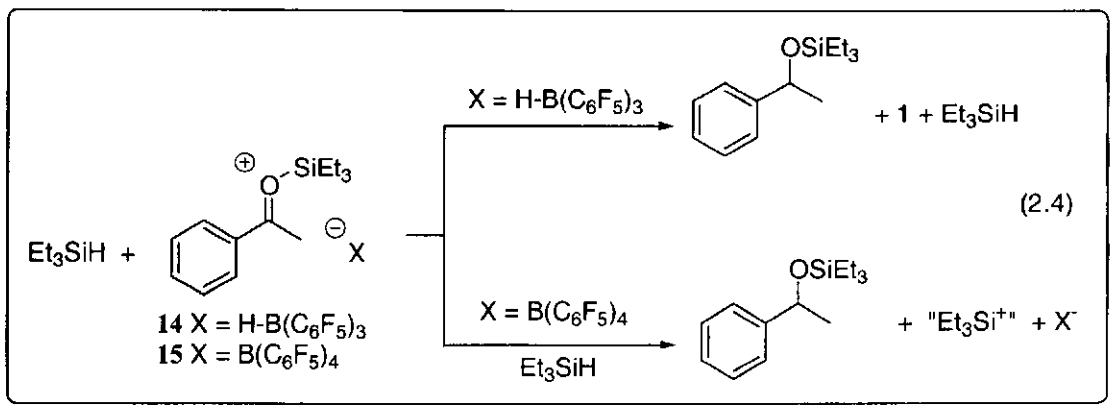

(2.4)

Other observations that discount silane delivery of hydride have been made by studying the reactivity of Lambert's $[Et_3Si(arene)]^+[B(C_6F_5)_4]^-$ reagent, **2**, as a catalyst for the hydrosilation. The primary difference between using this reagent versus **1** as the catalyst would be the nature of the counterion, both reactions proceeding through silylcarboxonium intermediates, **14** and **15** respectively, equation 2.4. With Lambert's reagent, hydridoborate delivery is not an option; C-H bond formation must proceed through silane delivery.

Ion-pair **2** was indeed shown to catalyze the hydrosilation of acetophenone; however, subsequent deoxygenation occurs leading to ethylbenzene, $Et_3SiOSiEt_3$ and unreacted acetophenone presumably via the intermediacy of **16**. A clear difference in reactivity is thus observed between **1** and **2**. Although **1** has been shown to catalyze reductive deoxygenation reactions with excess silane, controlled hydrosilation to silyl ether takes place with one equivalent of silane. The observation of deoxygenation reactions is reminiscent of Olah's use of TMSOTf to catalyze hydrosilation reactions. These results indicate that under borane catalysis, the ability of the hydridoborate anion

[i] Trace quantities of **5** were observed but test studies show they originate from trace amounts of Ph_3SiH present in the Ph_3SiD sample used.

to deliver hydride prevents further reaction from occurring. **1** is regenerated which then reenters the catalytic cycle; the initial silyl ether product is unlikely to coordinate **1** strongly. A silane delivery pathway (as for $[Et_3Si(arene)]^+[B(C_6F_5)_4]^-$ or TMSOTf) generates a new highly reactive trialkylsilylium species which is immediately sequestered by the proximal silyloxy group as in **16**. This species is highly susceptible to reductive cleavage of the C-O bond consuming a second equivalent of silane.

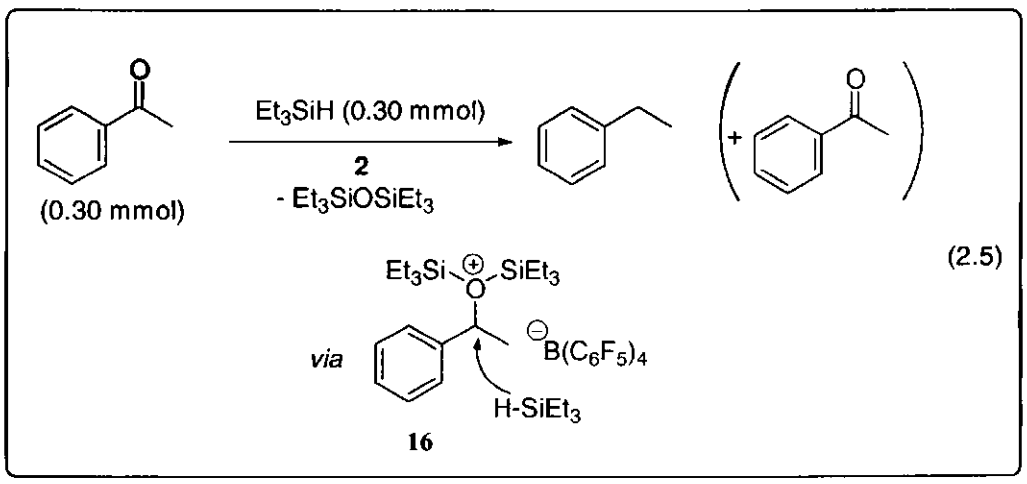

Interestingly, using the diborane **17**[72] as a catalyst for the reaction of acetophenone and one equivalent of Et_3SiH also leads to deoxygenation. Hence, this catalyst is more similar in its reactivity to **2** rather than to **1** consistent with the greater hydride affinity of **17** compared to **1**. In fact, it has been shown that **17** does abstract hydride from $PhMe_2SiH$ in the presence of $PhNMe_2$ where the hydride is bridged tightly between the two boron atoms.[73] Thus as a catalyst for hydrosilation, hydride abstraction would lead to a new unreactive anion which does not subsequently participate in C-H bond formation. Hydride delivery occurs from the silane, prompting the deoxygenative pathway to occur.

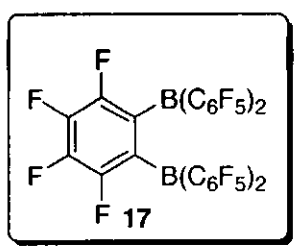

In conclusion then, the hydridoborate counterion is responsible for hydride delivery to acetophenone activated by a silylium cation. Of course, this mechanism could vary depending on the silane, carbonyl substrate, solvent *etc.* For example, in certain cases, $B(C_6F_5)_3$ could be responsible for Lewis acid activation of the carbonyl as is observed for the initial stages of allylstannation (see Chapter 4). On the other hand, this type of mechanism could take place in hydrosilation reactions of carbonyls catalyzed by other Lewis acids.

2.2.3 1,4-Hydrosilation of Enones

Borane **1** is also an effective catalyst for carrying out the synthetically useful 1,4-hydrosilation of α,β-unsaturated ketones, Table 2.2. In general, these exothermic reactions are high yielding, requiring small catalyst loadings and purification is convenient consisting simply of passing the reaction mixtures through silica using Et_3N/hexanes mixtures. In cases where high yields of the 1,4-addition products are isolated, GC-MS analysis does indicate that small amounts of the 1,2-addition product are formed. Reactions of 3-methyl-2-cyclopentenone and methyl vinyl ketone lead to complex reaction mixtures possibly through oligomerization reactions. Some oligomerization/polymerization likely occurs in all cases; interestingly for 2-cyclopentenone, clean 1,4-hydrosilation occurs at room temperature whereas an NMR tube experiment at low temperature led to formation of a complex reaction mixture.

Table 2.2: $B(C_6F_5)_3$-Catalyzed Hydrosilation of Enones.

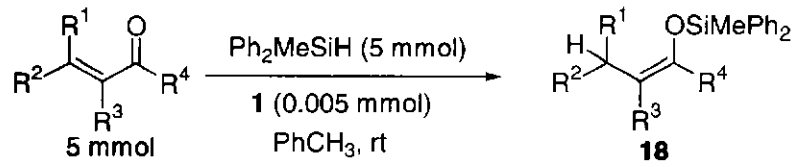

Entry	enone/enal	Products	Isolated Yield
1	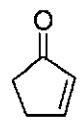	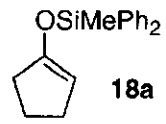 **18a**	81%
2	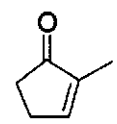	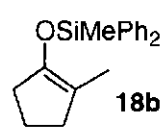 **18b**	90%
3	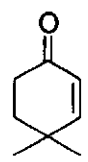	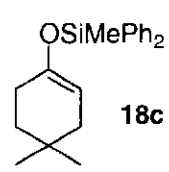 **18c**	96%
4	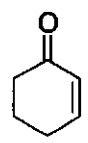	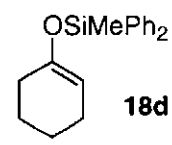 **18d**	82%
5	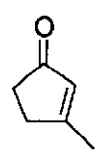	complex reaction mixture	---
6	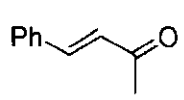	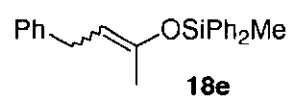 **18e** 3:2 *E*:*Z*	85%
7	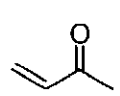	complex reaction mixture	---

Reaction of methyl vinyl ketone leads to a complex mixture of products presumably through oligomerization reactions.[74] Not shown, an enal, *trans*-cinnamaldehyde, undergoes predominant 1,2-hydrosilation leading to PhCH=CH-

$CH_2OSiMePh_2$, **19**; only small amounts of 1,4-hydrosilation are indicated by GC-MS analysis of the reaction mixtures. A variety of other commercially available silanes can be employed, although $^iPr_3SiH$ does not react, Table 2.3.

Table 2.3: $B(C_6F_5)_3$-Catalyzed Hydrosilation of 4,4-Dimethyl-2-cyclohexen-1-one.

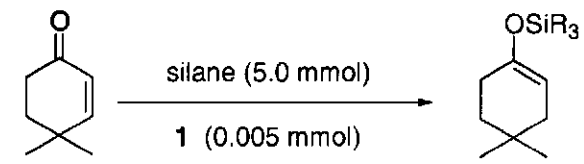

5.0 mmol

Entry	silane	Product	Isolated Yield
1	Ph_2MeSiH	**18c**	96%
2	$^tBuMe_2SiH$	**18f**	86%
3	$PhMe_2SiH$	**18g**	88%
4	Et_3SiH	**18h**	91%
5	Ph_3SiH	**18i**	86%
6	$^iPr_3SiH$	---	---

Although there exist many methods to effect the conjugate addition of hydride to enones, this method is attractive for a number of reasons. Small catalyst loadings are used (1%) and the products are readily purified by column chromatography using Et_3N/hexanes as eluent or by distillation. Unlike many other 1,4-reduction protocols, the products formed retain the "enolate" functionality in the useful form of a silyl enol ether. As mentioned in section 2.1.2, this functional group is extremely important in organic synthesis especially for C-C bond formation reactions such as aldol reactions. In fact,

Yamamoto has reported that **1** can be used to catalyze aldol reactions of silyl enol ethers with aldehydes and imines.[75]

The potential then exists for developing tandem one-pot 1,4-hydrosilation/aldol or other alkylation reaction protocols where both reactions are catalyzed by **1**. Alternatively, the silyl enol ether products can be readily hydrolyzed leading to the saturated ketone derivatives providing another means for the selective reduction of the "ene" portion of enones.

Scheme 2.9: Proposed Mechanism for 1,4-Hydrosilation.

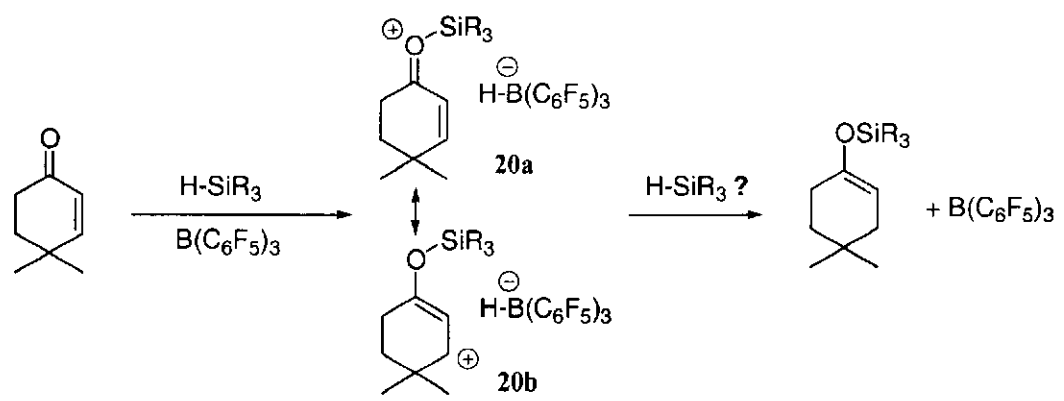

Extensive mechanistic studies have not been carried out although it seems likely that activation of silane by **1** leading to silylcarboxonium intermediates, **20a/b** is important as it is for saturated ketones, Scheme 2.9. ^{19}F NMR analysis of a mixture of 4,4-dimethyl-2-cyclohexen-1-one, $B(C_6F_5)_3$ and $PhMe_2SiH$ at -40 °C (a temperature at which reaction is occurring) reveals only the presence of the borane/ketone adduct, **21**. No evidence for formation of a hydridoborate anion is obtained. Whether silane addition or hydridoborate addition to the silylcarboxonium intermediate occurs awaits further cross-over studies similar to those carried out for acetophenone.

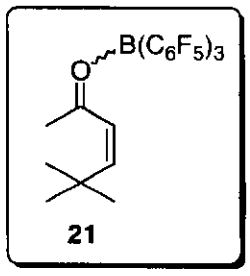

21

2.2.4 $B(C_6F_5)_3$-Catalyzed Hydrosilation of Silyl Enol Ethers

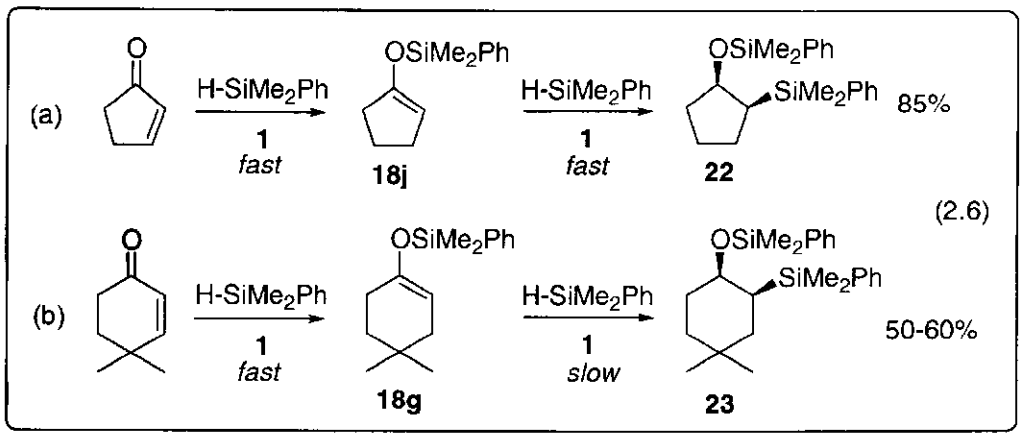

(2.6)

The silyl enol ethers **18j** and **18g** can be elaborated further through a second stereoselective hydrosilation reaction, equation 2.6. The resulting β-siloxy alkylsilanes **22** and **23** were purified by column chromatography. The siloxy and silyl groups in **22** are tentatively assigned a *cis*-disposition by nOe experiments. Irradiation of H_a leads to enhancement in H_b and *vice versa*. A decoupling experiment has shown the coupling constant between H_a and H_b to be 5.5 Hz. This value is most consistent with a *cis*-orientation; vicinal *trans*-hydrogens on a cyclopentane ring are expected to experience little coupling compared to 8 Hz coupling expected for vicinal *cis*-hydrogens.[76] Fleming has prepared *trans*-2-(dimethylphenylsilyl)cyclopentanol ($J(H_a/H_b)$ = 4.8 Hz).[77] Complete hydrosilation of silyl enol ether **18g** to **23** requires > 40 hours at room temperature whereas an NMR tube experiment has shown that hydrosilation of **18j** occurs rapidly even at -70 °C. **23** could not be purified completely from $PhMe_2SiOSiMe_2Ph$ and thus the yield of **23** is estimated as 50-60%. This byproduct presumably forms from **23**

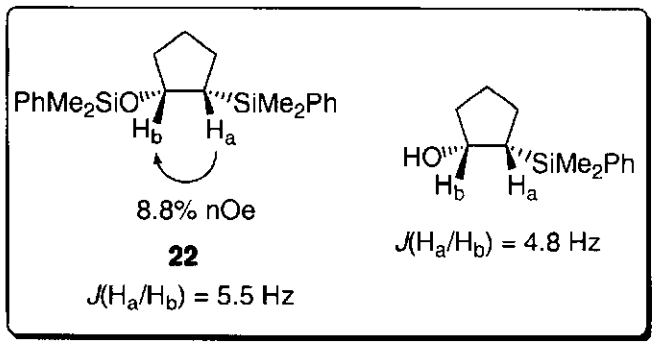

during the purification through silica gel. No attempts at optimization have yet been made. Similar NMR characterization supports a *cis*-substituted cyclohexane (see experimental section).

Surprisingly, hydrosilation of silyl enol ethers has not been reported. Larson and co-workers however have shown that hydroboration of silyl enol ethers is possible but this reaction did not require Lewis acid actvation.[78] For hydrosilation, one possible mechanism involves borane activation of silane followed by reaction with the silyl enol ether, Scheme 2.10. A silylcarboxonium intermediate **24** is predicted which possesses a trialkylsilyl group β- to the carbocationic center.

Scheme 2.10: Proposed Mechanism for Hydrosilation of Silyl Enol Ether.

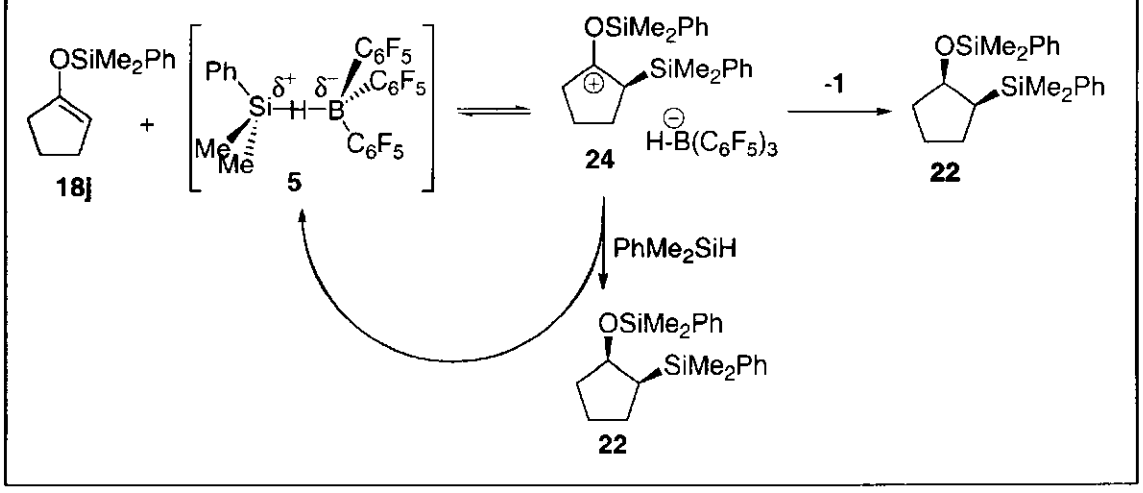

Observation of intermediate **24** by ^{19}F NMR analysis was not possible since

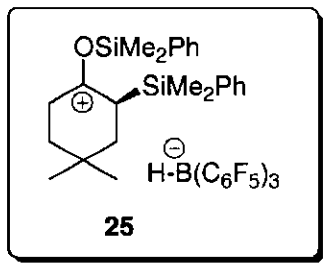

reaction of $PhMe_2SiH$ and silyl enol ether **18j** occurs instantaneously even at -70 °C. However, observation of an ion-pair, **25**, formed by mixing silyl enol ether **18g**, $PhMe_2SiH$ and **1** was possible. 4,4-dimethyl-2-cyclohexen-1-one was mixed with approximately 20% **1** in C_7D_8 in an NMR tube at -40 °C, Figure 2.1a. One

equivalent of $PhMe_2SiH$ was added leading to the silyl enol ether **18g**. At -40 °C, ^1H and ^{19}F NMR analysis revealed that an adduct was not formed between the silyl enol ether and **1**, Figure 2.1b.

Figure 2.1: 282 MHz ^{19}F NMR Spectra at -40 °C showing (a) enone + 20 mol% 1 (b) after one equivalent of $PhMe_2SiH$ and (c) after two equivalents of $PhMe_2SiH$.

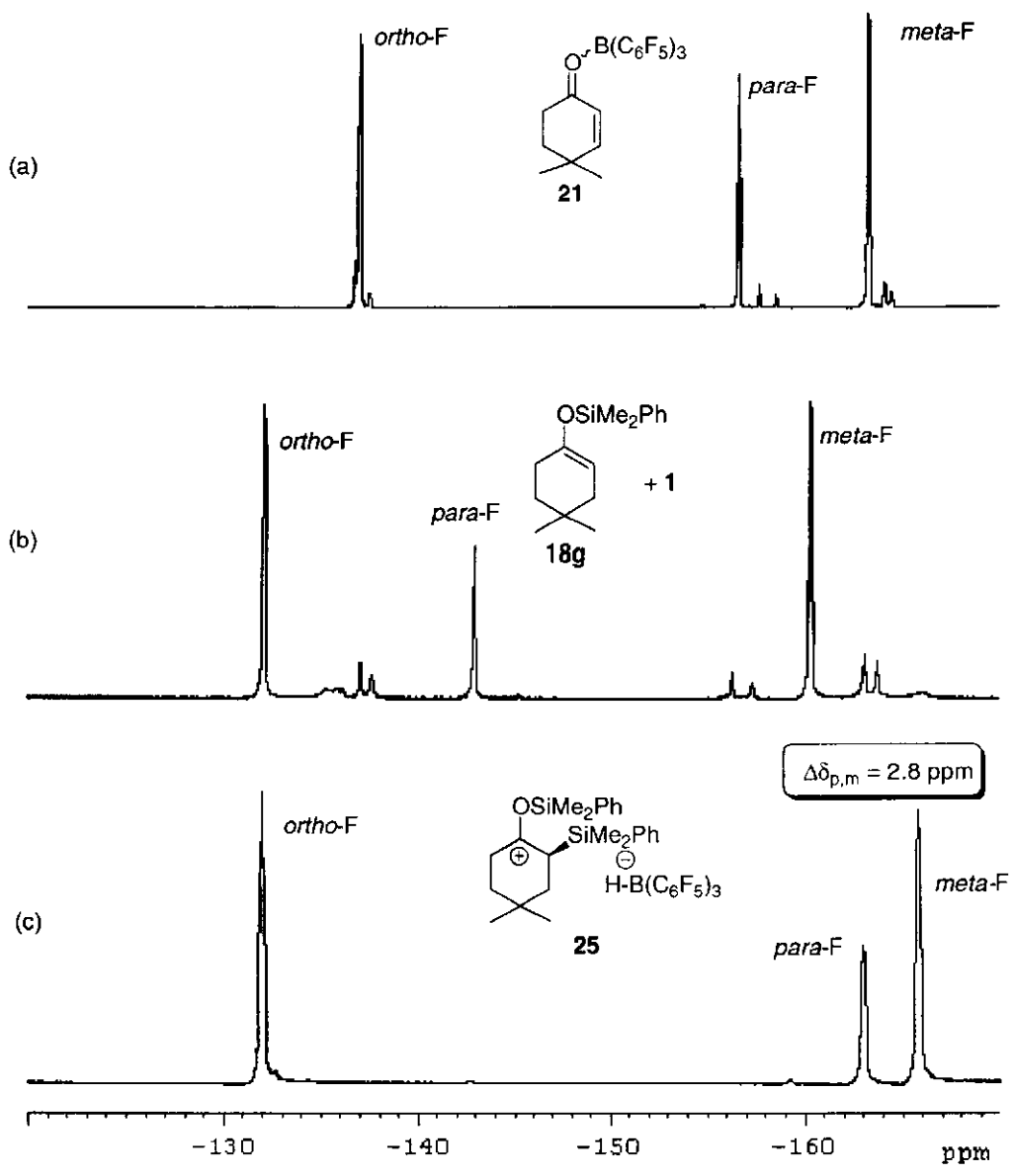

To this mixture at -78 °C was added a second equivalent of $PhMe_2SiH$. ^{19}F NMR analysis of this reaction mixture warmed to -40 °C indicated that a reaction involving **1** had taken place, Figure 2.1c. The signals for **1** are completely replaced by a new set of signals. Significantly, the value for $\Delta\delta_{p,m}$ is 2.8 ppm indicating that an anionic borate had been formed which is separated from its countercation (see Section 1.2.5).

Scheme 2.11: Synthesis of $[Bu_4N]^+[H\text{-}B(C_6F_5)_3]^-$.

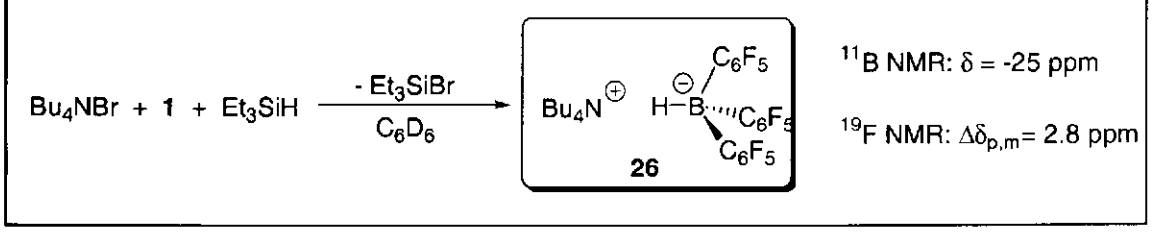

The ^{11}B NMR shift for **25** was measured to be -25 ppm, again consistent with an anionic borate. Comparison of spectral data of **25** to $[Bu_4N]^+[H\text{-}B(C_6F_5)_3]^-$, **26**, helped to confirm that this species was indeed a hydridoborate anion. Furthermore, the reaction mixture separates into two-layers, the bottom layer containing the ion-pair. This behavior is common to many reactions where a perfluoroaryl borate counterion is formed.[79] ^{29}Si NMR showed two signals at 46 ppm and 7 ppm. The former signal is consistent with the silicon from a silylcarboxonium intermediate.[80] The corresponding values for the hydrosilated product, **23**, are 3.4 ppm (O-Si) and -1.1 ppm (C-Si). Clearly, a significant shift in the value for the O-Si NMR shift is observed reflective of the partial positive charge on the Si atom. This mechanistic proposal is consistent with formation of the *cis*-substituted products. Formation of zwitterions **22** or **23** is followed by selective attack of the hydride *trans* to the bulky silyl group leading to the *cis* products. Thus the hydrosilane is delivered stepwise in a *trans* fashion.

2.2.5 Related/Future Work

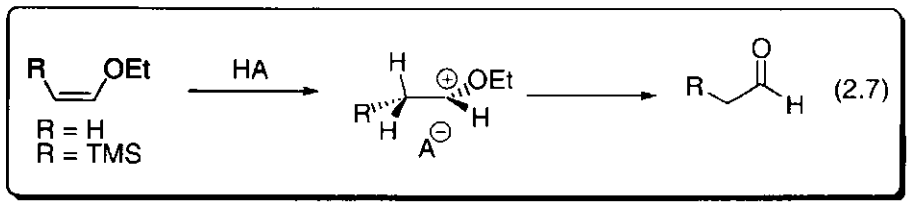

(2.7)

Two other examples of β-silyl-alkoxy-substituted cations have been reported, one of which is shown in equation 2.7.[81] The β-stabilizing effect of the silyl group was found to be attenuated by the presence of the alkoxy group relative to other β-silyl carbocations. Prakash, Olah and co-workers have also generated stabilized carbocations by reactions of esters with "Me_3Si^+" including an α-silyl-substituted ester.[82]

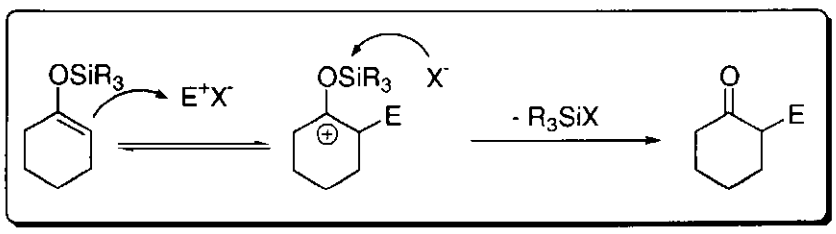

Reactions of silyl enol ethers with electrophiles are proposed to take place via initial C-attack by the electrophile. Hence, silylcarboxonium species are the presumed intermediates, the electrophilic Si subsequently being attacked by a nucleophile to generate a C=O double bond. However, until now, direct NMR observation of these intermediates by NMR spectroscopy or other means is without precedent.

An interesting aspect of the hydrosilation chemistry results from the possibility for attack of the nucleophile (hydridoborate or hydrosilane) at either of two electropositive centers, Scheme 2.12. Either hydride addition to the carbocationic center can ensue leading directly to the observed product or hydride attack could take place at the electrophilic silicon center generating hydrosilane and an α-silyl ketone (silyl enol ether

tautomer). Hydrosilation of the keto functionality could then take place also leading to the observed product. Initial tautomerization of the silyl enol ether to an α-silyl ketone could also take place prior to reaction with hydrosilane. Cross-over studies could potentially be used to differentiate between these possibilities.

Scheme 2.12: Mechanistic Possibilities for Hydrosilation of Silyl Enol Ethers.

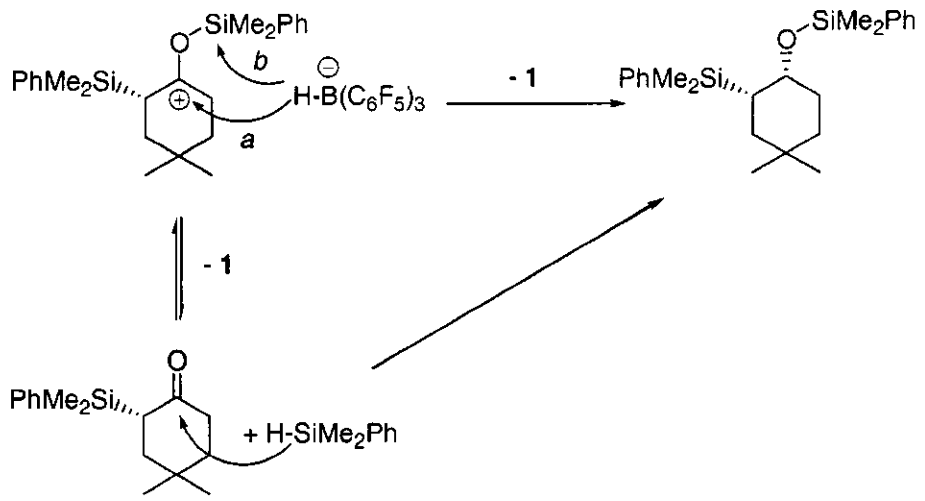

A number of reagents of general form X-Y (allylsilanes and-stannanes, TMS-CN, $TMSN_3$ etc.) could be imagined to proceed via similar reaction pathways with silyl enol ethers catalyzed by **1**.

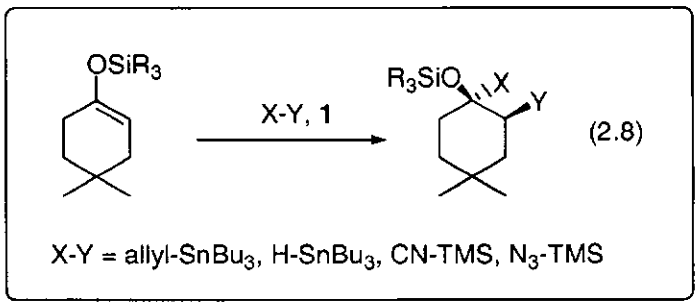

Furthermore, the reaction products could be potentially transformed further into useful functional groups. For example, deoxygenation of silyl ethers which is known to

be catalyzed by **1** in the presence of hydrosilane (see 2.3.6) could lead to alkyl silane formation.

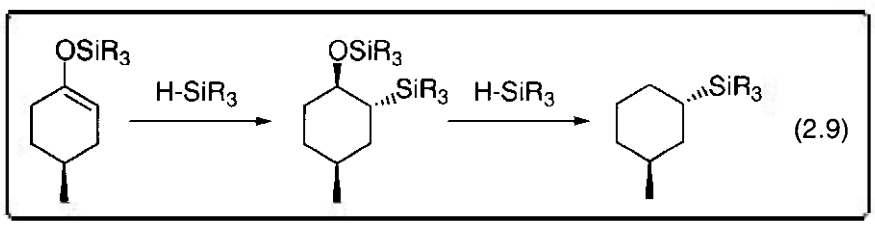

(2.9)

Typified by its role in the Petersen olefination reaction, the β-silylalkoxy functionality is prone to acid or base induced elimination reactions.[83] Thus, this protocol could provide a means of effecting a novel transformation, enone to alkene with vinylic group transposition in one pot.

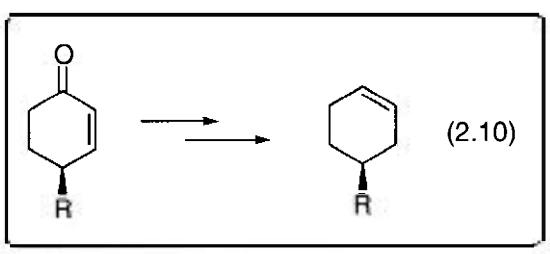

(2.10)

2.3 $B(C_6F_5)_3$-Catalyzed Silation of Alcohols

A convenient procedure for the protection of a diverse range of alcohols using a number of useful silyl groups has been developed with the technical assistance of undergraduate researchers Katie Foster and Vickie Beck. Preliminary observations made by Dr. Dan Parks inspired this research. The alcohol silation procedure uses **1** as a catalyst in conjunction with hydrosilanes. Most commonly, alcohols are protected as silyl ethers using the appropriate silyl chloride or triflate and a stoichiometric quantity of a base such as Et_3N to neutralize the acid byproduct. Although this strategy works admirably for most alcohols, there can be some disadvantages. For instance, a full equivalent of base is required leading to production of an ammonium hydrochloride such as Et_3NHCl. Base sensitive functional groups are often not tolerated or lead to the epimerization of stereocenters. Finally, bulky alcohols often react sluggishly or not at all.[84]

As discussed in Section 2.1.4, a number of alcohol silation strategies which employ hydrosilanes and a transition metal catalyst have been reported; however, most of these protocols suffer from one or more disadvantages such as poor functional group tolerance, slow reaction rates of tertiary alcohols with bulky/useful silanes, the requirement for rigorously anaerobic and/or water-free reaction conditions and the lack of a commercial source of the catalyst. As will become clear, the strategy presented herein addresses many of these issues. The majority of this work has been published including a detailed experimental section.[85]

2.3.1 Technical Details of Silation Procedure

In general, reactions are carried out by adding catalytic amounts of **1** (1-8 mol%) to a solution of the alcohol and silane in toluene or CH_2Cl_2. Reactions are generally very clean and quantitative where the only byproduct is H_2. Thus, isolation of the silyl ether byproducts is trivial involving concentration of the reaction mixture followed by column chromatography. Although, typically, scrupulously dried solvents and sublimed **1** were employed, test reactions have shown that such stringent conditions are not required. When "wet" **1** is used, the water is eventually silated although an induction period is usually observed prior to alcohol silation. Likewise, less-rigorously dried solvent and even solvent directly from a freshly opened bottle can be used with the same delay in reaction being observed.

2.3.2 Silation of 1°, 2°and 3°Alcohols and Phenols

A range of silyl ethers are obtained in high yield from the corresponding alcohols, Table 2.4. Primary, secondary and phenolic alcohols are cleanly silated to their respective triphenylsilyl ethers. For tertiary alcohols (entries 8 and 9), the use of Et_3SiH was necessary, again leading to high yields of the silyl ether products. The reactions were carried out on 5 mmol scale using 1-5 mol% of **1** as catalyst. To demonstrate the scalability of the reaction, 100 mmol of 2,6-dimethyl phenol was hydrosilated in >95% yield using Et_3SiH and 0.5 mol% **1**. The relative reactivity for silation of the alcohols used varies considerably. Interestingly, primary alcohols undergo silation slower than secondary alcohols, which do so slower than tertiary alcohols. This order of reactivity is unusual compared to typical procedures, especially base-catalyzed conditions where

tertiary alcohols are often unreactive. The mechanistic implications of this unusual reactivity order are discussed in Section 2.3.6.

Table 2.4: Silation of 1°, 2°, 3° Alcohols and Phenols.

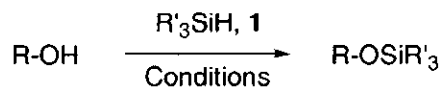

Entry	ROH	Silane	Cond.	Time (h)	Yield (%)
1	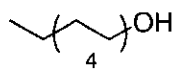	Ph_3SiH	A	24	80
2	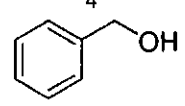	Ph_3SiH	A	20	93
3	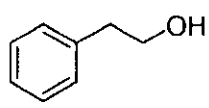	Ph_3SiH	A	144	87
4	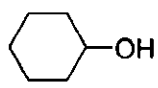	Ph_3SiH	A	1	95
5	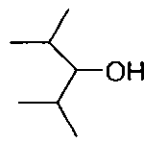	Ph_3SiH	A	2	95
6	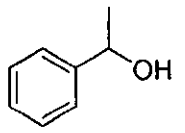	Ph_3SiH	A	48	87
7	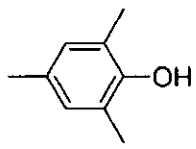	Ph_3SiH	A	2	75
8	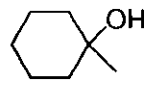	Et_3SiH	B	<1	91
9	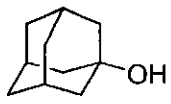	Et_3SiH	B	<1	79

A: ROH (5 mmol), **1** (0.1 mmol), C_7H_8, rt
B: ROH (5 mmol), **1** (0.05 mmol), C_7H_8, rt

2.3.3 Functional Group Tolerance

Table 2.5: Functional Group Tolerance in the Silation of 1^0, 2^0, 3^0 Alcohols

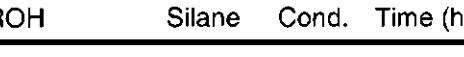

Entry	ROH	Silane	Cond.	Time (h)	Yield (%)
1	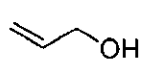	Ph_3SiH	A	72	78
2	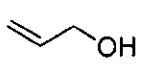	Ph_3SiH	B	4	95
3	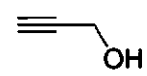	Ph_3SiH	A	2	**95**
4	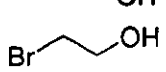	Ph_3SiH	A	1	**93**
5	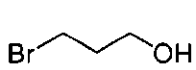	Ph_3SiH	A	16	**85**
6	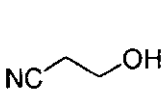	Ph_3SiH	A	84	55
7		Ph_3SiH	A	1	**86**
8	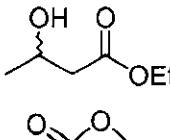	Ph_3SiH	C	2	**83**
9	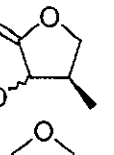	Ph_3SiH	A	2	**93**
10	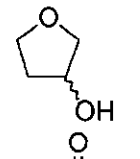	Et_3SiH	C	20	**86**

A: ROH (5 mmol), **1** (0.1 mmol), C_7H_8, rt
B: ROH (5 mmol), **1** (0.4 mmol), C_7H_8, rt
C: ROH (2.5 mmol), **1** (0.125 mmol), CH_2Cl_2, rt

One of the disadvantages of other alcohol silation strategies using hydrosilanes is the lack of functional group tolerance. In spite of the propensity for **1** to catalyze a number of reactions in league with hydrosilanes, considerable tolerance for other

potentially reactive functional groups is observed, Table 2.5. For example, alkenes and alkynes are tolerated (Table 2.5, entries 1-3). Transition metal catalysts that have been used for alcohol silation are often also proficient at alkene/alkyne hydrosilation. Alcohol silation in the presence of other functional groups such as bromo (entries 4 and 5), cyano (entry 6), ester (entries 7 and 8), ether (entry 9) and ketone (entry 10) proceed in good yield. Although the cyano group is not competitively hydrosilated, it does coordinate the borane catalyst leading to reduced reaction rates. As entries 7-10 illustrate, even carbonyl and ether functions which are known to react with hydrosilanes in the presence of **1** do not significantly compete with alcohol silation.

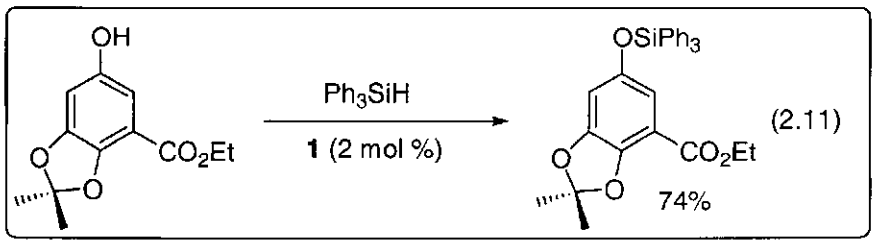

However, functional group tolerance is not guaranteed and should be addressed on a case by case basis, Table 2.6. Phenol groups are silated preferentially over ether (entries 1 and 2), ester (entry 3) and nitro (entry 4) groups; however, aldehyde (entries 6 and 8) and ketone (entries 7 and 9) groups undergo competitive reactions. Aldehyde and keto functions both *meta*- (non-conjugated) and *para*- (conjugated) to the hydroxy group interfered with alcohol silation. A more functionalized phenol was also silated efficiently, equation 2.11.

Table 2.6: Functional Group Tolerance in Silation of Phenols.

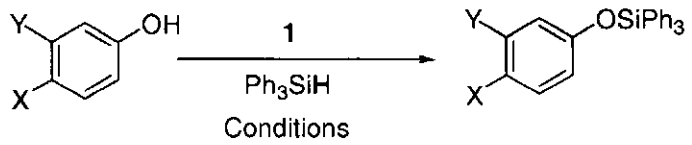

Entry	X	Y	Cond.	Time (h)	Yield
1	OMe	H	A	20	95
2	OBn	H	A	20	92
3	CO_2Me	H	A,B	20	87
4	H	NO_2	A	2	91
5	CH_2CN	H	A,B	240	12
6*	C(O)H	H	C		
7*	C(O)Me	H	C		
8*	H	C(O)H	C		
9*	H	C(O)Me	C		

A: ROH (2.5 mmol), **1** (0.125 mmol), C_7H_8 or CH_2Cl_2, rt
B: same as A, except 40 °C (refluxing CH_2Cl_2)
C: ROH (0.1 mmol), **1** (0.005 mmol), $CDCl_3$, rt

* competitive hydrosilation of carbonyl function

2.3.4 Variation in Silane

Table 2.6: Variation in Hydrosilane.

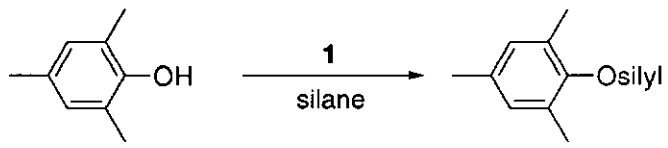

Entry	X	Cond.	Time (h)	Yield
1	$HSiEt_3$	A	2	95
2	$HSiPh_3$	A	2	72
3	$HSiMe_2{}^tBu$	A	12	95
4	$HSiMe_2Ph$	A	1	80
5	$HSiMe_2Cl$	A	2	79
6	H_2SiPh_2	A	<1	95*
7	$HSiBn_3$	B	---	n.r.
8	HSi^iPr_3	B	---	n.r.

A: ROH (5 mmol), **1** (0.1 mmol), C_7H_8, rt
B: ROH (5 mmol), **1** (0.1 mmol), C_7H_8, 110°C

* crude yield

Using 2,4,6-trimethylphenol as a representative substrate (moderate reactivity), other commercially available silanes were studied, Table 2.7. In addition to Ph_3SiH and Et_3SiH, useful silanes such as $^tBuMe_2SiH$, $PhMe_2SiH$, $ClMe_2SiH$ and Ph_2SiH_2 undergo efficient silation reactions. Bn_3SiH and $^iPr_3SiH$ were completely unreactive. In particular, *tert*-butyldimethylsilyl ether[86] and dimethylphenylsilyl ether protecting groups are used extensively in organic synthesis. With $ClMe_2SiH$ and Ph_2SiH_2, the resulting silyl ether products possess a functionalizable silicon center (Si-Cl and Si-H bonds respectively) which could potentially be utilized for the popular strategy of adjoining two reactants by a removable silicon tether.[87]

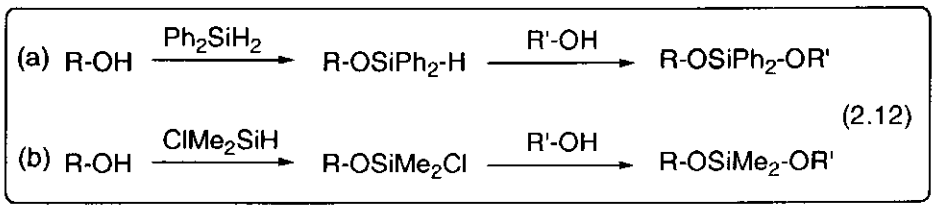

(2.12)

Ph_2SiH_2 has also been used to protect 1,2- and 1,3- diols as cyclic siloxanes in moderate, unoptimized yield, equation 2.13.

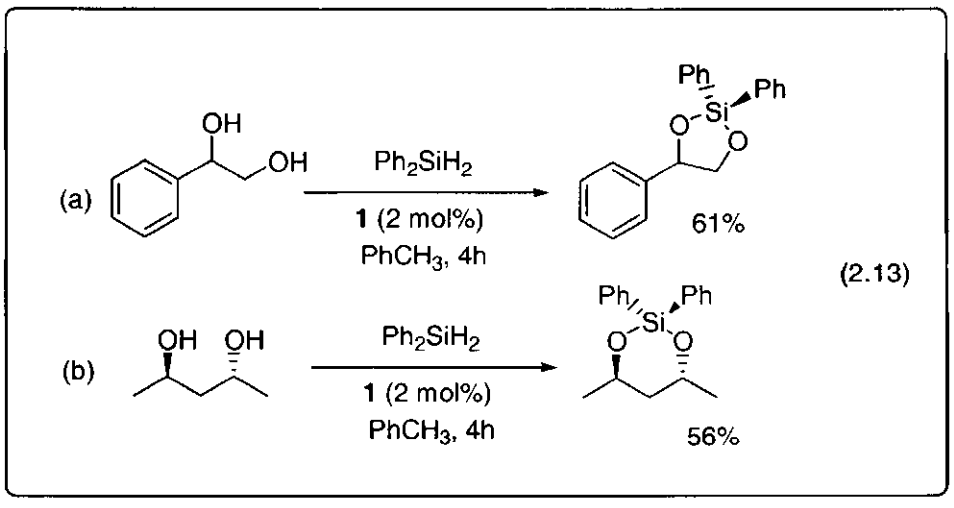

(2.13)

2.3.5 Mechanistic Insight

Scheme 2.13: Mechanistic Possibilities for Alcohol Silation.

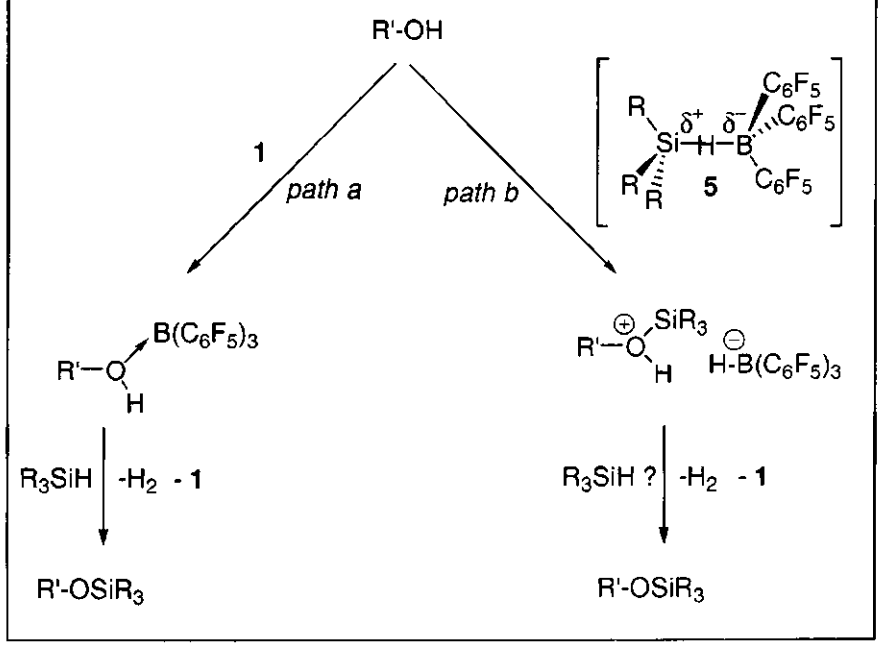

Two mechanisms are proposed in Scheme 2.13 differentiated primarily by the identity of the Lewis acid (**1** or "R_3Si^+") which coordinates/activates the hydroxy group to dehydrocoupling with either hydrosilane (path *a* or *b*) or hydridoborate (path *b*). Although both pathways are reasonable and competition between the two is possible, qualitative observations suggest pathway *b* to be the most prominent.

In support of mechanistic pathway *a*, aqua and alcohol adducts of **1** are well-precedented in the literature.[88] In fact, the pK_a of $(C_6F_5)_3B(OH_2)$ in acetonitrile was estimated to be 8.4 making its acidity comparable to that of HCl in acetonitrile.[88c] Silation of H_2O, which is necessary for alcohol silation to ensue if wet borane or solvent is used, could reasonably take place where $(C_6F_5)_3B(OH_2)$ acts as a strong acid in a dehydrocoupling reaction with hydrosilane. In fact, $(C_6F_5)_3B(OH_2)$ has been used as a

Brønsted acid in a number of applications including the protonolysis of metal alkyl bonds[89] and protonation of a zinc hydroxide to an aquated zinc cation.[90]

The acidity of coordinated alcohols would certainly also be enhanced; however, observations suggest that alcohol silation via path *a* is not important. First, the order of reactivity of alcohols to silation is tertiary > secondary > primary although presumably less hindered alcohols should coordinate **1** more strongly. This unusual order of reactivity is similar to that observed for carbonyl silation where it was shown that an ester ($PhCO_2Et$) is hydrosilated faster than a ketone (PhCOMe) and an aldehyde (PhCHO). This inverted order was attributed to the requirement that dissociation of the carbonyl borane adduct was necessary before hydrosilation could take place. PhCHO more effectively sequesters **1** thus leading to a decrease in reactivity. Tertiary alcohols (which show no evidence for coordination to **1** by ^{19}F NMR analysis) are silated instantly and exothermically. Silation of primary alcohols such as benzyl alcohol proceeds slowly in spite of its superior basicity toward **1**.

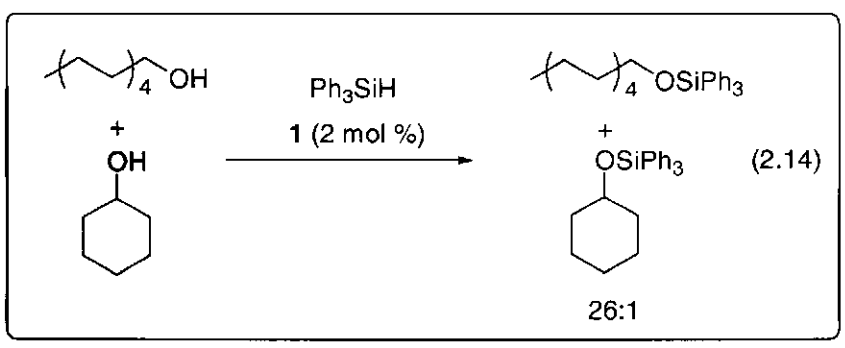

Furthermore, when a 1:1 mixture of decyl alcohol and cyclohexanol are reacted with Ph_3SiH, decyl alcohol is silated preferentially (26:1), equation 2.14. In independent reactions, silation of decyl alcohol requires 24 hours to reach completion whereas cyclohexanol is silated in less than two hours. Based on mechanistic pathway *b*, it is

proposed that the primary alcohol is a stronger Lewis base to both **1** and "Ph_3Si^+" than is cyclohexanol. Greater basicity of decyl alcohol to **1** leads to longer reaction times since **1** is not available to activate silane. However, when decyl alcohol and cyclohexanol are in direct competition for "Ph_3Si^+", the greater basicity of the primary alcohol leads to preferential silation.

2.4 Related Work

Scheme 2.14: Other Reactions of Silanes Catalyzed by 1

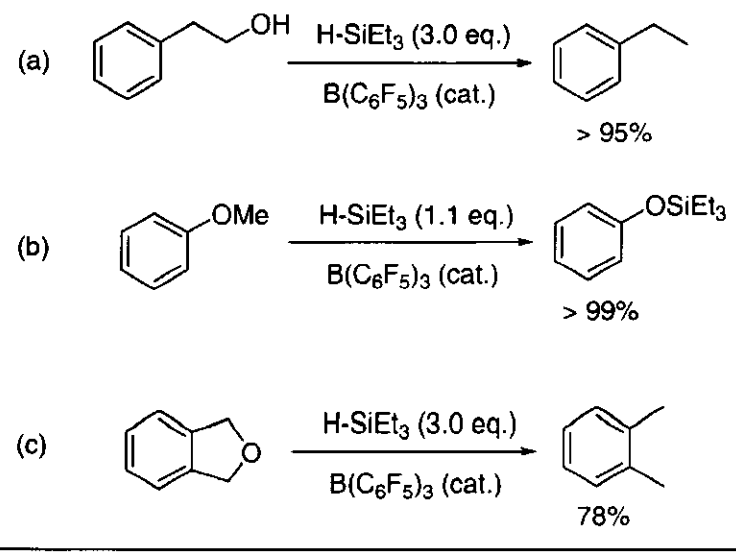

Concurrent to our work, H. Yamamoto and Gevorgyan have also studied reactions of hydrosilanes catalyzed by **1**.[91,92] For example, in the presence of excess Et_3SiH, alcohols can be reduced fully to the corresponding alkane, Scheme 2.14a. Various ethers can be cleaved to the corresponding silyl ether, Scheme 2.14b, or completely to the alkane, Scheme 2.14c.

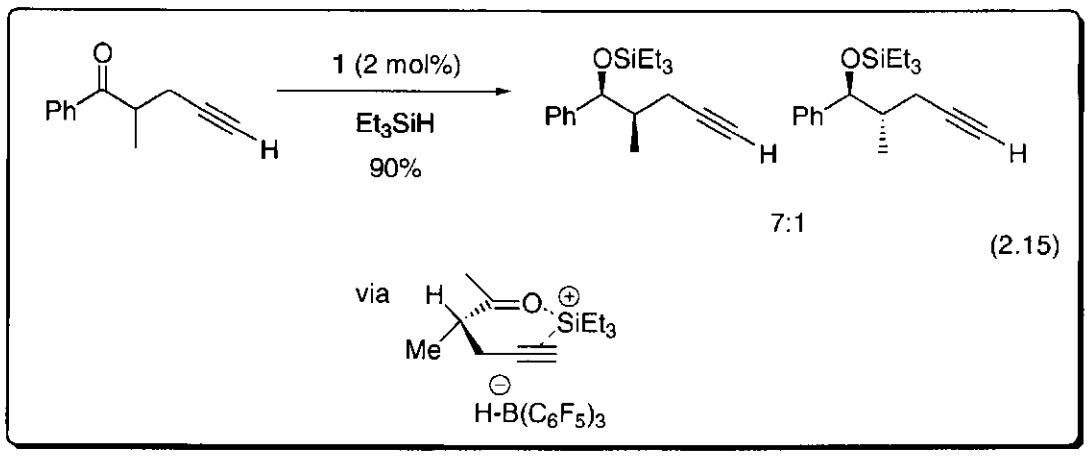

Y. Yamamoto and co-workers have invoked the mechanism described above for the hydrosilation of carbonyls to rationalize selectivity in the hydrosilation of alkynyl-substituted ketones.[93] The authors propose that a trialkylsilylium cation, "R_3Si^+", generated by activation of silane by **1** is chelated by a ketone and alkyne, equation 2.15.

2.5 Conclusions/Future Work

As the Piers' group and others have shown, the combination of hydrosilanes and catalytic **1** is a potent method for generating electrophilic silylium species *in situ* via activated silane complex **5**. Although, **5** is not observed spectroscopically, mechanistic and qualitative observations support its intermediacy in a number of reactions. Although **5** and preformed silylium Lewis acids can catalyze similar reaction chemistry, advantages of using **1** to transiently generate silylium Lewis acids has been demonstrated. This is particularly clear in carbonyl hydrosilation where hydride delivery by hydridoborate allows controlled reduction of carbonyl functions to silyl ethers. Furthermore, the transient nature of complex **5** allows reactions to be carried out in solvents such as CH_2Cl_2 in which silylium Lewis acids such as **2** are relatively unstable.

Future research goals of the Piers group are aimed at developing asymmetric hydrosilation reactions. These include ketone reductions and alcohol resolution

strategies. The most attractive possibility for effecting enantioslective reactions involves using chiral perfluoroarylboranes as Lewis acids and efforts toward this end are underway. It is largely because of this goal that obtaining a solid understanding of the activation and hydride delivery steps was deemed so important. The finding that carbonyl hydrosilation proceeds via silylium activation suggests that a chiral borane Lewis acid would be inappropriate for effecting enantiocontrol. However, it was also discovered that hydridoborate anion delivers the hydride; with a chiral borane, a chiral hydridoborate nucleophile would be responsible for C-H bond formation. The promise of this approach then rests on the effectiveness of the chiral nucleophile differentiating between the two enantiotopic faces of a silylcarboxonium cation. A number of choices of hydrosilane will facilitate optimization of the reaction.

---

[1] (a) Brook, M. A. *Silicon in Organic, Organometallic and Polymer Chemistry* John Wiley & Sons: Toronto, 2000, pp. 401-421. (b) Reichl, J. A.; Berry, D. H. *Adv. Organomet. Chem.* **1999**, *43*, 197.

[2] *Aldrich Handbook of Fine Chemicals and Laboratory Equipment*, Canada, 2000-2001, (prices in Canadian funds).

[3] See reference 1a, p. 28.

[4] see Greeves, N. in *Comprehensive Organic Synthesis* Trost, B. M.; Fleming, I., Eds.; Pergamon Press: New York, 1991; Vol. 1, p.1 and references therein.

[5] For a review on carbon based reducing agents (transfer hydrogenation), see Kellogg, R. M. in *Comprehensive Organic Synthesis*; Trost, B. M.; Fleming, I., Eds.; Pergamon Press: New York, 1991; Vol. 1, p.79.

[6] For a review on ionic hydrogenation, see Kursanov, D. N.; Parnes, Z. N.; Loim, N. M. *Synthesis* **1974**, 633.

[7] (a) Boyer, J.; Corriu, R. J. P.; Perz, R.; Rye, C. *J. Organomet. Chem.* **1978**, *157*, 153 and references therein.

[8] (a) Fujita, M.; Hiyama, T. *J. Am. Chem. Soc.* **1984**, *106*, 4629. (b) Hiyama, T.; Kobayashi, K.; Fujita, M. *Tetrahedron Lett.* **1984**, *25*, 4959. (c) Fujita, M.; Hiyama, T. *J. Am. Chem. Soc.* **1985**, *107*, 8294. (d) Fujita, M.; Hiyama, T. *Tetrahedron Lett.* **1987**, *28*, 2263. (e) Fujita, M.; Hiyama, T. *J. Org. Chem.* **1988**, *53*, 5406.

[9] (a) Doyle, M.P.; DeBruyn, D. J.; Kooistra, D. A. *J. Am. Chem. Soc.* **1972**, *94*, 3659. (b) Doyle, M. P.; West, C. T. *J. Org. Chem.* **1975**, *40*, 3835 and references therein.

[10] Doyle, M. P.; West, C. T.; Donnelly, S. J.; McOsker, C. C. *J. Organomet. Chem.* **1976**, *117*, 129.

[11] Fry, J. L.; Orfanopoulos, M.; Adlington, M. G.; Dittman Jr.; W. R.; Silverman, S. B. *J. Org. Chem.* **1977**, *43*, 375.

[12] Tsunoda, T.; Suzuki, M.; Noyori, R. *Tetrahedron Lett.* **1979**, 4679.

[13] Kato, J.; Iwasawa, N. Mukaiyama, T. *Chem. Lett.* **1985**, 743.

[14] Sassaman, M. B.; Kotian, K. D.; Prakash, G. K. S.; Olah, G. A. *J. Org. Chem.* **1987**, *52*, 4314.

[15] Komatsu, N.; Ishida, J. -Y.; Suzuki, H. *Tetrahedron Lett.* **1997**, *38*, 7219.

[16] Nishizawa, M.; Noyori, R. in *Comprehensive Organic Synthesis* Trost, B. M.; Fleming, I., Eds.; Pergamon Press: New York, 1991; Vol. 1, p.159 and references therein.

[17] For recent examples, see (a) Haag, D.; Runsink, J.; Scharf, H. -D. *Organometallics*, **1998**, *17*, 398. (b) Nishibayashi, Y.; Takei, I.; Uemura, S.; Hidai, M. *Organometallics* **1998**, *17*, 3420. (c) Herrmann, W. A.; Goosen, L. J.; Kücher, C.; Artus, G. R. *Angew. Chem. Int. Ed. Engl.* **1996**, *35*, 2805.

[18] (a) Carter, M. B.; Schiott, B.; Gutierrez, A.; Buchwald, S. L.; *J. Am. Chem. Soc.* **1994**, *116*, 11667. (b) Yun, J.; Buchwald, S. L. *J. Am. Chem. Soc.* **1999**, *121*, 5640 and references therein.

[19] Holmes, R. R. *Chem. Rev.* **1996**, *96*, 927 and references therein.

[20] Keinan, E.; Greenspoon, N. in *Comprehensive Organic Synthesis*; Trost, B. M.; Fleming, I., Eds.; Pergamon Press: New York, 1991; Vol. 3, p.523 and references therein.

[21] Yoshii, E.; Koizumi, T.; Hayashi, I.; Hiroi, Y. *Chem. Pharm. Bull.* **1977**, *25*, 1468.

[22] Ojima, I.; Kogure, T. *Organometallics* **1982**, *1*, 1390.

[23] Revis, A.; Hilty, K. Y. *J. Org. Chem.* **1990**, *55*, 2972.

[24] Chan, T. C.; Zheng, G. Z. *Tetrahedron Lett.* **1993**, *34*, 3095.

[25] Johnson, C. R.; Raheja, R. K. *J. Org. Chem.* **1994**, *59*, 2287.

[26] Lipshutz, B. H.; Chrisman, W.; Noson, K.; Papa, P.; Sclafani, J. A.; Vivian, R. W.; Keith, J. M. *Tetrahedron*, **2000**, *56*, 2779.

[27] See reference 1a, pp. 215-239.

[28] Hiyama, T.; Kusomoto, T. in *Comprehensive Organic Synthesis* Trost, B. M.; Fleming, I., eds.; Pergamon Press: New York, 1991; Vol. 3, p.763.

[29] For a review on Lewis acid-catalyzed hydrometallations of alkynes, see Asao, N.; Yamamoto, Y. *Bull. Chem. Soc. Jpn.* **2000**, *73*, 1071.

[30] Finke, U.; Moretto, H. *Ger. Pat.* 2,804.204, **1979**.

[31] Oertle, K.; Wetter, K. F. *Tetrahedron Lett.* **1985**, *26*, 5511.

[32] (a) Voronkov, M. G.; Adamovich, S. N.; Pukhnarevich, V. B. *J. Gen. Chem. USSR (Engl. Transl.)* **1982**, *52*, 2058. (b) Voronkov, M. G.; Adamovich, S. N.; Sherstyannikova, L. V.; Pukhnarevich, V. B. *J. Gen. Chem. USSR (Engl. Transl.)* **1983**, *53*, 706.

[33] (a) Song, Y. -S.; Yoo, B. R.; Lee, G. -Y.; Jung, I. N. *Organometallics,* **1999**, *18*, 3109. (b) Asao, N.; Sudo, T.; Yamamoto, Y. *J. Org. Chem.* **1996**, *61*, 7654. (c) Sudo, T.; Asao, N., Gevorgyan, V.; Yamamoto,

Y. *J. Org. Chem.* **1999**, *64*, 2494. (d) Sudo, T.; Asao, N.; Yamamoto, Y. *J. Org. Chem.* **2000**, *65*, 8919. (e) Buriak, J. M.; Allen, M. J. *J. Am. Chem. Soc.* **1998**, *120*, 1339. (f) Yamamoto, K.; Takamae, M. *Synlett*, **1990**, 259.

[34] (a) *Comprehensive Handbook on Hydrosilylation* Marciniec, B., Ed.; Pergamon Press: Oxford, U.K., 1992. (b) Ojima, I. in *The Chemistry of Organic Silicon Compounds* Patai, S., Rappoport, Z., Eds.; Wiley: New York, 1989. (c) Hiyama, T.; Kusomoto, T. in *Comprehensive Organic Synthesis* Trost, B. M.; Fleming, I., Eds.; Pergamon Press: Oxford, 1991, Vol. 8, p. 763.

[35] (a) Snyder, D. C. *J. Organomet. Chem.* **1986**, *301*, 137. (b) Ikeda, S.; Chatani, N.; Kajikawa, Y.; Ohe, K.; Murai, S. *J. Org. Chem.* **1992**, *57*, 2.

[36] (a) Skola-Foldes, R.; Kollar, L.; Balint, H. *J. Organomet. Chem.* **1991**, *408*, 297. (b) Murai, T.; Kimura, F.; Tsutsui, K.; Hasegawa, K.; Kato, S. *Organometallics*, **1998**, *17*, 926.

[37] (a) Gregg, B. T.; Cutler, A. R. *J. Am. Chem. Soc.* **1996**, *118*, 10069. (b) Mao, Z.; Gregg, B. T.; Cutler, A. R. *Organometallics*, **1998**, *17*, 1993.

[38] Chatani, N.; Shinohara, M.; Ikeda, S. -I.; Murai, S. *J. Am. Chem. Soc.* **1997**, *119*, 4303.

[39] (a) Akita, M.; Hua, R.; Oku, T.; Moro-oka, Y. *Organometallics,* **1996**, *15*, 2548 (b) Akita, M.; Hua, R.; Oku, T.; Tanaka, M.; Moro-oka, Y. *Organometallics,* **1996**, *15*, 4162.

[40] Murai, Y.; Yasui, E.; Kato, S.; Hatayama, Y.; Suzuki, S.; Yamasaki, Y.; Sonoda, N.; Kurosawa, H.; Kawasaki, Y.; Murai, S. *J. Am. Chem. Soc.* **1989**, *111*, 7938.

[41] (a) Corey, J. Y.; Braddock-Wilking, J. *Chem. Rev.* **1999**, *99*, 175. (b) see Hengge, E.; Stüger, H. in reference 33b, pp.2177-2216. (c) see reference 1a, pp.340-355.

[42] Lickiss, P. D. *Adv. Inorg. Chem.* **1995**, *42*, 147.

[43] (a) Lukevics, E.; Dzintara, M. *J. Organomet. Chem.* **1985**, *295*, 265 and references therein. (b) Corey, J. Y. *Adv. Silicon Chemistry* **1991**, *1*, 327 and references therein.

[44] (a) Schubert, U.; Lorenz, C. *Inorg. Chem.* **1997**, *36*, 1258. (b) Chalk, A. J. *J. Chem. Soc., Chem. Commun.* **1970**, 847.

[45] (a) Sommer, L. H.; Citron, J. D. *J. Org. Chem.* **1967**, *32*, 2470. (b) Blum, Y.; Laine, R. M. *Organometallics*, **1986**, *5*, 2081. (c) Liu, H. Q.; Harrod, J. F. *Can. J. Chem.* **1992**, *70*, 107. (d) Liu, H. Q.; Harrod, J. F. *Organometallics,* **1992**, *11*, 822. (e) Takaki, K.; Kamata, T.; Miura, Y.; Shishido, T.; Takehira, K. *J. Org. Chem.* **1999**, *64*, 3891.

[46] (a) Nesmayanov, A. N.; Friedlina, R. K.; Chukovskaya, E. C.; Petrova, R. G.; Belyavsky, A. B. *Tetrahedron* **1962**, *17*, 62. (b) For a recent review, see reference 43b.

[47] Jun, C. -H.; Crabtree, R. H. *J. Organomet. Chem.* **1993**, *447*, 177. (b) Takaki, K.; Kurioka, M.; Kamata, T.; Takehira, K.; Makioka, Y.; Fujiwara, Y. *J. Org. Chem* **1998**, *63*, 9265.

[48] see reference 1a, pp. 198-203.

[49] Nakano, T.; Nagai, Y. *Chem. Express* **1990**, *5*, 21.

[50] Bedard, T. C.; Corey, J. Y. *J. Organomet. Chem.* **1992**, *428*, 315.

[51] Lorenz, C.; Schubert, U. *Chem. Ber.* **1995**, *128*, 1267l.

[52] Barton, D. H. R.; Kelly, M. J. *Tetrahedron Lett.* **1992**, *33*, 5041.

[53] Doyle, M. P.; High, K. G.; Bagheri, V.; Pieters, R. J.; Lewis, P. J.; Pearson, M. M. *J. Org. Chem.* **1990**, *55*, 6082.

[54] Luo, X. -L.; Crabtree, R. H. *J. Am. Chem. Soc.* **1989**, *111*, 2527.

[55] Oehmichen, U.; Singer, H. *J. Organomet. Chem.* **1983**, *243*, 199.

[56] Chalk, A. J. *J. Chem. Soc., Chem. Commun.* **1970**, 847.

[57] Gregg, B. T.; Cutler, A. R. *Organometallics*, **1994**, *13*, 1039.

[58] Burn, M. J.; Bergman, R. G. *J. Organomet. Chem.* **1994**, *472*, 43.

[59] Corriu, R. J. P.; Perz, R.; Reye, C. *Tetrahedron* **1983**, *39*, 999.

[60] Tanabe, Y.; Okumura, H.; Maeda, A.; Murakami, M. *Tetrahedron Lett.* **1994**, *35*, 8413.

[61] Bideau, F.; Coradin, T.; Hénique, J.; Samuel, E. *Chem. Commun.* **2001**, 1408.

[62] Adlington, M. G.; Orfanopoulos, M.; Fry, J. L. *Tetrahedron Lett.* **1976**, 2955.

[63] Li, Y.; Kawakami, Y. *Macromolecules* **1999**, *32*, 3540.

[64] Li, Y.; Kawakami, Y. *Macromolecules* **1999**, *32*, 6871.

[65] Zhang, C.; Laine, R. M. *J. Am. Chem. Soc.* **2000**, *122*, 6979.

[66] Crabtree, R. H. *Angew. Chem. Int. Ed. Engl.* **1993**, *32*, 789.

[67] Parks, D. *Pentafluorophenylboranes in Synthesis* Ph. D. Dissertation, **1998**.

[68] (a) Parks, D. J.; Piers, W. E. *J. Am. Chem. Soc.* **1996**, *118*, 9440. (b) Parks, D. J.; Blackwell, J. M.; Piers, W. E. *J. Org. Chem.* **2000**, *65*, 3090.

[69] A five-coordinate *bis*-ligated species is unlikely based on literature precedents for coordinated trialkylsilicon cations, see Chapter 1.

[70] Parks, D. J.; Piers, W. E.; Parvez, M.; Atencio, R.; Zaworotko, M. J. *Organometallics*, **1998**, *17*, 1369.

[71] Mayr, H.; Basso, N.; Hagen, G. *J. Am. Chem. Soc.* **1992**, *114*, 3060.

[72] Williams, V. C.; Piers, W. E.; Clegg, W.; Elsegood, M. R. J.; Collins, S.; Marder, T. B. *J. Am. Chem. Soc.* **1999**, *121*, 3244.

[73] Henderson, L. D.; Piers, W. E. unpublished results.

[74] Silyl enol ethers react in Michael additions with enones, see (a) Narasaka, K.; Soai, K.; Mukaiyama, T. *Chem. Lett.* **2000**, 1223. (b) Narasaka, K.; Soai, K.; Aikawa, Y.; Mukaiyama, T. *Bull. Chem. Soc. Japan*, **1976**, *49*, 779. (c) RajanBabu, T. V. *J. Org. Chem.* **1984**, *25*, 495.

[75] (a) Ishihara, K.; Hanaki, N.; Yamamoto, H. *Synlett*, **1993**, 577. (b) Ishihara, K.; Funahashi, M.; Hanaki, N.; Miyata, M.; Yamamoto, H. *Synlett*, **1994**, 963.

[76] Silverstein, R. M.; Webster, F. X. *Spectrometric Identification of Organic Compounds* 6th ed., John Wiley & Sons: Toronto, 1998, p.186.

[77] Fleming, I.; Lawrence, N. J. *J. Chem. Soc. Perkin Trans. 1* **1992**, 3309.

[78] Larson, G. L.; Prieto, J. A. *Tetrahedron* **1983**, *39*, 855 and references therein.

[79] Lambert, J. B.; Zhang, S.; Ciro, S. M. *Organometallics* **1994**, *13*, 2430.

[80] Kira reported a value of 52.3 ppm in CD_2Cl_2 for $[Ph_2C{=}O\text{-}TMS]^+[B(C_6H_3(CF_3)_2\text{-}3,5]_4^-$, see Kira, M.; Hino, T.; Sakurai, H. *Chem. Lett.* **1992**, 555.

[81] (a) Kresge, A. J.; Tobin, J. B. *J. Phys. Org. Chem.* **1991**, *4*, 587. (b) Gabelica, V.; Kresge, A. J. *J. Am. Chem. Soc.* **1996**, *118*, 3838.

[82] Prakash, G. K. S.; Wang, Q.; Rasul, G.; Olah, G. A. *J. Organomet. Chem.* **1998**, *550*, 119.

[83] March, J, *Advanced Organic* Chemistry, 4th ed., John Wiley & Sons: Toronto, 1992, p. 952.

[84] Greene, T. W.; Wuts, P. G. *Protective Groups in Organic Synthesis*, 3rd ed.; John Wiley & Sons: New York, 1999.

[85] Blackwell, J. M.; Foster, K. L.; Beck, V. H.; Piers, W. E. *J. Org. Chem.* **1999**, *64*, 4887.

[86] Corey, E. J.; Venkateswarlu, A. *J. Am. Chem. Soc.* **1972**, *94*, 6190.

[87] See reference 1a, 209-215.

[88] (a) Siedle, A. R.; Lamanna, W. M. US Patent No. 5,296,433, March 22, 1994. (b) Bradley, D. C.; Harding, I. S.; Keefe, A. D.; Motevalli, M.; Zheng, D. H. *J. Chem. Soc., Dalton Trans.* **1996**, 3931. (c) Bergquist, C.; Bridgewater, B. M.; Harlan, C. J.; Norton, J. R.; Friesner, R. A.; Parkin, G. *J. Am. Chem. Soc.* **2000**, *122*, 10581. (d) Beringhelli, T.; Maggioni, D.; D'Alfonso, G. *Organometallics*, **2001**, *20*, published on web Oct.3, 2001.

[89] Hill, G. S.; Manojlovic-Muir, L.; Muir, K. W.; Puddephatt, R. J. *Organometallics*, **1997**, *16*, 525.

[90] Bergquist, C.; Parkin, G. *J. Am. Chem. Soc.* **1999**, *121*, 6322.

[91] (a) Gevorgyan, V.; Liu, J. -X.; Rubin, M.; Benson, S.; Yamamoto, Y. *Tetrahedron Lett.* **1999**, *40*, 8919. (b) Gevorgyan, V.; Rubin, M.; Benson, S.; Liu, J. -X.; Yamamoto, Y. *J. Org. Chem.* **2000**, *65*, 6179.

[92] See also, Rubin, M.; Gevorgyan, V. *Org. Lett.* **2001**, *3*, 2705.

[93] Asao, N.; Ohishi, T.; Sato, K.; Yamamoto, Y. *J. Am. Chem. Soc.* **2001**, *123*, 6931.

Chapter 3

The Chemistry of $B(C_6F_5)_3$ with Imines

3.1 Lewis Acid-Catalyzed Reactions Involving Imines

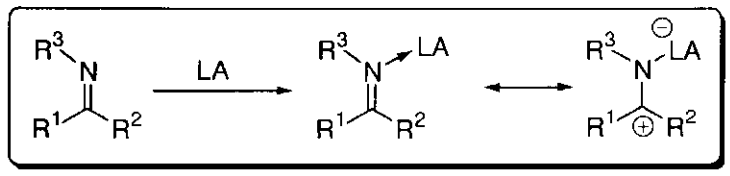

The conversion of imines to amines is an extremely important transformation in organic synthesis since the amine functional group is found in a number of natural products.[1] Access to imines from the corresponding aldehyde or ketone is convenient and a wide range of N-substituents can be used. Although addition of many powerful nucleophiles can occur without external activation, many weak nucleophiles require assistance by a Lewis acid. Even with strong nucleophiles, Lewis acid activation can be advantageous in order to modulate the reactivity or control the stereoselectivity.

3.1.1 Reduction of Imines

There exist a number of methods for effecting the reduction of imines to amines, the vast majority of which use borohydride and aluminum hydride reagents such as $NaBH_4$, $NaBH_3CN$, $LiH(sec\text{-}Bu)_3$ and $LiAlH_4$ alone or in conjunction with a Lewis acid.[2] Other sources for the hydride include H_2, BH_3, $^iBu_2AlH$ and less commonly, hydrosilanes. Asymmetric reductions have been developed by using chiral borane reagents such as oxazaborolidines.[3,4] In many instances, selective reduction of an imine over a carbonyl precursor is possible enabling *in situ* generation of the imine from the carbonyl in the presence of the reducing agent (reductive amination).[5]

Transition metal catalysts used in conjunction with H_2, hydrosilanes or to mediate hydrogen transfer reactions are finding increasing application especially for asymmetric reductions.[6] Catalysts based on Rh,[7,8] Ir,[9] Ru,[10] and Ti[11] can promote asymmetric reductions of ketimines in the presence of H_2. Transition metal catalyzed hydrosilation of imines has gained increasing popularity since early reports.[12] In 1973, Kagan reported the first enantioselective transition metal catalyzed hydrosilation reaction, equation 3.1.[13] Ten years later, Brunner showed that oximes and cyclic imines could be hydrosilated with moderate enantioselectivity using $[Rh(cod)Cl]_2$ as a catalyst precursor in the presence of chiral *bis*-phosphine ligand, (-)-DIOP.[14] In recent years, a number of asymmetric hydrosilation reactions have been disclosed notably those from the groups of Buchwald (chiral titanocene catalyst)[15] and Uemura and Hidai (chiral Rh and Ir catalysts).[16]

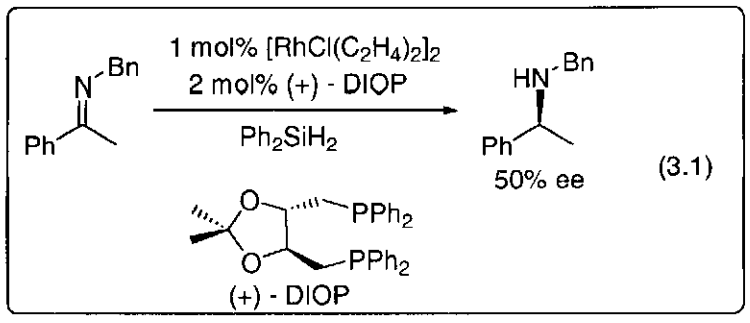

(3.1)

Lewis acid catalyzed methods for the hydrosilation of imines include the use of either Et_3SiH or $PhMe_2SiH$ with CF_3CO_2H (ionic hydrogenation).[1] Both nickel[17] and ytterbium[18] complexes have recently been shown to be effective Lewis acid catalysts when partnered with silanes. In related chemistry, Bu_2SnHCl[19] and Bu_3SnH[20] have been employed in reductive amination chemistry. Fu has shown that polymethylhydrosilane (PMHS) can serve as the stoichiometric source of reductive power when used in

conjunction with catalytic amounts of a hydrostannane.[21] A one-pot reductive amination strategy using $Ti(O^iPr)_4$ and polymethylhydrosiloxane has also recently been published.[22] Compared to the hydrosilation of carbonyl compounds, very few general methods exist for the hydrosilation of imines catalyzed or promoted by main group Lewis acids.

Hydrosilation of imines leads to the formation of silylated amines. Although this could be potentially advantageous in some situations, the sensitivity of the Si-N bond to hydrolysis makes isolation non-trivial. However, upon hydrolysis, the Si-N bond is replaced by a N-H bond; thus, hydrosilation generally results in net addition of H_2 across the C=N bond.

3.1.2 Other Reactions of Imines

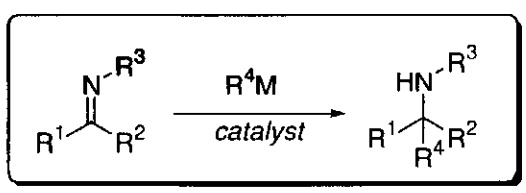

A tremendous amount of research has been carried out on reactions of imines with various nucleophiles and in cycloaddition reactions. A number of reviews have been written in recent years.[23] Nucleophilic additions of strong nucleophiles such as organolithium and organomagnesium compounds often do not require Lewis acidic activation; however, these reactions are often complicated by side reactions such as deprotonation of α-hydrogens. To overcome these problems, a number of solutions have emerged. One general strategy uses organolithium reagents in tandem with Lewis acids such as $BF_3 \cdot OEt_2$,[24] $CeCl_3$[25] or Cu catalysts.[26] A second approach uses less nucleophilic reagents in conjunction with a Lewis acid. For example, allylstannanes,[27] -silanes,[28] and

boranes,[29] dienes,[30] silyl ketene acetals,[31] alkylcopper reagents,[32] and alkylzinc reagents can all add to imines in the presence of main group and transition metal Lewis acids. Mechanistic details of these approaches will be discussed in the next section.

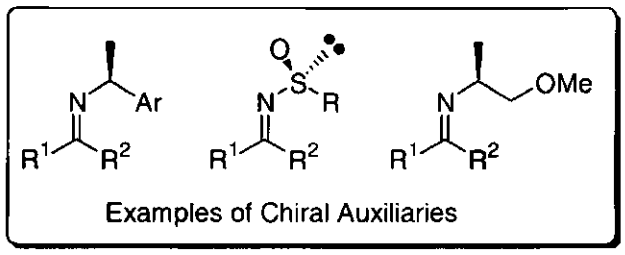

Many of the above reactions can be carried out enantioselectively by using chiral Lewis acids.[23] However, another strategy for preparing enantio-enriched amines involves stereoselective addition to enantiopure imines. Chiral non-racemic imines can be readily prepared from a chiral amine and aldehyde or ketone. After nucleophilic addition, diastereomeric amines can be separated and the chiral auxiliary can then be cleaved to afford the free amine. A number of chiral auxiliaries have been used including α-phenylethyl (-N-CH(Me)Ph),[33] α-(2-methoxyphenyl)ethyl,[34] α-naphthylethyl,[35] sulfinimes (N-S(O)Ar),[36] amino acid esters (N-CH(^{i}Pr)CO_2R),[37] and others.[38]

3.1.3 Mechanisms for Lewis Acid-Catalyzed/Promoted Reactions of Imines

Two general mechanistic pathways for Lewis acid promoted additions to imines are summarized in Schemes 3.1 and 3.2. The two pathways differ foremost in the role of the Lewis acid, either (a) to activate the imine or (b) to react with the nucleophile. Although extensive mechanistic studies on additions to imines in the presence of Lewis acids are lacking, some general points can be made.

Scheme 3.1: General Mechanism No. 1 for Lewis Acid Catalyzed Addition to Imine:Lewis Acid Activation of Imine.

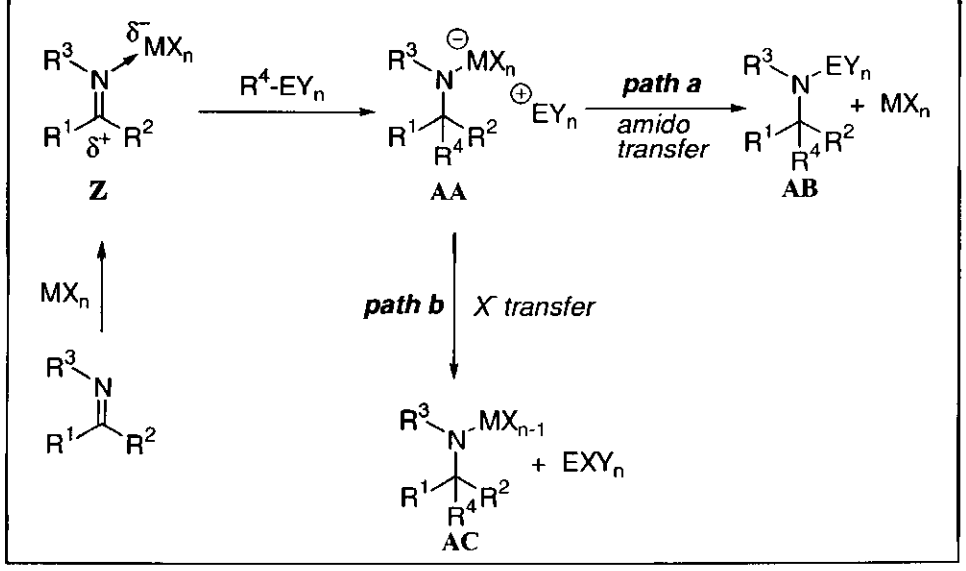

In the most commonly invoked mechanism, the Lewis acid activates the imine to nuclephilic attack, **Z**, Scheme 3.1. After nucleophilic attack, the Lewis acid (MX_n) is ligated by an anionic amido ligand, **AA**; two neutralization reactions can occur at this stage. First, transfer of the amido group to the metal cation (EY_n^+) often occurs regenerating the Lewis acid and **AB**, Scheme 3.1, path a. Alternatively, if the Lewis acid possesses labile substituents such as halides, they can be preferentially transferred to the cationic, often halophilic, metal species leading to **AC**, Scheme 3.1, path b. Stoichiometric quantities of the Lewis acid are thus often required to compensate for this "decomposition" pathway. Typically, chiral Lewis acids do not possess labile ligands in order to avoid this complication and thus can be used in catalytic quantities.

Lewis acid activation of the imine is tacitly assumed to occur (and likely does) in most addition reactions although little mechanistic work has actually been reported. In one recent study, Collum has carefully studied the addition of lithium phenylacetylide to

imines promoted by BF_3. Lithium phenylacetylide does react with BF_3:S complexes (S = Et_2O, THF, Bu_3N) in the absence of imine to give lithium borate salts; however, in the presence of imine, reaction of the imine:BF_3 complex with lithium phenylacetylide occurs immediately. Lithium borate salts were shown to be much less reactive.

Scheme 3.2: General Mechanism No.2 for Lewis Acid Catalyzed Additions to Imines: Activation of Nucleophile.

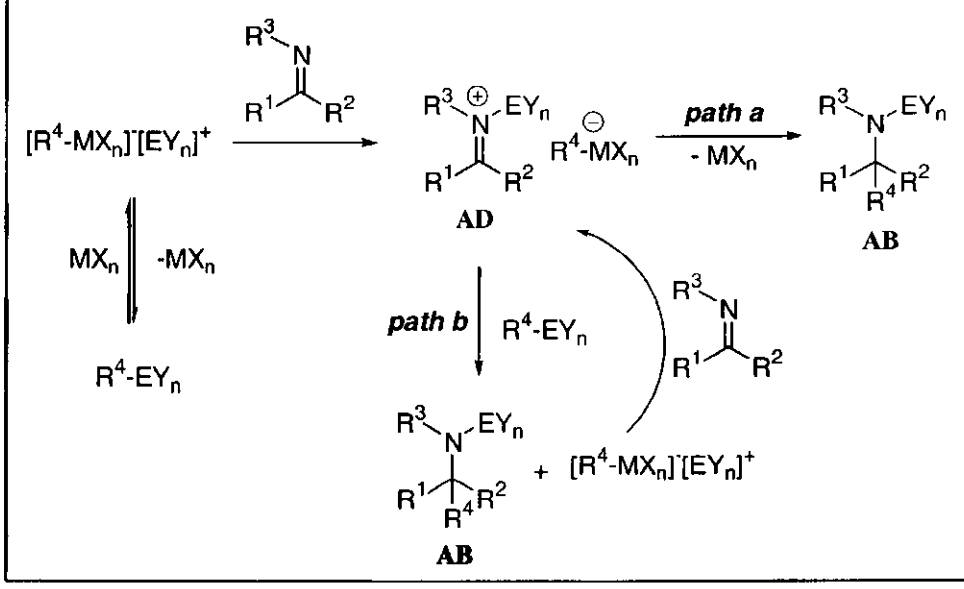

The potential does however exist for another reaction pathway in which the nucleophile reacts initially with the Lewis acid instead of the imine, Scheme 3.2. In this mechanism, the nucleophile first reacts with the Lewis acid and then this ionic reagent reacts with imine to give the addition product. This process leads to a new cationic Lewis acid (EY_n^+) that can react with the imine to generate an iminium cation, **AD**. The Lewis acid is aptly viewed as a co-catalyst responsible for generating another Lewis acid which activates the imine. This reactive iminium electrophile can react by two pathways both leading directly to the product of R^4-EY_n addition across the C=N bond, **AB**. First, delivery of R^4 by the anionic component of the ion pair can occur thereby regenerating

the neutral Lewis acid MX_n, Scheme 3.2, path a. The second possibility involves addition of a second equivalent of R^4-EY_n to the iminium cation, Scheme 3.2, path b. Upon addition, the incipient "EY_n^+" cation can be coordinated by another imine leading to a new iminium electrophile where the anion has remained intact. This scenario was encountered in the hydrosilation of carbonyls catalyzed by **1** where either hydridoborate or hydrosilane could act as the nucleophile (see Chapter 2).

Mechanistic studies in support of such a pathway have not been reported for additions to imines. There is no evidence to suggest that reaction of a neutral Lewis acid with the nucleophile can promote an ionic reaction pathway. There are however, a number of examples where iminium ion intermediates are certainly involved in addition reactions.[39] For example, activation of imines to nucleophilic attack by discrete cationic Lewis acids or ionizable Lewis acids undoubtedly involve ionic intermediates (eg. TMSOTf[40]).

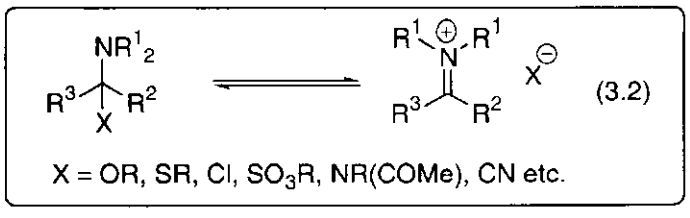

Other methods for producing reactive iminium ions both as preformed entities or *in situ* have been developed.[41] For example, various geminally substituted amines can be converted to iminium cations (often aided by a Lewis acid), equation 3.2. Secondary amines can react with aldehydes or ketones to generate N,N-dialkyliminium compounds. Iminium salts can also be generated electrochemically from tertiary amines.[42] In particular, the N-acyliminium class of compounds has found extensive application as reactive electrophiles. Mayr has estimated the electrophilicities of dialkyl iminium ions

relative to a range of nucleophiles.[43] Thus the formation of cationic iminium cations is an effective strategy for generating highly reactive species where activation by a neutral Lewis acid is oftentimes insufficient.

3.1.4 Coordination Chemistry of Imines and Lewis Acids

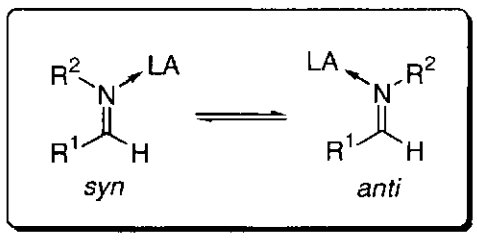

It is widely acknowledged that the possibility exists for geometrical isomers (*syn vs anti*)[i] of imine adducts of Lewis acids.[44] Often it has been hypothesized that competitive reaction via the isomers can affect the stereoselectivity of a nucleophilic addition. However, only in a few studies has any type of experimental evidence been reported that supports the notion that *syn-anti* isomerism is an important factor to consider. Invariably, the few existing studies rely on NMR spectroscopic observation of adducts or product analysis to make claims that competitive reaction via the two isomers is likely occurring.

For example, Keck has rationalized temperature and mixing effects on the observed stereoselectivity of addition of crotyltributylstannane to aldimines based on the potential for reaction via two different complexes, **AE** and **AF**, Scheme 3.3.[27a] At higher temperatures, the sterically preferred isomer **AF** is formed in greater amounts leading to a diminished stereoselectivity. These studies suggested that **AE** and **AF** can interconvert at higher temperatures; however, no suggestion of how this isomerization occurs was

---

[i] In this description, the syn/anti designation refers to the relative orientation of R^1 and R^2 and thus is consistent with the designation for the free imine.

advanced. Additionally, it was reasoned that $TiCl_4$ must be more sterically demanding than the benzyl group thus leading to conversion to **AF** where the $TiCl_4$ group is *syn* to the hydrogen. No NMR or other experimental observation for adducts **AE** or **AF** was provided.

Scheme 3.3: Temperature Effects on Crotylstannation of Imines.

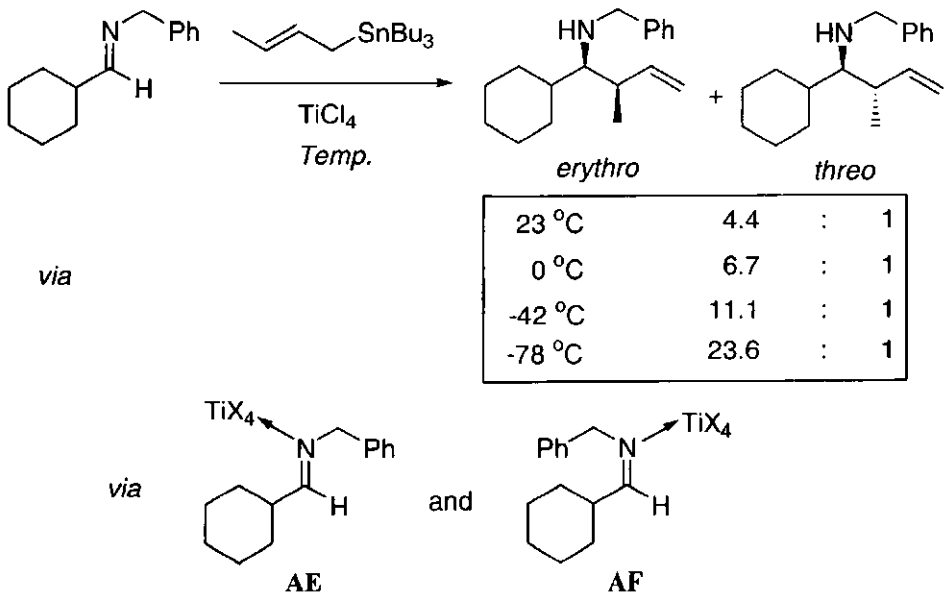

In another example, Fujisawa has rationalized a switchover in selectivity in an addition reaction to **AG** when the Lewis acid was switched from TiF_4 to $TiCl_4$ based on the formation of two "different types of complexes" although this was not specifically related to *syn/anti* isomerism.[31] As the sole supporting piece of evidence aside from product analysis, the ^1H NMR spectrum of **AG**:TiF_4 showed the imino proton at 8.47 versus 8.92 ppm for **AG**:$TiCl_4$ Temperature was also shown to have a noticeable effect on stereoselectivities, but no reasoning was provided for this observation.

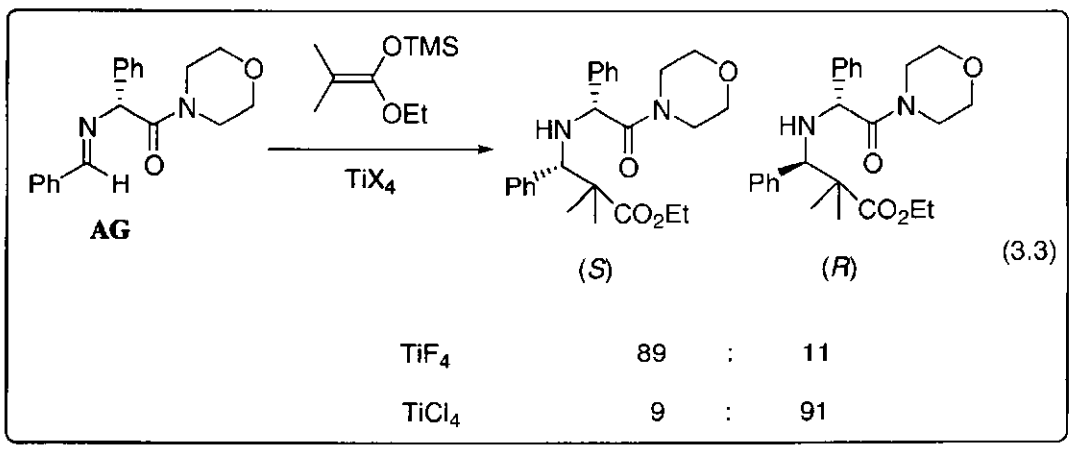

(3.3)

Brown and co-workers have recently reported the synthesis of N-unsubstituted imine trialkylborane adducts from the corresponding N-silyl imines via protonation by MeOH.[45] Although it was schematically implied that the protonation reactions occur from the isomer with the boron *syn* to the hydrogen of aldimines, **AH**, this was not explicitly proven. Protonation could occur from the other isomer, **AI**, followed by isomerization of the primary imine:borane adduct. In either case, isomerization about the C=N bond clearly does take place at one stage of the reaction.

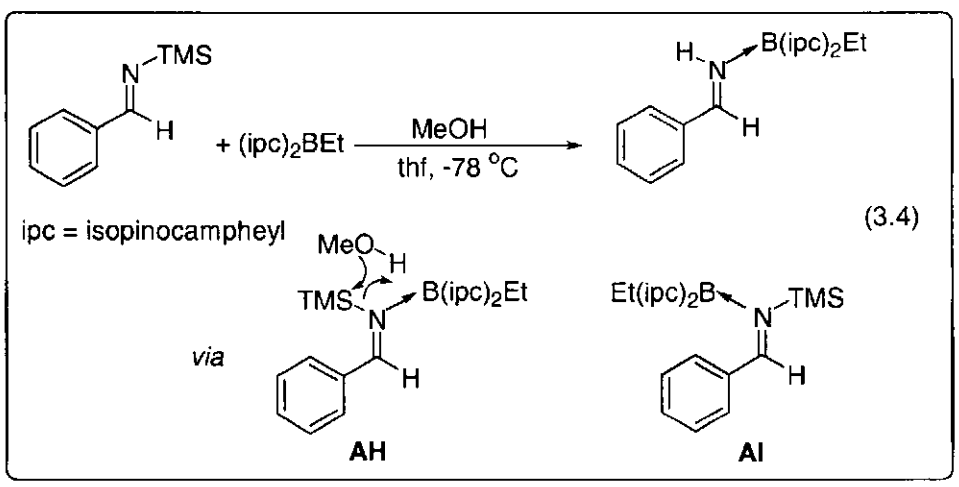

(3.4)

The importance of *syn/anti* isomerism was clearly shown by the Buchwald group in asymmetric hydrogenations catalyzed by chiral titanocene complexes, Scheme 3.4.[11] However, again all suppositions made were based on product analysis and not by direct

observation of imine:Lewis acid (Ti) intermediates. In this work, it was suggested that low enantioselectivities were a result of competitive reaction of both the syn and anti imine isomers. In the presence of an enantiopure catalyst, it is speculated that the *anti* imine is selectively transformed to the (*R*)-amine whereas the *syn* imine leads preferentially to the (*S*)-amine.

Scheme 3.4: Mechanistic Proposal for Asymmetric Hydrogenation of Imines by Chiral Titanocene Catalyst

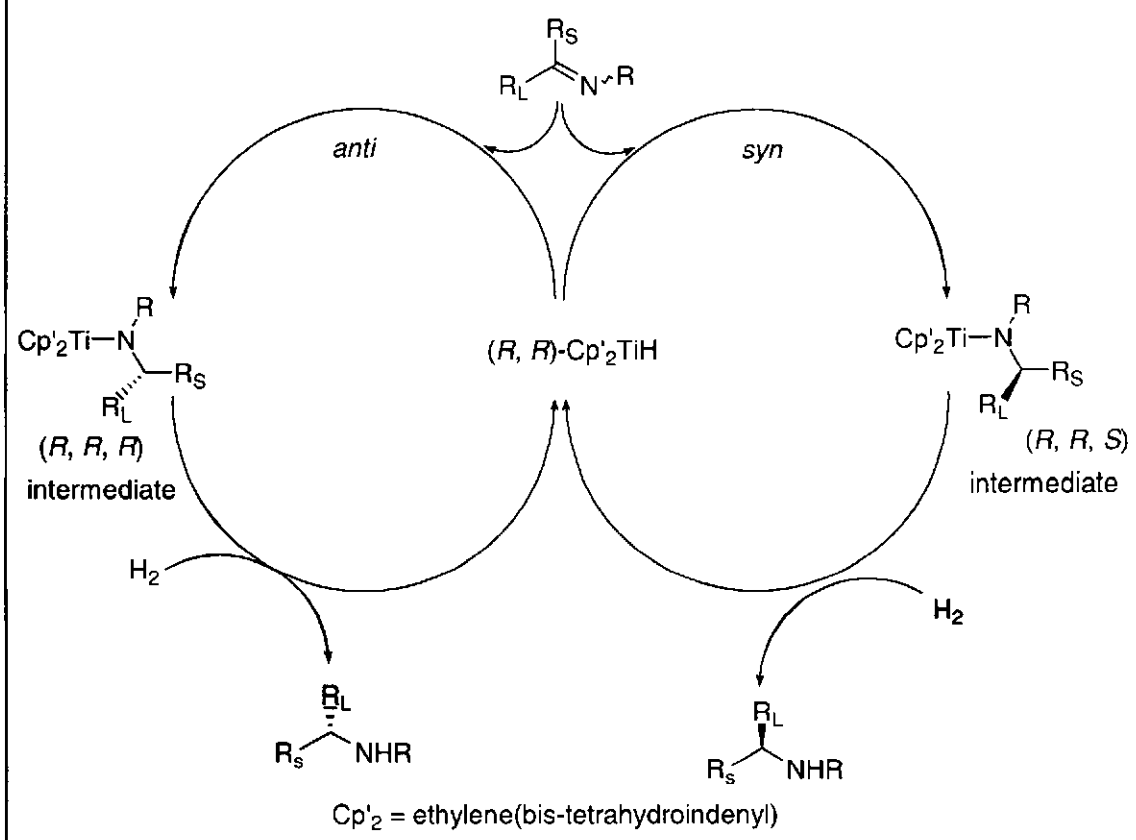

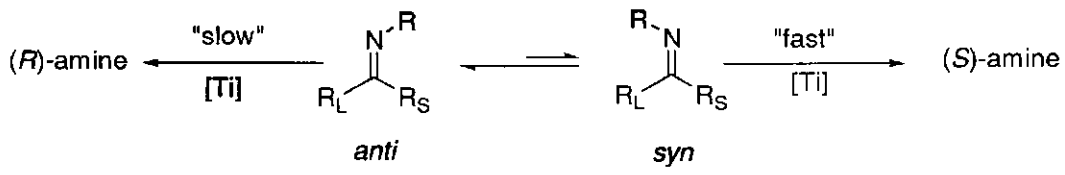

For imines known to exist as mixtures of *syn* and *anti* isomers, enantioselectivities are thus low. Interestingly, reductions under lower pressures of dihydrogen led to a decrease in the enantioselectivity where the authors reasoned that the lower hydrogenation rates enable imine isomerization to take place[46] and thus more of the reaction occurs via the faster reacting *syn* isomer. Although the *syn* isomer is sterically disfavored, when complexed to Ti, this effect is lessened or even reversed; that is, the titanium fragment coordinates more readily *syn* to the small substituent, R_s. As the *syn* isomer is consumed, reequilibration of unreacted imine generates more syn isomer.

In one case, the enantioselectivity could be reversed depending on H_2 pressure, albeit from 79% (*R*) isomer to 4% (*S*) isomer. Much higher enantioselectivities were observed for cyclic imines where *syn/anti* isomerization is not a factor. This work underscores the importance of *syn/anti* isomerism in asymmetric reactions and that controlling which Lewis acid:imine complex reacts predominantly can be crucial to success. This is particularly true if the two isomers react via opposite enantiofaces and is relevant to strategies employing either chiral Lewis acids or chiral N-substituents.

Very few reports of X-ray structures of adducts of mono-functional, non-chelating imines with main group Lewis acids have appeared. Most examples involve transition metals and are not directly related to studies on nucleophilic additions to imines.[46] In other cases, X-ray structures of metals coordinated by primary imines (N-substituent equals hydrogen) have been reported but are not of much relevance to typical imines used in addition reactions.[47] Additionally, a number of X-ray structures have been reported of imines incorporated into a multidentate ligand such as the salicylaldiminato class of

ligands where again, study of addition reactions to the imine is not the focus of the chemistry.

3.2 $B(C_6F_5)_3$-Catalyzed Hydrosilation of Imines

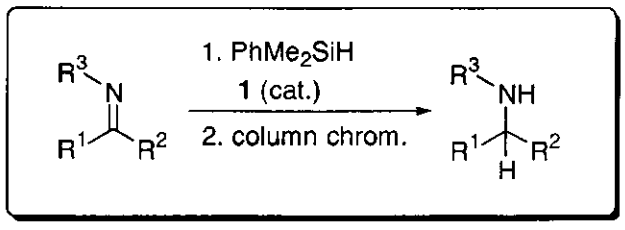

A convenient and general method for the hydrosilation of a variety of imines catalyzed by **1** has been developed with the technical assistance of undergraduate researchers Eric Sommor and Tiziana Scocitti. Upon purification by column chromatography, the silated amines are hydrolyzed to secondary amines that can be isolated in generally high yields. Furthermore, this chemistry has been adapted to a one-pot reductive amination protocol where aldimines can be generated *in situ* from aldehydes and subsequently reduced to the secondary amines.

3.2.1 Imine Hydrosilation

A variety of benzaldimines have been hydrosilated in high yields using $PhMe_2SiH$, Et_3SiH or Ph_2SiH_2, Table 3.1. In general, reactions proceed much quicker using $PhMe_2SiH$ or Ph_2SiH_2. The reaction times and temperatures varied considerably amongst the substrates. Less basic imines particularly those possessing electron-withdrawing N-substituents are hydrosilated most readily. Imines possessing bulky groups are rapidly hydrosilated as well (eg. entry 5 vs entry 12). In section 3.2.3, these reactivity differences are discussed in relation to the proposed mechanism.

Table 3.1: Hydrosilation of Aromatic Aldimines

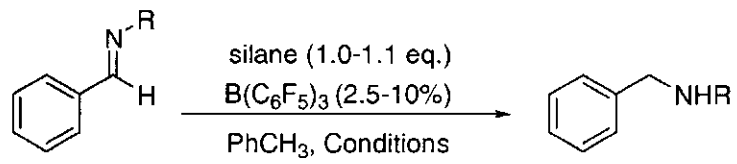

Entry	R	silane	Conditions	Yield
1	**Ph**	Et_3SiH	12 h, 70 °C	90%
2	**Ph**	$PhMe_2SiH$	1h, rt	>95%
3	**Ph**	Ph_2SiH_2	1h, rt	>95%
4	**^{t}Bu**	Et_3SiH	20 h, 70 °C	30%
5	**^{t}Bu**	$PhMe_2SiH$	30 min, rt	80%
6	**^{t}Bu**	Ph_2SiH_2	30 min, rt	61%
7	SO_2Ph	Et_3SiH	30 min, rt	89%
8	SO_2Ph	$PhMe_2SiH$	30 min, rt	93%
9	SO_2Ph	Ph_2SiH_2	1h, rt	>95%
10	**Bn**	Et_3SiH	16 h, 70 °C	84%
11	**Bn**	$PhMe_2SiH$	3h, 70 °C	91%
12	**Me**	$PhMe_2SiH$	72 h, 70 °C	n.r.
13	allyl	$PhMe_2SiH$	26 h, 70 °C	57%
14	allyl	Ph_2SiH_2	20 h, 70 °C	63%
15	^{t}Boc	Et_3SiH	30 min, rt	60%
16	^{t}Boc	Ph_2SiH_2	30 min, rt	60%

Ketimines can also be hydrosilated in high yields, Table 3.2. Interestingly, relative to comparable aldimines, ketimines tend to react faster (cg. Table 3.1, entry 11 vs

Table 3.2, entry 2). Again, a rationale for this is discussed in Section 3.2.3 in reference to the proposed mechanism.

Table 3.2: Hydrosilation of Ketimines

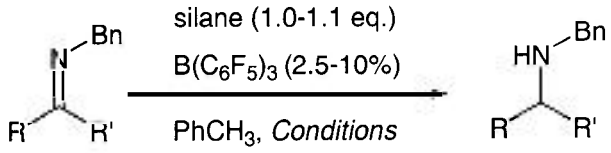

Entry	R	R'	silane	Conditions	Yield
1	Ph	Me	Et_3SiH	4 h, 70 °C	89%
2	Ph	Me	$PhMe_2SiH$	4h, rt	>95%
3	Ph	Me	Ph_2SiH_2	4h, rt	87%
4	Ph	Ph	Et_3SiH	20 h, 70 °C	n.r.
5	Ph	Ph	$PhMe_2SiH$	96 h, rt	96%
6	Ph	Ph	Ph_2SiH_2	16h, rt	80%
7	^tBu	Me	Et_3SiH	48h, 70 °C	66%
8	^tBu	Me	$PhMe_2SiH$	42 h, 70 °C	87%
9	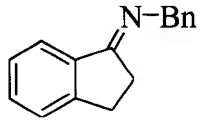		$PhMe_2SiH$ Ph_2SiH_2	21 h, rt 23 h, rt	>95% 91%

3.2.2 Reductive Amination

Table 3.3: Reductive Amination of Aldehydes

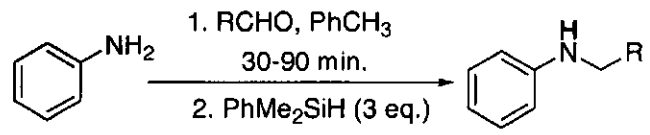

RCHO	Yield
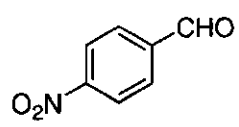	>95%
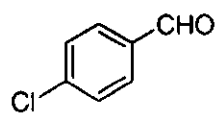	>95%
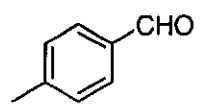	>95%
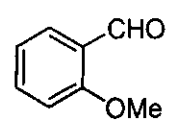	73%*
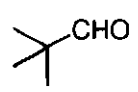	>95%
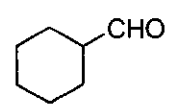	69%

* required 7 days at room temperature for second stage of reaction

Generation of imines from an aldehyde and an amine followed by *in situ* reduction is an important strategy for the formation of secondary amines and is referred to as reductive amination. The imine hydrosilation chemistry presented in Section 3.2.1 has been adapted to this end, Table 3.3. The procedure is convenient, consisting of

premixing the aldehyde with aniline, which generates the imine, followed by addition of three equivalents of silane and catalytic **1**. Two extra equivalents of silane are required to silate the water formed in the imine condensation reaction. The formation of $PhMe_2SiOSiMe_2Ph$ is confirmed by GC-MS analysis. Typically, after 24 hours, hydrosilation of the imine is complete (verified by GC-MS) except in the case of the imine derived from *ortho*-anisaldehyde (entry 4), which required 96 hours. Purification consists simply of placing the reaction mixture directly on a column packed with silica gel and eluting with hexanes/ethyl acetate mixtures.

In addition to aromatic aldimines, the procedure is applicable to aliphatic aldimines. This procedure has been adapted to the hydrosilation of one ketimine as well, equation 3.5. Since ketimine formation generally requires Lewis acid activation and or heat, simply mixing ketone and amine was not successful. However, when acetophenone and benzyl amine are refluxed in toluene in the presence of catalytic $ZnCl_2$, the ketimine PhC(Me)=NBn, is quantitatively formed. Cooling the reaction mixture to room temperature and adding **1** (5 mol%) and three equivalents of silane provides the secondary amine product in high yield after purification.

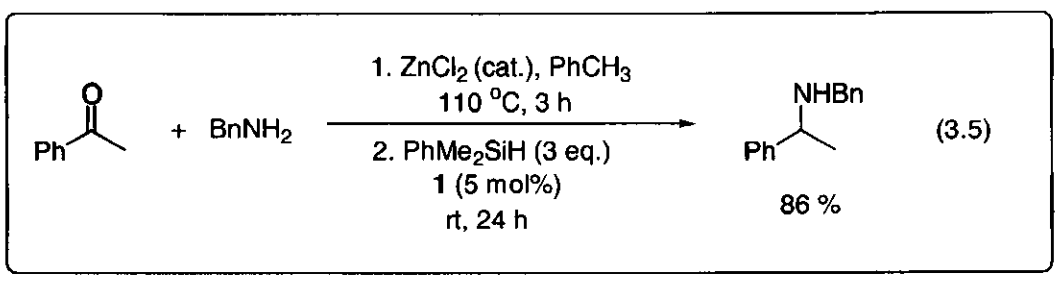

3.2.3 Mechanistic Proposal for Hydrosilation of Imines

Scheme 3.5: Proposed Mechanism for $B(C_6F_5)_3$-Catalyzed Imine Hydrosilation.

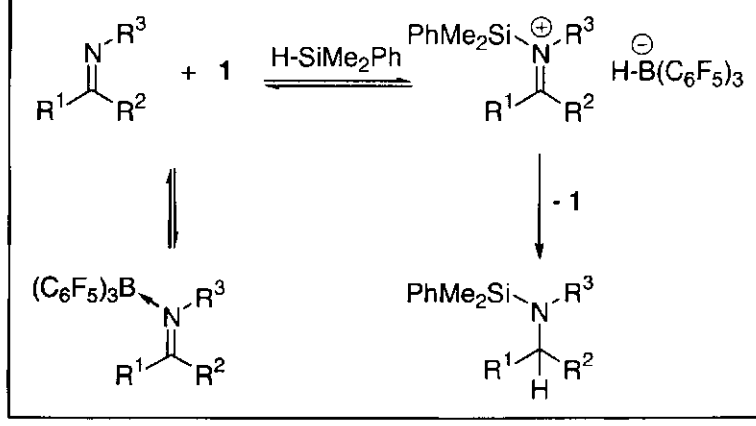

A mechanistic proposal for the hydrosilation of imines catalyzed by **1** is outlined in Scheme 3.5. This proposed mechanism is analogous to that described for the hydrosilation of aldehydes and ketones. Even though borane imine adducts are readily formed and have been extensively characterized (see below), these species are not believed to be direct intermediates in hydrosilation. As in the carbonyl hydrosilation studies, the proposed role of **1** is to activate the silane to nucleophilic attack, in this case, by an imine. This leads to the formation of a silyliminium intermediate with a hydridoborate counterion. It is this intermediate that participates in subsequent hydride delivery. Evidence suggests that hydridoborate delivery consummates the hydrosilation process.

Qualitative reactivity trends and NMR studies support this general mechanistic proposal. First, qualitative rate effects indicate that hydrosilations occur fastest for both sterically and electronically less basic imines. The manifestation of this trend is proposed to result from the requirement for access to uncoordinated **1** in order for silane activation to occur. Less basic imines do not sequester **1**. Aldimines are hydrosilated much slower

than analogous ketimines. For example, PhCH=NBn is hydrosilated much slower than PhC(Me)=NBn, Table 3.1, entry 2 and Table 3.2, entry 2. Hydrosilation of PhCH=NBn at room temperature occurs only very slowly over the course of days whereas PhC(Me)=NBn is completely hydrosilated after four hours at room temperature. If hydrosilation were to occur directly on the imine adducts of PhCH=NBn and PhC(Me)=NBn, then reaction would be predicted to occur fastest for PhCH=NBn based on steric arguments. This observation and rationalization is similar to that observed for relative rates of hydrosilation of esters, ketones and aldehydes.

The steric bulk of the N-substituent can also affect the propensity of an imine to undergo hydrosilation. For example, comparing the benzaldimines, PhCH=NMe versus PhCH=N^{t}Bu, a dramatic rate enhancement is observed for the bulky *tert*-butyl substituted imine, Table 3.1, entries 5 and 12. In fact, PhCH=NMe does not react at all. This difference is interpreted in terms of the relative binding abilities of the two imines to **1**. The bulky PhCH=N^{t}Bu is expected to bind **1** much less strongly than PhCH=NMe and therefore **1** is available to activate silane. In fact, ^{19}F NMR analysis of a 10:1 mixture of PhCH=N^{t}Bu and **1** reveals no strong interaction between the two.

Hydrosilation occurs much more readily for imines with electron-withdrawing N-substituents, most notably -SO_2Ph and -^{t}BOC. Although this may not be surprising since the C=N bond is more polarized, even dramatic increases are observed for N-benzylidine aniline versus N-benzylidine benzylamine, Table 3.1, entries 2 and 11. The hydrosilation of PhCH=NPh with $PhMe_2SiH$ occurs rapidly and exothermically whereas that of PhCH=NBn requires 3 hours at 70 °C. Again, it is proposed that this reactivity difference relates inversely to the binding of the imines to **1**. Comparison of bond lengths obtained

by X-ray crystallography for the borane adducts of PHCH=NPh and PHCH=NBn (see Section 3.3.2) confirm that **1** is bound more strongly in the latter case despite the fact PhCH=NBn is less reactive to hydrosilation. Also, when PhCH=NBn is mixed with preformed PhCH=NPh:$B(C_6F_5)_3$ in C_7D_8 at room temperature, complete conversion to PhCH=NBn:$B(C_6F_5)_3$ occurs after a few minutes.

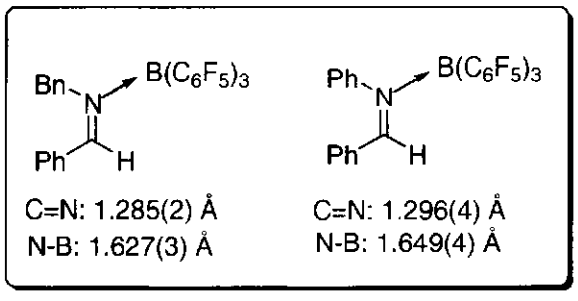

Spectroscopic evidence supporting the proposed mechanism has also been obtained. Using Ph_2C=NBn, **27**, it was possible to directly observe a key intermediate proposed in Scheme 3.5. When Ph_2C=NBn is mixed with equimolar quantities of $PhMe_2SiH$ and **1** in C_7D_8, ^1H, ^{19}F, ^{13}C, ^{11}B and ^{29}Si NMR analysis indicates that a new species is produced formulated as $[Ph_2C{=}N(Bn)SiMe_2Ph]^+[H\text{-}B(C_6F_5)_3]^-$, **28**. A two-layer mixture is formed in the NMR tube, typical of ion-pairs derived from perfluoroarylborate anions.[48] This type of behavior was encountered in Chapter 2 in the discussion on the formation of ion-pair **25** which also contained a hydridoborate counterion.

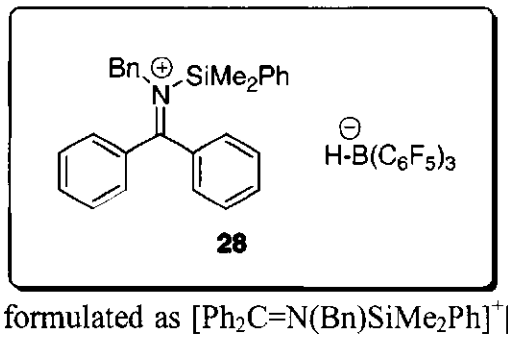

28

The reaction could be performed on large enough scale (0.20 mmol) allowing direct NMR analysis of the bottom layer. ^{19}F NMR analysis clearly indicates that an anionic borate has been formed ($\Delta\delta_{p,m}$ = 2.8 ppm). A negative value, -24.7 ppm, for the ^{11}B NMR shift of this compound also suggests formation of an anionic borate. The

identification of this anionic borate as $[H\text{-}B(C_6F_5)_3]^-$ was confirmed by carrying out a $^{11}B/^1H$ HETCOR NMR experiment. The ^{11}B NMR signal at -24.7 ppm correlated with a broad signal in the ^1H NMR at 5 ppm. The ^{11}B NMR resonance observed was broad and therefore coupling to the hydrogen was not detected. Notably, the ^1H, ^{11}B and ^{19}F NMR closely match the spectra for $[Bu_4N]^+[H\text{-}B(C_6F_5)_3]^-$, **26**, described in Chapter 2. A ^{29}Si NMR shift of 26.9 ppm was obtained consistent with other nitrogen-base coordinated silylium cations (see Chapter 1).[49] ^1H and ^{13}C NMR spectra were also consistent with formation of **28**. Ion pair **28** is surprisingly stable remaining intact over several hours. Over time, the two-layer reaction mixture is gradually converted into one layer and ^1H NMR analysis confirms that $Ph_2CH\text{-}N(Bn)SiMe_2Ph$, **29**, is slowly formed. Under catalytic conditions (10 mol% **1**), ^{19}F NMR confirms that **28** is present throughout the reaction as **29** is being formed.

Figure 3.1: ^{19}F, ^{29}Si and ^{11}B NMR Spectra of Ion-Pair 28.

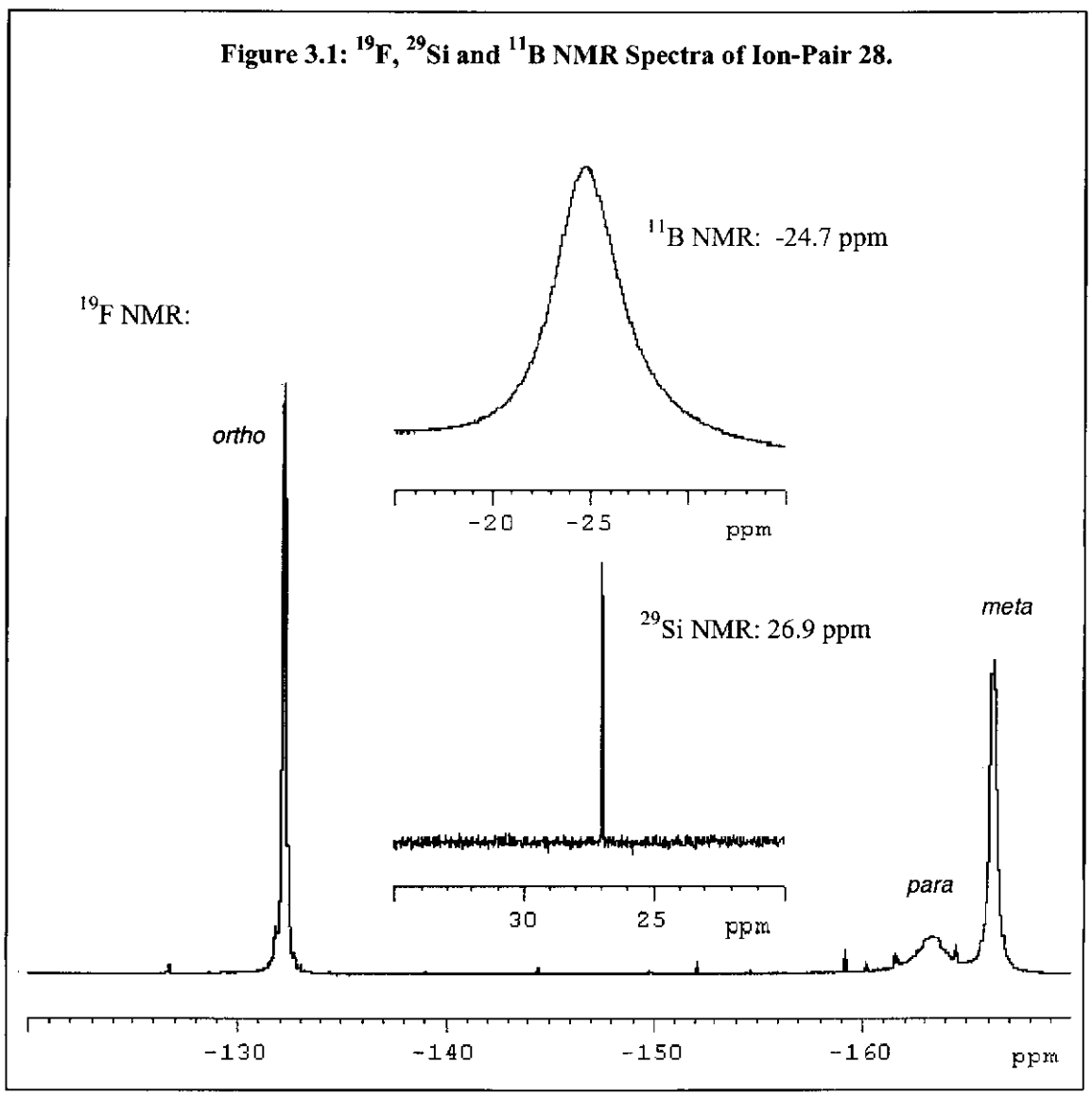

Evidence has been obtained that suggests that hydride delivery to the silyliminium intermediates occurs by the hydridoborate counterion although further work needs to be carried out to support this hypothesis. Cross-over studies similar to those described for the hydrosilation of acetophenone were found to be inappropriate since rapid H/D scrambling between silanes occurs. The evidence that has been obtained in support of hydridoborate delivery is the following. $[Et_3Si(arene)]^+[B(C_6F_5)_4]^-$, **2**, catalyzes both the reaction of PhCH=NPh with $PhMe_2SiH$ and PhC(Me)=NBn with $PhMe_2SiH$ in CD_2Cl_2,

but the reactions are much slower than reactions catalyzed by **1**. For example, **PhCH**=NPh is hydrosilated rapidly with $PhMe_2SiH$ at low temperature (~-40 °C) using ~5 mol% **1** as a catalyst whereas with >10 mol% **2** as catalyst, the reaction takes hours at room temperature to reach completion. With **2** as catalyst, hydrosilation does not occur to any significant extent in C_6D_6 even with heating although with **1** as catalyst, the reactions proceed smoothly. In the former case, a two-layer reaction mixture is formed where presumably the bottom layer contains the ion-pair formed from coordination of imine to "Et_3Si^+" (or "$PhMe_2Si^+$").[ii] In CD_2Cl_2, the ion pairs are soluble and thus reaction with silane is assisted yet still sluggish. Therefore, although hydrosilation can be catalyzed using a silylium activator where hydride delivery necessarily occurs from silane, the reactions are sluggish compared to reactions catalyzed by **1**. In the latter case, the possibility for hydridoborate delivery to the silyliminium cation exists. Silyliminium intermediates have previously been proposed as intermediates in imine reductions with silanes employing TMSOTf as catalyst.[40]

Of course, it is possible that formation of ion-pairs such as **28** is actually a dead-end in the reaction pathway and that reversal to the neutral components **1**, $PhMe_2SiH$ and **27** is necessary for productive reaction to ensue via a more conventional reaction pathway. However, the collective evidence indicates that imine hydrosilation catalyzed by **1** proceeds via silyliminium intermediates. This mechanistic proposal therefore represents an example of mechanistic pathway 2 described in Scheme 3.2 where the role of the Lewis acid (**1**) is to react/activate the nucleophile ($H\text{-}SiR_3$). This leads to *in situ*

[ii] $[Et_3Si]^+[B(C_6F_5)_4]^-$ was used rather than $[PhMe_2Si]^+[B(C_6F_5)_4]^-$ since formation of the latter by reaction with $[Ph_3C]^+[B(C_6F_5)_4]^-$ is not a clean reaction. $PhMe_2SiH$ was used since reactions with Et_3SiH were very slow.

generation of a new Lewis acid ("R_3Si^+") which then activates the imine to nucleophilic attack by formation of a silyliminium intermediate. Aside from the evidence provided herein, this type of mechanism has not been shown to occur in other Lewis acid catalyzed additions to imines. Finally, differences in reactivity between catalysis by **1** and $[Et_3Si(arene)]^+[B(C_6F_5)_4]^-$ suggest that hydridoborate delivery to the silyliminium intermediate occurs when catalyzed by **1**.

3.3 Coordination of Imines to $B(C_6F_5)_3$

As mentioned, few studies of Lewis acid complexes of imines have been reported. Although, it turns out that imine adducts of **1** are not likely to be direct intermediates in the hydrosilation reaction (see Section 3.2.3), some features both in solution and in the solid state are of potentially broader interest. Furthermore, **1** can be viewed as a model for BF_3 which is used to catalyze a number of addition reactions to imines. Reactions (other than hydrosilation) could be developed that do directly involve the intermediacy of imine adducts of **1**.

3.3.1 NMR Characterization/Dynamics

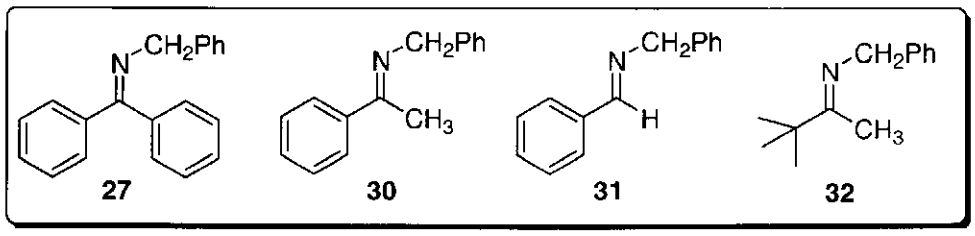

The solution behavior of four N-benzyl substituted imines, **27**, **30-32**, was studied by ^{1}H and ^{19}F NMR spectroscopy. This group includes a symmetrical ketimine, **27**, two unsymmetrical ketimines, **30** and **32**, and an aldimine, **31**.

Figure 3.2: 282 MHz ^{19}F NMR spectra of Adduct 33 at (a) -40 °C, (b) 25 °C and (c) 60 °C.

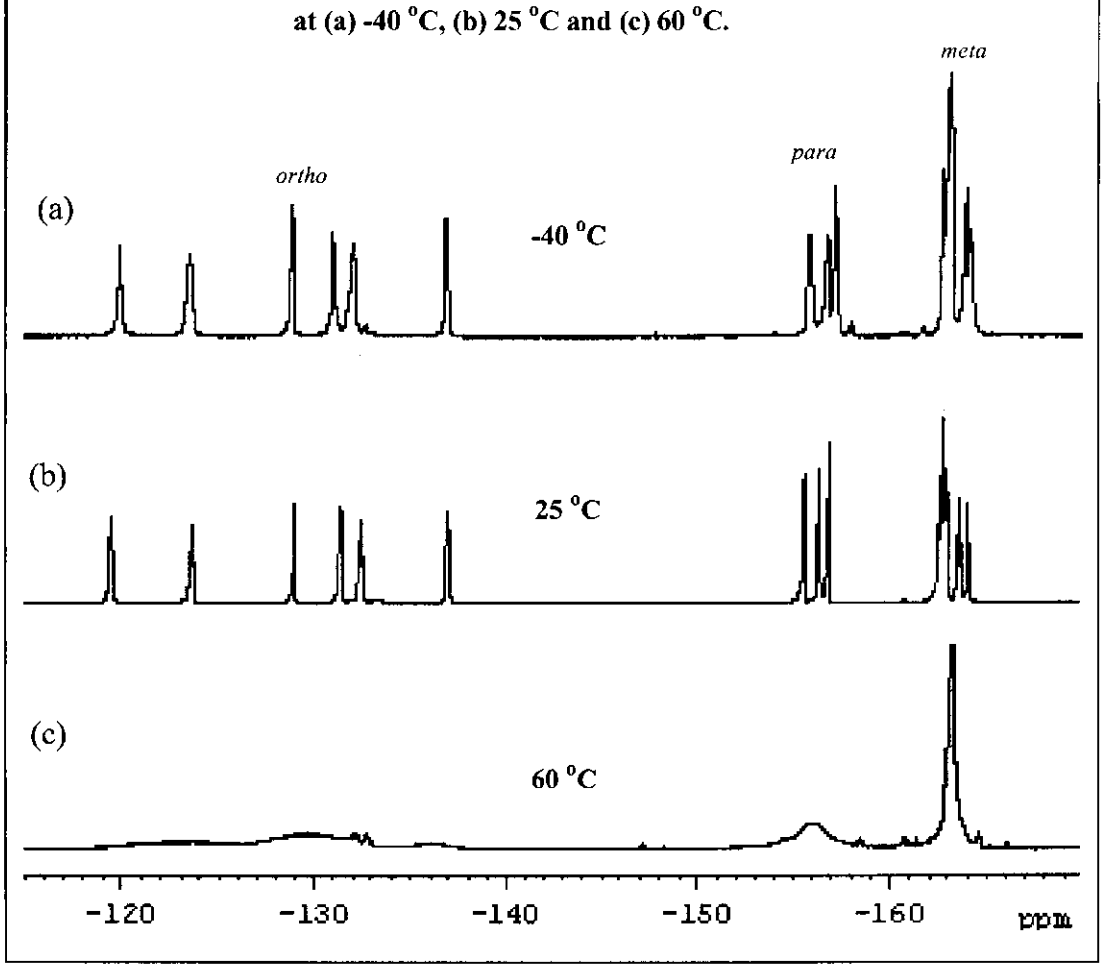

When ketimine **27** is mixed with an equivalent of of **1** in C_7D_8 at low temperature, a complex ^{19}F NMR spectrum is obtained for adduct **33** at -40 °C, Figure 3.2a. Six separate signals are observed for both the *ortho* (-119 to -137 ppm) and *meta* (-162 to -164 ppm) signals and three separate signals are observed for the *para* (-155 to -157 ppm) signals. The three pentafluorophenyl groups are all different and furthermore, the symmetry of each ring is lost. Rotation about the B-N bond and the three B-C bonds is restricted; the likely origins for this rigidity are discussed in section 3.3.2. Based on the severely broadened spectrum obtained at 60 °C, Figure 3.2c, some freedom to rotate is allowed at higher temperature. The ^1H NMR spectrum at low temperature indicates restricted rotation as well, Figure 3.3a. Specifically, two distinct resonances are observed for the benzylic hydrogens. Coalescence of these two signals is observed at ~40 °C ($\Delta G^{\ddagger} = 59.9$ kJmol^{-1}).

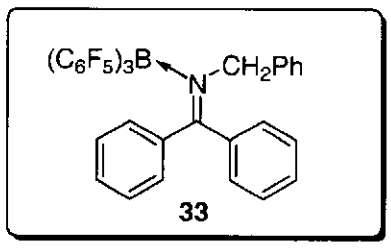

33

Figure 3.3: 300 MHz NMR Spectra of Adduct 33 Showing Coalescence of Benzylic Hydrogens

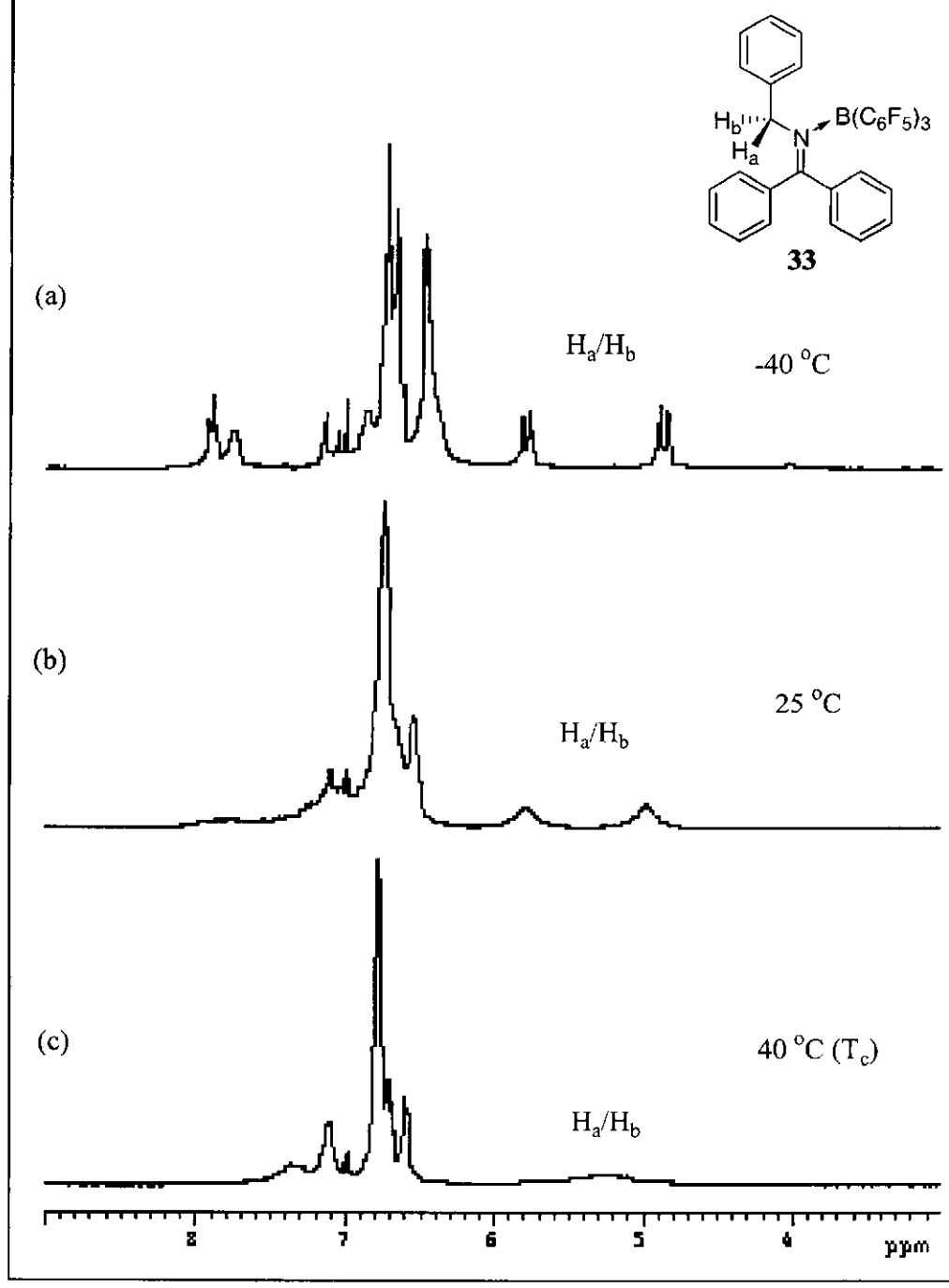

Figure 3.4: 282 MHz ^{19}NMR Spectra (C_7D_8) of (a) Adduct 34-k at -40 °C and (b) Adduct 34-t at -40 °C

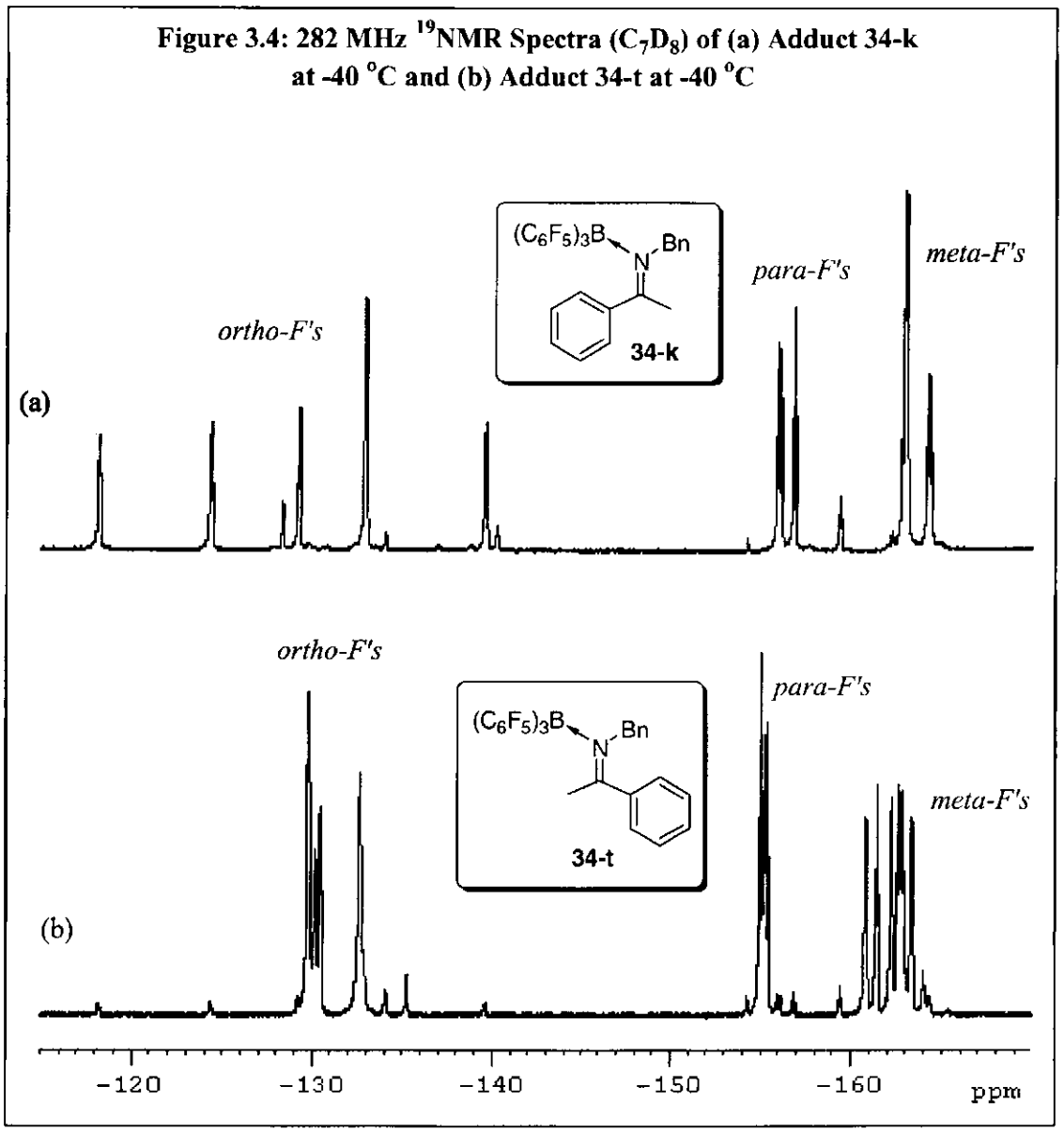

A similar ^{19}F NMR spectrum was obtained for adduct **34-k** (formed at low temperature, **k** for kinetic) at -40 °C, Figure 3.4a. The ^{1}H NMR spectrum however shows only one broad signal for the benzylic hydrogens at this temperature. Upon warming, adduct **34-k** is converted almost completely to a second adduct **34-t** (**t** for thermodynamic) resulting in an approximately

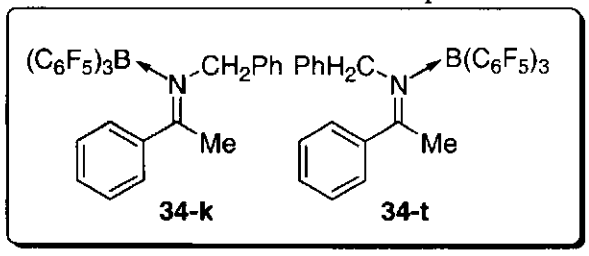

10:1 ratio of **34-t**:**34-k**.[iii] This isomerization between the two Lewis acid adducts is believed to take place via the uncoordinated imines; that is, dissociation followed by imine isomerization followed by recoordination converts **34-k** into **34-t**. The isomerization is greatly slowed down in the presence of excess **1** supporting this hypothesis, Scheme 3.5.

Scheme 3.5: Isomerization of 34-k to 34-t via Free Imines.

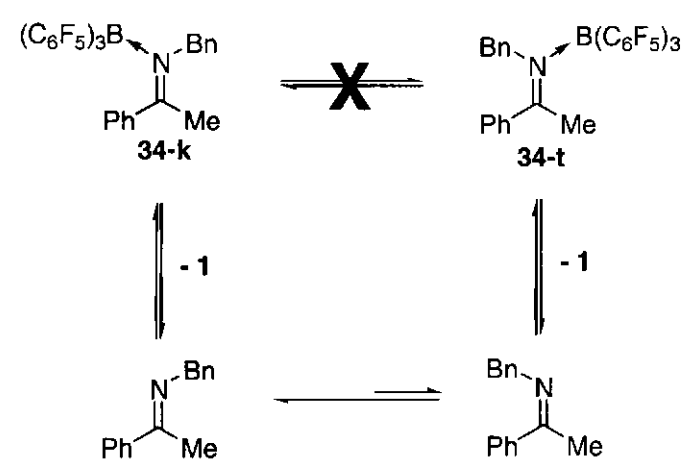

Again ^{19}F NMR analysis of the thermodynamic isomer (sample recooled to -40 °C) shows clear evidence for restricted rotation of the benzylic group, Figure 3.4b. The ^{1}H NMR spectrum of this thermodynamic isomer shows two signals for the benzylic hydrogens which coalesce at approximately 56 °C ($\Delta G^{\ddagger} = 66.6$ kJmol^{-1}).

The kinetic and thermodynamic adducts were characterized as **34-k** and **34-t** respectively based on the following evidence. First, ketimine **30** exists in solution as one predominant isomer with the benzyl group *anti* to the phenyl group.[50] The lone pair responsible for coordination to **1** is *syn* to the phenyl ring; coordination of **1** by this

[iii] This ratio does not change noticeably in temperature range of -70 °C to 25 °C. In C_6D_6, the ratio is approximately 5:1 **34-t**:**34-k**.

isomer would lead to **34-k**. A thermodynamic mixture (~5:1) of **34-t**:**34-k** in C_6D_6 was subjected to nOe NMR experiments. Irradiation of the benzylic ^{1}H's in **34-k** led to positive enhancement in the methyl ^{1}H's and *vice versa*. No such enhancements were observed for **34-t**. Additionally, a ^{19}F/^{1}H nOe experiment on adduct **34-t** reveals a positive enhancement in the methyl ^{1}H's upon individual irradiation of the six *ortho* F's. Furthermore, **34-t** would be expected to predominate under thermodynamic conditions since this isomer places the bulky borane substituent *syn* to the smaller methyl group.

Figure 3.5: 282 MHz ^{19}F NMR Spectra of (a) Adduct 35-k at -40 °C and (b) Adduct 35-t at -40 °C

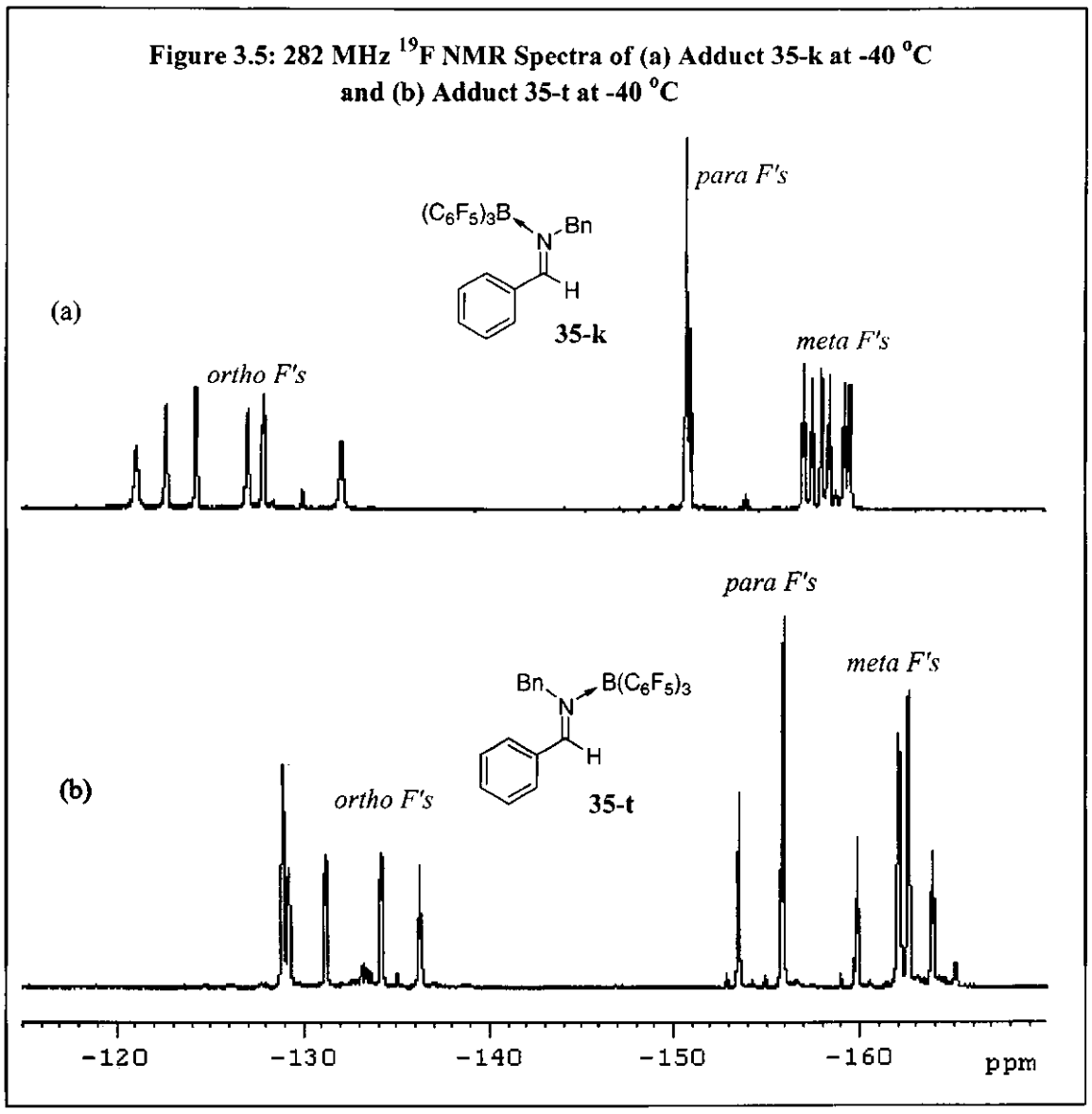

Two adducts of aldimine **31** have also been characterized by NMR spectroscopy, **35-k**/**35-t**, Figure 3.5. At -40 °C, adduct **35-k** is formed exclusively where presumably the borane group is syn to the phenyl ring through reaction of the predominant *anti*-imine isomer of **31**. Upon warming to room temperature, the thermodynamic adduct **35-t** forms quantitatively. The ^{19}F NMR spectra (both at -40 °C) for both compounds again illustrate an element of restricted rotation as all fifteen fluorines in each case are unique, Figure 3.5. In the ^{1}H NMR spectrum, two distinct benzylic signals are observed for each isomer at -40 °C. Interestingly, the benzylic signals for the thermodynamic isomer coalesce at a lower temperature (~ -10 °C, $\Delta G^{\ddagger} = 52.1$ kJmol^{-1}) relative to that for the kinetic isomer (~ 20 °C, $\Delta G^{\ddagger} = 58.5$ kJmol^{-1}). A possible reason for this disparity is discussed in the following section.

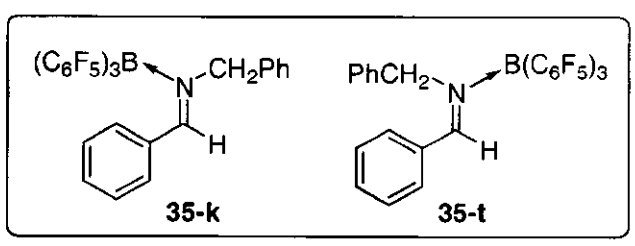

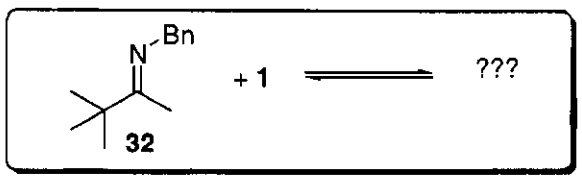

Imine **32** undergoes an unexpected reaction with **1**. Upon addition of one equivalent of **1** dissolved in C_6D_6, **32** is partially converted (~40% conversion) to a new compound for which the NMR spectral data is in disaccord with that expected for simple adducts **36-k** or **36-t**. When **32** and **1** are mixed in a 1:4 ratio, this new compound predominates allowing complete characterization by NMR spectroscopy. In

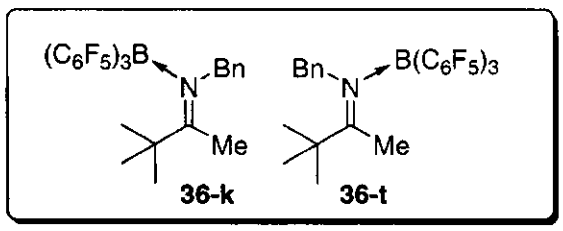

addition to ^{19}F resonances resulting from excess **1**, a new set of three signals is observed where the value for $\Delta\delta_{p,m}$ = 5.0 ppm. The ^{11}B NMR shift of the compound is -12.2 ppm. The ^{1}H NMR spectrum shows three non-aromatic signals integrating in a 2:2:9 ratio rather than a 2:3:9 ratio as observed for the imine **32**. The ^{13}C NMR spectrum shows four non-aromatic signals including one at 212.8 ppm confirming that the C=N bond is intact; however, it is shifted significantly downfield relative to that observed for **32** ($\delta_{C\text{-}N}$= 175.1 ppm) in C_6D_6. The NMR data is consistent with the iminium zwitterion **37**. This assignment was confirmed by X-ray crystallography of crystals obtained from benzene/hexane, Figure 3.6.

Figure 3.6: X-Ray Crystal Structure of Zwitterion 37.

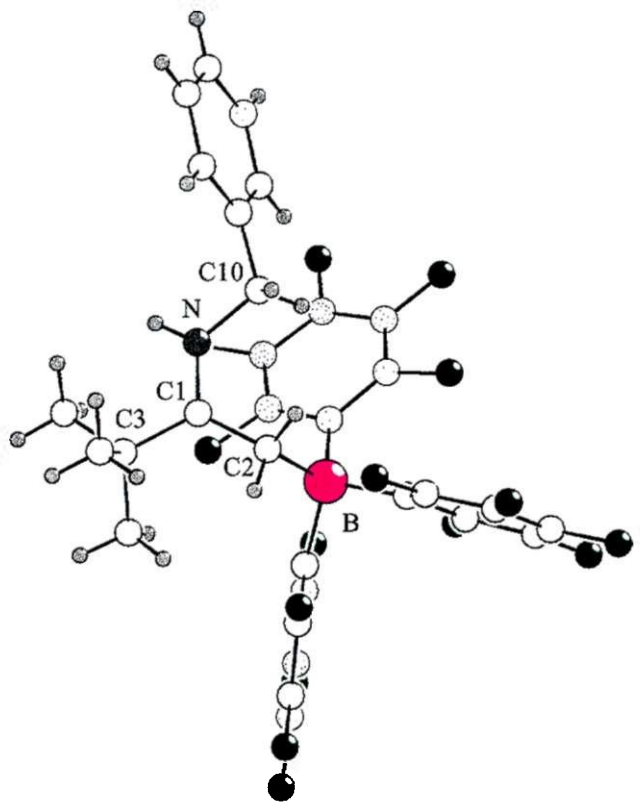

Bond Distances: C1-N, 1.305 Å; C2-B, 1.715 Å;
C10-N, 1.489 Å; C1-C2, 1.475 Å; C1-C3, 1.530 Å..
Bond Angles: <C1-N-C10 = 126.68°; <N-C1-C2 = 119.53°;
<N-C1-C3 = 117.23°; <C3-C1-C2 = 122.69°; <C1-C2-B = 121.6°.
Torsion Angles: <C10-N-C1-C2 = 6.56°; <C10-N-C1-C3 = 165.1°.

In the solid state, the benzyl group and $[\text{-}CH_2B(C_6F_5)_3]^-$ group are *syn*-disposed. A $^1H/^1H$ nOe experiment was carried out to confirm this geometry in solution; however, the results were consistent with both isomers. For example, irradiation of the ^{t}Bu H's led to enhancement in the NH ^1H and the benzylic ^1H's. This perhaps suggests that the *syn* and *anti* isomers of **37** are in rapid equilibrium with each other and that one isomer selectively crystallizes.

This species is presumably formed because steric effects destabilize the imine:borane adducts **36-k/t**. The sterically demanding *tert*-butyl group cannot

accommodate either the borane or the benzyl group in a *syn* orientation. Conversion of **32** to its enamine tautomer followed by reaction with **1** leads directly to **37**, equation 3.6. Hydrosilation of **32** does still occur in high yield, Table 3.2, entries 7 and 8 although it requires heating at 70 °C for several hours.

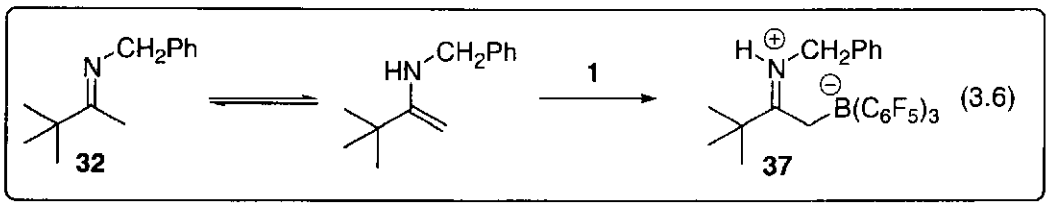

In conclusion, the lability of borane:imine adducts and steric effects have enabled indirect observation of two fundamental reactions of imines, *syn/anti*-isomerization and imine/enamine tautomerization. Thus for an unsymmetrical ketimine possessing α-protons, three pathways are available for reaction with a Lewis acid, two leading to Lewis acid adducts of the imine and the third, to an iminium zwitterion.

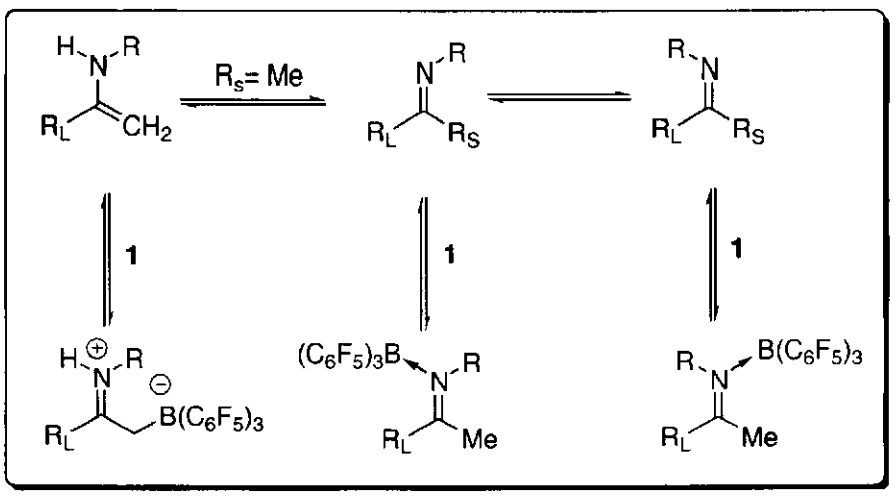

3.3.2 X-ray Structures of Imine/Borane Adducts

Table 3.4: Comparison of Metrical Prameters of Borane:Imine Adducts

Adduct	C=N (Å)	N-B (Å)	N-C_{Bn} (Å)	< C=N-C_{Bn}	< C=N-B	< C_{Bn}-N-B
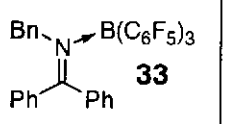 **33**	1.297(6)	1.642(8)	1.502(6)	117.0(4)	133.2(5)	109.6(4)
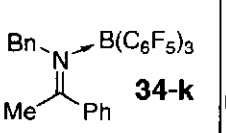 **34-k**	(a) 1.300(5) (b) 1.310(5)	1.630(6) 1.658(6)	1.504(5) 1.498(5)	116.8(4) 118.0(4)	132.2(4) 132.2(4)	110.6(3) 109.5(4)
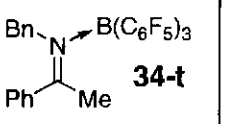 **34-t**	1.293(2)	1.640(2)	1.502(2)	118.11(14)	131.23(15)	110.51(13)
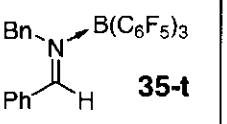 **35-t**	1.285(2)	1.627(3)	1.481(2)	121.08(16)	124.59(16)	114.26(14)
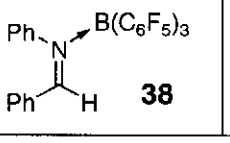 **38**	1.296(4)	1.649(4)	1.454(4)*	118.4(6)*	119.6(3)	121.8(2)*

* *ipso* carbon instead of C_{Bn}

X-ray crystal structures of **33**, **34-k**, **34-t** and **35-t** have been obtained, Figure 3.7. Key metrical parameters for these complexes are listed in Table 3.4. Data for **38** has been included for comparison. For adduct **34-k**, two sets of data are included for the two crystallographically independent molecules found. The bond lengths and angles obtained for the ketimine adducts are all very similar. Not surprisingly, the data for aldimine adduct **35-t** varies somewhat from the ketimine adducts. For instance, both the C=N and N-B bond lengths are shorter in **35-t**. Furthermore, the C=N-B angle is contracted considerably reflecting the lesser steric demands of the iminyl hydrogen relative to

phenyl or methyl groups providing more space for the bulky borane translating into a larger C_{Bn}-N-B angle.

Figure 3.7: X-ray Crystal Structures of Adducts 33, 34-k, 34-t and 35.

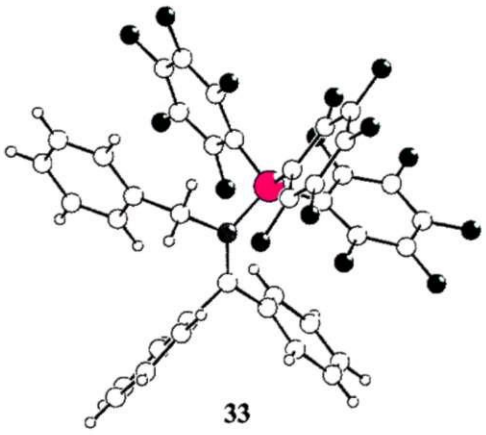

33

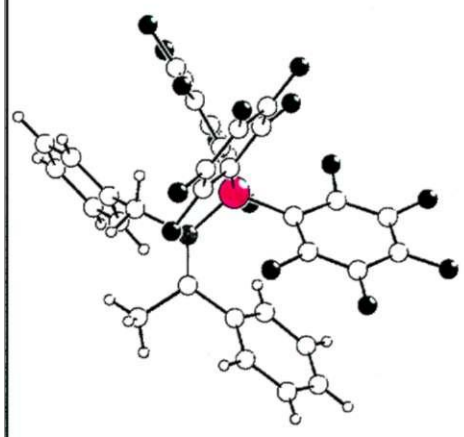

34-k

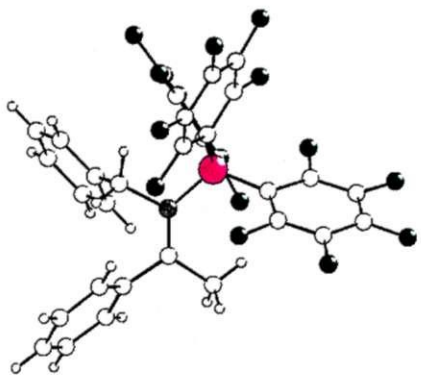

34-t

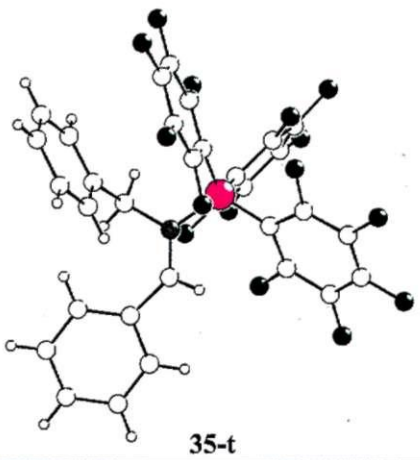

35-t

Figure 3.8: Adduct 33 showing π-stacking interactions.

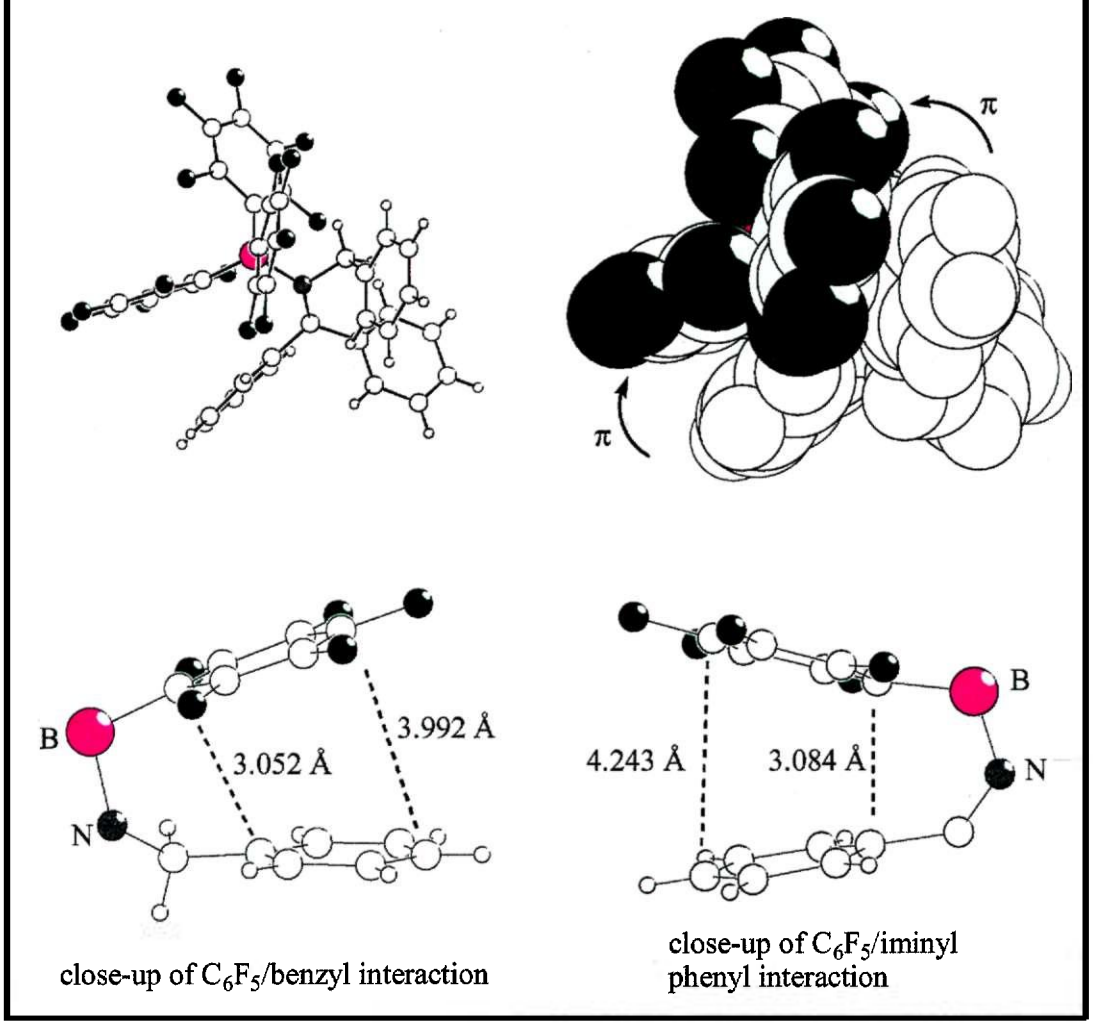

More importantly, examination of the crystal structures reveals a plausible origin for the restricted rotation observed in solution and the inequivalence of the benzylic hydrogens observed by ^{1}H NMR spectroscopy, Figure 3.8. For instance, in **33**, two of the C_6F_5 groups are engaged in π-stacking, one with the iminyl C_6H_5 group and one with the benzyl C_6H_5 group (see close-up views).

This stacking results in the two benzylic hydrogens occupying quite different environments, one hydrogen, H_a pointing toward the *syn* iminyl phenyl group and one hydrogen, H_b, pointing away. This arrangement is locked in place by the stacking interactions which prevent free rotation of the N-C bond. A similar arrangement is found in **34-k** where two stacking interactions can be accommodated, Figure 3.9.

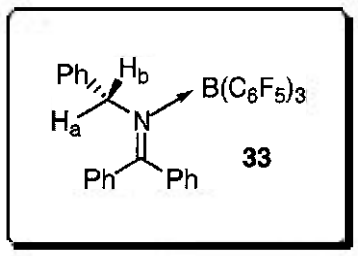

33

Figure 3.9: Views of the Two Stacking Interactions Present in the X-Ray Structure of Adduct 34-k

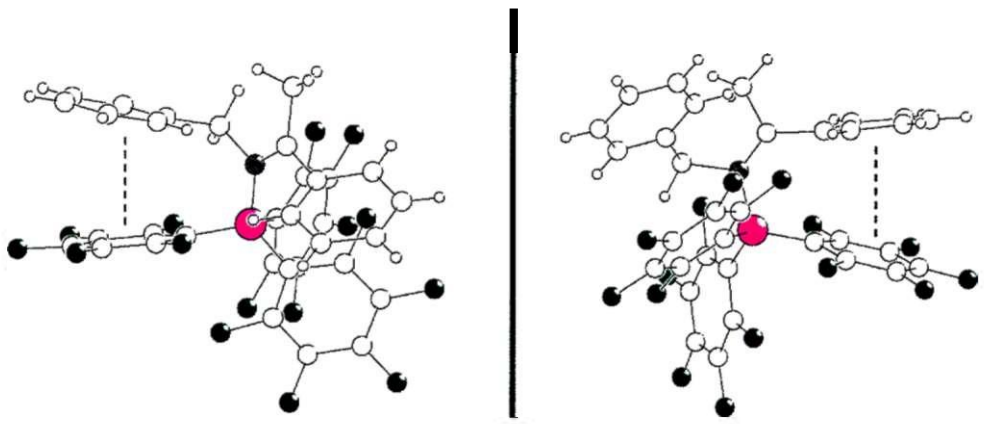

In **34-t** and **35-t**, only one C_6F_5 group can participate in π-stacking with the benzylic C_6H_5 group since the borane is *syn* to either a methyl group or the aldimine hydrogen, Figure 3.9. A list of C-C distances between the stacked rings for each of the adducts is provided in Tables 3.5 and 3.6. These values are within the range reported from other crystal structures which exhibit stacking between perfluoroaryl and protioaryl rings. The distances listed in Table 3.5 for **35-t** are generally shorter than those for **33**

and **34-k**, reflective of a stronger interaction. Geometrical constraints incurred by the presence of a second interaction in **33** and **34-k** could account for the weaker benzyl-C_6H_5/C_6F_5 interaction compared to that in **35-t**. The possibility for a second interaction exists for kinetic isomer **35-k**. However, suitable crystals of **35-k** could not be obtained as the adduct tended to precipitate as an amorphous powder at low temperatures.

Figure 3.10: View of the Lone Stacking Interaction Present in X-Ray Structure of Adduct 35-t.

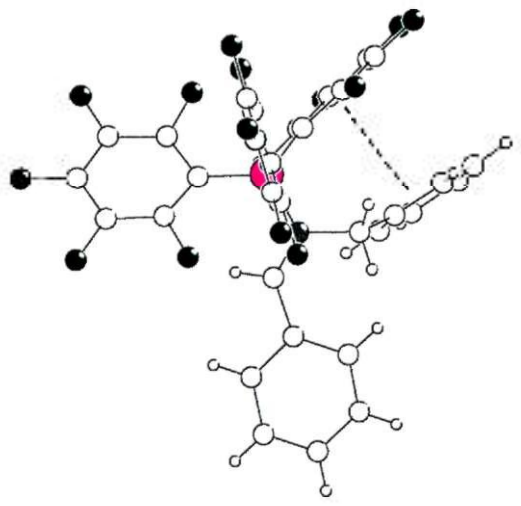

Table 3.5 List of Distances (Å) Between Atoms in Stacked C_6F_5 and Benzyl Rings.

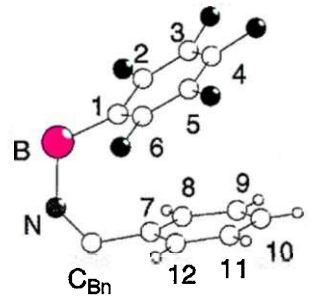

Positions	Distances (Å) **33**	**34-k** (mol. A)	**34-k** (mol. B)	**34-t**	**35-t**
1,7	3.052	3.123	3.092	3.121	3.062
2,8	3.338	3.503	3.476	3.392	3.119
3,9	3.829	3.905	3.945	3.769	3.454
4,10	3.992	3.977	4.018	3.935	3.710
5,11	3.691	3.652	3.621	3.686	3.655
6,12	3.212	3.219	3.178	3.237	3.336

Table 3.6 List of Distances (Å) Between Atoms in Stacked C_6F_5 and Iminyl Phenyl Rings

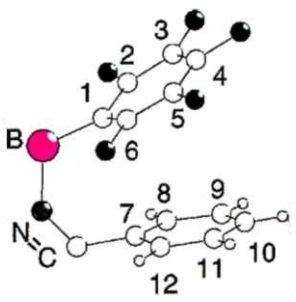

Positions	Distances (Å) **33**	**34-k** (mol. A)	**34-k** (mol. B)
1,7	3.084	3.062	3.017
2,8	3.579	3.534	3.445
3,9	4.176	4.121	3.887
4,10	4.243	4.224	3.901
5,11	3.795	3.756	3.543
6,12	3.313	3.258	3.173

Further analysis of the X-ray structure of **35-t** reveals that additional stacking interactions occur between individual adducts, Figure 3.10. The C_6F_5 group that is engaged in intramolecular stacking with the benzyl group is also engaged intermolecularly with another benzylic group from a second molecule. Not surprisingly, closer intramolecular than intermolecular contacts are formed. However, the

intermolecular contacts (3.340 - 3.967 Å) are well within the expected range of values for two stacked rings. Intermolecular stacking is a well-precedented phenomenon represented most commonly in crystals formed from a mixture of C_6H_6 and C_6F_6 and other arene mixtures.[51] These intermolecular interactions are not observed in the other adducts.

Figure 3.10: Two views of Adduct 35-t showing Intra- and Intermolecular π-Stacking Between Perfluoroaryl and Protioaryl Rings.

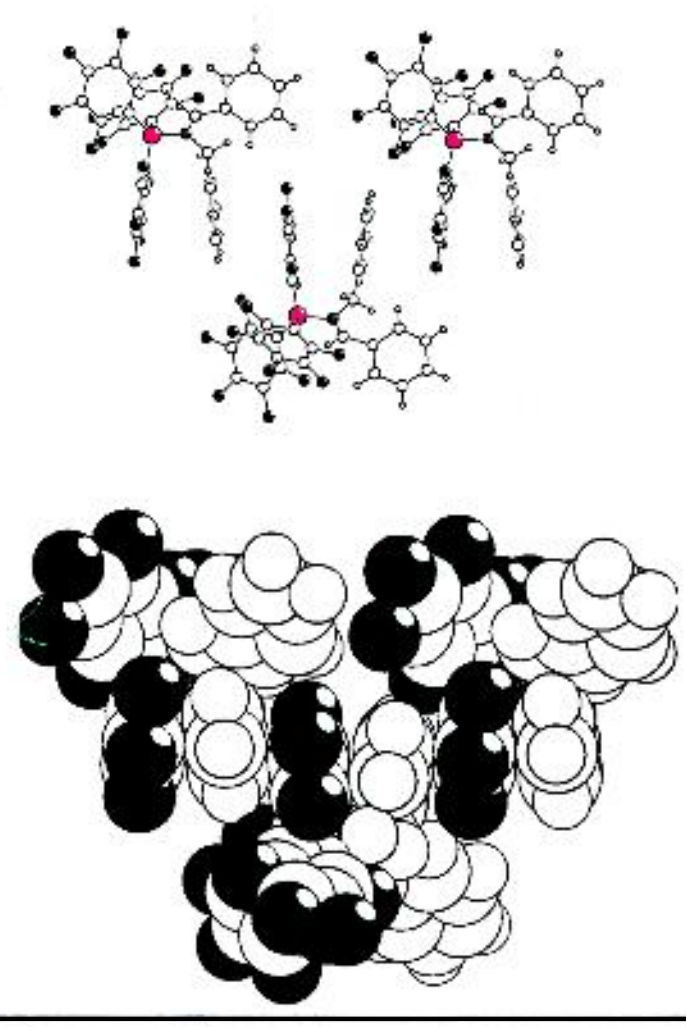

Electrostatic interactions between perfluororaryl and protioaryl groups are becoming increasingly common and have been used strategically for a number of purposes. The ability for these two groups to "stack" relates to their oppositely charged quadrupoles; perfluorinated rings are electron-poor above the aromatic plane whereas protioaryl rings are electron-rich.[51] The strength of these interactions is not great; however, weak energetic effects can have remarkable effects on subsequent chemistry.[52] For example, Grubbs and co-workers have shown that in the co-crystallization and solid-state photodimerization of a variety of C_6F_5- and C_6H_5-substituted alkenes, stacking interactions can be used to control regio- and stereoselectivity, equation 3.7.[52e]

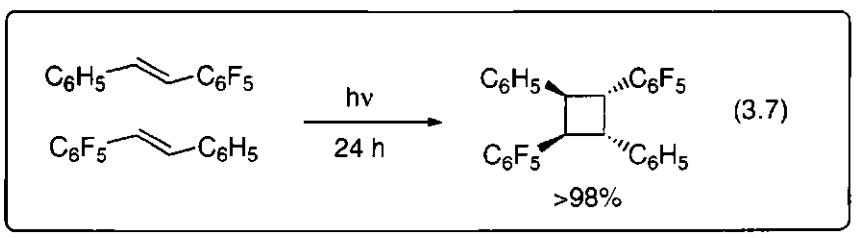

Cozzi, Siegel and co-workers have investigated the importance of quadrupolar interactions with respect to phenyl ring rotation in 1,8-diarylnaphthalenes, **AJ**.[53]

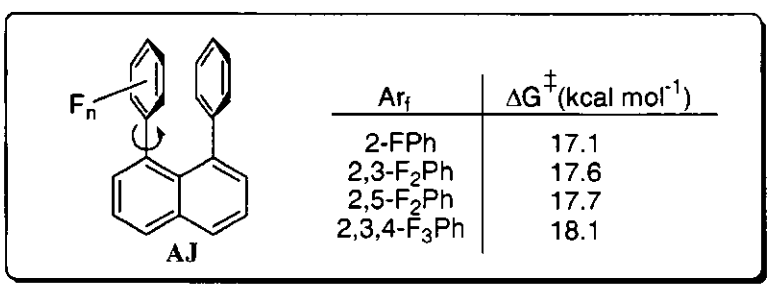

Consistent with greater attraction between the two rings, the barriers to rotation increase with increasing fluorine substitution of one of the aromatic rings (~ 0.5 kcal mol^{-1} per fluorine atom).

The weakness of these interactions in the imine adducts of **1** is evidenced by the thermodynamic preference for isomers **34-t** and **35-t** over **34-k** and **35-k** respectively. In the thermodynamic isomers **34-t** and **35-t**, there exists the possibility for only one

stacking interaction (with the benzylic C_6H_5) whereas in the kinetic isomers **34-k** and **35-k**, there exist the possibility for two interactions. Steric effects leading to the borane occupying the least congested position in the thermodynamic isomers clearly override any electronic stabilization associated with the second interaction. Nevertheless, observations do suggest that the second interaction does lend some degree of rigidity to the adducts in terms of rotation of the benzylic group. In adduct **33**, coalescence of the benzylic hydrogens occurs at approximately 40 °C corresponding to a value of $\Delta G^{\ddagger}$ = 60.0 $kJmol^{-1}$ for interconversion of the two rotamers **33'/33"**.[54] Interconversion simply requires partial rotation about the N-C bond which exchanges the environments of H_a and H_b. For this to occur, the interaction between the C_6F_5 group and the benzylic phenyl ring must clearly be broken.

Scheme 3.6: Interconversion of Rotamers of Imine Borane Adducts

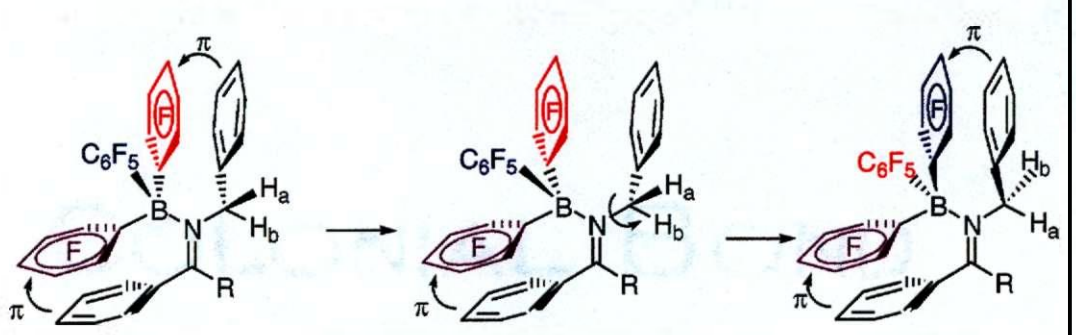

Evidence obtained through NMR studies of adducts **35-k/t** suggest that the second interaction must also be broken to allow interconversion of the rotamers. For adduct **35-k**, which also can engage in two π-interactions, the coalescence temperature observed is approximately 20 °C ($\Delta G^{\ddagger}$ = 58.5 $kJmol^{-1}$) compared to -10 °C ($\Delta G^{\ddagger}$ = 52.1 $kJmol^{-1}$)

for the thermodynamic isomer **35-t** containing only one quadrupolar interaction. As in **33**, in order for coalescence of the benzylic signals to occur, the interaction of the benzylic phenyl group with one of the C_6F_5 groups has to be disrupted followed by partial rotation around the N-C_{Bn} bond, Scheme 3.6. In the case of **35-k** this might be expected to actually be easier since the benzyl group is *syn* to the H. However, **35-k** exhibits a higher barrier to rotation than **35-t**. The second π-interaction conceivably plays a role at this stage by anchoring the borane in place thereby dissuading the C_6F_5 and benzylic C_6H_5 ring from separating sufficiently to allow rotation. It is thus speculated that both π-interactions must be broken in order for rotation to occur. For **33**, the same coalescence temperature was observed in the presence of excess **1** suggesting that complete dissociation of the adduct is not necessary.

3.4 Future Work

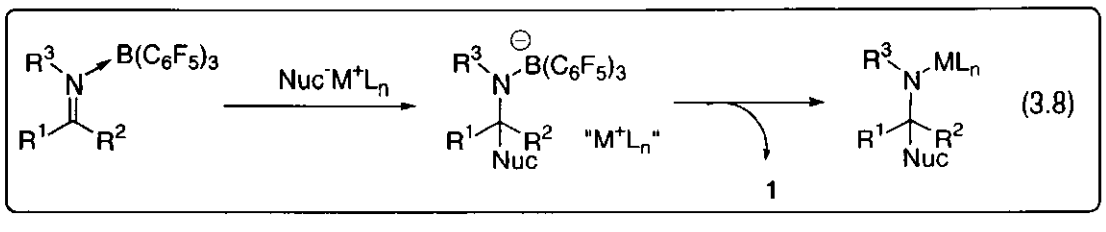

(3.8)

The adducts formed between imines and **1** do not appear to be directly relevant to the hydrosilation reaction. Nonetheless, it is conceivable that other addition reactions could proceed via borane adducts. For this to be useful, the Lewis acid and nucleophile will have to be compatible and ideally, regeneration of **1** will take place enabling reactions catalytic in borane to be developed. An eventual goal of the research is to develop asymmetric addition reactions using chiral boranes and thus it will be important to determine not only whether or not the reactions proceed via borane adducts, but also

whether the additions are likely to take place involving exclusively one of the isomeric adducts.

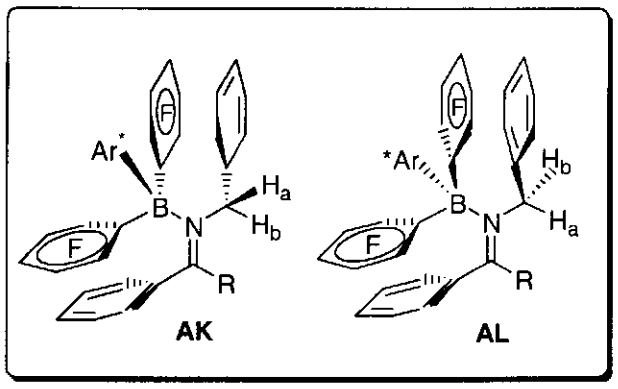

Stacking interactions could be used advantageously to influence the stereoselectivity of additions. For example, a chiral borane, $Ar^*B(C_6F_5)_2$, could be used to differentiate enantiotopic faces of an imine to nucleophilic attack. With the advent of one or two stacking interactions, coordination of the chiral Lewis acid may result in one face of the imine being more openly exposed to nucleophilic attack. The chiral Lewis acid, specifically the chiral aryl group, would provide the necessary discriminating effect between **AK** and **AL**. Furthermore, these stacking interactions could provide an extra means to favor either the *syn* or *anti* Lewis acid adduct.

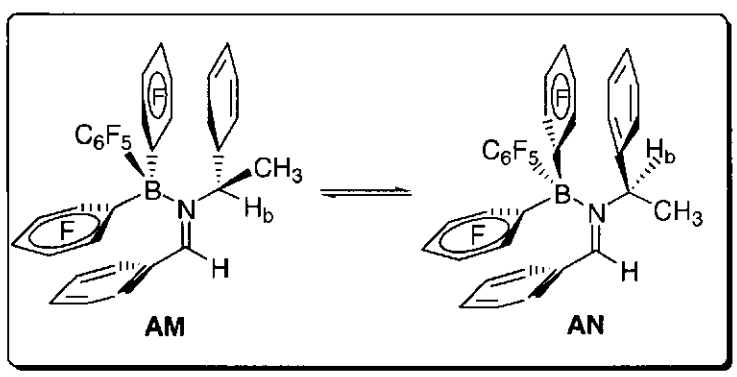

Alternatively, in conjunction with a chiral imine such as one derived from primary amine $PhCH(Me)NH_2$, coordination of **1** could potentially lead to formation of

predominantly one isomer (**AM** *vs* **AN**) controlled by the chiral benzylic center. This would lead to one enantioface being preferentially exposed to nucleophilic attack. The positioning of the methyl group in the diastereomeric adducts **AM/AN** could potentially control which isomer is favored and/or more reactive to addition. Although this strategy requires a stoichiometric amount of the source of chirality, it does not necessitate the preparation of novel chiral catalysts. A number of chiral imines prepared from readily available chiral amines are known; incorporation of the element of π-stacking using an achiral Lewis acid could provide a means for improving the discriminatory power of the chiral auxiliary.

Utilization of π-stacking to control the stereoselectivity of organic reactions has clearly been demonstrated on a number of occasions.[55] However, these studies generally involve an electron-rich aromatic ring interacting with an electron-poor olefin. The presence of π-stacking between perfluoroaryl and protiaryl rings has not yet been used in stereoselective organic synthesis although this strategy has been used in stereoselective polymer synthesis to control the tacticity of polypropylene produced by a zirconium catalyst.[52]

In conclusion, for either of the above strategies involving π-stacking to be effective, the nucleophilic additions must occur directly and exclusively on the borane imine adducts. Although hydrosilanes are likely to be inappropriate nucleophiles for this objective, a number of other nucleophiles are promising. In particular, nucleophiles that react directly with imines activated by BF_3 such as organotin, organozinc and organocopper reagents are strong candidates. Furthermore, for efficient enantioselectivity to be achieved, reaction exclusively via either the *syn* or *anti* Lewis

acid adduct will be necessary. Fully understanding the details of *syn-anti* isomerization of imines in the presence of the Lewis acid will therefore also be instrumental to success; preliminary advances in this regard have been made in the present study.

---

[1] Larock, R. C. *Comprehensive Organic Transformations* 2nd ed.; Wiley-VCH: Toronto, 1998. pp. 835-866.

[2] Harada, K. In *The Chemistry of the Carbon-Nitrogen Bond* Patai, S. ed.; Interscience (John Wiley & Sons): Toronto, 1970, pp.276-285.

[3] For early work see, (a) Yamada, K.; Takeda, M.; Iwakuma, T. *Tetrahedron Lett.* **1981**, *22*, 3869. (b) Yamada, K.; Takeda, M.; Iwakuma, T. *J. Chem. Soc., Perkin Trans. 1* **1983**, 265. (b) Itsuno, S.; Nakano, M.; Miyazaki, K.; Matsuda, H.; Ito, K.; Hirao, A. *J. Chem. Soc., Perkin Trans. 1* **1985**, 2039.

[4] (a) Inoue, T.; Sato, D.; Komura, K.; Itsuno, S. *Tetrahedron Lett.* **1999**, *40*, 5379. (b) Itsuno, S.; Matsumoto, T.; Sato, D.; Inoue, T. *J. Org. Chem* **2000**, *65*, 5879 (c) Hajpour, A. R.; Hantehzadeh, M. *J. Org. Chem.* **1999**, *64*, 8475.

[5] March, J. *Advanced Organic* Chemistry, 4th ed., John Wiley & Sons: Toronto, 1992, pp. 898-900.

[6] (a) Kobayashi, S.; Ishitani, H. *Chem. Rev.* **1999**, *99*, 1069. (b) Blaser, H. -U. in *Comprehensive Asymmetric Catalysis Vol. 1.* Jacobsen, E. N.; Pfaltz, A.; Yamamoto, H. eds.; Springer-Verlag, New York, 1999, pp.247-266.

[7] For early work, see (a) Boyle, P. H.; Keating, M. T. *J. Chem. Soc., Chem. Commun.* **1974**, 375. (b) Levi, A.; Modena, G.; Scorranno, G. *J. Chem. Soc., Chem. Commun.* **1975**, 6. (c) Bakos, J.; Tóth, I.; Hell, B.; Szalontai, G.; Párkányi, L.; Fülöp, V. *J. Organomet. Chem.* **1989**, *370*, 263. (d) Kang, G. -J.; Cullen, W. R.; Fryzuk, m. D.; James, B. R.; Kutney, J. P. *J. Chem. Soc., Chem. Commun.* **1988**, 1466.

[8] For reductions of oximes and hydrazones, see (a) Chan, A. S. C.; Chen, C. -C.; Lin, C. -W.; Lin, Y. -C.; Cheng, M. -C.; Peng, S. -M. *J. Chem. Soc., Chem. Commun.* **1995**, 1767. (b) Burk, M. J.; Martinez, J. P.; Feaster, J. E.; Cosford, N. *Tetrahedron*, **1994**, *50*, 4399.

[9] (a) Chan, Y. N. C.; Osborn, J. A. *J. Am. Chem. Soc.* **1990**, *112*, 9400. (b) Chan, Y. N. C.; Meyer, D.; Osborn, J. A. *J. Chem. Soc., Chem. Commun.* **1990**, 869. (c) Spindler, F.; Pugin, B.; Blaser, H. -U. *Angew. Chem. Int. Ed. Engl.* **1990**, *29*, 558. (d) Kainze, S.; Brinkmann, A.; Leitner, W.; Pfaltz, A. *J. Am. Chem. Soc.* **1999**, *121*, 6421 and references therein.

[10] (a) Oppolzer, W.; Wills, M.; Starkemann, C.; Bernardinelli, G. *Tetrahedron Lett.* **1990**, *31*, 4117. (b) Fogg, D. E.; James, B. R. *Inorg. Chim. Acta* **1994**, *222*, 85.

[11] Willoughby, C. A.; Buchwald, S. L. *J. Am. Chem. Soc.* **1994**, *116*, 8952 and references therein.

[12] Nishiyama, H. in *Comprehensive Asymmetric Catalysis Vol. 1.* Jacobsen, E. N.; Pfaltz, A.; Yamamoto, H. eds.; Springer-Verlag, New York, 1999, pp.267-286.

[13] (a) Langlois, N.; Dang, T. -P.; Kagan, H. B. *Tetrahedron Lett.* **1973**, 4865. (b) Kagan. H. B.; Langlois, N.; Dang, T. -P. *J. Organomet. Chem.* **1975**, *90*, 353.

[14] (a) Brunner, H.; Becker, R. *Angew. Chem Int. Ed. Engl.* **1984**, *23*, 222. (b) Becker, R.; Brunner, H.; Mahboobi, S.; Wiegrebe, W. *Angew. Chem. Int. Ed. Engl.* **1985**, *24*, 995.

[15] (a) Verdaguer, X.; Lange, U. E. W.; Reding, M. T.; Buchwald, S. L. *J. Am. Chem. Soc.* **1996**, *118*, 6784. (b) Verdaguer, X.; Lange, U. E. W.; Buchwald, S. L. *Angew. Chem. Int. Ed. Engl.* **1998**, *37*, 1103. (c) Hensen, M. C.; Buchwald, S. L. *Organic Lett.* **2000**, *2*, 713.

[16] (a) Nishibayashi, Y.; Takei, I.; Uemura, S.; Hidai, M. *Organometallics*, **1998**, *17*, 3420. (b) Takei, I.; Nishibayashi, Y.; Arikawa, Y.; Uemura, S.; Hidai, M. *Organometallics*, **1999**, *18*, 2271.

[17] Vetter, A. H.; Berkessel, A. *Synthesis*, **1995**, 419.

[18] Takaki, K.; Kamata, T.; Miura, Y.; Shishido, T.; Takehira, K. *J. Org. Chem.* **1999**, *64*, 3891.

[19] (a) Shibata, I.; Suwa, T.; Moriuchi-Kawakami, T.; Tanizawa, D.; Sugiyama, E.; Matsuda, H.; Baba, A. *J. Org. Chem.* **1998**, *63*, 383. (b) Shibata, I.; Suwa, T.; Sugiyama, E.; Baba, A. *Synlett*, **1998**, 1081.

[20] Suwa, T.; Sugiyama, E.; Shibata, I.; Baba, A. *Synlett*, **2000**, 558.

[21] Lopez, R. M.; Fu, G. C. *Tetrahedron* **1997**, *48*, 16349.

[22] Chandrasekhar, S.; Reddy, C. R.; Ahmed, M. *Synlett*, **2000**, 1655.

[23] (a) Denmark, S. E.; Nicaise, O. J. -C. in *Comprehensive Asymmetric Catalysis Vol. 2.* Jacobsen, E. N.; Pfaltz, A.; Yamamoto, H. eds.; Springer-Verlag, New York, 1999, pp.923-964. (b) Bloch, R. *Chem. Rev.* **1998**, *98*, 1407. (c) Enders, D.; Reinhold, U. *Tetrahedron: Asymmetry* **1997**, *8*, 1895.

[24] For examples, see (a) Wada, M.; Sakurai, Y.; Akiba, K. Y. *Tetrahedron Lett.* **1984**, *25*, 1083. (b) Uno, H.; Okada, S. -I.; Ono, T.; Shiraishi, Y.; Suzuki, H. *J. Org. Chem.* **1992**, *57*, 1504. (c) Aubrecht, K. B.; Winemiller, M. D.; Collum, D. B. *J. Am. Chem. Soc.* **2000**, *122*, 11084.

[25] For example, see Enders, D.; Schankat, J. *Helv. Chim. Acta* **1995**, *78*, 970.

[26] Denmark, S. E.; Stiff, C. M. *J. Org. Chem.* **2000**, *65*, 5875.

[27] (a) Keck, G. E.; Enholm, E. J. *J. Org. Chem.* **1985**, *50*, 147. (b) Ciufolini, M. A.; Spencer, G. O. *J. Org. Chem.* **1989**, *54*, 4739.

[28] (a) Panek, J. S.; Jain, N. F. *J. Org. Chem.* **1994**, *59*, 2674. (b) Fang, X.; Johannsen, M.; Yao, S.; Gathergood, N.; Hazell, R. G.; Jørgensen, K. A. *J. Org. Chem.* **1999**, *64*, 4844.

[29] (a) Yamamoto, Y.; Komatsu, T.; Maruyama, K. *J. Org. Chem.* **1985**, *50*, 3115. (b) Yamamoto, Y.; Nishii, S.; Maruyama, K.; Komatsu, T.; Ito, W. *J. Am. Chem. Soc.* **1986**, *108*, 7778.

[30] (a) Kerwin Jr., J. F.; Danishefsky, S. *Tetrahedron Lett.* **1982**, *23*, 3739. (b) Yao, S.; Saaby, S.; Hazell, R. G.; Jørgensen, K. A. *Chem. Eur. J.* **2000**, *6*, 2435.

[31] (a) Shimizu, M.; Kume, K.; Fujisawa, T. *Tetrahedron Lett.* **1995**, *36*, 5227. (b) Chen, J. -X.; Sakamoto, K.; Orita, A.; Otera, J. *J. Org. Chem.* **1998**, *63*, 9739.

[32] (a) Wada, M.; Sakurai, Y.; Akiba, K. -Y. *Tetrahedron Lett.* **1984**, *25*, 1079. (b) Boga, C.; Savoia, D.; Umani-Ronchi, A. *Tetrahedron: Asymmetry* **1990**, *1*, 291. (c) Alvaro, G.; Savoia, D.; Valentinetti, M. R. *Tetrahedron* **1996**, *52*, 12571.

[33] (a) Yamamoto, Y.; Komatsu, T.; Maruyama, K. *J. Am. Chem. Soc.* **1984**, *106*, 5031. (b) Bocoum, A.; Boga, C.; Savoia, D.; Umani-Ronchi, A. *Tetrahedron Lett.* **1991**, *32*, 1367.

[34] Hashimoto, Y.; Kobayashi, N.; Kai, A.; Saigo, K. *Synlett*, **1995**, 961.

[35] Yamada, H.; Kawate, T.; Nishida, A.; Nakagawa, M. *J. Org. Chem.* **1999**, *64*, 8821.

[36] Davis, F. A.; Zhou, P.; Chen, B. -C. *Chem. Soc. Rev.* **1998**, *27*, 13.

[37] Basile, T.; Bocoum, A.; Savoia, D.; Umani-ronchi, A. *J. Org. Chem.* **1994**, *59*, 7766.

[38] Beresford, K. J. M.; Howe, G. P.; Procter, G. *Tetrahedron Lett.* **1992**, *33*, 3355.(b) Ukaji, Y.; Watai, T.; Sumi, T.; Fujisawa, T. *Chem. Lett.* **1991**, 1555.

[39] See *Enamines* Cook, A. G. ed.; Marcel Dekker: New York, 1969.

[40] Jahangir; MacLean, D. B.; Brook, M. A.; Holland, H. L. *J. Chem Soc.; Chem. Commun.* **1986**, 1608. (b) Jahangir; MacLean, D. B.; Holland, H. L. *Can. J. Chem.* **1987**, *65*, 727. (c) Jahangir; Brook, M. A.; MacLean, D. B.; Holland, H. L. *Can. J. Chem.* **1987**, *65*, 2362. (d) Repke, D. B.; Jahangir; Clark, R. D.; MacLean, D. B. *J. Chem. Soc., Chem. Commun.* **1988**, 439.

[41] Böhme, H.; Viehe, H. G. *Iminium Salts in Organic Chemistry (Advances in Organic Chemistry, Vol 9)* Wiley: New York, 1976.

[42] Renaud, R. N.; Bérubé, D.; Stephens, C. J. *Can. J. Chem.* **1983**, *61*, 1379 and references therein.

[43] Mayr, H.; Ofial, A. R. *Tetrahedron Lett.* **1997**, *38*, 3503.

[44] (a) McCarty, C. G. in *The Chemistry of the Carbon-Nitrogen Bond* Patai, S. ed.; Interscience (John Wiley & Sons): Toronto, 1970, pp.363-464. (b) Smith, J. K.; Bergbreiter, D. E.; Newcomb, M. *J. Am. Chem. Soc.* **1983**, *105*, 4396.

[45] Chen, G. -M.; Brown, H. C. *J. Am. Chem. Soc.* **2000**, *122*, 4217.

[46] For example, see Cantrell, G. K.; Geib, S. J.; Meyer, T. Y. *Organometallics* **2000**, *19*, 3562.

[47] (a) Castarlenas, R.; Esteruelas, M. A.; Oñate, E. *Organometallics* **2000**, *19*, 5454. (b) Francisco, L. W.; White, P. S.; Templeton, J. L. *Organometallics* **1996**, *15*, 5127.

[48] Lambert, J. B.; Zhang, S.; Ciro, S. M. *Organometallics* **1994**, *13*, 2430.

[49] (a) Bahr, S. R.; Boudjouk, P. *J. Am. Chem. Soc.* **1993**, *115*, 4514. (b) Ichinohe, M.; Fukui, H.; Sekiguchi, A. *Chem. Lett.* **2000**, 600. (c) Xie, Z.; Liston, D. J.; Jelinek, T.; Mitro, V.; Bau, R.; Reed, C. A. *J. Chem. Soc., Chem. Commun.* **1993**, 384.

[50] Buchwald reports a 17:1 ratio of isomers, see reference 11.

[51] Williams, J. H. *Acc. Chem. Res.* **1993**, *26*, 593.

[52] (a) Coates, G. W.; Waymouth, R. M. *Science*, **1995**, *267*, 217. (b) Pietsch, M. A.; Rappé, A. K. *J. Am. Chem. Soc.* **1996**, *118*, 10908. (c) Coates, G. W.; Dunn, A. R.; Henling, L. M.; Dougherty, D. A.; Grubbs, R. H. *Angew. Chem. Int. Ed. Engl.* **1997**, *36*, 248. (d) Coates, G. W.; Dunn, A. R.; Henling, L. M.; Ziller, J.

W.; Lobkovsky, E. B.; Grubbs, R. H. *J. Am. Chem. Soc.* **1998**, *120*, 3641. (e) Weck, M.; Dunn, A. R.; Matsumoto, K.; Coates, G. W.; Lobkovsky, E. B.; Grubbs, R. H. *Angew. Chem. Int. Ed. Engl.* **1999**, *38*, 2741. (f) Dai, C.; Nguyen, P.; Marder, T. B.; Scott, A. J.; Clegg, W.; Viney, C. *Chem. Commun.* **1999**, 2493.

[53] Cozzi, F; Ponzini, F.; Annunziata, R.; Cinquini, M.; Siegel, J. S. *Angew. Chem. Int. Ed. Engl.* **1995**, *34*, 1019.

[54] Sandström, J. *Dynamic NMR Spectroscopy*, Academic Press: Toronto, 1982.

[55] Jones, G. B.; Chapman, B. J. *Synthesis*, **1995**, 475.

Chapter 4

$B(C_6F_5)_3$-Catalyzed Allylstannation of Carbonyls

4.1 Introduction to Allylstannation

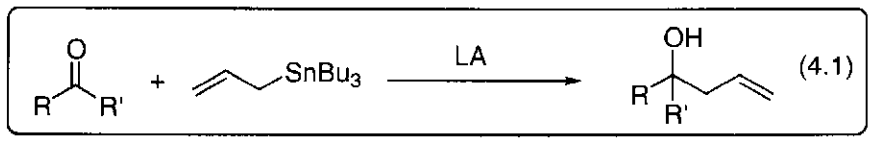

The allylstannation of carbonyls is a useful and important C-C bond forming reaction in organic synthesis, equation 4.1.[1] Typically, a stoichiometric amount of a Lewis acid is required leading to the description of these reactions as being "*Lewis acid promoted*". However, true catalytic systems have been developed, in particular, those protocols employing chiral Lewis acids.[2] By varying the Lewis acid, carbonyl substrate, allylstannane, and the reaction conditions, access to a diverse range of organic architectures important in natural product synthesis is feasible. In fact, from an early point, Denmark has described the allylstannation reaction as a "surrogate" for the hallowed aldol reaction since the allyl group can be oxidatively transformed into an aldehyde.[3] The large number of permutations possible from the aforementioned factors has made drawing definitive mechanistic conclusions difficult. Careful studies from a number of groups have led to the emergence of a number of general trends.[1,4]

4.1.1 Strategies to Increase the Synthetic Diversity of Allylstannation Reaction

Modification of Allylstannane: The groups of Yamamoto and Keck showed in the early 80's that by using substituted allylstannanes such as crotylstannanes, diastereoselective formation of homoallylic alcohols possessing two adjacent stereocenters could be achieved, equation 4.2.[5,6] Importantly, depending on the nature of the aldehyde and/or the

properties of the Lewis acid, access to either the *syn* or *anti* diastereomer is often possible. Soon thereafter, γ-alkoxy substituted allylstannanes were used effectively in diasteroselective additions to aldehydes.[7]

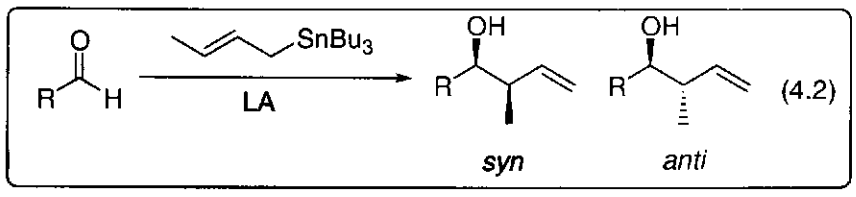

Marshall and others have demonstrated that chiral α-alkoxy allylstannanes are suitable nucleophiles allowing highly efficient chirality transfer to the newly forming stereocenter(s) in the allylated products, equation 4.3.[8,9] The development of reliable routes to enantioenriched γ-alkoxy and siloxy allylstannanes was followed by successful application as nucleophiles.[10] The chiral allylstannane strategy has allowed the preparation of important carbon skeletons possessing adjacent oxy-substituted stereocenters and has been applied to the synthesis of natural products.[11]

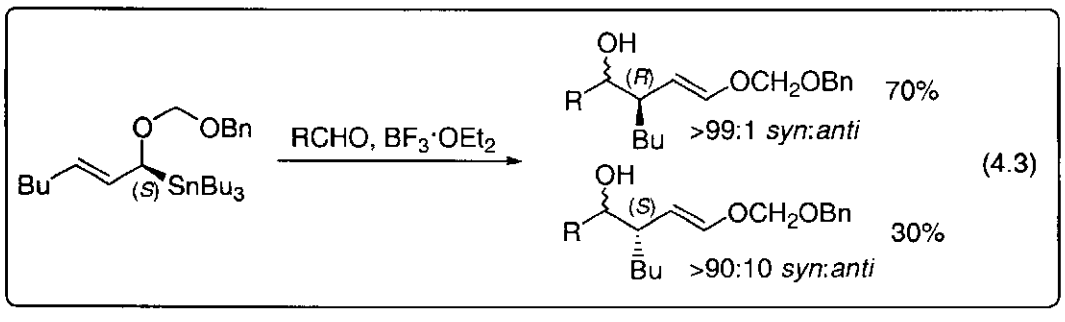

Other modifications to the allylstannane have been made including the use of bifunctional allylstannanes possessing two stannyl moieties.[12] Furthermore, *homo*-allylic stannanes have found application providing access to cyclopropyl-substituted carbinols.[13] Finally, allenyl- and propargylstannanes have found extensive use providing

homopropargyl and homoallenyl alcohols respectively.[8] Significant diversity in the alcohol products can be achieved by changing the nature of the stannane reagent used.

Substrate Control – Chiral Aldehydes:

Analogous to research on the aldol reaction, tremendous advances in stereoselective allylstannane chemistry were made by using chiral aldehyde substrates (substrate control).[1,14] Typically, these substrates possess alkoxy substituents either α- or β- to the carbonyl. Not only could the presence of a stereocenter control the stereochemistry of a newly forming one, but when used in conjunction with substituted allylstannanes, skeletons possessing three adjacent stereocenters could be prepared selectively, equation 4.4.[7a]

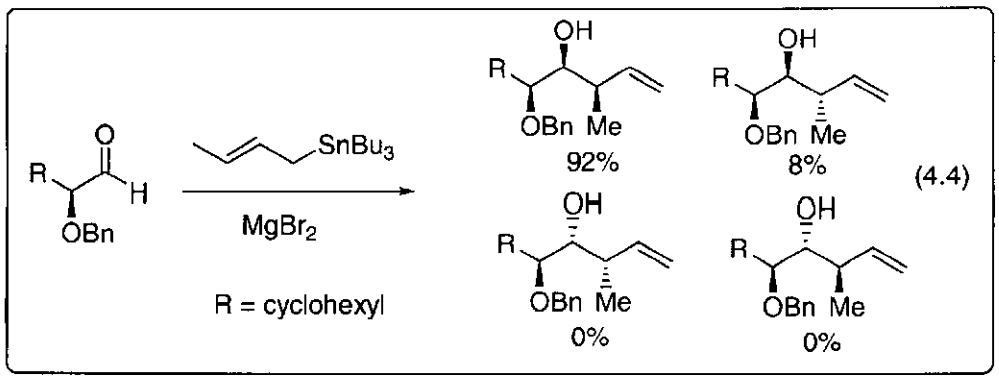

Properties of the Lewis Acid

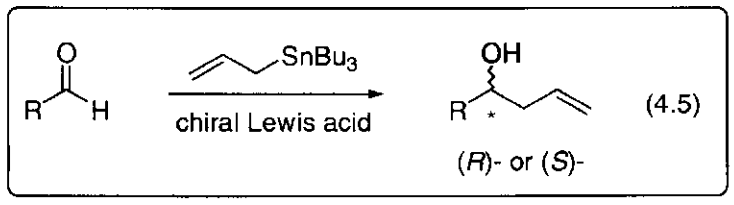

The scope of the allylstannation reaction has also been expanded through the use of chiral Lewis acids, although relative to aldol technology, few successful protocols exist.[15,16] Chiral Lewis acid catalysts based on boron, titanium, zirconium, rhodium, zinc

and silver have been used. The use of a chiral (non-racemic) Lewis acid allows the possibility for enantiotopic facial discrimination in the attack of an allylstannane on a carbonyl function. In the simple case of a non-chiral allylstannane, a chiral homo-allylic alcohol obtains where the enantioselectivity is controlled by the Lewis acid, equation 4.5. When a chiral Lewis acid is used with either a chiral aldehyde or a chiral allylstannane, both chiral sources can exert their own effect on the overall enantioselectivity either in concert or in opposition (matched/mismatched scenario).

The Lewis acid employed is also important when dealing with alkoxy-substituted aldehydes where the potential for chelation to the Lewis acid exists, equation 4.6.[7] For Lewis acids capable of hypercoordination such as $MgBr_2$ or $TiCl_4$, chelation to the metal by the alkoxy-substituent can occur leading to the formation of a cyclic intermediate[17] and subsequently, preferential attack at one face of the carbonyl. Although, in many instances, unambiguous experimental demonstration of chelated intermediates is used to rationalize the observed stereoselectivity, in other cases, only unsubstantiated hypotheses have been proposed. Other Lewis acids are incapable of chelation or prefer alternative binding modes (coordination of two carbonyls) and acyclic transition states are traversed often leading to products of the opposite stereoselectivity.

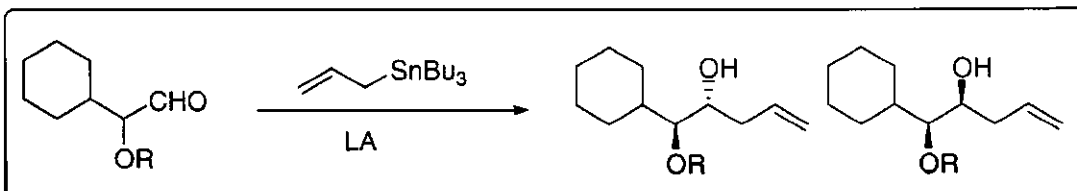

R	LA	Selectivity
^{t}BuMe$_2$Si	$BF_3{\cdot}OEt_2$	95:5
Bn	$MgBr_2$	1:>250

(4.6)

Reaction Conditions

Although variation of such features as temperature and concentration can have significant bearing on the level of stereoselectivity, a more important consideration is that of "order of reagent mixing". The order in which the reagents (Lewis acid, allylstannane, aldehyde) are mixed can affect the nature of the allylmetal reagent that actually reacts with the aldehyde.[18] Specifically, if the allylstannane and Lewis acid are premixed, a methathesis reaction can ensue involving transfer of the allyl group to the Lewis acidic metal with concomitant transfer of a labile group such as a halide from the Lewis acid to the tin atom (*eg.* allylSnBu$_3$ + SnCl$_4$ → Cl-SnBu$_3$ + allylSnCl$_3$).[19] Upon addition of aldehyde, the newly formed allylmetal reagent can react with aldehyde acting as both Lewis acid and the source of the allyl group. Such reactions are generally thought to proceed via six-membered cyclic transition states and can exhibit differing selectivity than the alternative acyclic transition state.

Premixing the Lewis acid with the carbonyl followed by addition of allylstannane, in general, leads to a conventional mechanistic pathway (Lewis acid activation of carbonyl to *intermolecular* nucleophilic attack). However, the possibility certainly exists for dissociation of the Lewis acid from the aldehyde enabling the metathesis pathway to compete and thus the accompanying possibility for diminution of stereoselectivity. Careful consideration of factors such as reagent stoichiometry and temperature are important in disfavoring this type of pathway.

4.1.2 Mechanistic Insight

Facilitating the important advances described above were simultaneous studies carried out by a number of groups aimed at elucidating a general mechanism for allylstannation reactions. Certainly, significant strides have been made in this area, but have lagged behind the synthetic applications.

Role of the Lewis Acid

Conventionally, the role of the Lewis acid in reactions involving nucleophilic attack at a carbonyl is to coordinate the carbonyl rendering it more electrophilic through polarization of the C=O bond. However, as mentioned earlier, precedence exists for another role; that is, the Lewis acid can react with the allylstannnane reagent leading (via a metathesis reaction) to a new allylmetal reagent. This new allylmetal reagent can itself react with the carbonyl since it often maintains sufficient Lewis acidity to both activate the carbonyl and intramolecularly deliver the allyl group. Clever experiments have been designed to probe the importance of the two often stereochemically divergent pathways.

Approach of the Allylstannane: C-C Bond Formation

Figure 4.1: Some Possible Transition States in Lewis Acid Promoted Crotylstannation of an Aldehyde via an Antiperiplanar Approach

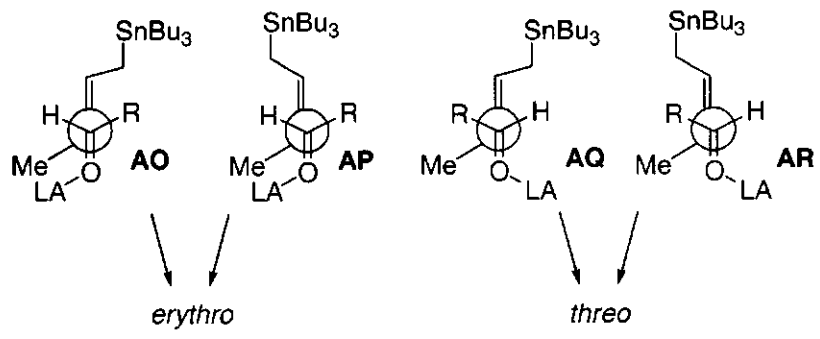

Initiated by Y. Yamamoto in the late 70's, considerable research has been extended toward establishing the geometry and nature of attack of the allylstannane toward a Lewis acid activated carbonyl. As illustrated in Figure 4.1, for crotyltributylstannane, a number of different modes of attack of the allylstannane can be envisioned. In general, attack via an acyclic, antiperiplanar transition state is considered to operate for most Lewis acid promoted allylstannation reaction although convincing evidence has been provided to support a synclinal mode in certain cases.[3,20] The pathway that predominates is often a function of the particular Lewis acid and allylstannane used.

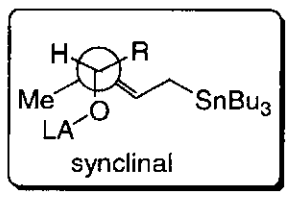

For each of the (*E*)- and (*Z*)-isomers of crotylstannanes, two possible approaches can occur producing either the *erythro* or *threo* diastereomer. For the antiperiplanar mode of attack, it is generally believed that approach of the crotyl group occurs which minimizes steric interaction between the methyl group of the stannane and the R group of the aldehyde as in **AO** and **AP**. The methyl group and the Lewis acid are placed in sterically most demanding positions with respect to each other. Larger Lewis acids can lead to decreased selectivity by favoring attack via transition states **AQ** or **AR**. In general, the reactive Sn-C bond orients itself perpendicular to the allyl π-system enabling the most effective stabilization of the positive charge that develops at the β-C during C-C bond formation.[21]

Ultimate Fate of the Trialkylstannyl Moiety

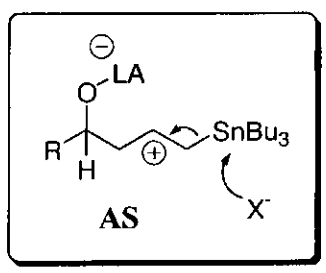

Scant mechanistic attention has been paid to the fate of the trialkyltin moiety upon consummation of C-C bond formation. Mechanistic proposals typically show removal of the "Bu_3Sn^+" by the attack of a nucleophile, X^-, (originating from the Lewis acid). No spectroscopic evidence has been provided to establish the intermediacy of **AS** at the commencement of C-C bond formation where positive charge is shared between the β-C and the trialkyltin moiety. Indeed, this stage of the reaction has remained somewhat of a "black-box".

Scheme 4.1: Consummation of Allylstannation - The Black Box.

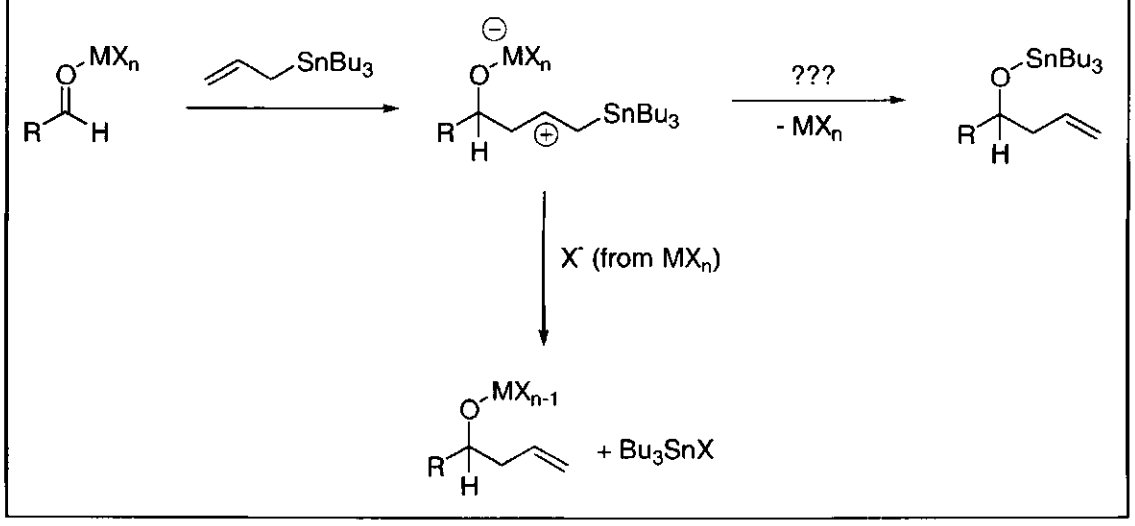

Certainly, formation of a naked "Bu_3Sn^+" species is untenable (see Section 1.4); that is, some type of Lewis base must participate in liberating this electron deficient group. A possibility not previously considered will be discussed in this chapter. The products isolated from the allylstannation of carbonyls are usually the homoallylic alcohols. Unless specific attempts have been made to analyze the products prior to

purification, it is difficult to conclude whether the trialkyltin moiety ultimately resides on the O (stannyl ether) or reacts with the Lewis acid to form a byproduct (*eg.* trialkylstannyl halide). When catalytic quantities of the Lewis acid are employed, presumably stannyl ether formation must occur. However, when a stoichiometric amount of Lewis acid is used (which is often the case), either situation could prevail.

4.1.3 Lewis Acid Catalyzed Isomerization of Allylstannanes

Scheme 4.2: Proposed Mechanism for Lewis Acid Catalyzed Isomerization of AllylStannanes

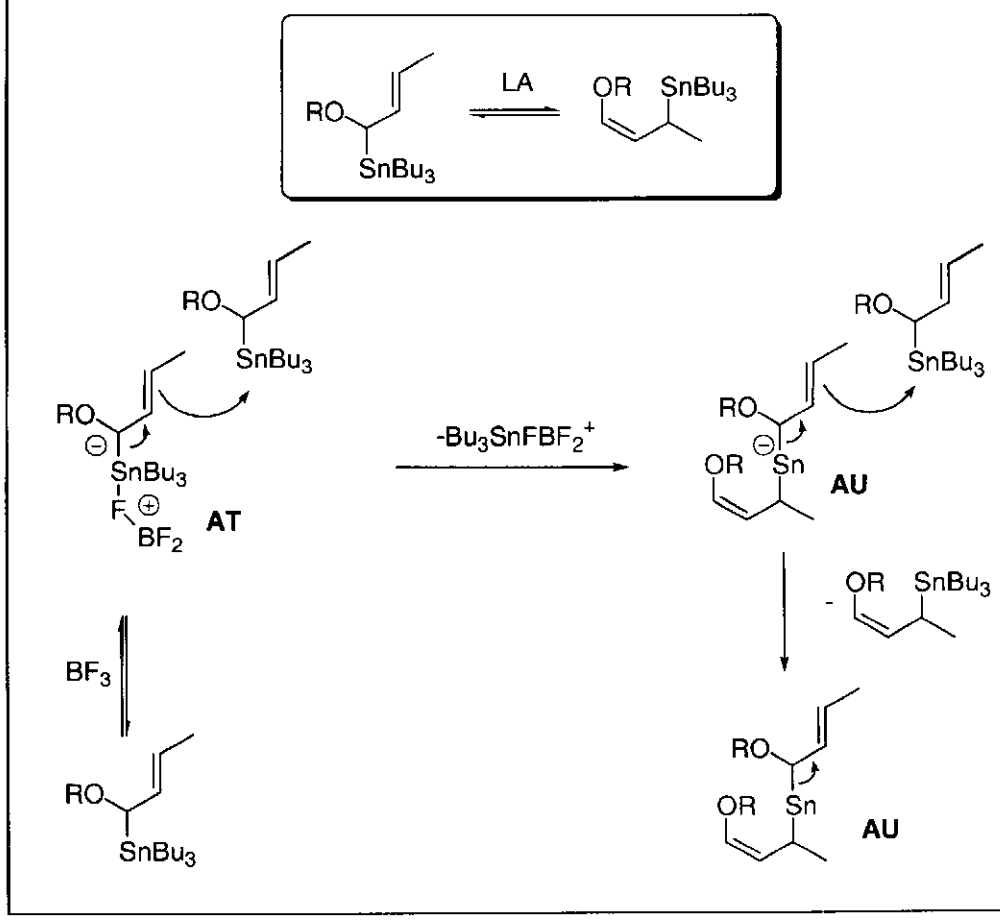

Lewis acids can also catalyze isomerization reactions of allylstannanes and are important in interconverting allenyl- and propargylstannanes.[8] Clear mechanistic insight

for this important process however is decidedly lacking. For instance, in order to explain isomerization in alkoxy-substituted allylstanannes, Marshall proposed the mechanism shown in Scheme 4.2.[9b] The authors ascribe a *Lewis basic* role to BF_3 where attack at the tin center by a fluoride group forms intermediate **AT** which initiates subsequent exchange of allyl groups between tin atoms via anionic tin species **AU**. Although this mechanism does rationalize the scrambling observed, no strong evidence was provided in its support. In fact, based on preliminary reports from the Piers group,[22] Marshall has reexamined the mechanism for isomerization of allylstannanes.[23] Denmark had hinted that γ-electrophilic attack of the Lewis acid on the allylstannane was important for isomerization, but provided no conclusive mechanism.[18] In this dissertation, an intermediate involved in the degenerate isomerization of allyl$SnBu_3$ catalyzed by **1** is characterized by NMR spectroscopy.

4.2 $B(C_6F_5)_3$-Catalyzed Allylstannation of Carbonyls

Scheme 4.3: Selectivity in Allylstannation of Aldehydes Catalyzed by $B(C_6F_5)_3$

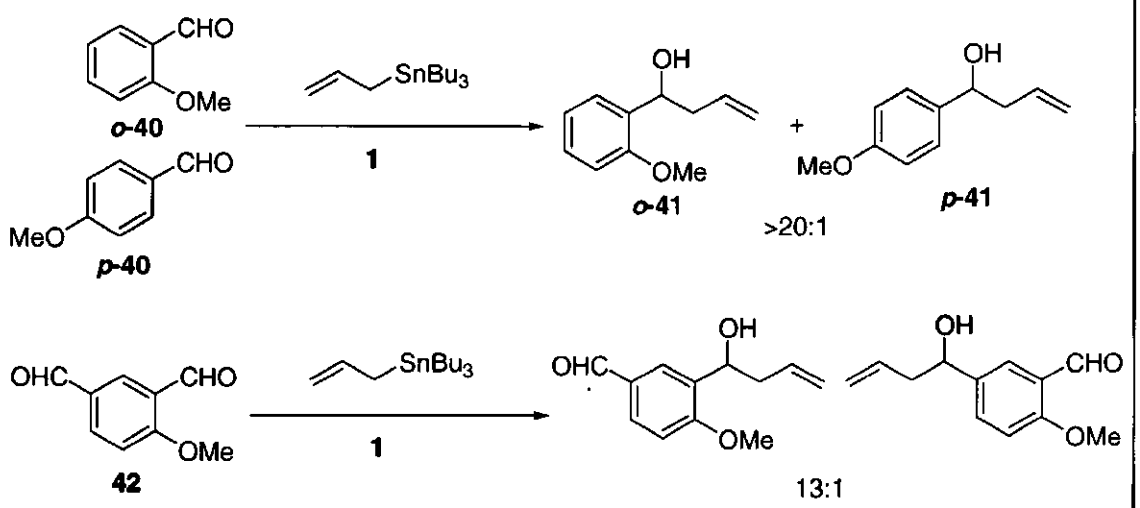

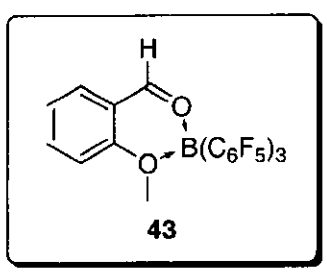

43

In 1998, Maruoka and coworkers reported that a stoichiometric amount of **1** promotes the allylstannation of carbonyls.[24] Allylstannation proceeded more facilely in those cases where a donor group was proximally located. For example, *ortho*-anisaldehyde, ***o*-40**, is allylated with >20:1 selectivity relative to the electronically similar *para*-anisaldehyde, ***p*-40**, Scheme 4.3. Furthermore, allylation of the dialdehyde **42** proceeds selectively (13:1) for the formyl group *ortho* to the methoxy group. To rationalize this remarkable selectivity, Maruoka proposed that the allylation of ***o*-40** proceeds via a hypercoordinate borane species, **43** where both the aldehyde and methoxy functions coordinate to **1**. This mode of bonding is not possible for coordination of *para*-anisaldehyde to **1**. No experimental evidence was included to support the intermediacy of a chelated species. Chelated intermediates have been shown unequivocally to form in other Lewis acid promoted reactions of carbonyls, however, the

central atom of the Lewis acids employed in these cases is considerably larger (Sn, Ti, Al) than B.[25] In fact, experimental demonstration of hypercoordination at boron is rare, consisting only of special examples contrived to favor this bonding mode.[26] The *conceptually*[27] new proposal that **1** could engage in hypercoordination should be viewed skeptically especially since no experimental evidence supports this claim.

4.3 Impetus for Mechanistic Study

The preliminary results reported by Maruoka clearly demonstrate the synthetic potential of $B(C_6F_5)_3$-catalyzed allylstannation of aldehydes. Coupled with the general importance of Lewis acid catalyzed allylstannation, development of an efficient asymmetric protocol would be highly desirable. A comprehensive understanding of the mechanism of this transformation, specifically elucidating the role of the Lewis acid **1**, will be invaluable in attaining this goal.

Our research on the hydrosilation of carbonyl and imine functions led to the proposal of a mechanism involving activation of the silane by **1** to transiently give **5**. Could analogous "activation" reactions be occurring in the allylstannation reaction or was a different complement of reactions involved? Would the same strategy designed for asymmetric hydrosilation reactions be suitable for allylstannation or would another strategy be more appropriate?

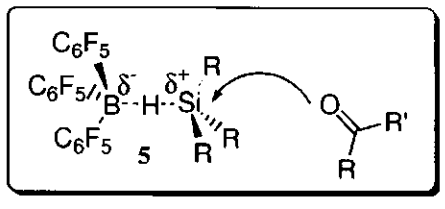

4.4 $B(C_6F_5)_3$-Catalyzed Allylstannation of Substituted Benzaldehydes

Table 4.1: Competitive Allylstannation Reactions of *ortho*- and *para*-Substitituted Benzaldehydes.

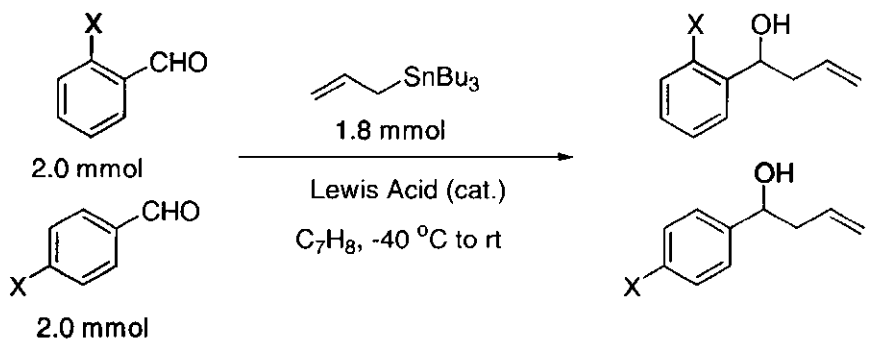

Entry	X	Lewis Acid	Ratio (*ortho*:*para*)
1	OMe	**1**	> 20:1
2	OTBS	**1**	> 20:1
3	F	**1**	**5:1**
4	Cl	**1**	**3:1**
5	Me	**1**	**1.1:1**
6	OMe	$[Bu_3Sn]^+[B(C_6F_5)_4]^-$	**12.5:1**
7	OMe	$BF_3{\cdot}OEt_2$	**7:1***

*1 eq. $BF_3{\cdot}OEt_2$ used in CH_2Cl_2, -78 °C to rt

Highly selective allylstannation of ***o*-40** versus ***p*-40** reported by Maruoka can be reproduced Table 4.1, entry 1; allylation of other substituted benzaldehyde mixtures range in selectivity, entries 2-5. Furthermore, the tabulated reactions occur using catalytic **1** whereas Maruoka used stoichiometric borane to promote the reactions. Selectivities were determined by ^1H NMR analysis after hydrolysis to the respective homoallylic alcohols. Interestingly, in the case of X = OTBS (entry 2, TBS = *tert*-butyldimethylsilyl) high selectivity was also observed in spite of the renowned inability

of silyloxy groups to chelate to Lewis acids.[28] Lower, yet still considerable selectivity was observed in the allylstannation of *ortho*/*para*-fluorobenzaldehyde (5:1, entry 3) and *ortho*/*para*-chlorobenzaldehyde (3:1, entry 4). Little or no selectivity was exhibited in the tolualdehyde competition experiment (entry 5). The selective allylstannation of *ortho*-anisaldehyde is not limited to catalysis by **1**; both $[Bu_3Sn]^+[B(C_6F_5)_4]^-$ (entry 6) and $BF_3{\bullet}OEt_2$ (entry 7) promote selective reactions as well. Although meaningful comparisons between the Lewis acids cannot be made since uniform reaction conditions could not be used, selectivity is not limited to carbonyls with proximal methoxy groups nor to catalysis by **1**.

4.5 $B(C_6F_5)_3$ Adducts of Aldehydes

Carbonyl functions coordinate strongly to **1** and indeed, Parks was able to fully characterize various carbonyl adducts both in solution and in the solid state.[29] Maruoka's proposal for the selectivity involving hypercoordinate boranes such as **43** was viewed to be chemically unreasonable based on the rarity of *bona fide* hypercoordinate borane compounds; therefore it was deemed unnecessary to exhaustively disprove its existence. However, the adducts of **1** and *ortho*- and *para*-anisaldehyde, ***o*-44** and ***p*-44** respectively, were characterized spectroscopically and in the solid state.

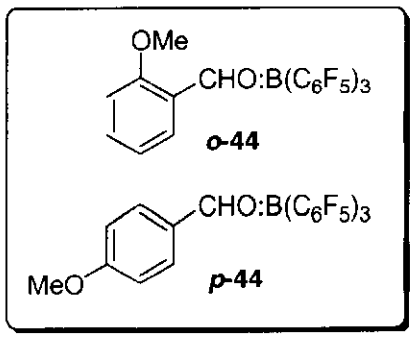

4.5.1 Characterization of Adducts

Solutions of ***o*-44** are bright yellow-green in color whereas solutions of ***p*-44** are colorless. Although, this observation suggests an obvious electronic difference between these two adducts, NMR analysis including nOe experiments provide no evidence for direct participation of the methoxy group via coordination to boron. Irradiation of the *ortho*- fluorine signal in ***o*-44** leads to no enhancement in the methoxy ^{1}H signal which would be expected if this group was coordinated to the boron atom especially since nOe effects between the *ortho*-fluorines and other ^{1}H's were observed.

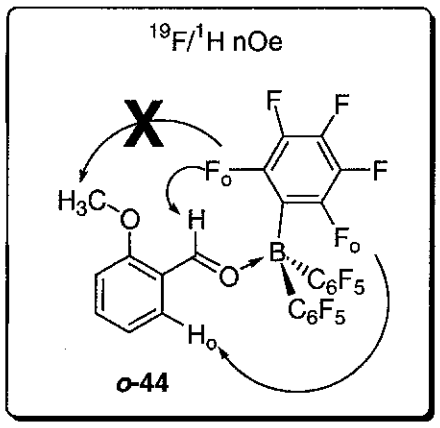

Both ^{11}B NMR and ^{19}F NMR spectroscopy provide no suggestive evidence for hypercoordination in ***o*-44**. The ^{11}B NMR shifts measured for ***o*-44** (3.3 ppm) and ***p*-44** (3.2 ppm) are consistent with coordination of a neutral ligand to **1** and are similar to those previously observed for carbonyl adducts of **1** (*eg.* PhCHO:**1**, δ = 5.0 ppm).[29] ^{19}F NMR spectroscopic data for ***o*-44** and ***p*-44** ($\Delta\delta_{p,m}$ = 7.2 and 7.1 ppm in CD_2Cl_2 at -60 °C) is consistent with neutral, four coordinate derivatives of **1** and the values are similar to those for other characterized carbonyl adducts of **1** (*eg.* $\Delta\delta_{p,m}$ = 8.2 ppm for PhCHO:**1** in C_6D_6).[29] No comparison can be made between this NMR data and that for hypercoordinate derivatives of **1**, but there is no reason based on the spectral data to suspect anything other than coordination solely by the carbonyl in ***o*-44**. Furthermore, there are no additional resonances observed in the ^{19}F NMR spectrum of ***o*-44** attributable to a minor isomer.

Figure 4.2: X-ray Structures of *o*-44, *p*-44 and 45.

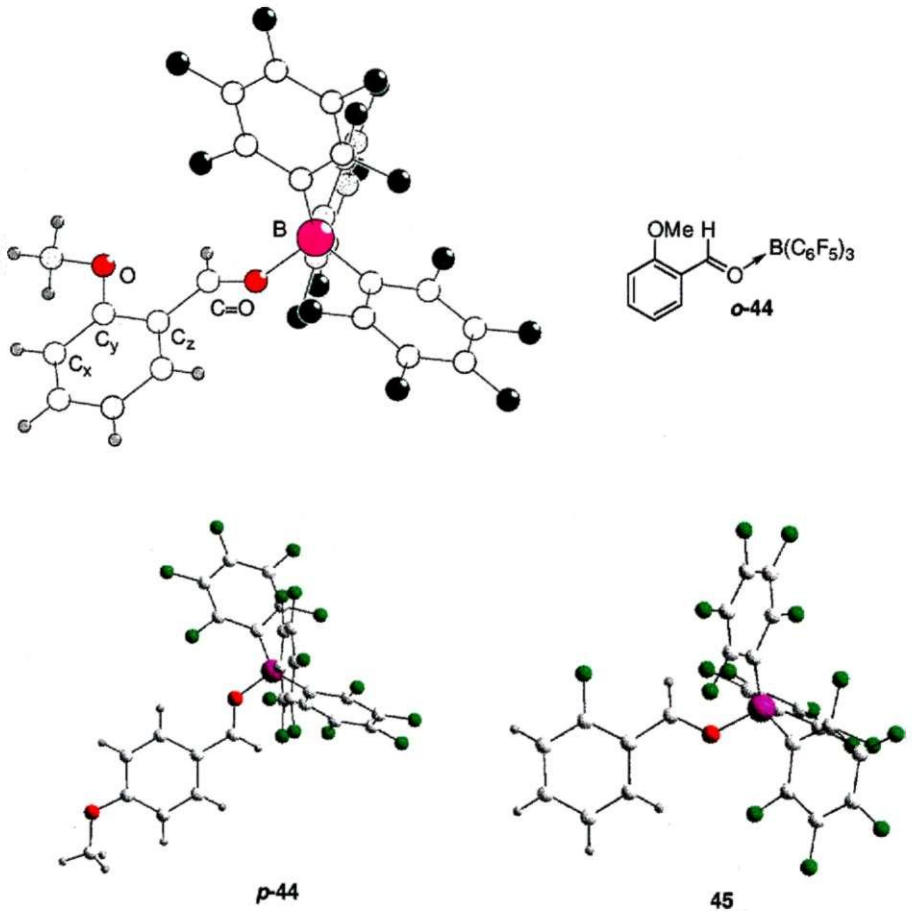

In the solid state, the methoxy group is not coordinated to the boron, Figure 4.2. The large Lewis acid **1** is coordinated in a bent fashion (< C-O-B = 127°) *syn* to the aldehydic H. The formyl:$B(C_6F_5)_3$ group orients itself to place the aldehydic hydrogen proximal to the methoxy group and the formyl unit is nearly coplanar with the aromatic ring. Based on the nOe studies described earlier, this type of conformation is favored in solution as well. The methoxy group is tilted slightly toward the formyl group (< O-C_y-C_z = 115.8° compared to < O-C_y-C_x = 124.8°) perhaps indicating a degree of hydrogen

bonding between the methoxy oxygen and formyl hydrogen;[30] the distance between the oxygen and formyl hydrogen is 2.33 Å which is within the sum of the van der Waals radii of H (1.20 Å) and O (1.52 Å).[31] An interaction between one of the *ortho*-fluorines and the formyl hydrogen is also suggested by a short distance of 2.40 Å. This type of interaction has previously been proposed for the adduct PhCHO:**1** where a distance of 2.56 Å was observed between the formyl hydrogen and one of the *ortho*-fluorines.[29] X-ray structures of ***p*-44** and *ortho*-fluorobenzaldehyde:$B(C_6F_5)_3$, **45**, were also obtained, Figure 4.2.

A comparison of some key metrical parameters between ***o*-44** and ***p*-44** is provided in Table 4.2. The C=O bond is slightly longer in ***o*-44** compared to ***p*-44** suggesting it is more activated; however, the O-B bond is shorter in ***p*-44** compared to ***o*-44** suggesting that the Lewis acid is more tightly bound to the *para*-congener. It is unwise to draw any firm conclusions based on these differences. The distances between the methoxy O and the directly bonded aryl carbon are almost identical in the two adducts showing that there is no substantial difference in resonance delocalization effects involving the methoxy groups (see ***o*-44'**). Again no evidence for hypercoordination involving participation of the fluorine is observed in the solid state structure of adduct **45**.

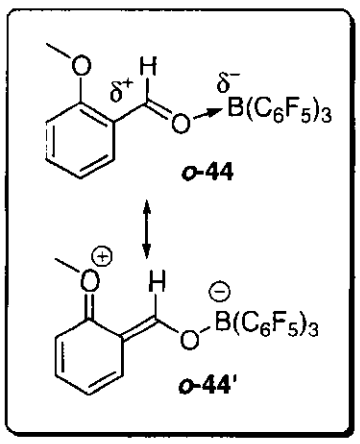

Table 4.2: Comparison of Metrical Parameters Between Aldehyde-Borane Adducts.

Adduct	C=O (Å)	O-B (Å)	MeO-C (Å)	< C-O-B
***o*-44**	1.263(12)	1.589(26)	1.345(17)	127.00(31)
***p*-44**	1.2523(16)	1.5743(17)	1.3420(17)	129.04(11)
45	1.247(4)	1.603(5)	---	126.41(25)

4.5.2 Selectivity in Binding $B(C_6F_5)_3$

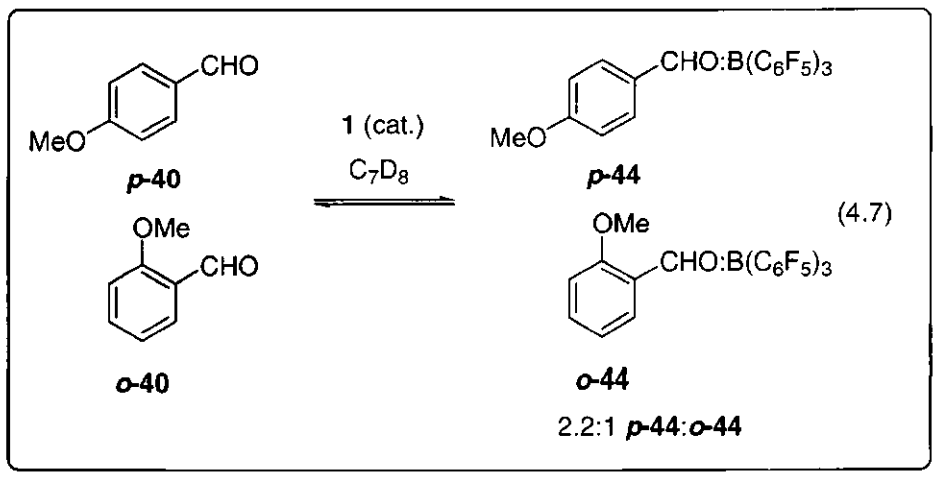

NMR studies pitting ***o*-40** in competition with ***p*-40** for **1** were carried out in order to test the hypothesis that the observed selectivity could simply result from preferential formation of ***o*-44**. However, when a 1:1 mixture of ***o*-/*p*-40** is mixed in C_7D_8 with a catalytic quantity of **1**, only modest selectivity is observed by ^{19}F NMR spectroscopy. In fact, preferential (2.2:1) formation of ***p*-44** is observed. Clearly, there is no inherent preference for formation of ***o*-44** eliminating selective coordination of **1** as a possible origin of the selectivity.

4.6 Reactions of $B(C_6F_5)_3$ with $AllylSnBu_3$

A key step in the hydrosilation of carbonyl functions and imines is the interaction of **1** with silane. NMR tube experiments were conducted to determine whether any interaction between **1** with $allylSnBu_3$, both in the absence and presence of a Lewis base, exists. In fact, substantial evidence has been compiled that demonstrates **1** and $allylSnBu_3$ do react. These observations have significant relevance to the poorly understood process of Lewis acid-catalyzed allylstannane isomerization reaction, but are less relevant to the allylstannation of aldehydes catalyzed by **1**.

4.6.1 Reaction of $B(C_6F_5)_3$ and 1 Equivalent of $AllylSnBu_3$

Scheme 4.4: Reactions of Allylstannanes with 1.

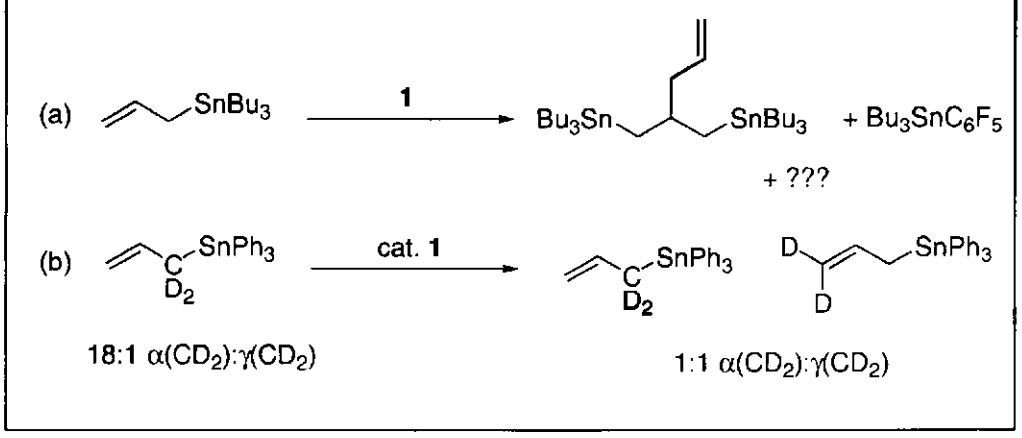

Borane **1** and $allylSnBu_3$ react with each other in the absence of external bases. First, when $allylSnBu_3$ and **1** are mixed in a 1:1 ratio at room temperature, the signals for the allyl protons in the ^1H NMR spectrum are all significantly broadened. Secondly, decomposition of these reagents occurs at room temperature leading to among other products, $Bu_3SnC_6F_5$ and $Bu_3SnCH_2CH(allyl)CH_2SnBu_3$ (the product from allylstannation of $allylSnBu_3$), Scheme 4.4a. Thirdly, when selectively dideuterated

allylSnPh$_3$[32] is treated with catalytic **1**, scrambling of the deuteriums occurs from the allylic positions (α to the Sn) into the terminal vinylic positions (γ to the Sn) leading to a ~1:1 mixture of isotopomers, Scheme 4.4b.

Figure 4.3: NMR Spectra (CD_2Cl_2, -60 °C) of 1:1 Mixture of AllylSnBu$_3$ and 1.

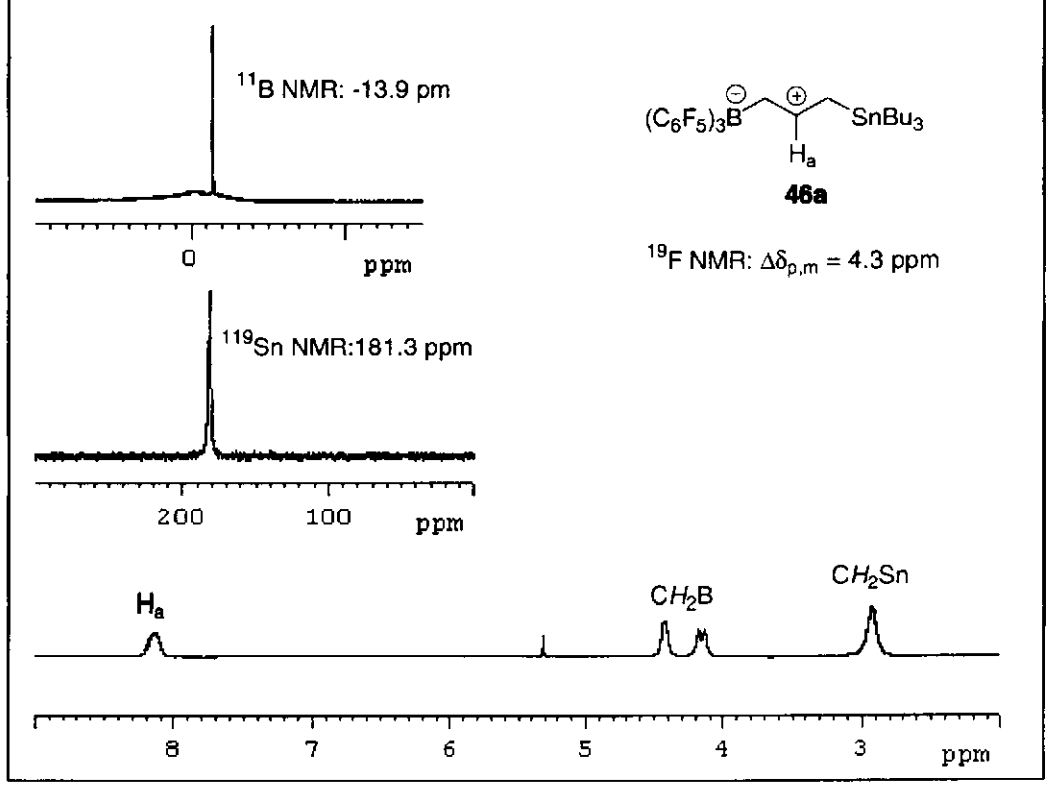

More importantly, low temperature NMR investigations enabled the characterization of a Lewis acid:base adduct, **46**, formed between allylSnBu$_3$ and **1**. When **1** and allylSnBu$_3$ are mixed in a 1:1 ratio in C_7D_8 or CD_2Cl_2 at room temperature, there is no noticeable change in the ^{19}F NMR spectrum (relative to free **1**). However, upon cooling, the ^{19}F NMR spectrum changes dramatically, the value for $\Delta\delta_{p,m}$ decreasing gradually from 18.1 ppm at 25 °C to 5.0 ppm in C_7D_8 and 4.3 ppm in CD_2Cl_2, both at -60 °C. This contracted value is consistent with formation of an anionic borate

species in which the corresponding countercation is still tightly associated (see Section 1.2.5). ^{1}H, ^{13}C, ^{11}B, and ^{119}Sn NMR spectroscopy at -60 °C all support this claim, Figures 4.3 and 4.4.

Figure 4.4: NMR Spectroscopic Characterization of 46a/b in CD_2Cl_2 at -60 °C

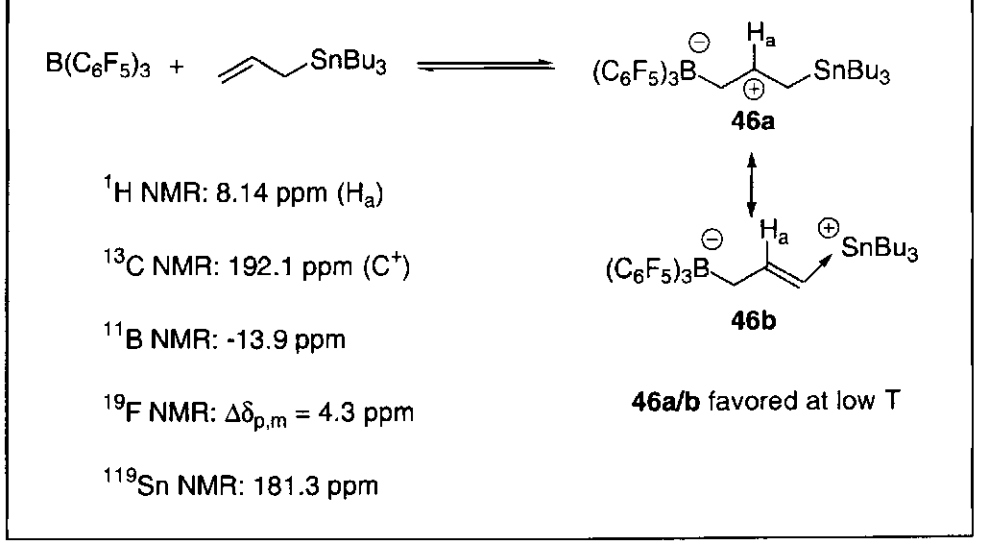

Based on the NMR measurements listed above, this new species has been characterized as the resonance hybrid **46a/b**. A negative ^{11}B NMR shift (-13.9 ppm) is consistent with an anionic borate compound. The ^{119}Sn NMR shift (181.3 ppm) is suggestive of only slight positive charge build-up at the tin (see Chapter 1). Finally ^{1}H and ^{13}C NMR both indicate substantial positive charge build-up at the middle carbon as in resonance form **46a**. Upon warming the solution, the zwitterionic species reverts back to the neutral reactants, **1** and allyl$SnBu_3$.

4.6.2 Excess Allylstannane - Isomerization of Allylstannanes

Figure 4.5: ^{1}H NMR Spectra (CD_2Cl_2, -60 °C) of AllylSnBu$_3$ and 1: (a) 1:1 (b) 2:1 and (c) 5:1

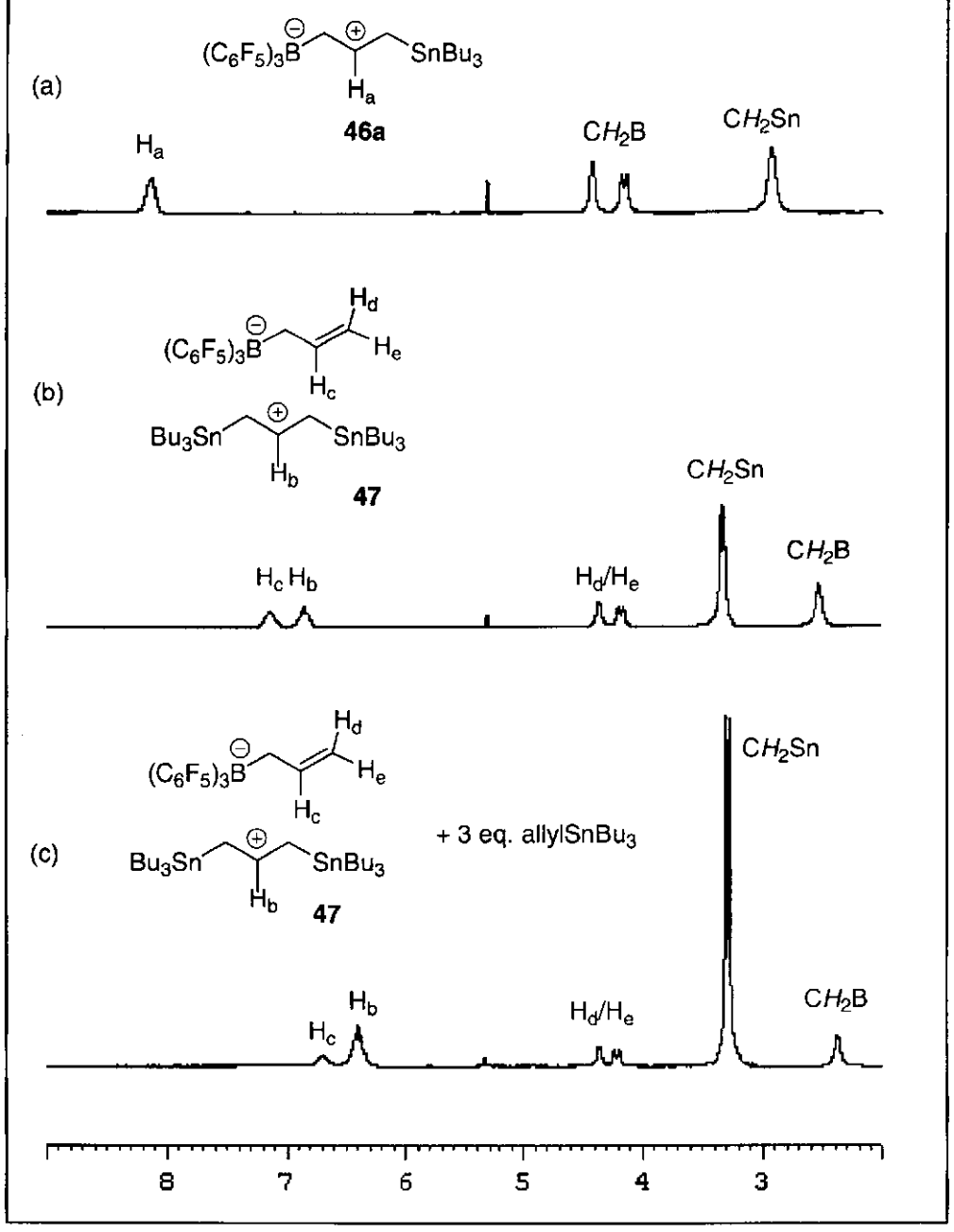

When allylSnBu$_3$ and **1** are mixed in a 2:1 ratio in CD_2Cl_2, NMR studies reveal interesting dynamic processes of mechanistic relevance to Lewis acid-catalyzed allylstannane isomerization. At elevated temperatures (>-40 °C), ^{19}F NMR spectroscopy is again consistent with anionic borate formation ($\Delta\delta_{p,m}$ = 3.9 ppm). However, only one set of extremely broadened ^1H resonances for the allyl group is distinguishable in the ^1H NMR spectrum. Free allylSnBu$_3$ is in rapid exchange with allylSnBu$_3$ incorporated in **46a/b**. However, at -60 °C, distinct ^1H NMR signals for the allylborate are now apparent. Additionally, ^1H NMR signals at 6.85 ppm (quint, 1H) and 3.33 ppm (d, 4H) are observed, Figure 4.5b.

Figure 4.6: NMR Data for Ion-Pair 47 in CD_2Cl_2 at -60 °C (2:1 AllylSnBu$_3$:B(C$_6$F$_5$)$_3$).

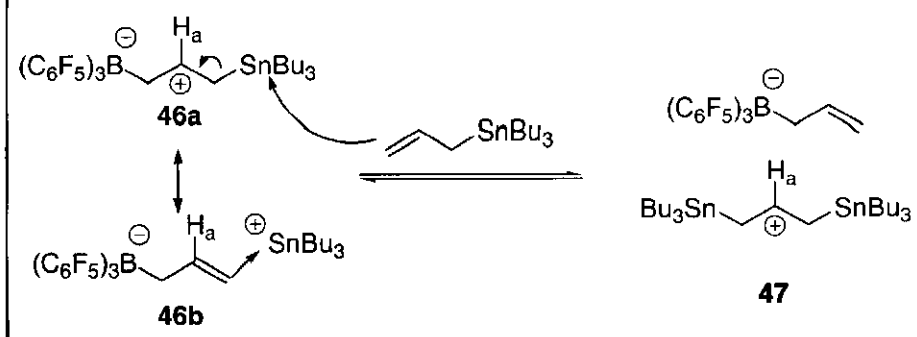

^1H NMR: 6.85 ppm (H_a)

^{13}C NMR:161.2 ppm (C^+)

^{11}B NMR: -14.2 ppm

^{19}F NMR: $\Delta\delta_{p,m}$ = 3.9 ppm

^{119}Sn NMR: 90.8 ppm

This ^{1}H NMR spectrum has been attributed to the ion-pair **47**, Figure 4.6. The second equivalent of allylSnBu$_3$ displaces the allylborate from the incipient "Bu$_3$Sn$^+$" in **46a/b** thereby producing the novel cation "Bu$_3$SnCH$_2$C$^+$HCH$_2$SnBu$_3$" where the cationic charge at the central carbon is stabilized by *two* electropositive tin atoms through hyperconjugation.[21] The aforementioned quintet and doublet result from this symmetrical carbocation. One ^{119}Sn NMR signal at 90.8 ppm is observed, intermediate between that observed for **46a/b** (181.3 ppm) and allylSnBu$_3$ (-17 ppm). At slightly higher temperatures, the anion, [allylB(C$_6$F$_5$)$_3$]$^-$, back-transfers an allyl group to one of the "Bu$_3$Sn$^+$" groups (regenerating **1** and two equivalents of allylSnBu$_3$) leading to the observed coalesence.

In the presence of five equivalents of allylSnBu$_3$, similar chemistry takes place. Again ^{1}H NMR signals for both [allylB(C$_6$F$_5$)$_3$]$^-$ and [Bu$_3$SnCH$_2$CHCH$_2$SnBu$_3$]$^+$ are distinguishable at -60 °C, Figure 4.5c. Now, however, the signals for the cation are of greater intensity relative to the anion since the cation and free allylSnBu$_3$ are exchanging rapidly even at this low temperature. This equilibrium is reflected by the fact that the ^{1}H NMR signals of the cation are now shifted closer to those observed for free allylSnBu$_3$. The ^{119}Sn NMR shift (38.3 ppm) is also shifted closer toward that of free allylSnBu$_3$ (-17 ppm).

Scheme 4.5: Degenerative Scrambling of $AllylSnBu_3$ via 47.

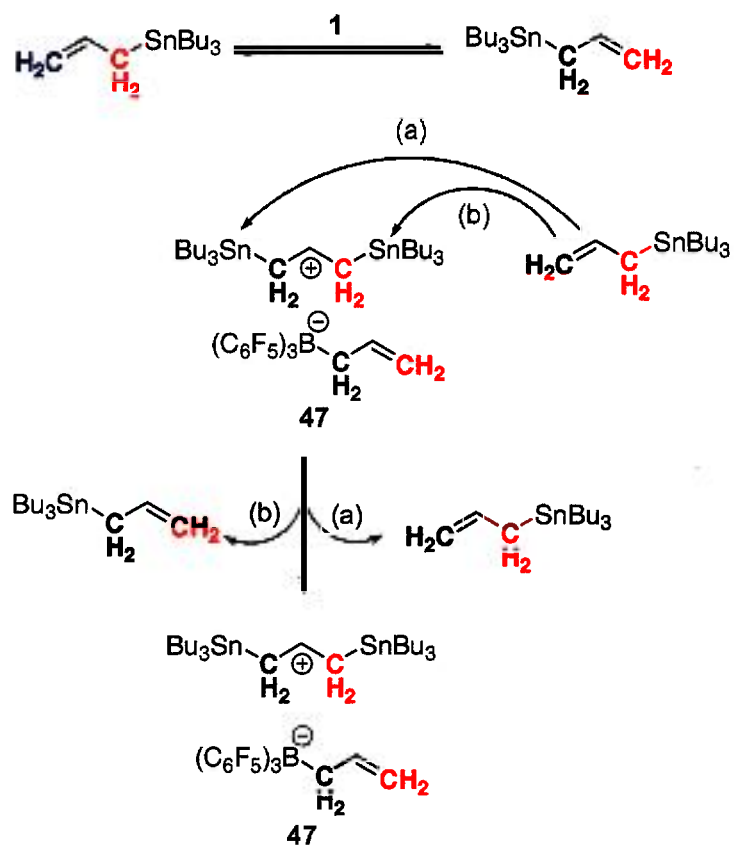

The chemistry described above results in the net degenerative scrambling of the α-CH_2 group and the γ-CH_2 groups of the allyl moiety, Scheme 4.5. Although, the cation "$Bu_3SnCH_2C^+HCH_2SnBu_3$" is not distinguishable at higher temperatures where scrambling is rapid, the intermediacy of ion-pair **47** is proposed.

Scheme 4.6: Synthesis of $[Bu_4N]^+[allylB(C_6F_5)_3]^-$.

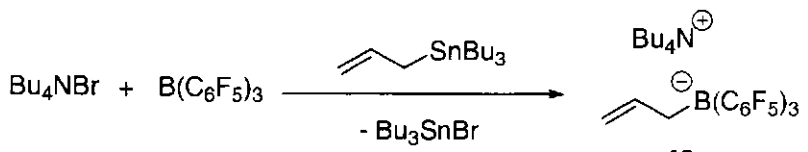

48

^{11}B NMR (CD_2Cl_2, -60 °C): δ -14.3 ppm

^{19}F NMR (CD_2Cl_2, -60 °C): $\Delta\delta_{p,m}$ = 3.2 ppm

The anionic and cationic portions of **47** were prepared independently with stable counterions in both cases. First, $[Bu_4N]^+[allylB(C_6F_5)_3]^-$, **48**, was prepared *in situ* according to Scheme 4.6. Abstraction of the allyl group from $allylSnBu_3$ by **1** is followed/accompanied by attack of bromide at the electropositive tin atom leading to Bu_3SnBr as a byproduct. ^1H, ^{13}C, ^{19}F NMR and in particular, ^{11}B NMR spectral data for **47** and **48** in CD_2Cl_2 at -60 °C, are similar as would be expected for the same anion. The ^{19}F NMR data for **47** and **48** are not identical (**47**, $\Delta\delta_{p,m}$ = 3.9 ppm; **48**, $\Delta\delta_{p,m}$ = 3.2 ppm) underscoring the fact that **47** is in equilibrium with neutral reagents. Indeed, excess $allylSnBu_3$ (5 equivalents total) shifts the equilibrium in favor of **47** ($\Delta\delta_{p,m}$ = 3.6 ppm).

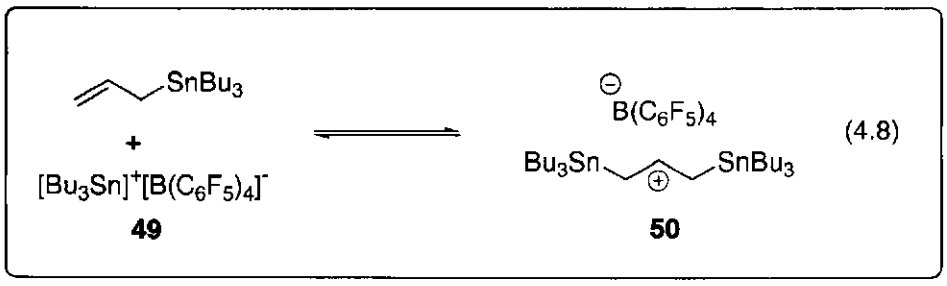

The cationic portion of **46** is modeled using Lambert's stannylium reagent, $[Bu_3Sn(toluene)]^+[B(C_6F_5)_4]^-$, **49**, as a stable source of "Bu_3Sn^+";[33] the *tetrakis*-pentafluorophenylborate counterion has been shown to be quite stable in solution at room

temperature to the solvated Lewis acidic stannylium species. This reagent is prepared in C_7D_8 by addition of $[Ph_3C]^+[B(C_6F_5)_4]^-$ to Bu_3SnH leading to formation of a two-layer mixture where **49** resides primarily in the bottom layer. If necessary, Ph_3CH can be removed by repeatedly extracting the bottom layer with additional toluene without removing significant amounts of **49**. The bottom layer is then dissolved in CD_2Cl_2 at low temperature followed by successive additions of approximately one and then four equivalents of allyl$SnBu_3$ leading to **50**.[i]

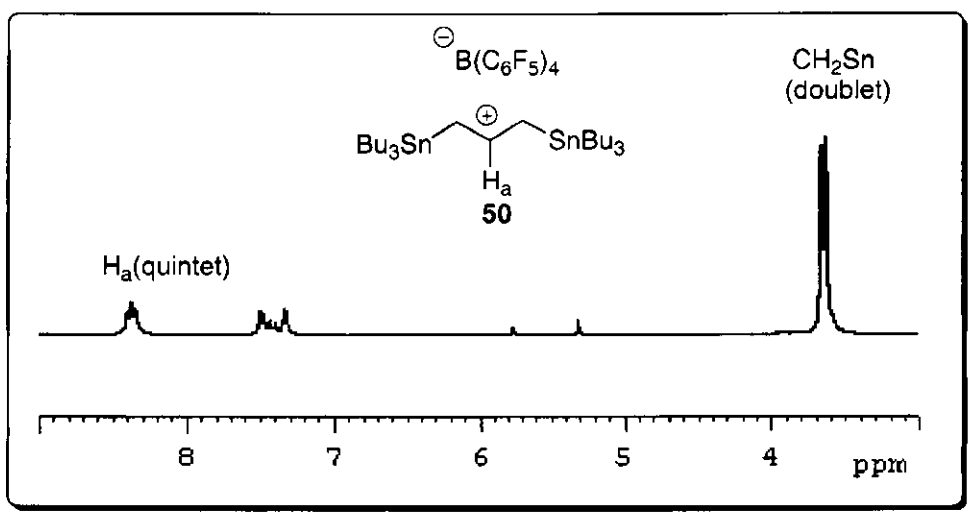

The distinct quintet/doublet observed for **47** and assigned to the cation $[Bu_3SnCH_2CHCH_2SnBu_3]^+$ is reproduced under these conditions. In the presence of excess allyl$SnBu_3$, rapid exchange between allyl$SnBu_3$ and the cation occurs at -60 °C. Again this is reflected in the ^{119}Sn NMR spectra where the value decreases from 434 ppm for **49**[ii], 184 ppm for **50** and 40 ppm in the presence of four equivalents of allyl$SnBu_3$. In the latter case, the observed value is an average of the ^{119}Sn NMR shifts of **50** and free

[i] $Bu_3Sn(toluene)]^+[B(C_6F_5)_4]^-$ decomposes in CD_2Cl_2 at room temperature.
[ii] This value is different than that reported by Lambert (262 ppm), see reference 33.

allylSnBu$_3$. This averaging was also observed for **47** in the presence of excess allylSnBu$_3$.

In summary, the identification of **47** as $[Bu_3SnCH_2C(H)CH_2SnBu_3]^+[allylB(C_6F_5)_3]^-$ is strongly supported by independent synthesis of both the anionic and cationic halves of the ion-pair with the stable counterions $[Bu_4N]^+$ and $[B(C_6F_5)_4]^-$ respectively. Ion-pair **47** is proposed to catalyze isomerization chemistry; that is, reaction of **1** with allylSnBu$_3$ generates a reactive stannylium species susceptible to attack by a second equivalent of allylSnBu$_3$. Although, other Lewis acids have not been specifically studied, it is suggested that similar intermediates could be involved in other isomerization reactions, especially in light of some of the "interesting" mechanisms described in the introduction to this chapter.

4.6.3 Reaction of Activated Allylstannane with other Nucleophiles

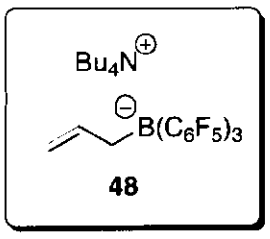

48

The observation that a mild nucleophile such as allylSnBu$_3$ is sufficiently reactive to displace "Bu_3Sn^+" from the zwitterionic **46a/b** resonance hybrid indicates that this interaction could be important in the allylstannation of aldehydes. Other nucleophiles have been shown to readily displace the allylborate anion. As mentioned, reaction of Bu$_4$NBr with one equivalent of each of allylSnBu$_3$ and **1** leads to the formation of ion-pair **48** and Bu$_3$SnBr presumably via the intermediacy of **46a/b**.

The reaction of dimethylaniline with allylSnBu$_3$ and **1** (4:1:1) also generates an ion-pair formulated as [(PhNMe$_2$)SnBu$_3$]$^+$[allylB(C$_6$F$_5$)$_3$]$^-$, **51**. The anion has been characterized by ^{1}H, ^{13}C, ^{19}F and ^{11}B NMR spectroscopy and closely matches that observed for **48**. The cation has been characterized as [(PhNMe$_2$)SnBu$_3$]$^+$ by comparison of its ^{119}Sn NMR shift to that obtained for **52** formed from the reaction of [Bu$_3$Sn(C$_7$D$_8$)]$^+$[B(C$_6$F$_5$)$_4$]$^-$ with one equivalent of PhNMe$_2$ (for both, ^{119}Sn NMR: δ = 272 ppm at -60 °C in CD_2Cl_2). No change in the ^{119}Sn NMR shift is observed upon addition of excess PhNMe$_2$ leading to the conclusion that only one equivalent of dimethylaniline coordinates. Rapid exchange of free and bound PhNMe$_2$ does however occur even at -60 °C.

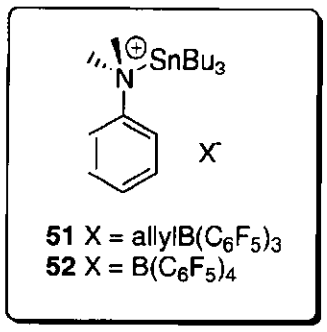

51 X = allylB(C$_6$F$_5$)$_3$
52 X = B(C$_6$F$_5$)$_4$

4.7 Reaction of B(C$_6$F$_5$)$_3$ with AllylSnBu$_3$ in the Presence of Aldehyde

The allylstannation of ***o*-40** catalyzed by **1** proceeds only slowly at -40 °C and therefore it was envisioned that NMR spectroscopic analysis at even lower temperature would enable observation of intermediates. As NMR solvents, both C_7D_8 and CD_2Cl_2 have been used. In C_7D_8, NMR analysis of ion-pairs is complicated by the fact that two-layer reaction mixtures are formed whereas in CD_2Cl_2, the reaction mixtures are homogeneous. The chemistry that occurs in each solvent has been judged to be the same; however, NMR analysis was more convenient using CD_2Cl_2 and therefore, was the solvent of choice for the following experiments. Although the mechanism for the allylstannation reaction and the origin of selectivity for ***o*-40** versus ***p*-40**, are closely entwined, the two features are disentangled in the following discussion. First, experiments are described that lead to a general mechanistic picture for the reaction in

terms of Lewis acid activation (B *vs* Sn), allyl delivery (C-C bond formation) and stannyl ether formation (O-Sn bond formation). This proposal is then contextualized with respect to the preference for allylation of aldehydes possessing proximal donor groups.

4.7.1 Observation of an Ion-Pair by NMR Spectroscopy

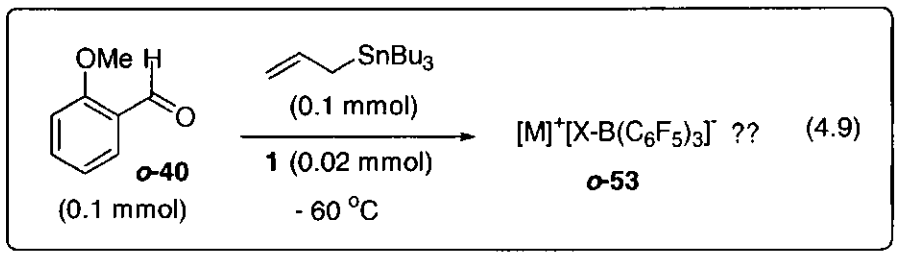

To mimic the catalytic conditions, allylSnBu$_3$ (0.1 mmol) was added slowly to a mixture of ***o*-40** (0.1 mmol) and **1** (0.02 mmol) in C_7D_8 or CD_2Cl_2 cooled to -78 °C. The reaction mixture was then placed in the NMR probe precooled to -60 °C and ^{19}F and ^{1}H NMR spectra were collected periodically. As shown by the series of ^{19}F NMR spectra in Figure 4.7, a clean reaction does occur. Similar spectra were obtained in CD_2Cl_2. Initially, the only ^{19}F containing species in solution is the borane adduct, ***o*-44**, Figure 4.7a, which are gradually supplanted by a new set of signals where $\Delta\delta_{p,m}$= 3.16 ppm. A stable ion-pair, "***o*-53**", is formed at -60 °C incorporating all of the available **1**.

Figure 4.7: Observation of an Ion-Pair by ^{19}F NMR Spectroscopy of 5:1:1 Mixture of *Ortho*-Anisaldehyde:allylSnBu$_3$:1 (CD_2Cl_2, -60 ^{o}C)

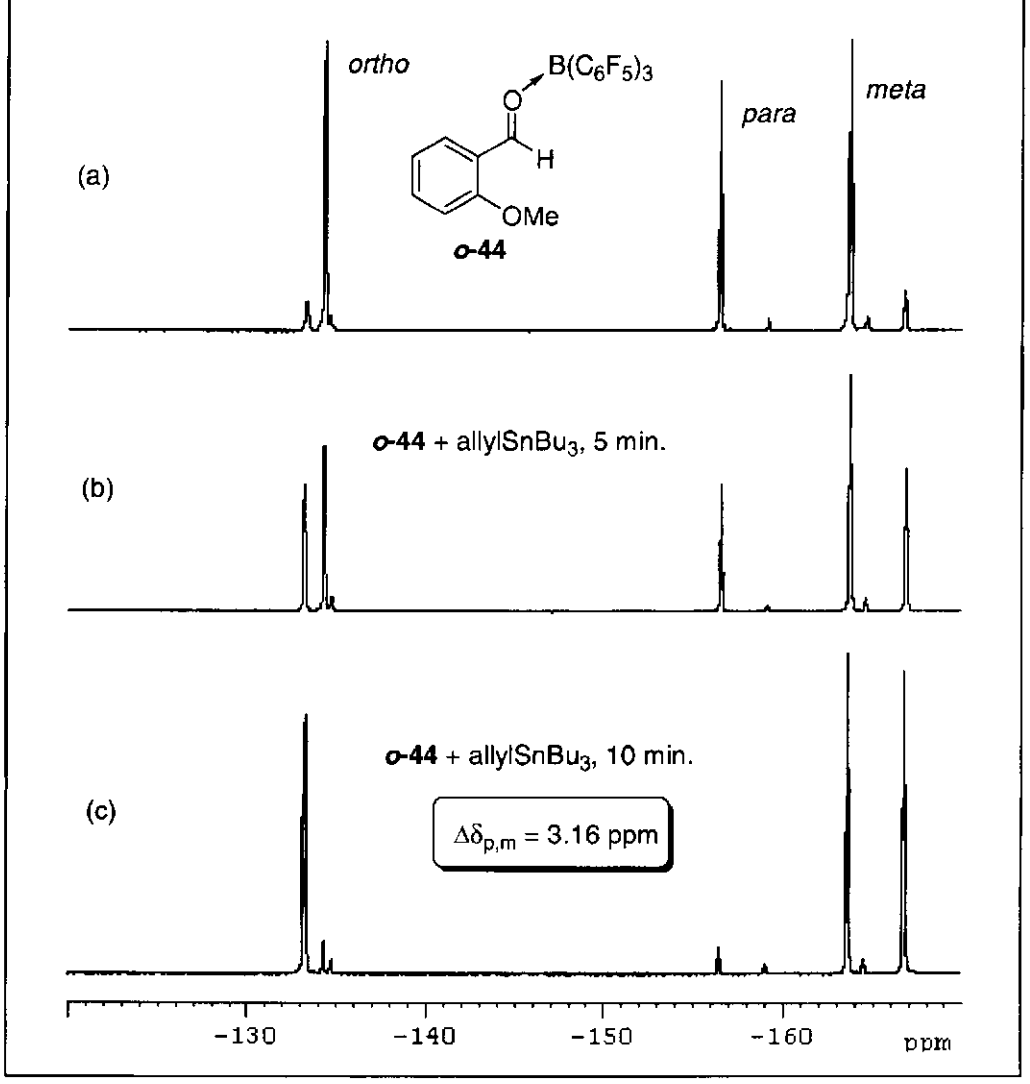

Similar NMR studies were effected using *para*-anisaldehyde, ***p*-40**, probing for any differences that might provide clues to explain Maruoka's results. Experiments have indeed shown that ***o*-40** reacts much faster and at lower temperatures than ***p*-40**. AllylSnBu$_3$, ***p*-40** and **1** were mixed in a 1:5:1 ratio at -60 °C and ^{1}H and ^{19}F NMR spectra were measured. Whereas complete ionization to ***o*-53** occurs promptly (15

minutes), over the same time, there is only a minor set of signals attributable to the ion-pair, ***p*-53**, in the ^{19}F NMR spectrum after 15 minutes. After 35 minutes at -60 °C, ^{19}F NMR spectroscopy indicates ~20% of **1** has been converted to an ion-pair. After four hours, conversion of **1** to an ion-pair is ~ 50% complete although the reaction is not as clean as reactions with ***o*-40**. Warming to -40 °C, does lead to faster conversion but subsequent reactions compete.

These results for the Lewis bases, ***o***- and ***p*-40**, would at first, appear to be analogous to the results obtained with allylSnBu$_3$, bromide and dimethylaniline which can displace [allylB$(C_6F_5)_3$]$^-$ from **46a/b**. However, careful analysis of ***o*-53** by ^1H, ^{13}C and ^{11}B NMR spectroscopy reveals that a different type of ion-pair is formed which does not involve nucleophilic attack on **46a/b** and that [allylB$(C_6F_5)_3$]$^-$ is not produced.

4.7.2 Characterization of the Anion

When allylSnBu$_3$ (0.033 mmol) is added to ***o*-40** (0.10 mmol) and **1** (0.033 mmol) in CD_2Cl_2 at -70 °C,[iii] ^1H NMR analysis shows clean formation of a new species possessing both aromatic and allylic signals that are clearly distinguishable from those still present for unreacted *ortho*-anisaldehyde, Figure 4.8. Complete consumption of the allylSnBu$_3$ occurs at -60 °C. Diagnostic ^1H NMR signals attributable to [allylB$(C_6F_5)_3$]$^-$ are *not* observed. The anion has been characterized by ^1H, ^{13}C, ^{11}B, and ^{19}F NMR spectroscopy and identified as an alkoxyborate anion, [(ortho-anisyl)CH(allyl)OB$(C_6F_5)_3$]$^-$.

[iii] A 3:1:1 ratio of *ortho*-anisaldehyde:**1**:allylSnBu$_3$ in CD_2Cl_2 was determined to be optimal mixture.

Figure 4.8: ^{1}H NMR Spectra (CD_2Cl_2, -60 °C) of (a) Ion-Pair *o*-53 and (b) Ion-pair *o*-54.

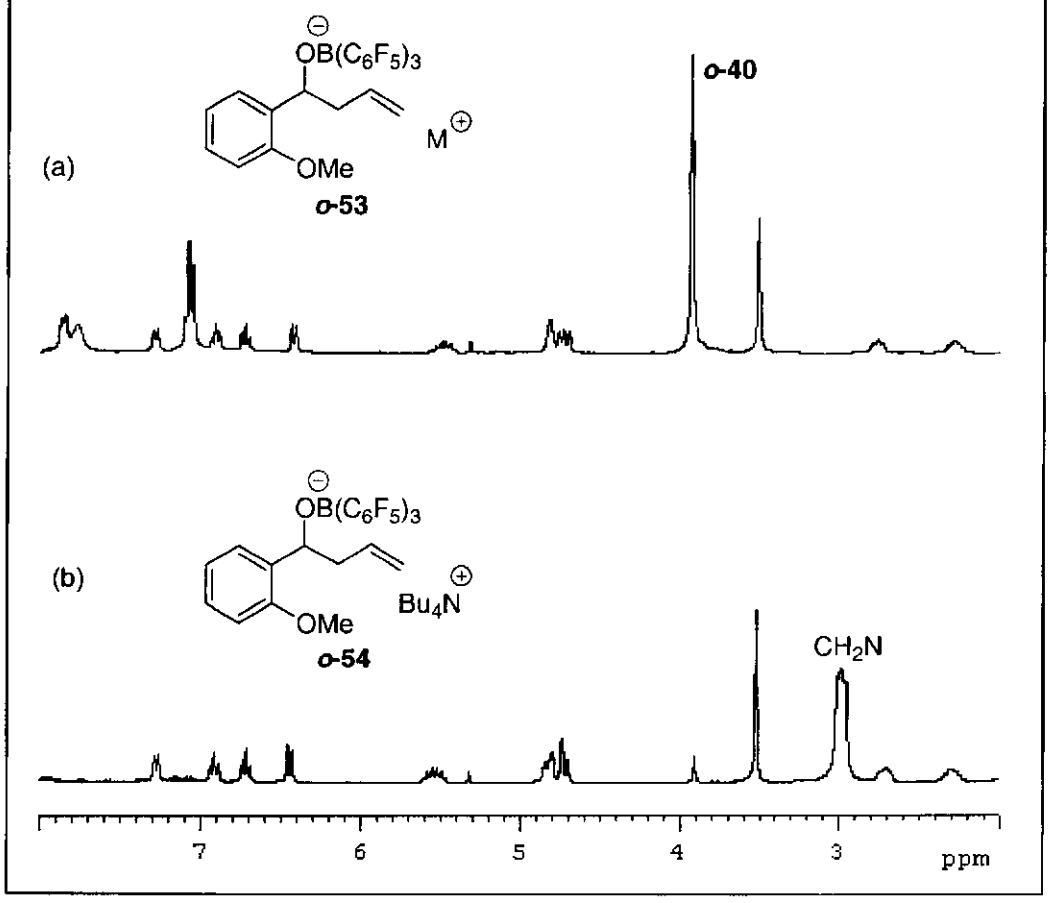

This identification has been confirmed by independent synthesis of $[Bu_4N]^+[(ortho\text{-anisyl})CH(allyl)OB(C_6F_5)_3]^-$, ***o*-54**, outlined in equation 4.10 where *in situ* generated **48** is added to ***o*-40** *catalyzed* by **1** at room temperature. The ^{1}H and ^{13}C NMR spectra of ***o*-53** and ***o*-54** are identical in the relevant regions, Figure 4.8. Identical values for the ^{11}B NMR shifts (-4.5 ppm) are obtained at -60 °C for ***o*-53** and ***o*-54**. These values are considerably different than the values (~ -14 ppm) obtained for the allylborate anions.

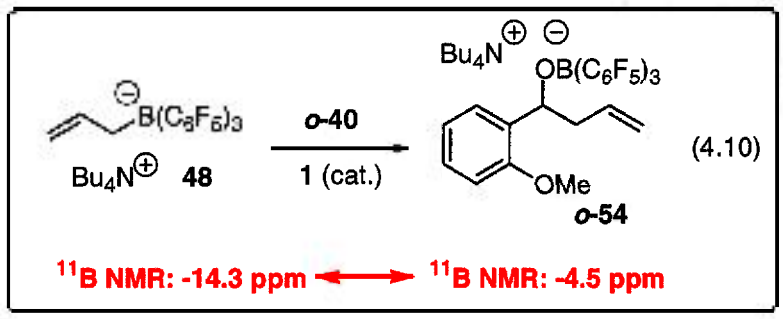

Although it could not be formed as cleanly, the anionic component of ion-pair ***p*-53** derived from ***p*-40** is confirmed to also be an alkoxyborate species, [(*para*-anisyl)CH(allyl)$OB(C_6F_5)_3$]$^-$, by NMR spectral comparison to the ion-pair, $[Bu_4N]^+$[(*para*-anisyl)CH($OB(C_6F_5)_3$)allyl]$^-$, ***p*-54**, prepared anogously to ***o*-54**.

4.7.3 Characterization of the Cation

Although the anionic component of the ion-pair is not consistent with [allyl$B(C_6F_5)_3$]$^-$, it was expected that an aldehyde-ligated "Bu_3Sn^+" species was still important. In order to establish the coordination environment at the cationic tin center, ^{119}Sn NMR spectroscopy was instrumental. Again, using Lambert's stannylium reagent, **49**, the ^{119}Sn NMR shifts in CD_2Cl_2 of [(***o*-40**)$SnBu_3$]$^+$[$B(C_6F_5)_4$]$^-$, ***o*-55**, and [(***o*-40**)$_2SnBu_3$]$^+$[$B(C_6F_5)_4$]$^-$, ***o*-56**, were measured as 297.6 ppm and 90.2 ppm respectively, Figure 4.9b/c.

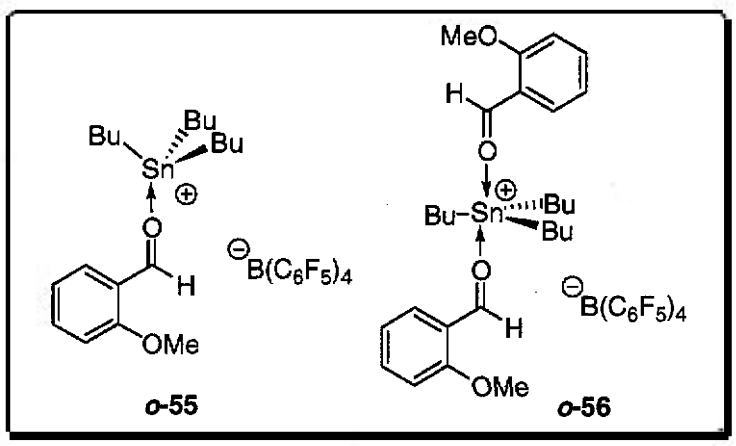

Figure 4.9: 149.2 MHz ^{119}Sn NMR Spectra (C_7D_8, -60 ^{o}C)
(a) Ion-pair 49 (b) 49 + 1 eq. *o*-40 (c) 49 + 2 eq. *o*-40.

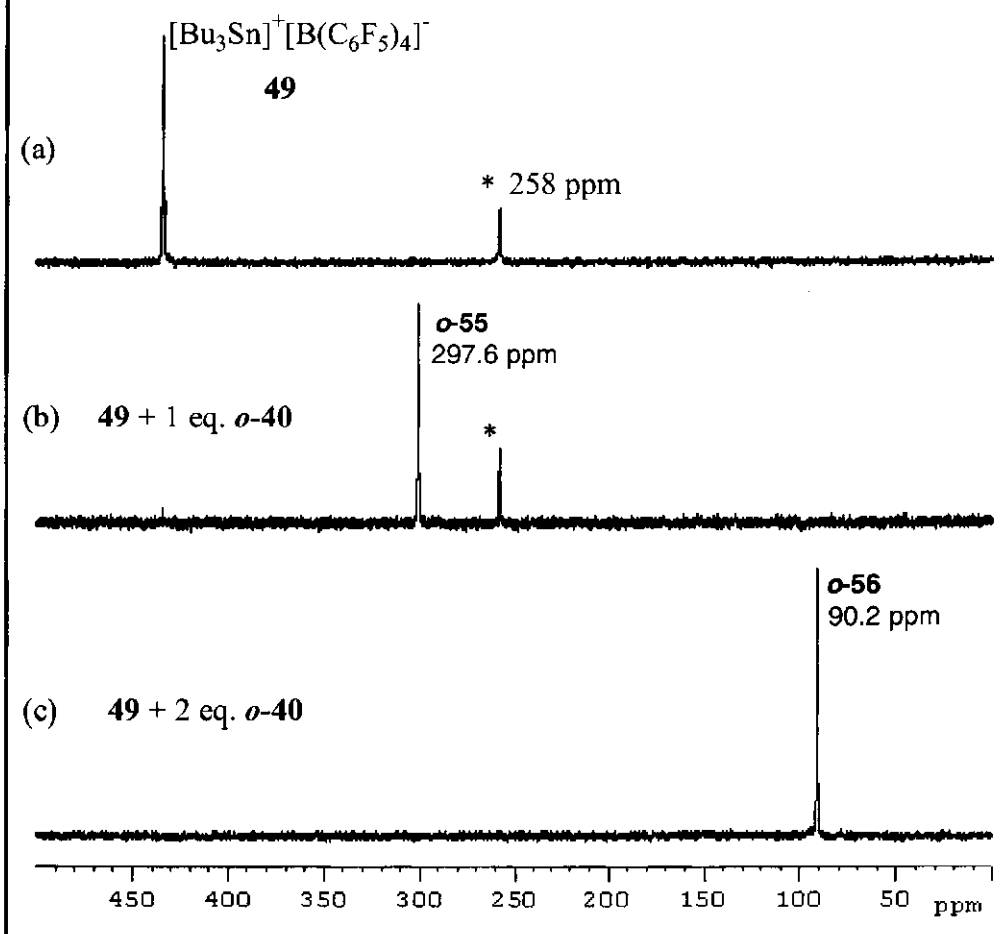

* unidentified peak, Lambert reported the NMR shift of **49** as 262.8 ppm (C_6D_6, r.t.), see reference 33.

Addition of greater than two equivalents of ***o*-40** led to no change in the ^{119}Sn NMR shift. However, ^{1}H NMR analysis reveals that rapid exchange between free and bound ***o*-40** occurs even at -60 °C. The ion-pair ***o*-53** (generated from a 5:1:1 ratio of ***o*-40**:**1**:allylSnBu$_3$) in CD_2Cl_2 at -60 °C exhibits a ^{119}Sn NMR signal at 90.1 ppm. It can be reliably concluded then that the cationic portion of the ion-pair observed under

catalytically relevant conditions is $[(\boldsymbol{o}\text{-}\mathbf{40})_2SnBu_3]^+$ where free and bound aldehyde exchange rapidly even at low temperature.

Similarly, $[(\boldsymbol{p}\text{-}\mathbf{40})SnBu_3]^+[B(C_6F_5)_4]^-$, ***p*-55**, and $[(\boldsymbol{p}\text{-}\mathbf{40})_2SnBu_3]^+[B(C_6F_5)_4]^-$, ***p*-56**, were analyzed by ^{119}Sn NMR spectroscopy. Values of 290.5 ppm and 82.5 ppm were obtained respectively at -60 °C. The ^{119}Sn NMR shift measured for ***p*-53** is 82.0 ppm; the cationic half of ***p*-53** has been identified as $[(\boldsymbol{p}\text{-}\mathbf{40})_2SnBu_3]^+$. These NMR shifts are 7.1 and 7.7 ppm upfield-shifted from those observed for ***o*-55** and ***o*-56** suggesting that *para*-anisaldehyde is more Lewis basic to "Bu_3Sn^+" than *ortho*-anisaldehyde.

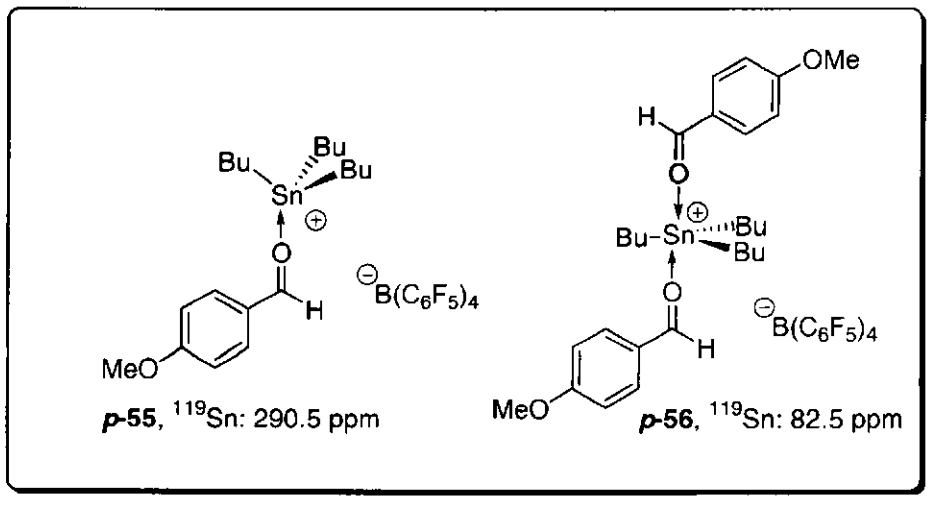

4.7.4 Summary of Formation of Ion-Pair *o*-53

The formation of ion-pair ***o*-53** involves direct reaction of borane adduct ***o*-44** with $allylSnBu_3$, Scheme 4.7. As C-C bond formation between the activated aldehyde and the allylstannane occurs, positive charge is developed at the β-C, stabilized through hyperconjugation by the "Bu_3Sn" moiety, as in hypothetical intermediate, ***o*-57**. The electrophilicity of the Sn atom is increased leading to consecutive coordination of two

molecules of *ortho*-anisaldehyde, completely displacing the "Bu_3Sn" from the allyl group via the unobserved intermediate ***o*-58**.

Scheme 4.7: Summary of formation of Ion-pair *o*-53.

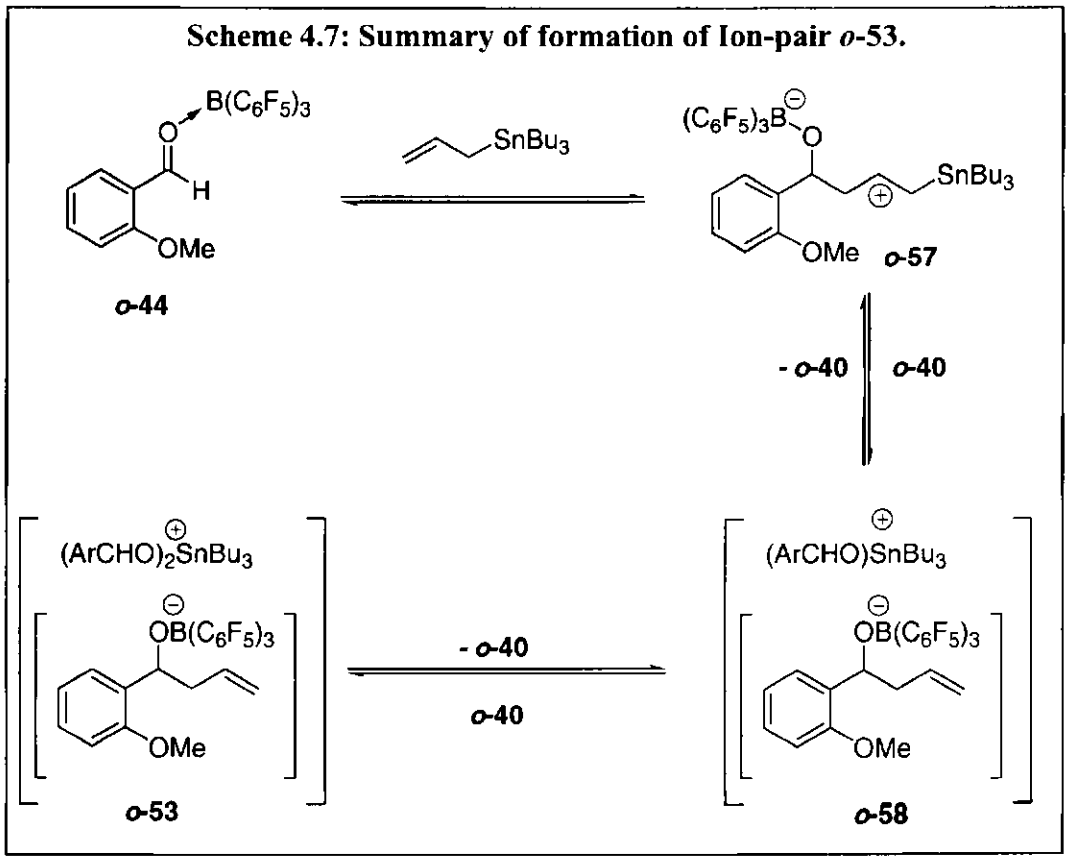

In general, this stage of the Lewis acid promoted allylstannation reaction determining the fate of the trialkyl tin moiety has not been extensively studied. In typical mechanistic proposals, either some anion, $[X]^-$, is shown to displace the "Bu_3Sn^+" group or direct formation of an O-Sn bond mysteriously occurs. Undoubtedly, general pathways such as these do occur but this research has revealed (*based on experimental results*) another option heretofore not considered where additional carbonyl substrate plays an important role.

4.8 $B(C_6F_5)_3$ versus "Bu_3Sn^+" activation

It should be emphasized that the observation of a chemical species in a catalytic cycle does not imply its direct intermediacy; that is, ***o*-53** is not necessarily a catalytic intermediate in the allylstannation reaction just because it is observed at low temperature. In fact, the chemistry to be discussed below suggests that the formation of ***o*-53** though crucial to commencement of catalysis, does not actually play a direct role in formation of the bulk of allylstannated product. It should also be pointed out that the conditions used in the NMR experiments described below are not directly representative of those used for the entries in Table 4.1. To facilitate NMR analysis, greater quantities of **1** have been used (20-50%) compared to the 1-5% typically required for catalysis. In Maruoka's original report, stoichiometric **1** was used. Since high selectivities were observed using both stoichiometric and catalytic **1**, the NMR experiments should be relevant to both extremes.

4.8.1 Conversion of *o*-53 to Stannyl Ether *o*-59 (no excess allylSnBu$_3$)

Ion-pair ***o*-53** is formed quantitatively at -60 °C in CD_2Cl_2 after which it is stable for hours at this temperature. However, upon warming to -20 °C, the formation of stannyl ether ***o*-59** commences as observed by ^1H NMR analysis. No reaction is observed at -40 °C. Experiments described in Section 4.8.3 indicate that conversion of ***o*-53** to ***o*-59** (in the absence of allylSnBu$_3$) proceeds via alkoxy transfer from the alkoxyborate to the "Bu_3Sn^+".

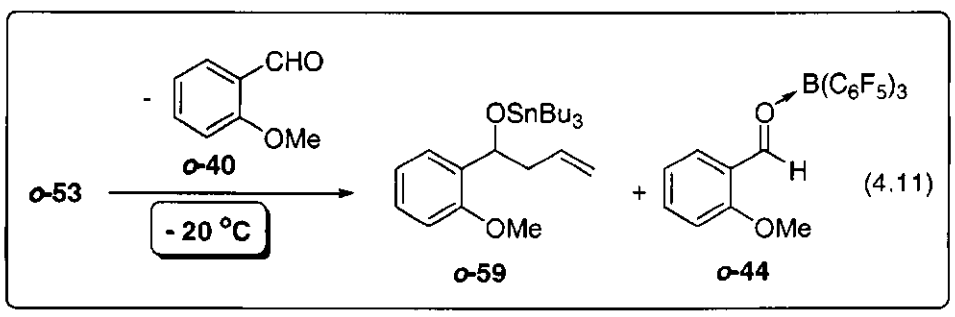

It is highly unlikely that alkoxy transfer occurs directly to $[(o\text{-}\mathbf{40})_2SnBu_3]^+$. Presumably either one, if not both aldehydes, must dissociate to enable the sterically crowded alkoxyborate oxygen to approach the "Bu_3Sn^+" moiety. Nonetheless, this reaction pathway does lead to the regeneration of ***o*-44** and would allow perpetuation of catalysis in the presence of more $allylSnBu_3$.

4.8.2 Conversion of *o*-53 to *o*-59 in presence of allylstannane

When ***o*-53** is generated in the presence of two equivalents of $allylSnBu_3$, again no reaction is observed at -60 °C. Upon warming to -40 °C however, the formation of ***o*-59** does occur as evidenced by ^1H NMR analysis. This reactivity is in contrast to that observed in the absence of $allylSnBu_3$ where formation of ***o*-59** does not occur at a significant rate until -20 °C.

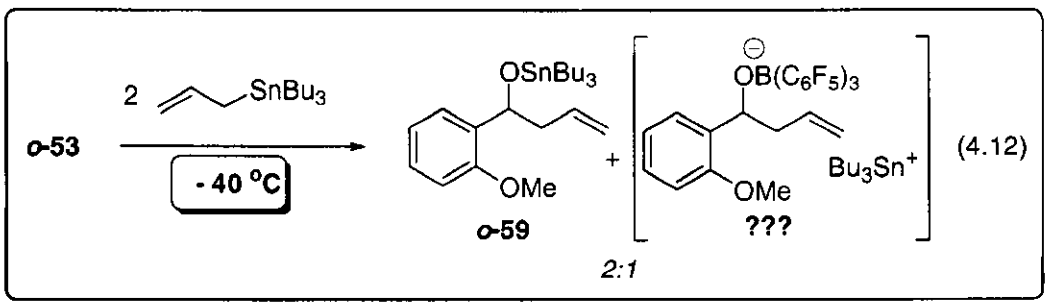

After formation of ***o*-59** at -40 °C, ^{19}F and ^1H NMR spectroscopy indicates that all of **1** remains incorporated as the same alkoxyborate counterion as in ***o*-53** now however,

possessing a different cation. Consideration of mass balance necessitates the formation of a species with the composition $[Bu_3Sn]^+[(ortho\text{-anisyl})CH(allyl)OB(C_6F_5)_3)]^-$. Characterization of this ion-pair will be discussed in more detail in Section 4.8.3. There is no evidence for regeneration of either **1** or borane adduct ***o*-44**. Although formation of ***o*-59** could still proceed via ion-collapse as suggested in Section 4.8.1 (alkoxy transfer), this does not rationalize why stannyl ether formation proceeds more rapidly in the presence of allyl$SnBu_3$.

Scheme 4.8: "Bu_3Sn^+"-Activation Pathway.

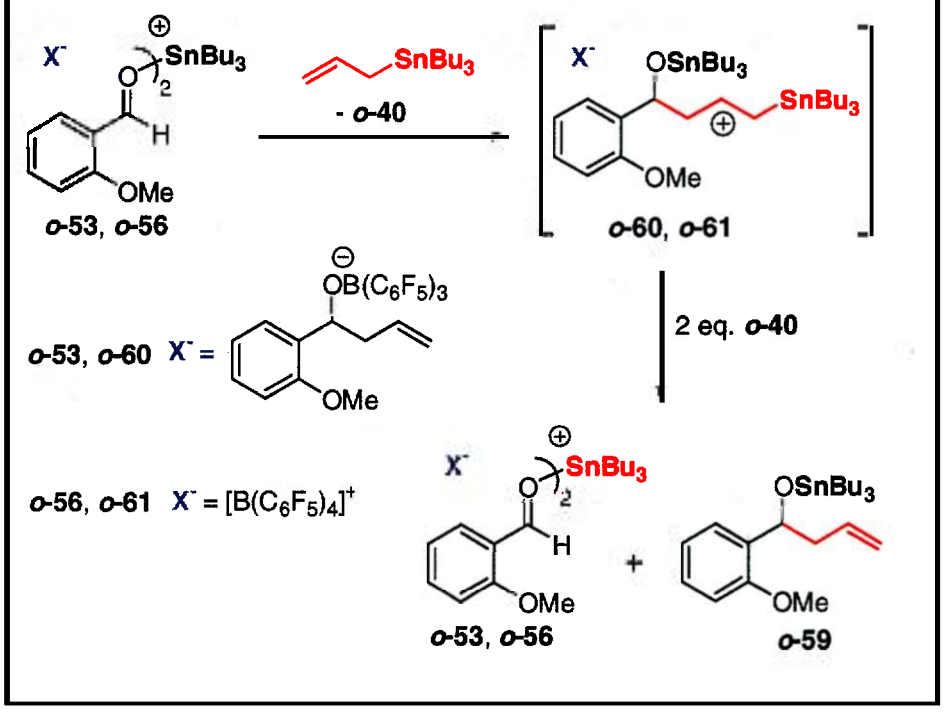

An alternate route leading from ***o*-55** to ***o*-60** is proposed involving reaction of the cationic half of ***o*-53** with allyl$SnBu_3$, Scheme 4.8. The anion is represented as X^- to emphasize its spectator role. Intervention of additional ***o*-40** regenerates the cationic portion where the "Bu_3Sn^+" has been derived from allyl$SnBu_3$ and the stannyl ether ***o*-59**

is formed directly through "Bu_3Sn^+" activation of ***o*-40**. This proposal is supported by the fact that stannylium reagent **49** also catalyzes the allylstannation of ***o*-40** at -40 °C via via attack at the stannylium-activated aldehyde, ***o*-56**. The primary difference then is the identity of the anion, X^-, either [(*ortho*-anisyl)CH(allyl)$OB(C_6F_5)_3$]$^-$ or $[B(C_6F_5)_4]^-$.

Certainly, collapse of ***o*-53** to ***o*-59** (alkoxy transfer) could occur regenerating **1** which immediately activates another molecule of ***o*-40** to allylation. Although this would explain why only alkoxyborate is observed by ^{19}F NMR, it does not rationalize the increased rate of formation of ***o*-59** in the presence of $allylSnBu_3$. Therefore, a mechanism where the bulk of catalysis proceeds via a "Bu_3Sn^+" activation pathway is proposed to predominate. Activation by **1** is important, but only to generate the true stannylium catalyst, $[(\textbf{\textit{o}}\textbf{-40})_2SnBu_3]^+$.

4.8.3 Monitoring the Reaction to Completion

Under conditions where a full equivalent of $allylSnBu_3$ relative to **o-40** is used, $allylSnBu_3$ and ***o*-40** do fully react, but with an unexpected result. In the absence of ***o*-40**, the anion [(*ortho*-anisyl)CH(allyl)$OB(C_6F_5)_3$]$^-$ is *stable at room temperature*. The reaction product formed under these conditions is proposed, based on NMR spectroscopic analysis, to be ion-pair ***o*-62**. The stannylium cation is ligated by one equivalent of the stannyl ether product ***o*-59**.

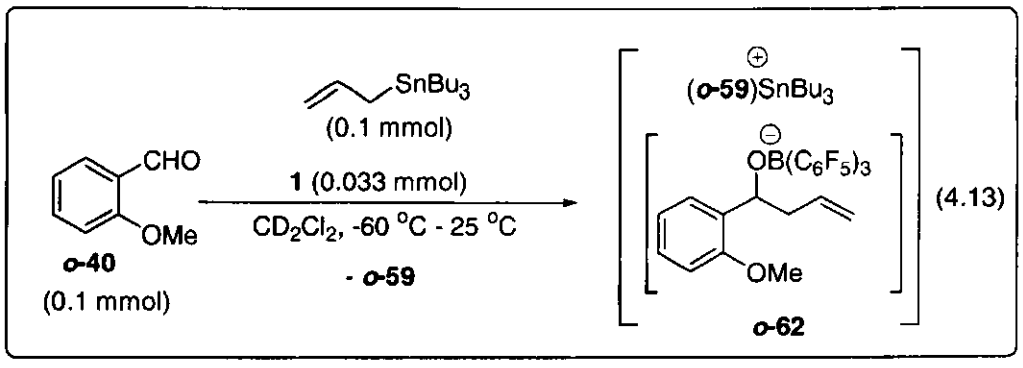

First, the anionic portion is identical by ^{1}H, ^{13}C, ^{19}F and ^{11}B NMR spectroscopic analysis to that of ***o*-53** and ammonium salt, ***o*-54**; that is, the alkoxyborate anion survives after all allyl$SnBu_3$ and aldehyde is consumed. In the cation, only one set of extremely broadened butyl ^{1}H and ^{13}C signals is discernible suggesting that free and bound stannyl ether, ***o*-59**, are exchanging rapidly on the NMR time scale at -60 °C. However, ^{119}Sn NMR spectroscopy shows the presence of both ***o*-59** (slightly downfield-shifted and broadened) and two broad signals at 220 and 240 ppm. These two signals are reflective of the two different coordination environments for the two "Bu_3Sn" groups in the cation $[(o\text{-}59)SnBu_3]^{+}$. The fact that these ^{119}Sn NMR signals are both downfield relative to that found for ***o*-53** indicates that the positive charge is less effectively delocalized with ***o*-59** as a ligand in lieu of two aldehydes. To confirm that only one equivalent of ***o*-59** is coordinated, the reaction was carried out with ½ equivalent of **1**. Similar NMR spectra are obtained, but now there is no free ***o*-59** present as judged by ^{119}Sn NMR spectroscopy. The ^{119}Sn NMR spectrum again possesses two broad signals at 220 and 240 ppm, however, now ^{1}H and ^{13}C NMR spectra are no longer broadened. Again, only one set of

butyl signals is observed by ^{13}C NMR analysis suggesting that on the ^{13}C NMR time scale, the tributyltin groups are rapidly exchanging.

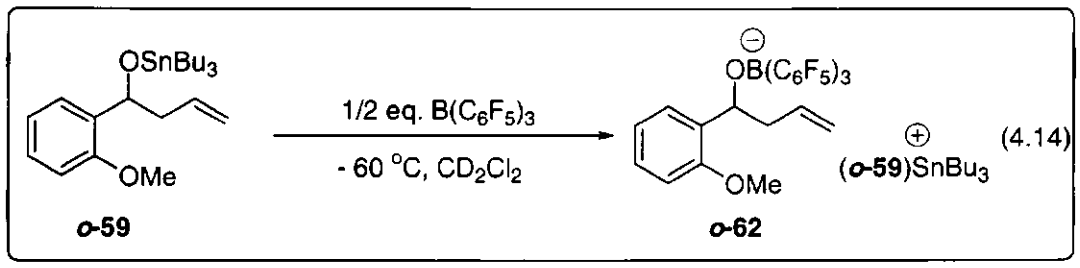

Ion-pair ***o*-62** can be prepared directly from stannyl ether ***o*-59** upon addition of ½ equivalent of **1**, its NMR signature being identical to that for the ion-pair formed by addition of allylSnBu$_3$ to a 2:1 mixture of ***o*-40** and **1**. This observation implies that in the absence of ***o*-40**, ion-pair ***o*-62** is thermodynamically favored over the neutral components ***o*-59** and **1**. In the presence of ***o*-40**, this equilibrium reverts back to stannyl ether and borane adduct ***o*-44**. Alkoxy transfer from stannyl ether to **1** occurs at temperatures below -60 °C whereas transfer from alkoxyborate to ligated "Bu$_3$Sn" begins to occur at -20 °C and above.

The pathway directly connecting ***o*-53** and stannyl ether, ***o*-59**, is certainly interesting and of some potential importance; however, it should be emphasized that it provides only a minor contribution to the bulk of the allylstannation of *ortho*-anisaldehyde, ***o*-40**. The primary pathway involves reaction of allylSnBu$_3$ with ***o*-40** activated by "Bu$_3$Sn$^+$". In the NMR tube experiments described above, inflated quantities of **1** are employed to facilitate NMR analysis. Catalyst loadings as low as 1 mol% have been used to effect the allylstannation reaction. Hence, the amount of

alkoxyborate formed will never exceed this amount. At the end of the reaction there will only be this amount of ***o*-62** remaining as well. Upon purification by column chromatography presumably ***o*-62** should be hydrolysed to two equivalents of the homoallylic alcohol ***o*-41**.

4.8.4 Reaction via *Mono*-Aldehyde or *Bis*-Aldehyde "Bu_3Sn^+" Complexes

Scheme 4.9: Allylation via *Mono*- or *Bis*-Aldehyde Complexes.

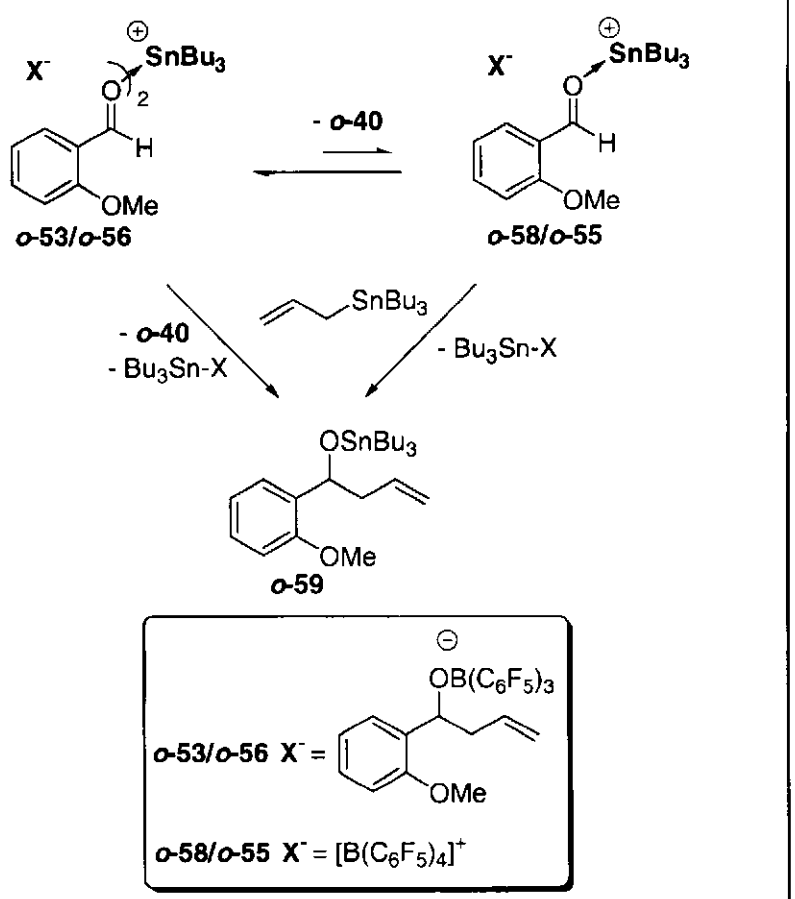

Scheme 4.10: Effect of [*o*-40] on Allylstannation Catalyzed by 49.

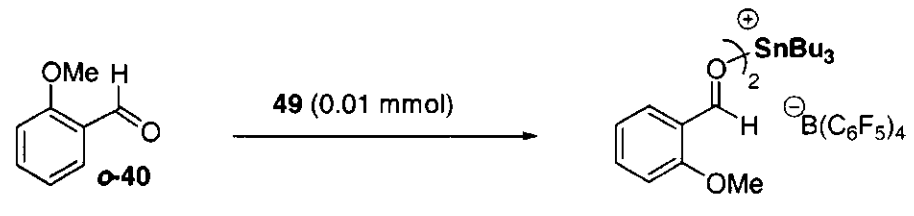

time (min)	percentage completion X = 0.1	0.2	0.3	1.0
10	30	33	38	24
15	37	40	45	36
20	42	46	51	44
25	48	51	56	48
30	53	56	61	52

The proposed mechanism involves reaction of allyl$SnBu_3$ with $[(\textbf{o-40})_2SnBu_3]^+$. Alternatively, reaction could take place on the *mono*-aldehyde adduct, $[(\textbf{o-40})SnBu_3]^+$, ***o*-58**, which should be more activated. By NMR analysis, only ***o*-53** is observed at temperatures where reaction occurs. However, this fact alone does not discount the possibility that ***o*-58** does form and then reacts immediately (either with more aldehyde to regenerate ***o*-53** or with allyl$SnBu_3$). If dissociation of ***o*-40** from ***o*-53** is important, then an inverse rate dependence on [***o*-40**] would be expected. This effect could not be directly studied for ***o*-53**; however, Lambert's stannylium reagent, **49**, was used to isolate this stage of the reaction. Using this reagent, no complications arise from the presence of another Lewis acid, **1**, in the reaction mixture. As shown in Scheme 4.10, the

concentration of aldehyde, ***o*-40**, had no appreciable effect on the reactivity leading to the conclusion that allylstannation does occur predominantly on the *bis*-aldehyde complex, ***o*-56** and by extension, ***o*-53**.

4.9 Selectivity in the Allystannation reaction.

With a clear mechanistic picture of the allylstannation reaction including insight into the role of Lewis acid **1** and various ionic intermediates, the question of selectivity could be addressed. The remarkable selectivity observed by Maruoka in the allylstannation of ***o*-40** versus ***p*-40** certainly suggests chelation by the *ortho*-methoxy group as one possible origin. Maruoka postulated that a hypercoordinate borane intermediate was involved. We have found no evidence to support this controversial proposal and have demonstrated that allylation proceeds predominantly via a "Bu_3Sn^+" activation pathway anyway. It is logical to thus question whether a chelated stannane intermediate could be involved. Hypercoordinate stannanes are well represented in the literature (see Chapter 1); the results reported in this section however discount this possibility too. A proposal for the origin of the selectivity is provided which is applicable to both borane and stannane Lewis acids.

4.9.1 Selectivity in Allyl Delivery to $B(C_6F_5)_3$-Activated Aldehydes

The allylation of ***o*-44** or ***p*-44** serves mainly to form the active catalyst, ***o*-53** or ***p*-53** respectively. Formation of ion-pair ***o*-53** is more facile than formation of ***p*-53**. This difference in reactivity is manifested in spite of the fact that ***p*-40** actually coordinates **1** in slight preference (2.2:1) when in competition with ***o*-40** (see Section 4.5.2). Addition of allylSnBu_3 (0.05 mmol) at -78 °C to a mixture of ***o*-40** (0.1 mmol), ***p*-40** (0.1 mmol) and **1** (0.05 mmol) followed by collection of ^{1}H NMR spectra at -60 °C leads to the series

of spectra in Figure 4.10 (methyl region shown). Spectra for the tetrabutylammonium alkoxyborate salts, ***o*-54** and ***p*-54** (at -60 °C) are included. Over the first 5 minutes, only ***o*-44** reacts leading to alkoxyborate derived from *ortho*-anisaldehyde, ***o*-40**. Concurrent ^{19}F NMR analysis shows that the ratio of ***p*-44**:***o*-44** increases; re-equilibration between the borane adducts is slow at -60 °C. Over the next 145 minutes, formation of alkoxyborate derived from ***p*-40** does form while simultaneously, ***o*-44** is regenerated from ***p*-44** and then rapidly allylated. The observed selectivity after complete consumption of allyl$SnBu_3$ is ~4.2:1, but the initial discrimination is much higher (>20:1); the decrease in the selectivity over time is a function of the equilibrium between the two borane adducts.

Figure 4.10: ^{1}H NMR Spectra (CD_2Cl_2, -60 °C) (a) 1:1 *o*-/*p*-40 + 1/2 eq. 1 (b) after addition of allylSnBu$_3$, 5 min (c) 150 min (d) *o*-54 (e) *p*-54

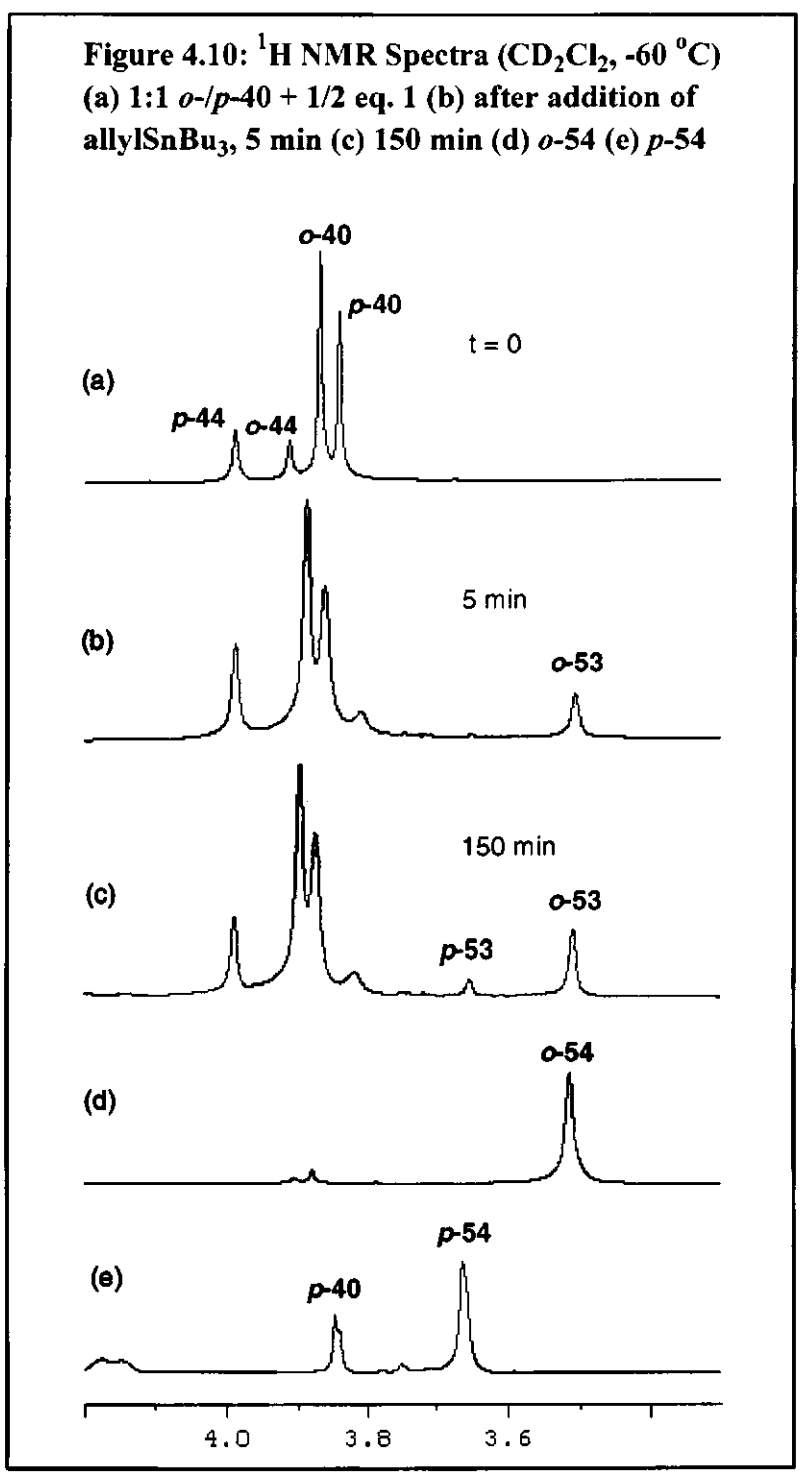

$[Bu_4N]^+[allylB(C_6F_5)_3]^-$ also selectively (>20:1) delivers an allyl group to ***o*-40** over ***p*-40** when activated by **1** at room temperature. In this case, the only Lewis acid available for activation of aldehyde is **1**; reactions must occur via ***o*-44** and ***p*-44**. The reaction is much less facile than the addition of $allylSnBu_3$ to ***o*-44** which occurs as low as -60 °C showing that $allylSnBu_3$ is a superior nucleophile than allylborate, at least to ***o*-44**.

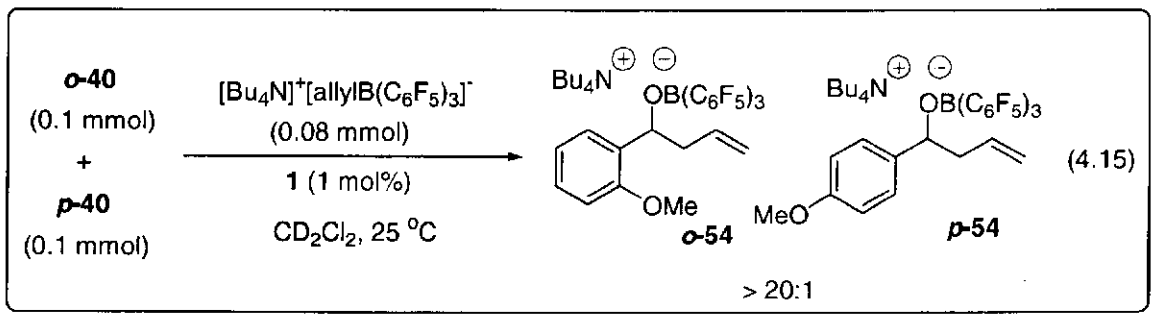

4.9.2 Selectivity in the Allylstannation of "Bu_3Sn^+"-Activated Aldehdyes

Stannylium reagent, **49**, selectively catalyzes the allylstannation of ***o*-40** over ***p*-40** (12.5:1) at -40 °C. Under typical $B(C_6F_5)_3$-catalyzed conditions at -40 °C, the proposed mechanism implies that only a minor contribution to the observed selectivity will directly originate from addition to borane/aldehyde adducts ***o*-44**/***p*-44**. If 5 mol% **1** is used, then only 5% of the allylated product should be formed via an alkoxyborate intermediate. The remainder of allylated product results from allylation of aldehyde activated by "Bu_3Sn^+". The overall selectivity of the reaction will thus be a composite of the selectivity observed for activation by **1** and that observed for activation by "Bu_3Sn^+", both of which have been shown to be selective.

4.9.3 Selectivity via Hypercoordinate Stannane

A number of observations suggest that intervention of a hypercoordinate tin species is not involved in the allylstannation of ***o*-40**. First, selective addition (of $allylSnBu_3$ and allylborate nucleophiles) to borane adduct ***o*-44** over ***p*-44** has been observed; that is, a Lewis acid, **1**, incapable of chelation can provide selectivity. The $BF_3{\bullet}OEt_2$-promoted reaction is also selective (7:1) for allylation of ***o*-40**. The ability to chelate is thus not a prerequisite, some other mechanism enables selectivity to manifest itself.

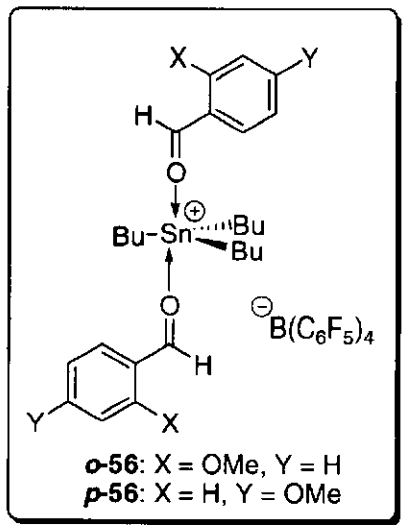

***o*-56**: X = OMe, Y = H
***p*-56**: X = H, Y = OMe

The second observation that refutes the intermediacy of a chelated species is the lack of any NMR or structural evidence in its support. In the presence of two equivalents of ***o*-40** or ***p*-40**, two molecules of aldehyde have been shown to coordinate Lambert's stannylium reagent, **49**, to give ***o*-56** or ***p*-56**. Although, these results do show that hypercoordination is favored, coordination of two aldehyde functions is preferred over chelation. In the presence of one equivalent of aldehyde, formation of the *mono*-coordinated species ***o*-55** results (as opposed to ½ equivalent of ***o*-56** and ½ equivalent of **49**). Furthermore, in ***o*-55** there is no evidence for coordination of the methoxy group to the cationic tin center. This species possesses a ^{119}Sn NMR shift of 297.6 ppm in CD_2Cl_2 whereas under the same conditions, $[(\textbf{\textit{p}-40})SnBu_3]^+[B(C_6F_5)_4]^-$, ***p*-55**, has a shift of 290.5 ppm. If methoxy coordinates to the tin atom in ***o*-55** it should

exhibit a significantly different (upfield shifted) ^{119}Sn NMR shift than that for ***p*-55** reflective of a second donor group.

Figure 4.11: 149.2 MHz ^{119}Sn NMR Spectrum (CD_2Cl_2, -80 °C) of 1:1 Mixture of *o*-40/*p*-40 and catalytic 49.

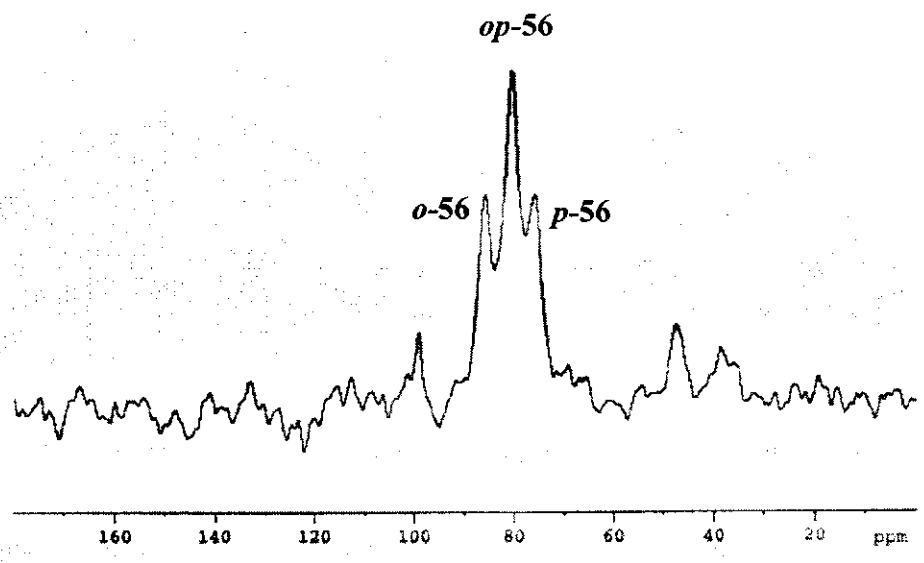

Third, when ***o*-40** and ***p*-40** are mixed with a catalytic amount of **49**, ^{119}Sn NMR spectroscopy at -80 °C in CD_2Cl_2 reveals that a statistical mixture of the three possible *bis*-adducts, ***o*-56**, ***p*-56** and ***op*-56** are formed, Figure 4.11. There is no inherent thermodynamic selectivity for coordination of ***o*-40** to "Bu_3Sn^+". Similarly, when ***o*-44** is selectively allylated at -60 °C over ***p*-44**, there is no subsequent selectivity in the formation of the cation; ***o*-40** and ***p*-40** competitively displace "Bu_3Sn^+" from its allyl

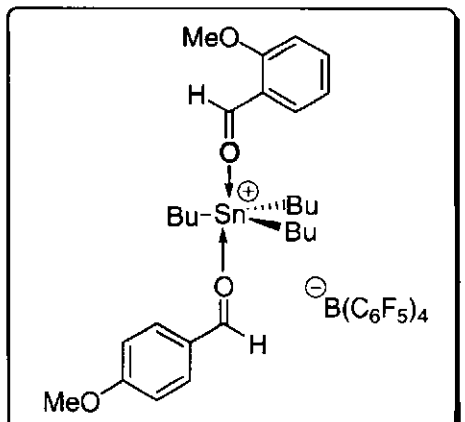

***op*-56**

group. This leads to a statistical mixture of the three ion-pairs ***o*-53**, ***o*-53'** and ***o*-53"**, differentiated only by the ligand environment of the cation, Scheme 4.10, as confirmed by ^{119}Sn NMR spectroscopy.

Scheme 4.11: Formation of Ion-Pairs *o*-53, *o*- 55' and *o*-55".

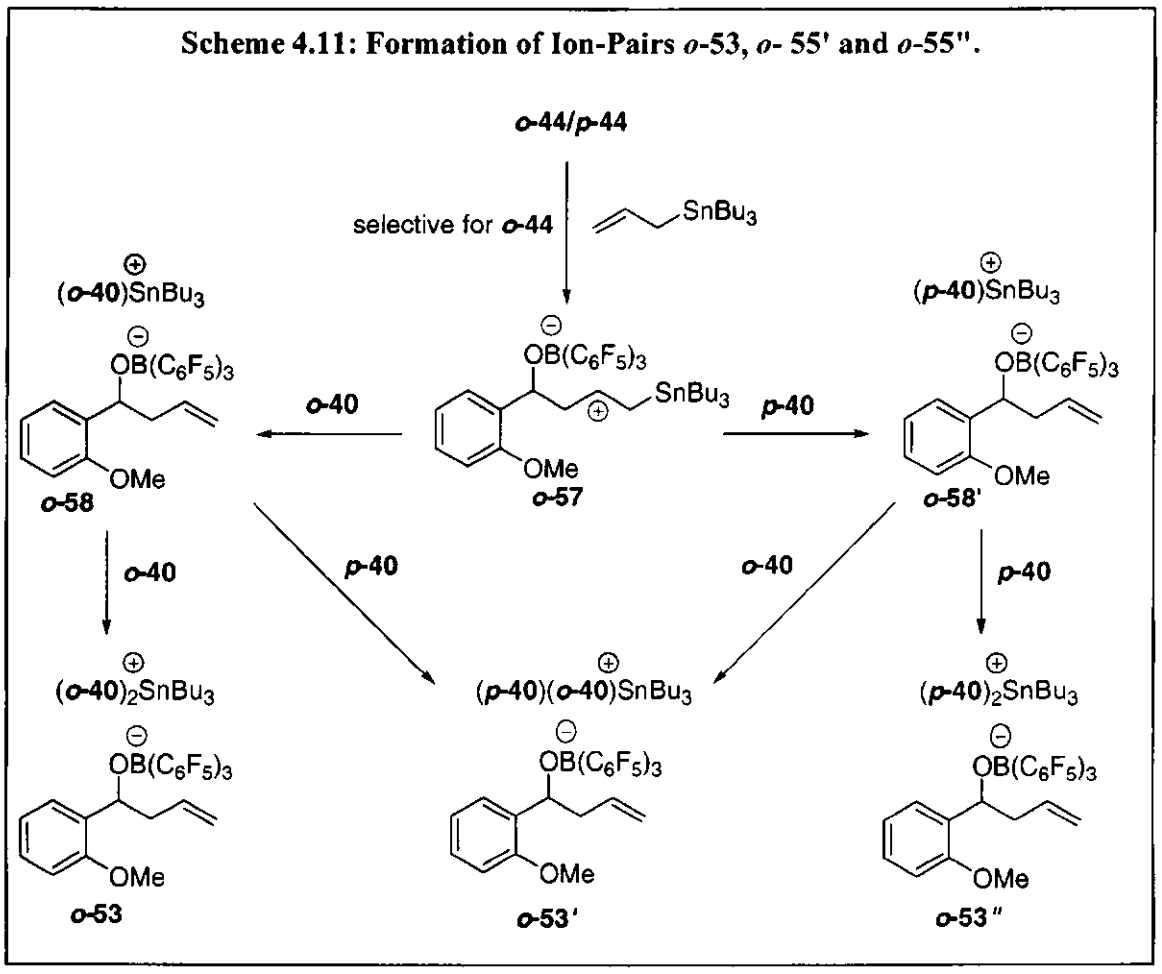

Attempts to grow X-ray quality crystals of any of the species with aldehyde coordinated to "Bu_3Sn^+" have been unsuccessful; however, an X-ray structure of [(***o*-40**)$SnMe_3$]$^+$[BF_4]$^-$, **63**, was obtained, Figure 4.13. The weakly coordinating BF_4^- outcompetes the methoxy group for the fifth coordination site at the tin center. In fact, the trimethyltin moiety is coordinated *trans* to the aryl group.

Figure 4.13: X-ray Structure of $[(o\text{-}40)SnMe_3]^+[BF_4]^-$, 63.

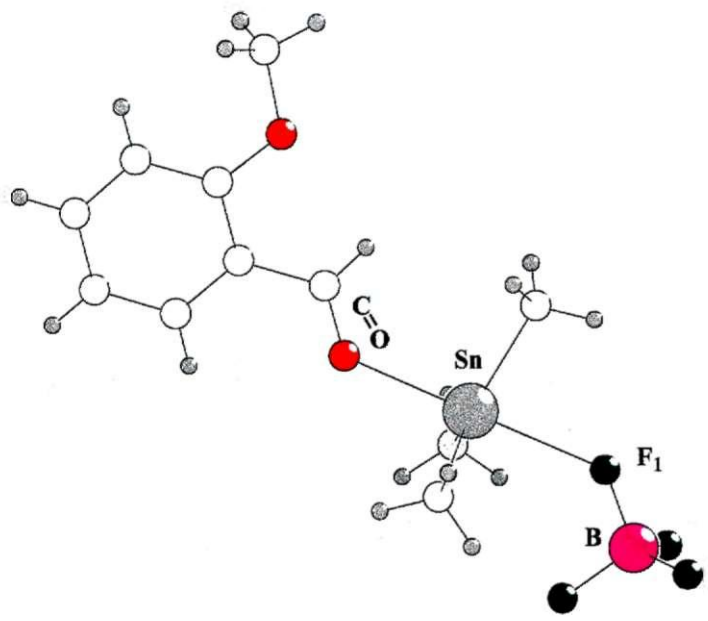

Bond Distances: C=O, 1.242 Å; MeO-C(aryl), 1.346 Å; O-Sn, 2.249 Å; Sn-F_1, 2.387 Å.

Bond Angles: < C-O-Sn, 127.7°; < O-Sn-F, 178.6°.

The fact that evidence for a chelated stannane is not available does not preclude it from being formed from the *bis*-adduct en route to product. If $[(o\text{-}40)_2SnBu_3]^+[B(C_6F_5)_4]^-$ must lose one coordinated ***o*-40** to form the active intermediate, then an inverse rate dependence on [***o*-40**] might be expected which is not oberved, Scheme 4.10. Again, the fact that [***o*-40**] does not affect the rate does not conclusively refute this mechanistic pathway. However, in conjunction with the above observations, chelated stannane intermediates are unlikely intermediates in the allylstannation. It should be emphasized that selective allylation of ***o*-44** occurs over ***p*-44** using either borane or tin Lewis acids establishing that selectivity does not require a Lewis acid capable of chelation.

4.9.4 Selectivity via Stabilization of Positive Charge in Transition State

In 1991, Yamataka and coworkers made the observation that BF_3-promoted allylstannation of substituted benzaldehydes proceeded at an anomalously high rate for 2-chloro and 2-fluorobenzaldehyde. The authors suggested that the *ortho* donor groups were able to stabilize incipient positive charge build-up during the transition state thereby lowering the barrier for C-C bond formation.[34]

A similar proposal is favored for the allylstannation catalyzed by **1**. It has been shown that the allylstannation of the C=O bond is stepwise. First C-C bond formation occurs accompanied/followed by C-Sn bond breakage. The "Bu_3Sn^+" group ultimately is stabilized by two molecules of aldehyde, this species then perpetuates catalysis. Coordination of aldehyde presumably drives the reaction forward as a solvated stannylium species would otherwise have to be released. Coordination of the methoxy group could provide electronic stabilization of the developing charge either at the the β-carbon, "Bu_3Sn^+" group or both, **64a/b**, Figure 4.14. An aesthetically satisfying six-membered ring is involved in the first case. Although this would decrease the positive charge build-up at the tin, it would also lessen the requirement for hyperconjugative stabilization by this group which could in turn facilitate coordination/displacement by the first molecule of aldehyde.

Figure 4.14: Electronic Stabilization of Incipient Positive Charge by *Ortho*-Methoxy Group.

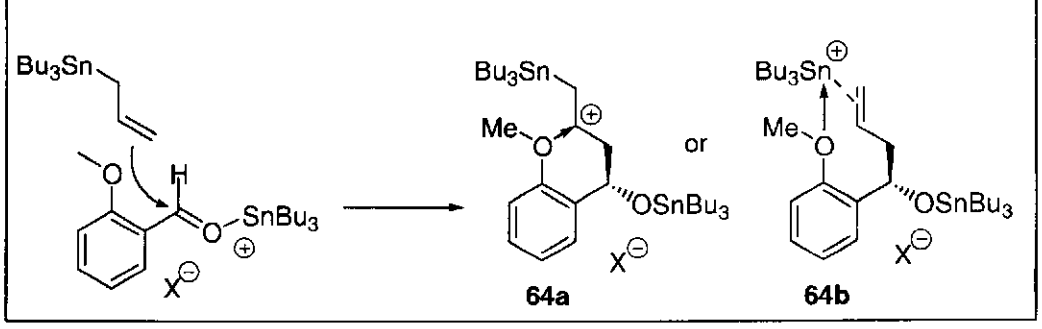

The high selectivity observed using $[Bu_4N]^+[allylB(C_6F_5)_3]^-$ as a nucleophile demonstrates that an anionic nucleophile can also be used without substantial diminution in selectivity. The production of a cationic transition state/intermediate during or after allyl delivery is not necessary for high selectivity. If the proposed rationale for the selectivity is correct, then the energy of the transition state for allyl delivery from allylborate must also be significantly lowered by electronic stabilization provided by the *ortho*-methoxy group. It might be predicted that this would be less important than for $allylSnBu_3$ since a neutral "byproduct", **1**, is formed rather than the cationic "Bu_3Sn^+". However, allylborate is a much poorer nucleophile than $allylSnBu_3$ to adduct ***o*-44**; perhaps even a small stabilization effect is translated into high selectivity.

4.10 Mechanistic Summary

Scheme 4.12: Summary of $B(C_6F_5)_3$-Catalyzed Allylstannation of *ortho*-Anisaldehyde.

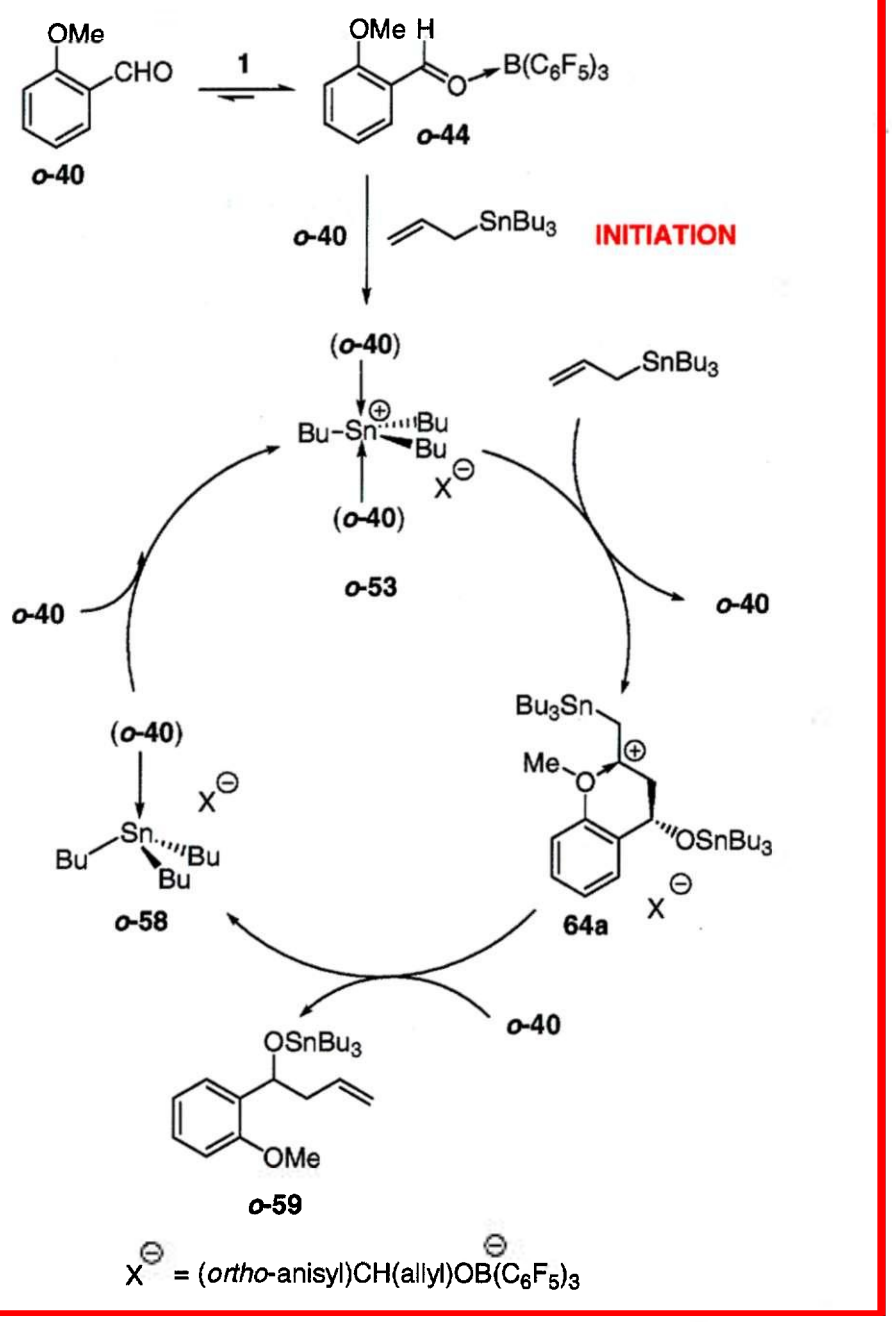

$B(C_6F_5)_3$, **1**, catalyzes the allylstannation of aldehydes such as *ortho*-anisaldehyde, ***o*-40** and selectively allylates *ortho*-anisaldehyde over *para*-anisaldehyde.

Initially, allylSnBu$_3$ delivers an allyl anion to borane adduct ***o*-44** providing ion-pair ***o*-53** (after coordination of two molecules of ***o*-40** to the incipient "Bu$_3$Sn$^+$"). One of the coordinated aldehydes is activated to attack by allylSnBu$_3$, directly producing stannyl ether, ***o*-59** and ion-pair ***o*-58**. Coordination of another equivalent of ***o*-40** to the tin regenerates ion-pair, ***o*-53**, which can perpetuates catalysis. The enhanced rate of allylstannation of ***o*-40** relative to ***p*-40**, is attributed to electronic stabilization of the carbocationic charge that develops during allyl transfer from allylSnBu$_3$ to ***o*-53**.

4.11 Conclusions/Future Work

A detailed mechanism has been proposed for the allylstannation of *ortho*-anisaldehyde catalyzed by **1**. This proposal reveals a catalyst activating role for **1** and also suggests a plausible reason to account for selectivity in competition reactions between *ortho*- and *para*-substituted benzaldehydes. Although this mechanistic proposal should not be immediately invoked for the allylstannation of all carbonyl functions catalyzed by **1** and by other Lewis acids, it does warrant serious consideration. Indeed, preliminary studies with benzophenone suggest another mechanism could take place in certain cases. When mixed with allylSnBu$_3$ and **1**, ion-pair formation is observed, equation 4.16. However, rather than an alkoxyborate-based ion-pair analogous to ***o*-53** being formed, instead an [allylB(C$_6$F$_5$)$_3$]$^-$-based ion-pair, **65**, is formed. Formation of ion-pair **65** is temperature dependent, **65** being favored at low temperatures, adduct **66**, at high temperatures. If allylation were to ensue from **65**, this type of mechanism would be analogous to that proposed for the hydrosilation of carbonyl functions where the role of **1** is to electrophilically activate the nucleophile (either hydrosilane or allylSnBu$_3$). However, allylation of benzophenone is not observed.

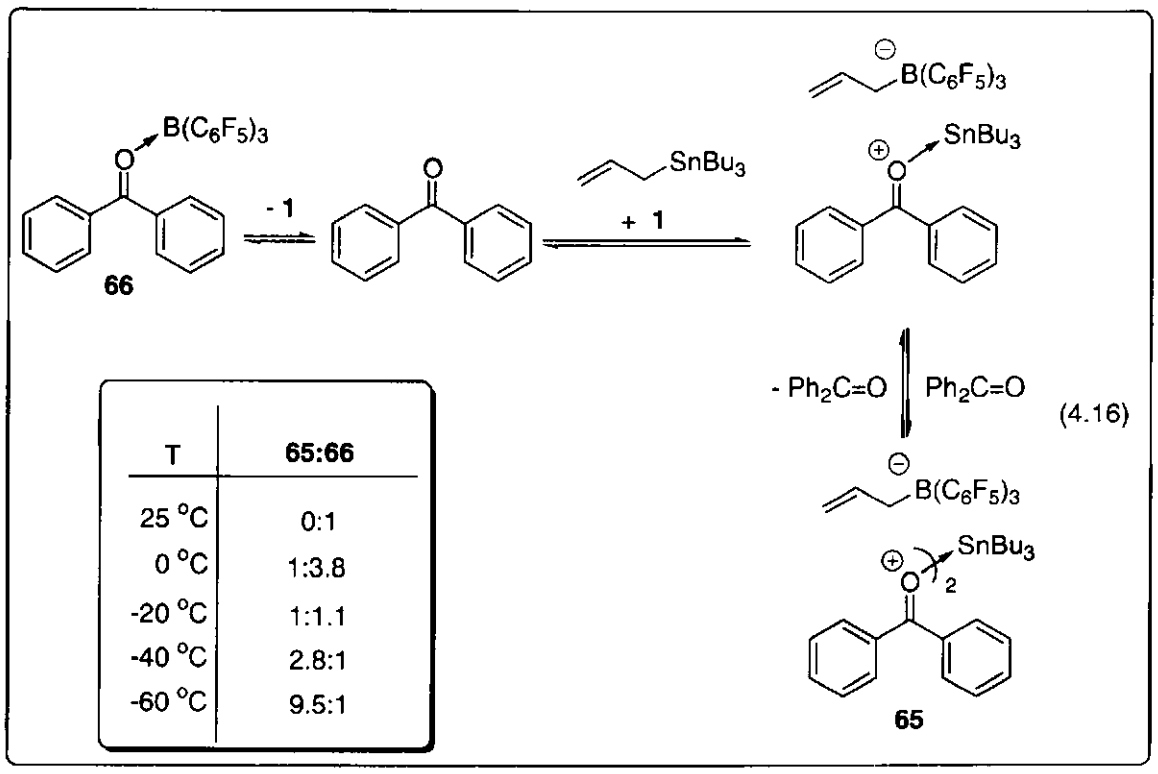

T	65:66
25 °C	0:1
0 °C	1:3.8
-20 °C	1:1.1
-40 °C	2.8:1
-60 °C	9.5:1

A research project under investigation in the Piers' research group involves preparing chiral, perfluoroaryl borane Lewis acids to use in asymmetric hydrosilation, allylstannation and other reactions. In light of the mechanistic proposal's ascription of an initiating role to **1** for allylstannation, it might seem that this approach would be ineffective; the bulk of carbonyl activation occurs by the achiral Lewis acid, "Bu_3Sn^+". Formation of stannyl ether can occur by two pathways, one denoted "chiral", the other "achiral", equation 4.17. The "chiral" pathway involves alkoxy transfer from borate to "Bu_3Sn^+". The enantiomeric excess of stannyl ether formed by this pathway would be the equal to that that for allylation of the chiral borane/aldehyde adduct. The "achiral" pathway involves "Bu_3Sn^+" activation of aldehyde which was shown to predominate for catalysis by **1**. The chiral borane has been relegated to a bystander role as the counterion

and is unlikely to exert significant enantiocontrol in the allylation of the achiral cationic complex. However, alkoxy transfer from borate to tin cation does occur in the absence of aldehyde. Traversal of the chiral pathway could be favored by (1) using stoichiometric chiral Lewis acid or more desirably, (2) adding the aldehyde slowly (syringe pump addition) to allylstannane and catalytic chiral borane at a temperature where allylation of borane adduct and subsequent alkoxy transfer occur readily.

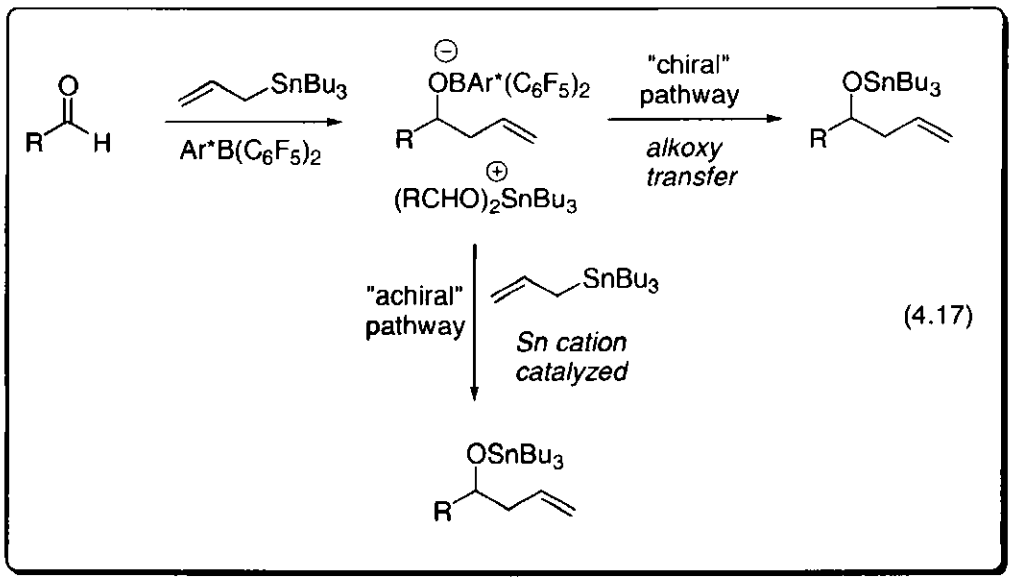

[1] For general reviews of Lewis acid promoted/catalyzed allylstannation of carbonyl groups, see (a) Santelli, M.; Pons, J. -M. in *Lewis Acids and Selectivity in Organic Synthesis*, CRC Press, **1996**, 91-184. (b) Fleming, I. In *Comprehensive Organic Synthesis* Trost, B. M.; Fleming, I. Eds.; Pergamon Press: New York, 1991; Vol.2, 563.

[2] *Comprehensive Asymmetric Catalysis* Jacobsen, E.N.; Pfaltz, A.; Yamamoto, H. eds.; Springer-Verlag: New York, 1999.

[3] Denmark, S. E.; Weber, E. J. *J. Am. Chem. Soc.* **1984**, *106*, 7970.

[4] (a) Yamamoto, Y.; Yatagai, H.; Ishihara, Y.; Maeda, N.; Maruyama, K. *Tetrahedron* **1984**, *40*, 2239. (b) Yamamoto, Y. in *Advances in Detailed Reaction Mechanisms* JAI Press Inc.:Greenwich, **1994**, 1-44.

[5] For reviews on the use of crotylmetal reagents in stereoselective synthesis, see (a) Yamamoto, Y.; Asao, N. *Chem. Rev.* **1993**, *93*, 2207. (b) Hoffmann, R. W. *Angew. Chem. Int. Ed. Engl.* **1982**, *21*, 555.

[6] (a) Yamamoto, Y.; Yatagai, H.; Naruta, Y.; Maruyama, K. *J. Am. Chem. Soc.* **1980**, *102*, 7107. (b) Keck, G. E.; Boden, F. P. *Tetrahedron Lett.* **1984**, *25*, 1879. (c) Keck, G. E.; Abbott, D. E. *Tetrahedron Lett.* **1984**, *25*, 1883. (d) Keck, G. E.; Abbott, D. E.; Boden, F. P.; Enholm, E. J. *Tetrahedron Lett.* **1984**, *25*, 3927.

[7] (a) Keck, G. E.; Abbott, D. E.; Wiley, M. R. *Tetrahedron Lett.* **1987**, *28*, 139. (b) Koreeda, M.; Tanake, Y. *Tetrahedron Lett.* **1987**, *28*, 143.

[8] Marshall, J. A. *Chem. Rev.* **1996**, *96*, 31.

[9] (a) Marshall, J. A.; Gung, W. -Y. *Tetrahedron* **1989**, *45*, 1043. (b) Marshall, J. A.; Welmaker, G. S.; Gung, B. W. *J. Am. Chem. Soc.* **1991**, *113*, 647. (c) Quintard, J. -P.; Dumartin, G.; Elissondo, B.; Rahm, A.; Pereyre, M. *Tetrahedron*, **1989**, *45*, 1017.

[10] (a) Marshall, J. A.; Jablonowski, J. A.; Elliott, L. M. *J. Org. Chem.* **1995**, *60*, 2662. (b) Marshall, J. A.; Welmaker, G. S. *J. Org. Chem.* **1992**, *57*, 7158.

[11] For example, see (a) Marshall, J. A.; Welmaker, G. S. *J. Org. Chem.* **1994**, *59*, 4122. (b) Ikemoto, N.; Schreiber, S. *J. Am. Chem. Soc.* **1992**, *114*, 2524.

[12] Sana, H.; Okawara, M.; Ueno, Y. *Synthesis*, **1984**, 933.

[13] Sugawara, M.; Yoshida, J. -I. *Chem. Commun.* **1999**, 505.

[14] Reetz, M. T. *Angew. Chem. Int. Ed. Engl.* **1984**, *23*, 556.

[15] (a) Marshall, J. A.; Tang, Y. *Synlett*, **1992**, 653. (b) Keck, G. E.; Tarbet, K. H.; Geraci, L. S. *J. Am. Chem. Soc.* **1993**, *115*, 8467. (c) Keck, G. E.; Geraci, L. S. *Tetrahedon Lett.* **1993**, *34*, 7827. (d) Keck, G. E.; Krishnamurthy, D.; Grier, M. C. *J. Org. Chem.* **1993**, *58*, 6543

[16] Yanigisawa, A. in *Comprehensive Asymmetric Catalysis* Jacobsen, E.N.; Pfaltz, A.; Yamamoto, H. eds.; Springer-Verlag: New York, 1999, pp. 965-979.

[17] Reetz, M. T. *Acc. Chem. Res.* **1993**, *26*, 462.

[18] For the clearest demonstration of the importance of order of reagent mixing, see (a) Denmark, S. E.; Wilson, T.; Willson, T. M. *J. Am. Chem. Soc.* **1988**, *110*, 984. (b) Keck, G. E.; Andrus, M. B.; Castellino, S. *J. Am. Chem. Soc.* **1989**, *111*, 8136.

[19] For lead references, see (a) Tagliavini, G.; Peruzzo, V.; Plazzogna, G.; Marton, D. *Inorg. Chim. Acta* **1977**, *24*, L47. (b) Fishwick, M. F.; Wallbridge, M. G. H. *J. Organomet. Chem.* **1977**, *136*, C46. (c) Gambaro, A.; Marton, D.; Tagliavini, G. *J. Organomet. Chem.* **1981**, *210*, 57. (d) Gambaro, A.; Marton, D.; Peruzzo, V.; Tagliavini, G. *J. Organomet. Chem.* **1982**, *226*, 149. (e) Boaretto, A.; Marton, D.; Tagliavini, G. *J. Organomet. Chem.* **1987**, *321*, 199. (f) Naruta, Y.; Nishigaichi, Y.; Maruyama, K. *Tetrahedron*, **1989**, *45*, 1067.

[20] Denmark, S. E.; Weber, E.J.; Wilson, T. M.; Willson, T. M. *Tetrahedron*, **1989**, *45*, 1053.

[21] Lambert, J. B.; *Tetrahedron* **1990**, *46*, 2677.

[22] Blackwell, J. M.; Piers, W. E.; Parvez, M. *Organic Lett.* **2000**, *2*, 695.

[23] Marshall, J. A.; Gill, K. *J. Organomet. Chem.* **2001**, *624*, 294.

[24] Ooi, T.; Uraguchi, D.; Kagushima, N.; Maruoka, K. *J. Am. Chem. Soc.* **1998**, *120*, 5327.

[25] *The Chemistry of Hypervalent Compounds* Akiba, K., ed.; Wiley-VCH: New York, 1999.

[26] (a) Lee, D. Y.; Martin, J. C. *J. Am. Chem. Soc.* **1984**, *106*, 5745. (b) Yamashita, M.; Yamamoto, Y.; Akiba, K.; Nagase, S. *Angew. Chem. Int. Ed. Engl.* **2000**, *39*, 4055.

[27] Maruoka, K.; Ooi, T. *Chem. Eur. J.* **1999**, *5*, 829.

[28] Kahn, S. D.; Keck, G. E.; Hehre, W. J. *Tetrahedron Lett.* **1987**, *28*, 279.

[29] Parks, D. J.; Piers, W. E.; Parvez, M.; Atencio, R.; Zaworotko, M. J. *Organometallics*, **1998**, *17*, 1369.

[30] Hydrogen bonding between formyl hydrogens and basic atoms such as oxygen have been proposed, (a) Corey, E.J.; Rohde, J. J.; Fischer, A.; Azimiora, M. D. *Tetrahedron Lett.* **1997**, *38*, 33. (b) Corey, E. J.; Lee, T. W. *Chem Commun.* **2001**, 1321.

[31] Bondi, A. *J. Phys. Chem.* **1964**, *68*, 441.

[32] Baldwin, J. E.; Adlington, R. M.; Birch, D. J.; Crawford, J. A.; Sweeney, J. B. *J. Chem. Soc., Chem. Commun.* **1986** , 1339.

[33] Lambert, J. B.; Zhao, Y.; Wu, H.; Tse, W. C.; Kuhlmann, B. *J. Am. Chem. Soc.* **1999**, *121*, 5001.

[34] Yamataka, H.; Nishikawa, K.; Hanafusa, T. *Chem. Lett.* **1990**, 1711.

Chapter 5

Experimental Procedures

5.1 General

5.1.1 Starting materials and solvents: $B(C_6F_5)_3$ was purchased from Boulder Scientific and was dried with Cl_2SiMe_2, sublimed under vacuum at ~100 °C and stored in a glove box. $[Ph_3C]^+[B(C_6F_5)_4]^-$ was received as a generous gift from NOVA Chemicals. $AgBF_4$ and Bu_4NBr were purchased from Aldrich and used as is. Silanes and allyl$SnBu_3$ were purchased from Aldrich and used without further purification. All aldehydes, ketones and alcohols were purchased from Aldrich and generally used as is except for both *ortho*- and *para*-anisaldehyde which were distilled before use. Imines were either purchased from Aldrich and used as is or were prepared by standard methods.[1] Aldimines were generally prepared by condensing aldehyde and amine in CH_2Cl_2 followed by purification by recrystallization or distillation; ketimines were prepared by mixing ketone and amine in toluene and heating to reflux (4-24 hours) using Dean-Stark apparatus in the presence of catalytic $ZnCl_2$ and then purified by recrystallization or distillation. Toluene was purified using the Grubbs' method.[2] All deuterated solvents were purchased from Cambridge Isotopes. C_7D_8 and C_6D_6 were distilled from Na/benzophenone. CD_2Cl_2 was distilled from CaH_2.

5.1.2 Spectroscopy/Analysis: NMR spectra were obtained on either a Bruker AMX300 or Bruker AM-400 spectrometer. All ^1H and ^{13}C spectra were referenced externally to Me_4Si at 0 ppm by referencing the solvent peak (^1H NMR: $CDCl_3$, 7.24 ppm; C_6D_6, 7.15 ppm, C_7D_8, 2.09 ppm; CD_2Cl_2, 5.32 ppm. ^{13}C NMR: $CDCl_3$, 77.0 ppm; C_6D_6, 128.4 ppm, C_7D_8, 20.4 ppm; CD_2Cl_2, 54.0 ppm). ^{11}B NMR spectra were referenced relative to

BF_3•Et_2O at 0 ppm. ^{19}F NMR spectra were referenced externally to C_6F_6 at -163 ppm relative to $CFCl_3$ at 0 ppm. ^{29}Si NMR spectra were referenced relative to Me_4Si at 0 ppm. ^{119}Sn NMR spectra were referenced relative to Me_4Sn at 0 ppm. Low temperature reactions are referenced to the appropriate standard at that temperature and in the same solvent. For example, low temperature ^{119}Sn NMR spectra in CD_2Cl_2 were referenced (0 ppm) using a solution of Me_4Sn in CD_2Cl_2 cooled to the same temperature. Significant changes in the ^{119}Sn NMR shifts are observed with variation in temperature. IR spectra were obtained on neat samples for liquids and as KBr disks for solids using a Mattson Instruments 4030 Galaxy Series spectrometer. Elemental analyses were performed by D. Fox using a Control Equipment Corporation 440 Elemental Analyzer. High resolution mass spectra were obtained by D. Fox using Kratos MS-80 spectrometer.

5.1.3 NMR Tube Reactions: NMR tube reactions were generally carried out by charging an NMR tube with the initial reagents in glove box under an argon atmosphere using scrupulously dried deuterated solvents. Subsequent reagents were introduced by syringe to the septa-sealed NMR tubes at the appropriate temperature. For low temperature reactions, reactants were typically mixed at -78 °C and the placed in NMR probe at appropriate temperature. In some cases, the NMR tube, after being submerged in dry ice/acetone, was shaken once to ensure proper mixing mindful of the potential for premature heating.[3] In cases where premature reaction occurs, the reactions were repeated.

5.2 Experimental Details for Chapter 2

5.2.1 $B(C_6F_5)_3$-Catalyzed Hydrosilation of Carbonyl Functions

Experimental details for this section have previously been published.[4]

$B(C_6F_5)_3$-Catalyzed 1,4-Hydrosilation of Enones

General Procedure for Enone Hydrosilation (Tables 2.2 and 2.3)

A round bottom flask or 10 dram vial was charged with the enone (5.0 mmol), **1** (51 mg, 0.01 mmol) and toluene (5.0 mL). The silane (5.0 mmol) was then added to the reaction mixture via syringe (except for Ph_3SiH which is a solid) all at once. Typically, after 1-5 minute period of time, the reaction mixture heated up considerably and turned yellow or orange in color. Stirring was continued for 30-60 minutes and the reaction mixtures were analyzed by GC-MS. Usually, one major peak is observed corresponding to the molecular weight of the silyl enol ether accompanied by smaller peak(s) from compounds of the same molecular weight. These minor peaks are interpreted to result from either 1,2-hydrosilation or the presence of isomers in the initial enone sample. In some cases competitive or predominant 1,2-hydrosilation is observed. The products were purified by column chromatography (silica gel, 2% Et_3N/hexanes as eluent) and characterized by ^1H and ^{13}C NMR spectroscopy and high resolution mass spectroscopy or by comparison of ^1H NMR data to literature values. The purity of the samples was generally greater than 95%. In some cases, small amounts of $R_3SiOSiR_3$ formed via hydrolysis of the silyl enol ether was observed.

1-Diphenylmethylsiloxycyclopentene (18a):

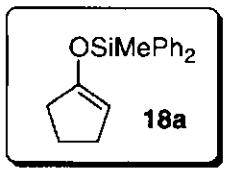

Yield: 90% of colorless oil. HRMS: Mass calcd for $C_{18}H_{20}OSi$, 280.1283; Found, 280.1294. **18a** is a known compound.[5]

1-Diphenylmethylsiloxy-2-methylcyclopentene (18b):

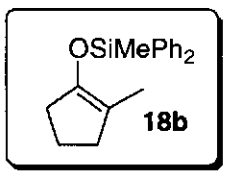

Yield: 90% of colorless oil. ^{1}H NMR ($CDCl_3$, 400 MHz): δ 7.74-7.69 (m, 4H), 7.51-7.40 (m, 6H), 2.25 (app. td, 4H, J = 1.6, 7.2 Hz), 1.79 (m, 2H), 1.65 (s, 3H), 0.79 (s, 3H). ^{13}C NMR ($CDCl_3$, 100 MHz): δ 146.12, 136.27, 134.19, 129.85, 127.78, 113.29, 33.58, 33.39, 19.73, 11.92, -1.99. HRMS: Mass calcd for $C_{19}H_{22}OSi$, 294.1440; Found, 294.1413.

4,4-Dimethyl-1-diphenylmethylsiloxycyclohexene (18c):

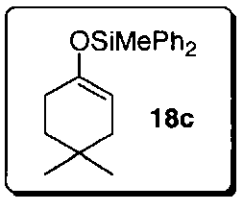

Yield: 96% of colorless oil. ^{1}H NMR ($CDCl_3$, 400 MHz): δ 7.75-7.70 (m, 4H), 7.48-7.42 (m, 6H), 4.90 (tt, 1H, J = 1.3, 4.1 Hz), 2.13 (m, 2H), 1.84 (td, 2H, J = 2.3, 3.8 Hz), 1.46 (t, 2H, 6.4 Hz), 0.95 (s, 6H), 0.81 (s, 3H). ^{13}C NMR ($CDCl_3$, 100 MHz): δ 149.19, 136.26, 134.28, 129.79, 127.78, 104.04, 37.80, 35.84, 28.52, 27.85, 27.51, -2.48. HRMS: Mass calcd for $C_{21}H_{26}OSi$, 322.1753; Found, 322.1751.

1-Diphenylmethylsiloxycyclohexene (18d):

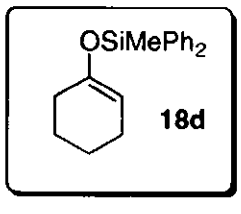

Yield: 96% of colorless oil. HRMS: Mass calcd for $C_{19}H_{22}OSi$, 294.1256; Found, 294.1439. **18d** is a known compound.[6]

(*E*/*Z*)-2-(Diphenylmethylsiloxy)-4-phenyl-2-butene ((*E*)- and (*Z*)-18e):

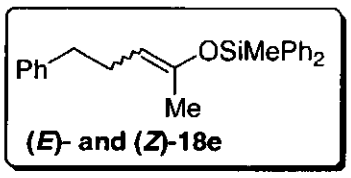

Yield: 85% as 3:2 mixture of *E*:*Z* isomers. Both isomers have previously been characterized.[6]

4,4-Dimethyl-1- ((*tert*)-butyldimethylsiloxy)cyclohexene (18f):

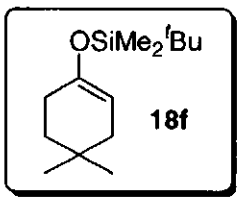

Yield: 86% of colorless oil. ^{1}H NMR ($CDCl_3$, 400 MHz): δ 4.75 (t, 1H, *J* = 3.9 Hz, C=C*H*), 1.98 (m, 2H), 1.79 (dt, 2H, *J* = 2.2, 4.0 Hz), 1.38 (t, 2H, *J* = 6.5 Hz), 0.90 (s, 9H), 0.90 (s, 6H, CH_3), 0.64 (s, 6H). ^{13}C NMR ($CDCl_3$, 100 MHz): δ 149.44, 103.20, 37.94, 35.97, 28.62, 28.03, 27.55, 25.77, 18.02, -4.38. HRMS: Mass calcd for $C_{14}H_{28}OSi$, 240.1909; Found, 240.1912.

4,4-Dimethyl-1-(dimethylphenylsiloxy)cyclohexene (18g):

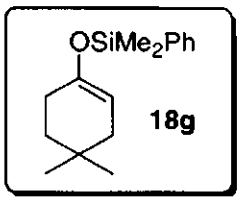

Yield: 88% of colorless oil. ^{1}H NMR (C_7D_8, 400 MHz): δ 7.60-7.50 (m, 2H), 7.20-7.10 (m, 3H), 4.82 (tt, 1H, *J* = 1.3, 4.0 Hz), 2.02 (m, 2H), 1.71 (dt, 2H, *J* = 2.1, 4.2 Hz), 1.26 (t, 2H, 6.6 Hz), 0.82 (s, 6H), 0.39 (s, 3H). **18g** is a known compound.[7]

4,4-Dimethyl-1-(triethylsiloxy)cyclohexene (18h):

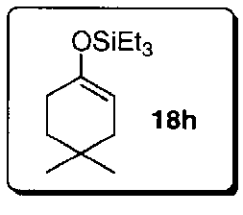

Yield: 91% of colorless oil. ^{1}H NMR ($CDCl_3$, 400 MHz): δ 4.74 (tt, 1H, J = 1.2, 4.0 Hz, C=C*H*), 1.99 (m, 2H), 1.78 (dt, 2H, J = 2.2, 4.1 Hz), 1.38 (t, 2H, J = 6.6 Hz), 0.96 (t, 9H, J = 8.0 Hz, $SiCH_2CH_3$), 0.90 (s, 6H, CH_3), 0.64 (q, 6H, J = 8.0Hz, $SiCH_2CH_3$). ^{13}C NMR ($CDCl_3$, 100 MHz): δ 149.31, 102.72, 37.90, 35.97, 28.58, 27.94, 27.46, 6.69, 4.92. HRMS: Mass calcd for $C_{14}H_{28}OSi$, 240.1909; Found, 240.1918.

4,4-Dimethyl-1-(triphenylsiloxy)cyclohexene (18i):

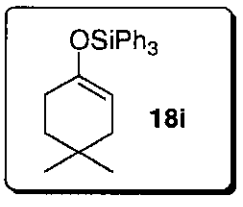

Yield: 86% of white solid. ^{1}H NMR ($CDCl_3$, 400 MHz): δ 7.69-7.61 (m, 6H), 7.46-7.33 (m, 9H), 4.84 (t, 1H, J = 4.1 Hz), 2.01 (m, 2H), 1.68 (dt, 2H, 2.2, 3.8Hz), 1.32 (t, 2H, J = 6.4 Hz), 0.78 (s, 6H). ^{13}C NMR ($CDCl_3$, 100 MHz): δ 149.16, 135.43, 134.34, 129.99, 127.74, 104.69, 37.76, 35.81, 28.46, 27.80, 27.56. HRMS: Mass calcd for $C_{26}H_{28}OSi$, 384.1909; Found, 384.1947.

1-(Dimethylphenylsiloxy)-1-cyclopentene, 18j:

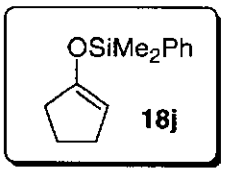

^{1}H NMR ($CDCl_3$, 400 MHz): δ 7.69-7.61 (m, 6H), 7.46-7.33 (m, 9H), 4.84 (t, 1H, J = 4.1 Hz), 2.01 (m, 2H), 1.68 (dt, 2H, 2.2, 3.8Hz), 1.32 (t, 2H, J = 6.4 Hz), 0.78 (s, 6H). δ HRMS: Mass calcd for $C_{13}H_{18}OSi$, 218.1127; Found, 218.1137.

(*E*)-3-(Diphenylmethylsiloxy)-1-phenyl-1-propene(19):

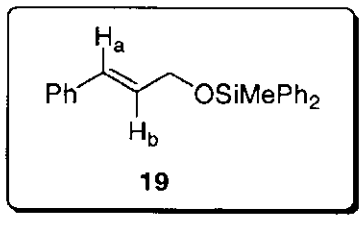

19

Yield: 88% of colorless oil. ^{1}H NMR ($CDCl_3$, 400 MHz): δ 7.80-7.67 (m, 2H), 7.55-7.26 (m, 6H), 6.69 (dt, 1H, J = 1.5, 15.9 Hz, H_a), 6.39 (dt, 1H, J = 5.3, 15.9 Hz, H_b), 4.52 (dd, 1H, J = 1.6, 5.3 Hz, CH_2O), 0.80 (s, 3H, $SiCH_3$). ^{13}C NMR ($CDCl_3$, 100 MHz): δ 136.92, 135.81, 134.37, 133.95, 130.26, 129.86, 128.44, 127.87, 127.37, 126.38, 64.22, -2.85. HRMS: Mass calcd for $C_{22}H_{22}OSi$, 330.1268; Found, 330.1281.

5.2.3 $B(C_6F_5)_3$-Catalyzed Hydrosilation of Silyl Enol Ethers

1-(Dimethylphenylsilyl)-2-(dimethylphenylsiloxy)cyclopentane, 22:

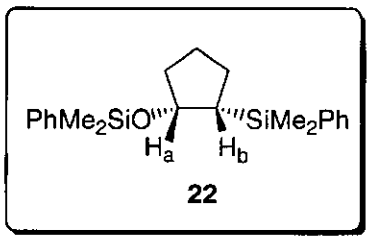

22

A round-bottom flask was charged with **1** (51 mg, 0.10 mmol), 2-cyclopenten-1-one (420 μL, 5.0 mmol) and toluene (5.0 mL). $PhMe_2SiH$ (1.61 mL, 10.5 mmol) was added via syringe all at once. The mixture heats up considerably and then was stirred at room temperature for thirty minutes. The mixture was concentrated *in vacuo* and then purified by column chromatography (silica gel, hexanes then 2% ethyl acetate/hexanes as eluent) affording a colorless oil (1.5 g, 85%). A small amount of $PhMe_2SiOSiMe_2Ph$ was present but could be removed by purifying a second time by column chromatography. ^{1}H NMR (C_6D_6, 400 MHz): δ 7.55 (dd, 2H, J = 1.9, 7.3 Hz), 7.48 (dd, 2H, J = 3.6, 6.6 Hz), 7.29-7.17 (m, 6H), 4.36 (ddd, 1H, 2.2, ~5.0, ~5.0 Hz, H_a), 1.85-1.67 (m, 2H), 1.65-1.51 (m, 2H), 1.47-1.29 (m, 2H), 1.12 (ddd, 1H, J = 5.5, 8.8, 10.4 Hz, H_b), 0.41 (s, 3H), 0.36 (s, 3H), 0.27 (s, 3H), 0.25 (s, 3H). ^{13}C NMR (C_6D_6, 100 MHz): δ 141.10, 139.08, 134.59, 134.26, 130.08, 129.21, 128.33 (one aryl C missing), 78.36, 38.05, 35.43, 26.94, 25.29, -0.28, -1.14, -1.72, -2.42. Anal. Calcd for

$C_{16}H_{30}OSi_2$: C, 71.12%; H, 8.53%. Found: C, 71.45%; 8.23%. ^{1}H NMR decoupling experiments showed that $J(H_a/H_b)$ = 5.5 Hz. In nOe experiments, irradiation of H_a led to enhancement in H_b (8.0%) and *vice versa* (11.0%).

4,4-Dimethyl-1-(dimethylphenylsilyl)-2-(dimethylphenylsiloxy)cyclopentane, 23:

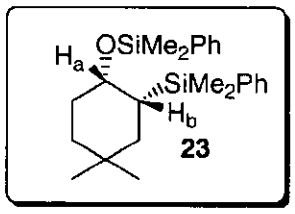

23

A round-bottom flask was charged with **1** (51 mg, 0.10 mmol), 4,4-dimethyl-2-cyclohexen-1-one (658 μL, 5.0 mmol) and toluene (5.0 mL). $PhMe_2SiH$ (1.61 mL, 10.5 mmol) was added via syringe all at once. The mixture heats up considerably and then was stirred at room temperature for 40 hours. The mixture was concentrated *in vacuo* and then purified by column chromatography (silica gel, 2% ethyl acetate/hexanes as eluent) affording a colorless oil (1.41 g). $PhMe_2SiOSiMe_2Ph$ was present but could not be removed by purifying again by column chromatography. The yield of **23** is approximately 60% taking this into account. ^{1}H NMR (C_6D_6, 400 MHz): δ 7.60 (m, 4H), 7.54-7.49 (m, 6H), 4.03 (m, 1H, H_a), 1.84 (t, 1H, J = 13.1 Hz), 1.66 (td, 1H, J = 4.1, 13.7 Hz), 1.50 (dq, 1H, J = 3.2, 14.5 Hz), 1.32 (tdd, 1H, J = 2.6, 3.8, 14.2 Hz), 1.21-1.09 (m, 2H, one of them H_b), 0.92 (s, 3H), 0.80 (s, 3H), 0.35 (s, 6H), 0.33 (s, 3H), 0.31 (s, 3H). ^{13}C NMR (C_6D_6, 100 MHz): δ 140.29, 139.84, 134.67, 134.29, 130.09, 130.02, 129.38, 128.48, 69.63, 35.19, 33.81, 33.61, 31.31, 30.44, 28.20, 24.14, -0.12, -0.61, -2.90, -3.44. ^{29}Si NMR: (C_6D_6, 79.5 MHz): δ 3.4, -1.1. ^{1}H, ^{13}C NMR and ^{29}Si resonances from $PhMe_2SiOSiMe_2Ph$ are not included. HRMS: Calcd for $C_{24}H_{34}OSi_2$, 396.2305; Found, 396.2312. ^{1}H NMR nOe experiments were used to establish the *cis*-relationship of H_a and H_b. First, H_b was assigned using a DEPT ^{13}C NMR experiment to identify the two CH carbons and an HMQC NMR experiment to identify the attached ^{1}H. Irradiation of

H_a led to a 6.3% nuclear Overhauser enhancement in H_b. The coupling constant between H_a and H_b could not be obtained, but is less than 3 Hz based on the appearance of H_a in the ^{1}H NMR spectrum. If the silyl and siloxy groups were *trans*-disposed they would be expected to occupy equatorial sites whereas H_a and H_b would both occupy axial sites; the expected coupling constant would be 10-14 Hz.[8] In a *cis*-substituted cyclohexane, one of H_a/H_b would be axial and the other equatorial leading to a small coupling constant (0-3Hz).

Characterization of Ion-Pair 25 by NMR Spectroscopy:

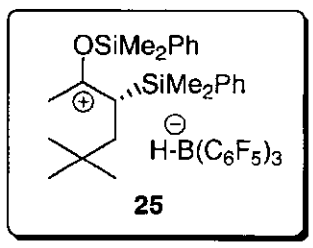

25

An NMR tube was charged with 4,4-dimethyl-2-cyclohexen-1-one (28 μL, 0.20 mmol), **1** (20 mg, 0.04 mmol) and C_7D_8 (~500 μL). $PhMe_2SiH$ (32 μL, 0.20 mmol) was added via syringe causing the solution to heat up immediately. ^{1}H NMR confirmed that clean hydrosilation to silylenol ether **8g** had occurred. ^{19}F NMR at -40 °C showed NMR signals predominantly for uncoordinated **1**. A second equivalent of $PhMe_2SiH$ (32 μL, 0.20 mmol) was added at to the NMR tube cooled to -78 °C. The tube was placed in the NMR probe precooled to -60 °C and ^{1}H, ^{19}F and ^{11}B NMR showed that reaction had taken place. A two-layer reaction mixture is formed under these conditions. All of **1** was incorporated into new compound with the following ^{19}F and ^{11}B NMR spectroscopic data. ^{19}F NMR (C_7D_8, 282 MHz, -60 °C): δ -132.0 (br., 2F, *o*-F's), -62.8 (br., 1F, *p*-F's), -165.6 (br., 2F, *m*-F's). ^{11}B NMR (C_7D_8, 128.4 MHz, -60 °C): δ -25. ^{29}Si NMR (C_7D_8, 76.5 MHz, -60 °C): δ 46, 7. ^{1}H and ^{13}C NMR spectra are very broad.

Synthesis of $[Bu_4N]^+[H\text{-}B(C_6F_5)_3]^-$, 26:

Ion-pair **15** was generated *in situ* by mixing $B(C_6F_5)_3$, Bu_4NBr and Et_3SiH in 1:1:1 molar ratio (0.20 mmol) in C_6D_6. ^1H NMR (400 MHz): δ 4.16 (br. d, 1H, B*H*), 2.44 (m, 8H, NCH_2), 1.01 (m, 16H), 0.74 (br. t, 12H, J = 6.9). ^{13}C NMR (100 MHz): δ 149.4 (dm, J = 235 Hz, *C*-F), 138.9 (dm, J = 240 Hz, *C*-F), 137.5 (dm, J = 246 Hz, *C*-F), 126.7 (br., *C*-B), 58.98 (N*C*H_2), 24.02, 19.97, 13.58. ^{19}F NMR (282 MHz): δ -133.0 (d, 2F, *o*-F's), -163.9 (t, 1F, *p*-F's), -166.9 (m, 2F, *m*-F's). ^{11}B NMR (128.34 MHz): δ -25.5 (d, J = 58 Hz). Ion-pair **26** can be isolated as a solid by mixing reactants together (1:1:1) in CH_2Cl_2 under argon atmosphere, removing CH_2Cl_2 *in vacuo*, and adding hexane to the resulting oily residue which leads to a white solid upon sonication. The hexane is removed by filtration, more hexane is added and removed by filtration. ^{19}F NMR and elemental analysis of the resulting white powder confirmed that it was **26**. This material decomposes at room temperature over weeks. Anal. Calcd for $C_{34}H_{37}NBF_{15}$: C, 54.05%; H, 4.94%; N, 1.85%. Found: C, 53.68%; 4.65%, N 1.85%.

5.2.4 $B(C_6F_5)_3$-Catalyzed Silation of Alcohols

Complete experimental details for Section 2.3 have previously been published.[9]

5.3 Experimental Details for Chapter 3

5.3.1 Hydrosilation of Imines

General Procedure for Hydrosilation of Imines

The imine (1.0 mmol) and **1** (26-51 mg, 5-10 mol%) were mixed in toluene (1.0 mL) in a round-bottom flask or Kontes-sealed reaction bomb. Silane (1.0 mmol) was then added via syringe. The reaction mixtures were then either stirred at room temperature or placed in oil bath at 70 °C. The progress of the hydrosilation reactions was monitored by GC-

MS analysis to determine when reactions were complete. Upon completion, the reaction mixtures were directly purified by column chromatography using hexanes/ethyl acetate mixtures as eluent. The collected fractions containing secondary amine were combined and concentrated *in vacuo* and analyzed by ^{1}H NMR spectroscopy and compared to literature data.[10]

General Procedure for Reductive Amination of Aldehydes:

The aldehyde (1.0 mmol) and aniline (100 μL, 1.0 mmol) were mixed together in 1.0 mL of toluene (used directly from solvent bottle without drying) in a vial and stirred at room temperature for 30-60 minutes. Over this time, the initially homogeneous solutions become cloudy with formation of H_2O droplets on side of vial. $PhMe_2SiH$ (800 μL, 3.05 mmol) and **1** (51 mg, 0.10 mmol) were added and reaction mixtures were stirred at room temperature for 24-168 hours. The progress of the reaction was monitored by GC-MS analysis. Upon completion of reaction, the mixtures were purified by column chromatography using hexanes/ethyl acetate mixtures as the eluent. ^{1}H NMR analysis of the purified (desilated) secondary amine products was carried out; the NMR spectra were compared to previously reported data.[9]

Reductive Amination Reaction Between Acetophenone and Benzyl Amine: Acetophenone (600 μL, 5.0 mmol) and benzyl amine (545 μL, 5.0 mmol) were dissolved in toluene (5.0 mL). A catalytic amount of $ZnCl_2$ (10 mg) was added and the reaction mixture was refluxed for 4 hours after which GC-MS analysis confirmed that imine formation was complete. The reaction mixture was cooled to room temperature and $PhMe_2SiH$ (2.4 mL, 15 mmol) and **1** (51 mg, 0.10 mmol) were added. The mixture was stirred at room temperature for 24 hours, GC-MS analysis confirming that hydrosilation

of the imine was complete. The mixture was then purified by column chromatography using ethyl acetate/hexanes as eluent (5%-50% gradient). The secondary amine (PhCH(Me)-NHBn) was isolated in 86% yield as a colorless oil.

5.3.2 Mechanistic Studies

Formation of Ion-Pair 28:

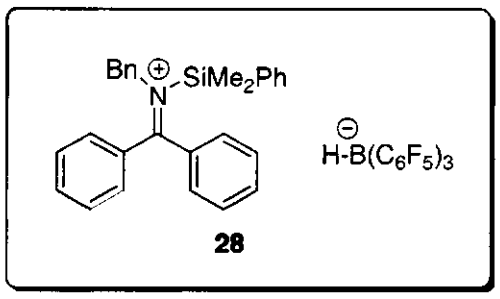

28

Ph_2C=NBn (54 mg, 0.20 mmol) and **1** (102 mg, 0.20 mmol) were dissolved in C_6D_6 (approximately 0.5 mL) in an NMR tube packed under argon and sealed with rubber septum. $PhMe_2SiH$ (32 μL, 0.20 mmol) was then added via syringe leading instantly to a colorless two-layer reaction mixture. ^{1}H, ^{13}C, ^{19}F, ^{11}B and ^{29}Si NMR spectra of the bottom layer were recorded at 25 °C. ^{1}H NMR (400 MHz): δ 7.21-7.01 (m, 10H), 6.92-6.84 (m, 4H), 6.81 (d, 2H), 6.70 (d, 2H), 6.64 (m, 2H), 5.20-4.20 (br. s, 1H, B-*H*), 4.63 (s, 2H, CH_2Ph), 0.00 (s, 6H, SiCH_3). ^{13}C NMR (100 MHz): δ 197.6 (*C*=N), 137.8, 136.7, 136.1, 135.1, 133.8, 133.6, 132.3, 131.8, 131.6, 131.5, 130.2, 130.1, 129.9, 129.8, 129.4, 129.1, 61.8 (*C*H_2Ph), -0.2 (Si*C*H_3). ^{19}F NMR (282 MHz): δ -132.4 ppm (m, 6 F, *o*-F's), -163.8 ppm (m, 3 F, *p*-F's), -166.6 ppm (m, 6 F, *m*-F's). ^{11}B NMR (128.34 MHz): δ -24.7 ppm. ^{29}Si NMR (79.5 MHz): δ 26.9 ppm. Observation of a cross-peak (centered at 4.7 ppm of ^{1}H NMR axis and -24 ppm of ^{11}B NMR axis) in a ^{1}H-^{11}B HETCOR experiment confirmed the direct H-B bonding relationship.

NMR analysis of $B(C_6F_5)_3$ catalyzed hydrosilation of Ph_2C=NBn: To an NMR tube containing Ph_2C=NBn (27 mg, 0.10 mmol) and $B(C_6F_5)_3$ (5 mg, 0.010 mmol) dissolved in C_6D_6 was added $PhMe_2SiH$ (16 μL, 0.10 mmol) via syringe. ^{19}F NMR analysis at

room temperature showed only the borane:imine adduct to be present. Upon heating to 70 °C, ^{19}F NMR analysis revealed that all of **1** was converted to ion-pair **28** after a period of 90 minutes. ^{1}H NMR confirmed that hydrosilation was occurring at this temperature.

NMR Analysis of $B(C_6F_5)_3$-Catalyzed Hydrosilation of PhC(Me)=NBn: To an NMR tube containing PhC(Me)=NBn (21 mg, 0.10 mmol) and $B(C_6F_5)_3$ (5 mg, 0.010 mmol) dissolved in C_6D_6 was added $PhMe_2SiH$ (16 μL, 0.10 mmol) via syringe. The reaction mixture was checked immediately by ^{1}H and ^{19}F NMR spectroscopy showing only partial reaction; the reaction is complete after 75 minutes. Initially signals for a different compound appear which are eventually converted to the main silyl amine product. This initial product is tentatively interpreted to be a rotameric isomer which eventually isomerizes although other possibilities exist. ^{19}F NMR analysis revealed no indication of an anionic borate being formed. NMR data for PhCH(Me)-N(Bn)$SiMe_2$Ph. ^{1}H NMR (C_6D_6, 400 MHz): δ 7.62-7.58 (m, 2H), 7.28-7.00 (m, 13H), 4.33 (q, 1H, J = 7.0 Hz), 3.94 (d, 1H, J = 16.1 Hz), 3.87 (d, 1H, J = 16.1 Hz), 1.27 (d, 7.0 Hz, 3H), 0.37 (s, 3H). ^{13}C NMR (C_6D_6, 100 MHz): δ 144.96, 143.54, 140.25, 134.31, 129.32, 128.12, 128.11, one aryl C missing, 55.96, 49.32, 20.92, 0.02, -0.16. ^{29}Si NMR (C_6D_6, 79.46 MHz): δ -0.50.

Hydrosilation Attempt Using $[Et_3Si(C_6D_6)]^+[B(C_6F_5)_4]^-$:

Et_3SiH (18 μL, 0.11 mmol) was added to an NMR tube charged with $[Ph_3C]^+[B(C_6F_5)_4]^-$ (9.2 mg, 0.01 mmol) and C_6D_6 (~500 μL). The orange-red two-layer mixture becomes colorless (still two layers) and PhC(Me)=NBn (21 mg, 0.10 mmol) dissolved in C_6D_6 was immediately added (still two layers). No reaction was observed over an hour at room

temperature by ^{1}H NMR spectroscopy. The mixture was heated at 70 °C for 36 hours (still two layers). ^{1}H NMR analysis showed that hydrosilation had not taken place under these conditions. The reaction was also attempted using catalytic $[Et_3Si]^+[B(C_6F_5)_4]^-$ and $PhMe_2SiH$ as silane since $PhMe_2SiH$ is more reactive using **1** as catalyst; however, no hydrosilation was observed even with heating.

NMR Analysis of $B(C_6F_5)_3$-Catalyzed Hydrosilation of PhCH=NPh: To an NMR tube charged with PhCH=NPh (18 mg, 0.10 mmol) and **1** (5 mg, 0.01 mmol) in CD_2Cl_2 at -40 °C was added $PhMe_2SiH$ (16 mL, 0.10 mmol). A ^{1}H NMR spectrum was immediately obtained at -40 °C showing that complete consumption of imine had occurred providing $PhCH_2N(Ph)SiMe_2Ph$, **29**, cleanly. ^{1}H NMR (CD_2Cl_2, 400 MHz): δ 7.70-7.20 (m, 10H), 7.15-7.08 (m, 2H), 6.93 (d, 2H, J = 8.2 Hz), 6.79 (t, 1H, J = 7.5 Hz), 4.73 (s, 2H), 0.59 (s, 6H). ^{13}C NMR (CD_2Cl_2, 100 MHz): δ 149.62, 141.54, 139.22, 134.09, 129.74, 128.87, 128.73, 128.38, 128.08, 126.89, 126.83, 119.94, 119.64, 52.59, -0.31.

$[Et_3Si]^+[B(C_6F_5)_4]^-$-Catalyzed Hydrosilation of PhCH=NPh: An NMR tube was charged with PhCH=NPh (18 mg, 0.10 mmol), $PhMe_2SiH$ (16 mL, 0.10 mmol) and CD_2Cl_2. $Et_3SiB(C_6F_5)_4$ (~20 mol%) prepared in C_6D_6 was added via syringe and ^{1}H NMR spectra were recorded over the next 4½ hours showing that slow (relative to catalysis with **1**) formation of $PhCH_2N(Ph)SiMe_2Ph$ does occur.

Competition Between PhCH=NBn and PhCH=NPh for Coordination of $B(C_6F_5)_3$: An NMR tube was charged with PhCH=NPh (18 mg, 0.10 mmol) and **1** (10 mg, 0.02 mmol) and C_7D_8 (~500 μL). ^{1}H and ^{19}F NMR spectra were recorded at 25 °C showing the presence of **38**. PhCH=NBn (19 uL, 0.10 mmol) was added to the NMR tube at 25 °C

via syringe. Initially, ^{1}H NMR analysis showed a mixture of two adducts (**38** and **35-t**), but after 15 minutes, only signals for **35-t** were present in both the ^{1}H and ^{19}F NMR spectra.

5.3.3 Characterization of Imine Adducts of $B(C_6F_5)_3$

Adduct 20: Crystals of adduct **33** suitable for X-ray crystallography and elemental

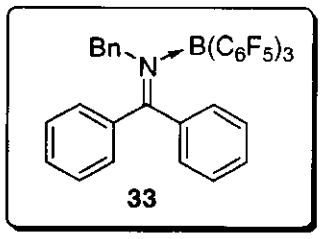

33

analysis were obtained by mixing **1** (51 mg, 0.10 mmol) and imine **27** (30 mg, 0.11 mmol) in toluene (approx ½ mL) in a small vial. Hexane was added until the mixture became cloudy and then the mixture was heated until all of the precipitate dissolved. The mixture was cooled to room temperature over which time colorless crystals formed (yields ranging from 50-90% from first crystallization). X-ray structural data is included on attached compact disk. NMR spectral characterization was carried out by mixing 1:1 ratio (0.1 mmol) of **1** and **33** in C_7D_8. ^{1}H NMR (C_7D_8, 300 MHz, -40 °C): δ 7.89 (t, 1H, J = 9.2 Hz), 7.75 (br. s, 1H), 6.95-6.24 (m, 13H), 5.79 (d, 1H, J = 15.6 Hz), 4.87 (d, 1H, J = 15.6 Hz); ^{1}H NMR (C_7D_8, 300 MHz, 25 °C) δ 8.20-6.24 (m, 15H), 5.79 (br. s, 1H), 4.98 (br. s, 1H). A series of ^{1}H NMR spectra were collected from -40 °C to 60 °C; coalescence of the benzylic ^{1}H's was observed at 40 °C. In the presence of excess **1** (two and four equivalents), no change in the coalescence temperature was observed. ^{13}C NMR (C_6D_6, 100 MHz, -40 °C): δ 190.2 (C=N), 139.4, 138.2, 136.3, 136.2, 133.8, 132.0, 131.7, 131.1, 129.3, 128.4, 128.1, 128.0, 127.4, 127.2, 126.9, 126.0, 125.4, 124.4, 61.1 (d), 21.8 (broad resonances from $B(C_6F_5)_3$ not included). ^{19}F NMR (C_7D_8, 282 MHz, -40 °C): δ -119.5 (app. t, 1F, *o*-F), -123.6 (app. t, 1F, *o*-F), -129.0 (d, 1F, *o*-F), -131.4 (d, 1F, *o*-F), -132.5 (app. t, 1F, *o*-F), -137.0 (app. t, 1F, *o*-F), -

155.6 (app.t, 1F, *p*-F), -156.4 (app. t, 1F, *p*-F), -156.8 (app. t, 1F, *p*-F), -162 - -163 (m, 4F, *m*-F's), -163.8 (app. t, 1F, *m*-F), -164.2 (app. t, 1F, *m*-F). ^{11}B NMR (C_7D_8, 64.18 MHz, 25 °C): δ -3.7. IR (KBr, cm^{-1}): 1646 (C=N), 1573, 1513, 1470, 1282, 1088, 972, 796, 698. Anal. Calcd for $C_{38}H_{17}NBF_{15}$: C, 58.26%; H, 2.19%; N, 1.79%. Found: C, 58.17%; 2.28%, N 1.75%.

Adduct 34-k (Kinetic isomer):

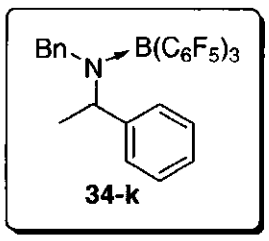

34-k

Crystals of adduct **34-k** were obtained while attempting to isolate the thermodynamic isomer, **34-t**. Imine **30** and **1** were mixed in a 1:1 ratio (0.10 mmol) in toluene. A white precipitate fomed that was heated into solution and allowed to cool slowly to room temperature. X-ray quality crystals deposited from this mixture which presumably contained both **34-k** and **34-t**. The crystal structure obtained was of the kinetic isomer **34-k**. NMR analysis of the crystals to confirm that they were predominantly **34-k** was not possible since it was necessary to heat the NMR tube in order to re-dissolve the crystals. In order to characterize **34-k** by NMR spectroscopy, the adduct was generated at low temperature by adding a solution of **1** in C_7D_8 to **30** dissolved in C_7D_8 in NMR tube cooled to -78 °C. ^{1}H NMR (C_7D_8, 400 MHz, -20 °C): δ 7.38 (t, 1H), 6.89 (t, 1H), 6.82-6.76 (m, 3H), 6.71 (t, 1H), 6.52 (br. s, 1H), 6.34-6.22 (m, 3H), 4.69 (br. s, 2H, CH_2), 1.51 (s, 3H, CH_3). ^{19}F NMR (C_7D_8, 282 MHz, -40 °C): δ -118.1 (br. t, 1F, *o*-F), -124.4 (t, 1F, *o*-F), -129.3 (d, 1F, *o*-F), -133.0 (m, 2F, *o*-F's), -139.6 (s, 1F, *o*-F), -155.9 (t, 1F, *p*-F), -156.1 (t, 1F, *p*-F), -156.9 (t, 1F, *p*-F), -162.4 to -163.2 (m, 4F, *m*-F's), -164.1 to -164.6 (m, 2F, *m*-F's). ^{13}C NMR analysis was precluded by the propensity of **21-k** to precipitate over longer periods of time in C_7D_8, CD_2Cl_2 and other solvents. From the ^{13}C NMR

spectrum obtained under thermodynamic conditions in C_6D_6 (5:1 **34-t**:**34-k**), the following ^{13}C NMR resonances could be attributed to **34-k**. ^{13}C NMR (C_6D_6, 25 °C, 100 MHz): 60.02 (CH_2), 30.61 (CH_3). A $^1H/^1H$ nOe experiment was carried out on the thermodynamic mixture in C_6D_6 confirming that in the minor isomer, **34-k**, the methyl and benzyl groups are *syn*. Specifically, irradiation of the benzylic signal led to an 8.2% enhancement in the methyl signal while irradiation of the methyl signal led to a 7.1% enhancement in the benzylic signal. The infrared spectrum and elemental analysis were obtained on solid that immediately precipitates when **30** and **1** are mixed at low temperature. IR (KBr, cm^{-1}): 1639 (C=N), 1601, 1515, 1459, 1278, 1088, 979, 760, 698, 504. Anal. Calcd for $C_{33}H_{15}NBF_{15}$: C, 54.95%; H, 2.10%; N, 1.94%. Found: C, 54.54%; H 2.05%, N 1.94%.

Adduct 34-t (Thermodynamic isomer):

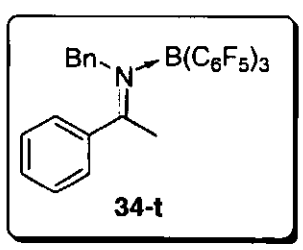

34-t

Crystals of **34-t** were obtained from a 10:1 mixture of **34-t**:**34-k** (0.10 mmol) dissolved in C_7D_8 in an NMR tube (see Structure Report on attached compact disk). This thermodynamic mixture was prepared by mixing imine **30** and **1** in C_7D_8 followed by heating to redissolve precipiate that initially forms. Complete NMR spectral characterization was carried out. ^1H NMR (300 MHz, -40 °C): δ 7.25-6.35 (m, 8H), 6.08 (m, 2H), 5.27 (d, 1H, J = 16.9 Hz), 5.02 (d, 1H, J = 16.9 Hz), 1.94 (s, 3H); ^1H NMR (300 MHz, 25 °C): δ 6.83-6.52 (m, 8H), 6.16 (m, 2H), 5.23 (d, 1H, J =16.4 Hz), 5.03 (d, 1H, J = 16.4 Hz), 2.09 (br. s, 3H). ^{19}F NMR (282 MHz, -40 °C): δ -129.8 (br. s, 2F, *o*-F's), -130.2 (d, 1F, *o*-F), -130.5 (d, 1F, *o*-F), -132.7 (br. s, 2F, *o*-F's), -155.0 (app. t, 1F, *p*-F), -155.2 (app. t, 1F, *p*-F), -155.4 (app. t, 1F, *p*-F), -160.8 (app. t, 1F, *m*-F), -161.4 (app. t,

1F, *m*-F), -162.2 (app. t, 1F, *m*-F), -162.6 (m, 1F, *m*-F), -162.9 (m, 1F, *m*-F), -163.4 (app. t, 1F, *m*-F) (plus minor resonances for **34-k**). ^{13}C NMR (C_6D_6, 100 MHz, 25 °C): δ 191.82 (*C*=N), 138.31, 135.14, 130.30, 128.76, 128.05, 127.15, 125.48, 124.82, 60.55 (m, CH_2), 28.94 (m, CH_3). ^{11}B NMR (128.34 MHz, 25 °C): δ -4.7. A $^{19}F/^{1}H$ heteronuclear Overhauser (hOe) experiment was carried out. Irradiation of each of the six different *ortho* F's led to enhancement in the methyl ^{1}H's and the benzylic ^{1}H's although this should not be viewed as conclusive proof for the *syn* orientation of **1** and the methyl group since the perfluoroaryl groups do occupy large volume of space. A $^{1}H/^{1}H$ nOe experiment on a 5:1 mixture of **34-t**:**34-k** in C_6D_6 showed no enhancement in the two benzylic signals upon irradiation of the methyl signal and *vice versa*. IR (KBr, cm^{-1}): 1651 (C=N), 1596, 1519, 1454 (br.), 1372, 1279, 1105 (br.), 968. Anal. Calcd for $C_{33}H_{15}NBF_{15}$: C, 54.95%; H, 2.10%; N, 1.94%. Found: C, 54.51%; H, 1.93%, N 1.99%. Note that IR spectral and analytical data were obtained on crystalline material obtained under thermodynamic conditions.

Adduct 35-k (Kinetic isomer):

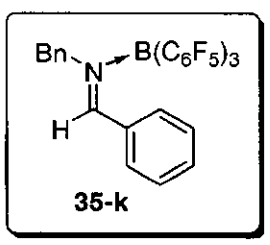

35-k

Owing to its insolubility, **35-k** could only be partially characterized by NMR spectroscopy. Adduct **35-k** was generated at low temperature by adding a solution of **1** (26 mg, 0.05 mmol) to imine **31** (9 mg, 0.05 mmol) dissolved in C_7D_8 in an NMR tube at low temperature. ^{1}H and ^{19}F NMR spectra could be obtained, but a ^{13}C NMR spectrum was not obtained since **35-k** precipitates in the NMR tube soon after it is formed. Warming the reaction mixture to room temperature leads to conversion of adduct **35-k** to adduct **35-t**. When **35-k** is generated in the presence of excess **1**, this isomerization reaction is

suppressed at room temperature. ^{1}H NMR (C_7D_8, 300 MHz, -40 °C): δ 7.69 (s, 1H), 7.04 (d, 2H, *J* =9.8 Hz), 6.86-6.66 (m, 4H), 6.54 (t, 2H, *J* = 8.5 Hz), 6.32 (d, 2H, *J* = 6.9 Hz), 4.68 (d, 1H, *J* = 14.9 Hz), 4.31 (d, 1H, *J* = 14.9 Hz). A series of ^{1}H NMR spectra were recorded between -40 °C and 25 °C; the coalescence temperature for the benzylic H's was observed to be 20 °C. Conversion to the thermodynamic isomer does not take place substantially until after warming to 25 °C. ^{19}F NMR (C_7D_8, 282 MHz, -40 °C): δ -121.1 (br. s, 1F, *o*-F), -122.6 (app. t, 1F, *o*-F), -124.3 (d, 1F, *o*-F), -127.0 (br. s, 1F, *o*-F), -127.9 (d, 1F, *o*-F), -132.0 (br. s, 1F, *o*-F), -150.7 (app. t, 2F, *p*-F), -150.9 (app. t, 1F, *p*-F), -157.0 (app. td, 1F, *m*-F), -157.5 (app. td, 1F, *m*-F), -158.0 (app. td, 1F, *m*-F), -158.3 (app. td, 1F, *m*-F), -159.2 (app. td, 1F, *m*-F), -159.5 (app. td, 1F, *m*-F). ^{11}B NMR (C_6D_6, 64.18 MHz, 25 °C): δ -6.6 (sample prepared from 2:1 ratio of **1**:**31** in order to suppress isomerization to **35-t** during collection of NMR spectrum). IR (KBr, cm^{-1}): 1651 (C=N), 1531, 1383, 1290, 1115 (br.), 963 (br.), 793. Anal. Calcd for $C_{33}H_{13}NBF_{15}$: C, 54.34%; H, 1.85%; N, 1.98%. Found: C, 54.84%; H 2.00%, N 1.89%. Infrared spectral and analytical data were obtained on precipitate formed at low temperature.

Adduct 35-t (Thermodynamic Isomer): Colorless crystals of **35-t** were obtained by dissolving a 1:1 mixture of **1** and **31** (0.1 mmol) in toluene, adding hexane until cloudy, heating into solution and then letting stand at room temperature. Characterization by NMR spectroscopy was carried out on samples prepared by mixing **1** and **31** in a 1:1 ratio (0.1 mmol each) at room temperature in C_7D_8 in NMR tube. If precipitate formed immediately, than the NMR tube was heated until solid re-dissolved. ^{1}H NMR (300 MHz, -40 °C): δ 8.68 (d, 1H, *J* = 7.2 Hz, C*H*=N), 7.05 (br.s,

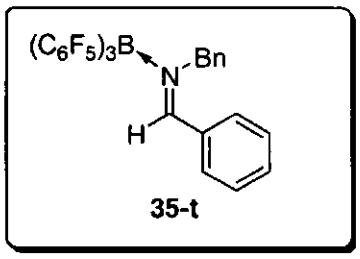

35-t

2H), 6.79 (t, 1H, J = 7.4 Hz), 6.70-6.63 (m, 3H), 6.57 (t, 2H, J = 7.4 Hz), 6.35 (m, 2H), 5.25 (d, 1H, J = 15.6 Hz), 4.87 (d, 1H, J = 15.6 Hz). ^{19}F NMR (282 MHz, -40 °C): δ -129.0 (m, 2F, *o*-F's), -129.2 (br. s, 1F, *o*-F), -131.2 (d, 1F, *o*-F), -134.2 (d, 1F, *o*-F), -136.3 (app. t, 1F, *o*-F), -153.5 (app. t, 1F, *p*-F), -155.9 (app. t, 1F, *p*-F), -156.0 (app. t, 1F, *p*-F), -159.8 (app. td, 1F, *m*-F), -161.8 - -162.3 (m, 2F, *m*-F's), -162.5 - -162.8 (m, 2F, *m*-F's), -163.9 (m, 1F, *m*-F). A series of ^{19}F NMR spectra were recorded between -60 °C and 25 °C showing gradual coalescence of *ortho*-, *para*- and *meta*-fluorines. ^{13}C NMR ($CDCl_3$, 100 MHz, -40 °C): δ 171.0 (*C*=N), 135.6, 132.8, 132.4, 130.2, 128.6, 128.4, 127.8, 125.3, 56.2 (d, CH_2), (broad resonances from $B(C_6F_5)_3$ not included). ^{11}B NMR (C_7D_8, 64.18 MHz, 25 °C): δ -3.3. Anal. Calcd for $C_{32}H_{12}NBF_{15}$: C, 54.34%; H, 1.85%; N, 1.98%. Found: C, 54.19%; H 1.58%, N 1.98%. Infrared spectral and analytical data was obtained on crystalline material obtained under thermodynamic conditions.

Zwitterion 37:

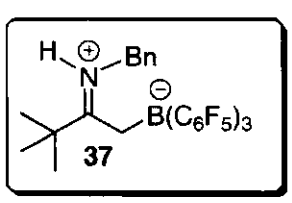

37

Colorless crystals of **37** were obtained in 44% yield by mixing **1** and **32** in 1:1 ratio (0.1 mmol each) in toluene at room temperature followed by cooling to -30 °C (see attached compact disk for structure report of **37**). Characterization of **37** in solution was achieved by the following means. First, **1** and **32** were mixed in a 1:1 ratio in an NMR tube in C_6D_6 at room temperature. ^{1}H and ^{19}F NMR showed only partial conversion to **37**. In the presence of excess **1** (4 eq. total), **32** is almost completely converted to **37** (7:1 **37**:**32**). ^{1}H NMR (400 MHz, C_6D_6): δ 7.07 (br. s, 1H, N*H*), 7.00-6.80 (m, 3H), 6.36 (d, 2H, J = 6.9 Hz), 3.40 (br. s, 2H, CH_2B), 3.30 (d, 2H, J = 5.7 Hz, NCH_2Ph), 0.36 (s, 9H). ^{13}C NMR (100 MHz, C_6D_6): δ 212.87 (*C*=N), 132.39, 130.07, 130.00, 127.58, 50.60, 42.99,

42.95 ($C(CH_3)_3$), 27.07 (CH_3). ^{19}F NMR (282 MHz, C_6D_6): δ -131.41 (br. s, 2F, *o*-F), -158.88 (br. s, 1F, *p*-F), -164.24 (br.s, 2F, *m*-F). ^{11}B NMR (128.4 MHz, C_6D_6): δ -12.2. Infrared spectral and analytical data was obtained on crystalline **37** that had been crushed into a powder. IR (KBr, cm^{-1}): 3632 (w), 3540 (w), 3356 (s, NH), 2972, 1644 (C=N), 1618, 1516, 1454, 1368, 1270, 1148, 1081, 974, 862, 754, 688. Anal. Calcd for $C_{31}H_{19}NBF_{15}$: C, 53.09%; H, 2.73%, N, 2.00%. Found: C, 53.09%; H, 2.20%; 1.96%.

Adduct 38:

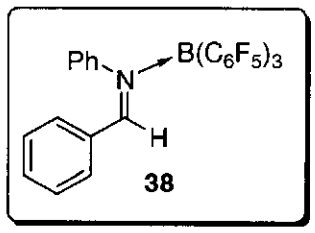

38

An NMR tube was charged with PhCH=NPh (18 mg, 0.10 mmol), **1** (51 mg, 0.10 mmol) and C_7D_8 (~500 μL). NMR spectra of this compound were measured. ^1H NMR (C_7D_8, 300 MHz, 25 °C): δ 7.89 (s, 1H, C(*H*)=N), 7.20-6.50 (m, 10H). ^{13}C NMR (C_6D_6, 25 °C): 174.76, 151.03, 143.11, 135.28, 134.61, 133.14, 131.47, 130.02, 129.90, 129.79, 129.57, 129.41, 125.81. ^{19}F NMR (C_7D_8, 282 MHz, -20 °C): -122.1 (d, 1F, *o*-F), -126.1 (d, 1F, *o*-F), -126.9 (d, 1F, *o*-F), -132.4 (s, 1F, *o*-F), -133.8 (d, 1F, *o*-F), -138.6 (d, 1F, *o*-F), -155.0 (app.t, 1F, *p*-F), -155.7 (app. t, 1F, *p*-F), -155.9 (app. t, 1F, *p*-F), -162.4 (m, 1F, *m*-F), -162.9 (m, 1F, *m*-F), -163.4 to –163.7 (m, 2F, *m*-F's), -164.9 (m, 1F, *m*-F), -165.1 (m, 1F, *m*-F). Crystals suitable for X-ray analysis were obtained from the NMR tube and the structure report is included on attached compact disk. IR spectral and analytical data was performed on this crystalline material. IR (KBr, cm^{-1}): 1667 (C=N), 1651, 1596, 1520, 1088, 766. Anal. Calcd for $C_{31}H_{11}NBF_{15}$: C, 53.45%; H, 1.60%, N, 2.02%. Found: C, 53.71%; H, 1.43%; 2.06%.

Calculation of Barriers to Rotation of Benzyl Groups: Coalescence temperatures for the benzylic hydrogens in adducts **33**, **34-t**, **35-k** and **35-t** were obtained under similar conditions (approx 0.1 mmol in 500 μL of C_7D_8). These values were then used in the following equation: $\Delta G = aT_c[9.972 + \log(T_c/\delta\nu)]$ where $a = 1.914 \times 10^{-2}$ for calculation in kJ mol^{-1}.[11] The values for δν (separation in Hz of benzylic H's) were obtained at -60 °C.

Adduct	T_c (K)	δν (Hz)	$\Delta G^{\ddagger}$ ($kJmol^{-1}$)
33	313	285.7	59.98
34-t	329	80.5	66.64
35-k	293	103.6	58.46
35-t	263	110.3	52.10

5.4 Experimental Details for Chapter 4

Representative Procedure for Competitive Allylstannation Reactions of Aromatic Aldehydes (Entries 1-5, Table 4.1): Entry 1. A mixture of *ortho*-anisaldehyde, ***o*-40**, (272 mg, 2.0 mmol), *para*-anisaldehyde, ***p*-40**, (240 uL, 2.0 mmol) and $B(C_6F_5)_3$ (51 mg, 0.01 mmol) dissolved in toluene (5.0 mL) was cooled to -40 °C using a dry ice/CH_3CN cold bath. $AllylSnBu_3$ (570 μL, 1.8 mmol) was added via syringe and the reaction mixture was stirred for 2 h and then warmed to room temperature by removing cold bath. The reaction mixture was placed directly on a silica-packed column that had been prepared from a hexanes/silica gel slurry. Hexanes, 10% ethyl acetate/hexanes and 20% ethyl acetate/hexanes were used as eluents. All fractions containing the homoallylic alcohols (visualized by TLC using *para*-anisaldehyde stain and UV light) were combined

and concentrated *in vacuo*. ^{1}H NMR spectroscopy was then used to calculate the ratio of the two homoallylic alcohols, ***o*-41** and ***p*-41**, (>20:1). The alcohols were not separated completely from residual aldehyde. However, the alcohols were prepared and purified individually in order to calculate the above ratio. ***o*-41:** ^{1}H NMR ($CDCl_3$): δ 7.34 (dd, 1H, J = 1.8, 7.6 Hz), 7.23 (td, 1H, J = 1.8, 8.2 Hz), 6.95 (td, 1H, J = 1.1, 7.6 Hz), 6.86 (d, 1H, J = 8.1 Hz), 5.90-5.78 (m, 1H, C*H*=CH_2), 5.18-5.04 (m, 2H, CH=CH_2), 4.96 (dd, 1H, J = 4.8, 7.9 Hz), 3.83 (s, 3H, OCH_3), 2.66-2.44 (m, 3H, O*H* and CH_2CH=CH_2). ^{13}C NMR ($CDCl_3$): δ 156.3, 135.1, 131.8, 128.2, 126.7, 120.6, 117.4, 110.3, 69.4, 55.1, 41.8. A similar protocol was used to determine ratios listed for each of Entries 2-5, Table 4.1.[12]

$[Bu_3Sn]^+[B(C_6F_5)_4]^-$-Catalyzed Allylstannation of *o*-/*p*-40 (Entry 6, Table 4.1): A solution of *ortho*-anisaldehyde (272 mg, 2.0 mmol), *para*-anisaldehyde (240 uL, 2.0 mmol) and allyl$SnBu_3$ (570 mL, 1.8 mmol) in CH_2Cl_2 (5.0 mL) was cooled to -40 °C. A solution of $[Bu_3Sn(C_7H_8)]^+[B(C_6F_5)_4]^-$ was prepared by the addition of Bu_3SnH (30 uL, 0.1 mmol) to $[Ph_3C]^+[B(C_6F_5)_4]^-$ (91 mg, 0.1 mmol) in toluene. An aliquot (~ 0.01 mmol) of the bottom clathrate layer of this two-phase solution was added via syringe and the reaction mixture was stirred for two hours and then warmed to room temperature. The reaction mixture was concentrated *in vacuo* and then columned through silica gel using hexanes, 10% ethyl acetate/hexanes and 20% ethyl acetate/hexanes as eluents. All fractions containing the homoallylic alcohols were combined and concentrated *in vacuo*. ^{1}H NMR spectroscopy was then used to measure the ratio of ***o*-41**:***p*-41**, (12.5:1).

$BF_3{\cdot}OEt_2$-Promoted Allylstannation of *o*-/*p*-40 (Entry 7, Table 4.1): A mixture of ***o*-40** (272 mg, 2.0 mmol), ***p*-40** (240 μL, 2.0 mmol), and allyl$SnBu_3$ (570 μL, 1.8 mmol)

dissolved in CH_2Cl_2 was cooled to -78 °C. $BF_3{\cdot}OEt_2$ (280 uL, 2.0 mmol) was then added via syringe. The reaction mixture was concentrated and then columned through silica using hexanes, 10% ethyl acetate/hexanes and 20% ethyl acetate/hexanes as eluents. All fractions containing the homoallylic alcohols were combined and concentrated *in vacuo*. ^{1}H NMR spectroscopy was then used to measure the ratio of ***o*-41:*p*-41** (7:1).

Preparation of Aldehyde:$B(C_6F_5)_3$ Adducts, *o*-44, *p*-44 and 45: NMR samples were prepared by mixing $B(C_6F_5)_3$ (51 mg, 0.10 mmol) with aldehyde (0.10 mmol) in CD_2Cl_2 or C_6D_6 at room temperature. Samples for X-ray structure determination or elemental analysis were prepared by dissolving **1** and aldehyde (0.10 mmol each) in a 3 dram vial in the minimal amount of toluene. Hexane was then added until the solution turns cloudy and then the mixture was heated until adduct was solubilized again. The solution was cooled to room temperature or -30 °C, leading to crystal formation. Yields were not determined. The crystal of adduct ***p*-44** used for X-ray structure determination was obtained from C_7D_8 in an NMR tube cooled to -10 °C.

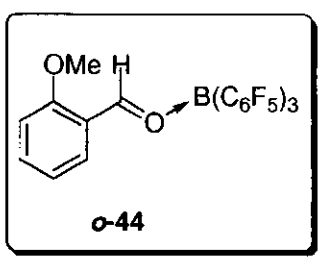

***o*-44**

***o*-44** (-60 °C, CD_2Cl_2): ^{1}H NMR: δ 9.54 (s, 1H, C*H*O), 8.16 (dd, 1H, J = 8.2, 1.8 Hz), 7.97 (m, 1H), 7.16 (app. t, 1H, J = 7.8 Hz), 7.09 (d, 1H, J = 8.8 Hz), 3.93 (s, 3H, OCH_3). ^{13}C NMR: δ 193.6 (*C*HO), 167.5 (Ar C), 147.8 (d, J = 242 Hz, C-F), 146.0 (Ar C), 140.1 (dm, J = 249 Hz, C-F), 136.9 (dm, J = 249 Hz, C-F), 132.4 (Ar C), 122.1 (Ar C), 119.6 (Ar C), 115.9 (m, ipso C Ar_f), 112.9 (Ar C), 56.8 (O*C*H$_3$). ^{19}F NMR: δ -134.4, -156.6, -163.8. ^{11}B NMR (room temp.): δ 3.3. Anal. Calcd for $C_{26}H_8O_2BF_{15}$: C, 48.18%, H, 1.24%. Found: C, 48.01%, H, 1.00%.

***p*-44** (-60 °C, CD_2Cl_2): ^1H NMR: δ 8.90 (s, 1H, C*H*O), 8.39 (d, *J* = 8.6 Hz), 8.04 (d, *J* = 7.7 Hz), 7.19 (d, *J* = 8.3 Hz), 7.13 (d, *J* = 7.6 Hz), 4.02 (s, 3H, OCH_3). ^{13}C NMR: δ 193.3 (*C*HO), 171.6 (Ar C), 147.7 (dm, *J* = 240 Hz, C-F), 144.0 (Ar C), 140.0 (dm, *J* = 250 Hz, C-F), 136.9 (dm, *J* = 249 Hz, C-F), 134.9 (Ar C), 123.7 (Ar C), 118.1 (Ar C), 116.0 (m, ipso C Ar_f), 114.0 (Ar C), 57.3 (OCH_3). ^{19}F NMR: δ -134.3, -156.6, -163.7. ^{11}B NMR (room temp.): δ 3.2. Anal. Calcd for $C_{26}H_8O_2BF_{15}$: C 48.18%, H, 1.24%. Found, C, 48.48%, H, 1.24%.

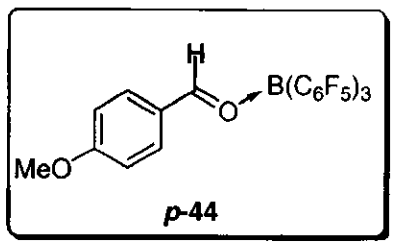

***p*-44**

45 (C_6D_6, 25 °C): ^1H NMR: δ 9.57 (s, 1H, C*H*O), 7.77 (ddd, 1H, *J* = 1.8, 6.4, 7.3 Hz), 6.77 (m, 1H), 6.41 (t, 1H, *J* = 7.9 Hz), 6.23 (t, 1H, *J* = 9.7 Hz). ^{13}C NMR: δ 194.72 (br.), 167.70 (d, *J* = 271.4 Hz), 148.98 (dm, *J* = 245 Hz, C(Ar_f)), 145.00 (d, *J* = 10.7 Hz), 141.70 (dm, *J* = 253 Hz C(Ar_f)), 138.30 (dm, *J* = 252 Hz, C(Ar_f)), 132.42, 126.58 (d, *J* = 3.1 Hz), 126.58 (d, *J* = 3.1 Hz), 120.27 (d, *J* = 6.9 Hz), 117.51 (d, *J* = 19.9 Hz), 115.8 (br. *ipso* C(Ar_f)). ^{19}F NMR: δ -109.3 (1F), -134.3 (6F), -155.9 (3F), -163.5 (6F). ^{11}B NMR: δ 4.5 ppm. Anal. Calcd for $C_{25}H_5OBF_{16}$: C, 47.20%, H, 0.79%. Found: C, 47.33, H, 0.35%.

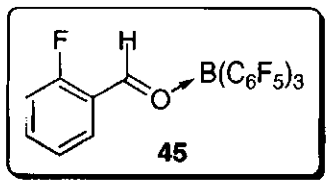

45

NMR Analysis of Ion-pair 46. An NMR tube was charged with $B(C_6F_5)_3$ (51 mg, 0.10 mmol) and CD_2Cl_2 (approx. 500 μL). $AllylSnBu_3$ (31 μL, 0.10 mmol) was added by syringe to the NMR tube cooled to -78 °C and the NMR tube was shaken and placed in the NMR probe at -60 °C. ^1H NMR: δ 8.14 (m, 1H, H_a), 4.42 (br. s, 1H, SnC*H*), 4.16 (d, 1H, J = 16.4 Hz, SnC*H*), 2.93 (br. s, 2H, BCH_2), 1.70-1.40 (m, 12H), 1.34-1.22 (m, 6H), 0.86 (t, 9H, J = 7.2 Hz). ^{19}F NMR: δ -133.4, -161.1, -165.4. ^{13}C NMR: δ 192.1 ($^1J_{C\text{-}H}$ = 149.7 Hz, C^+), 147.7 (d, J = 240 Hz, C-F), 138.3 (d, J = 248 Hz, C-F), 136.6 (d, J = 248 Hz, C-F), 122.4 (br. s, *ipso*) 88.7 (CH_2Sn), 40.5 (CH_2B), 28.2 ($^3J_{C\text{-}Sn}$ = 10.7 Hz), 27.4 ($^2J_{C\text{-}Sn}$ = 36.0 Hz), 18.0 ($^1J_{C\text{-}Sn(119)}$ = 137.3 Hz, $^1J_{C\text{-}Sn(117)}$ = 143.4 Hz, CH_2Sn), 13.6 (CH_3). ^{119}Sn NMR: δ 181.3. ^{11}B NMR: δ -13.9.

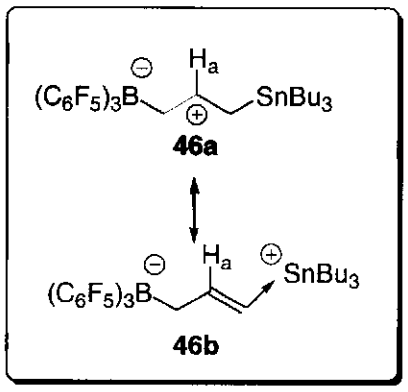

NMR Analysis of Ion-Pair 47. To the NMR tube above (adduct **46**) was added $allylSnBu_3$ at -78 °C. The NMR tube was shaken and placed in the NMR probe at -60 °C. After NMR measurements were complete, $allylSnBu_3$ (93 μL, 0.30 mmol) was added to this sample at -78 °C. The NMR tube was shaken and placed in the NMR probe at -60 °C. ^1H NMR: (anion) δ 7.14 (br. s, 1H, CH_2=C*H*CH_2B), 4.36 (d, 1H, J = 6.3 Hz, vinylic H), 4.18 (d, 1H, J = 16.7 Hz, vinylic H), 2.53 (br. s, 2H, CH_2B); (cation) δ 6.85 (m, 1H, CH^+), 3.33 (d, 4H, J = 10.8 Hz, CH_2), 1.60-1.35 (m,

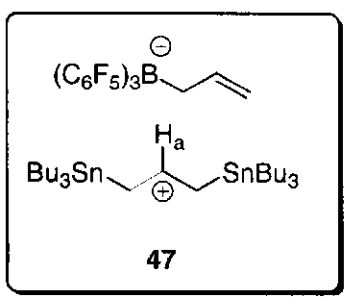

12H), 1.35-1.10 (m, 24H), 0.84 (t, 18H, J = 7.2 Hz). ^{19}F NMR: δ -133.2, -161.9, -165.8; ^{13}C NMR: (anion) δ 170.9 ($^{1}J_{C\text{-}H}$ = 151.8 Hz, CH_2=*C*HCH_2B), 147.7 (d, J = 236 Hz, C-F), 137.8 (d, J = 250 Hz, C-F), 136.3 (d, J = 246 Hz, C-F), 124.3 (br. s, *ipso*), 98.3 (*C*H_2=CH), 35.8 (br. s, *C*H_2B); (cation) δ 161.2 ($^{1}J_{C\text{-}H}$ = 158.0 Hz, *C*$^{+}$H), 58.7 (*C*H_2SnBu$_3$), 28.6 ($^{3}J_{C\text{-}Sn}$ = 10.7 Hz), 27.4 ($^{2}J_{C\text{-}Sn}$ = 33,7 Hz), 13.8 ($^{1}J_{C\text{-}Sn(119)}$ = 146.5 Hz, $^{1}J_{C\text{-}Sn(117)}$ = 152.6 Hz, *C*H_2Sn), 13.7 (*C*H_3). ^{119}Sn NMR: δ 90.8. ^{11}B NMR: δ -14.2. AllylSnBu$_3$ (93 μL, 0.30 mmol) was added to this NMR tube at -78 °C, the tube was shaken and placed in NMR probe at -60 °C. ^{1}H NMR: (anion) δ 7.14 (br. s, 1H, CH_2=C*H*CH_2B), 4.36 (d, 1H, J = 6.3 Hz, *trans* vinylic H), 4.18 (d, 1H, J = 16.7 Hz, *cis* vinylic H), 2.53 (br. s, 2H, C*H*$_2$B); (cation) δ 6.85 (m, 1H, C*H*$^{+}$), 3.33 (d, 4H, J = 10.8 Hz, C*H*$_2$), 1.60-1.35 (m, 12H), 1.35-1.10 (m, 24H), 0.84 (t, 18H, J = 7.2 Hz); ^{19}F NMR: δ -133.0, -162.5, -166.1. ^{13}C NMR: (anion) δ 161.5 (br. s, CH_2=*C*HCH_2B), 147.8 (d, J = 240 Hz, C-F), 137.86 (d, J = 248 Hz, C-F), 136.3 (d, J = 248 Hz, C-F), 125.0 (br. s, *ipso*), 102.5 (*C*H_2=CH), 33.7 (*C*H_2B); (cation) δ 149.6 (br. s, *C*H^{+}), 60.6 (*C*H_2SnBu$_3$), 29.0 ($^{3}J_{C\text{-}Sn}$ = 10.7 Hz), 27.6 ($^{2}J_{C\text{-}Sn}$ = 30.7 Hz), 13.9 (*C*H_3), 11.4 ($^{1}J_{C\text{-}Sn(119)}$ = 149.5 Hz, $^{1}J_{C\text{-}Sn(117)}$ = 156.4 Hz). ^{119}Sn NMR: δ 38.3. ^{11}B NMR: δ -14.3.

Preparation of [Bu$_4$N]$^{+}$[allylB(C$_6$F$_5$)$_3$]$^{-}$, 48. An NMR tube was charged with B(C$_6$F$_5$)$_3$ (51 mg, 0.10 mmol), Bu$_4$NBr (34 mg, 0.10 mmol) and CD_2Cl_2 (approx. 500 μL). AllylSnBu$_3$ was added at room temperature and the NMR tube was shaken vigorously. NMR spectra were measured at -60 °C. ^{1}H NMR: δ 5.90-5.76 (m, 1H, C*H*=CH$_2$), 4.28 (dd, 1H, J = 3.4, 10.2 Hz, CH=C*H*$_{(cis)}$H$_{(trans)}$, 4.20 (d, 1H, J = 17.2 Hz

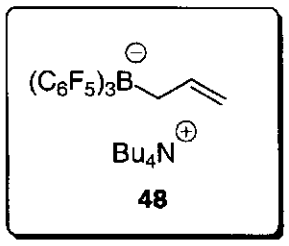

48

CH=CH$_{(cis)}$*H*$_{(trans)}$), 3.02 (m, 8H, C*H*$_2$N), 2.01 (d, 2H, *J* = 7.6 Hz, C*H*$_2$B) 1.60-1.23 (m, Bu_4N CH_2's + Bu_3SnBr), 0.92 (t, Bu_4N CH_3). ^{19}F NMR: δ -133.5, 163.3, -166.5. ^{13}C NMR: δ 147.7 (d, *J* = 238 Hz), 144.2 (vinylic C), 137.3 (d, *J* = 243 Hz), 136.0 (d, *J* = 244 Hz), 127.4-124.8 (br. *ipso*), 109.5 (vinylic C), 58.3 (*C*H$_2$N), 30.4 (br., *C*H$_2$B), 23.5 (Bu_4N *C*H$_2$), 19.6 (Bu_4N *C*H$_2$), 13.5 (Bu_4N *C*H$_3$). ^{11}B NMR: δ -14.3.

Preparation of $[Bu_4N]^+[$(*ortho*-anisylCH(allyl)OB$(C_6F_5)_3]^-$, *o*-54. An NMR tube containing **48** was prepared as described above. *Ortho*-anisaldehyde (14 mg, 0.1 mmol) and $B(C_6F_5)_3$ (approx. 2 mg) were added to the NMR tube and the reaction mixture was maintained at room temperature for two hours. NMR analysis at -60 °C revealed that a new ion-pair was formed. ^1H NMR: δ 7.28 (d, *J* = 7.6 Hz), 6.91 (app.t, *J* = 7.0), 6.72 (app. t, *J* = 7.2 Hz), 6.44 (d, *J* = 8.0 Hz), 5.58-5.45 (m, 1H, C*H*=CH$_2$), 4.87-4.68 (m, 3H, CH=C*H*$_2$, *CH*OB), 3.52 (s, 3H, OC*H*$_3$), 2.98 (m, 8H, C*H*$_2$N), 2.79-2.67 (m, 1H, C(*H*$_a$)H$_b$CH=CH$_2$), 2.36-2.21 (m, 1H, C(*H*$_b$)H$_a$CH=CH$_2$), 1.60-1.20 (m, 16H, Bu_4N C*H*$_2$'s), 0.91 (t, 12H, *J* = 5.6 Hz, Bu_4N C*H*$_3$). ^{19}F NMR: δ -133.2, -163.5, -166.6. ^{13}C NMR: δ 154.8, 147.4 (d, *J* = 240 Hz, C-F), 137.5 (d, *J* = 242 Hz, C-F), 136.3, 135.5 (d, *J* = 244 Hz, C-F), 134.9, 127.5, 127.3, 126.5-122.0 (br., *ipso* Ar$_f$), 125.8, 119.1, 114.9, 107.8, 67.4 (*C*HOSnBu_3), 58.2 (*C*H$_2$N), 54.4 (OC*H*$_3$), 44.6 (*C*H$_2$CH=CH$_2$), 23.4 (Bu_4N *C*H$_2$), 19.5 (Bu_4N *C*H$_2$), 13.4 (Bu_4N *C*H$_3$). ^{11}B NMR: δ -4.5.

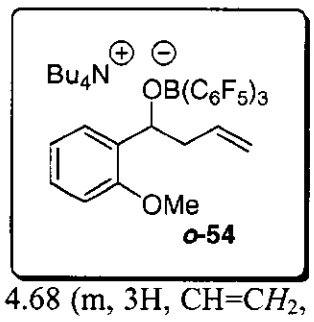

***o*-54**

The *para*-anisaldehyde congener, ***p*-54**, was prepared analogously. ^{1}H NMR: δ 6.86 (d, *J* = 8.2 Hz), 6.54 (d, *J* = 8.2 Hz), 5.41 (ddd, 1H, *J* = 7.3, 10.5, 17.1 Hz, C*H*=CH$_2$), 4.83-4.71 (m, 2H, CH=C*H*$_2$), 4.18 (d, 1H, *J* = 9.5 Hz, C*H*OB), 3.67 (s, 3H, OC*H*$_3$), 2.98 (m, 8H, C*H*$_2$N), 2.82-2.72 (m, 1H, C(*H*$_a$)H$_b$CH=CH$_2$), 2.37-2.21 (m, 1H, C(*H*$_b$)H$_a$CH=CH$_2$), 1.60-1.20 (m, 16H, Bu$_4$N C*H*$_2$'s), 0.91 (t, 12H, *J* = 7.3 Hz, Bu$_4$N C*H*$_3$). ^{13}C NMR: δ 157.0, 147.5 (d, *J* = 240 Hz, C-F), 138.6, 137.6 (d, *J* = 245 Hz, C-F), 136.5, 135.9 (d, *J* = 246 Hz, C-F), 127.3, 126.0-123.5 (br., *ipso* Ar$_f$), 115.4, 111.6, 76.8 (*C*HOSnBu$_3$), 58.3 (*C*H$_2$N), 55.0 (OCH$_3$), 45.4 (*C*H$_2$CH=CH$_2$), 23.4 (Bu$_4$N *C*H$_2$), 19.6 (Bu$_4$N *C*H$_2$), 13.5 (Bu$_4$N *C*H$_3$). ^{19}F NMR: δ -133.4, -163.4, -166.6. ^{11}B NMR: δ -4.5.

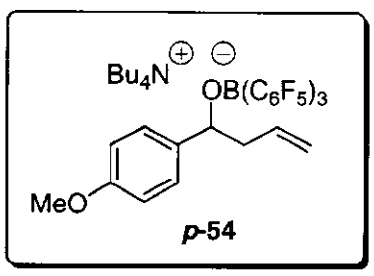

***p*-54**

Preparation of [Bu$_3$Sn]$^+$[B(C$_6$F$_5$)$_4$]$^-$, 49. Bu$_3$SnH (62 μL, 0.2 mmol) was added to a two-phase red-orange C$_7$D$_8$ solution (approximately 500 μL) of [Ph$_3$C]$^+$[B(C$_6$F$_5$)$_4$] (182 mg, 0.2 mmol) in an NMR tube leading to a colorless two-phase mixture. The top layer was removed via syringe and more C$_7$D$_8$ (approx. 300 μL) was added. The NMR tube was vigorously shaken, the top layer removed by syringe and then repeated. ^{119}Sn NMR analysis of the bottom clathrate layer (approx. 400 μL) at room temperature showed a sharp signal at 262 ppm and a very broad, weak signal centered at 420 ppm. The sample was cooled to -60 °C at which temperature, a sharp signal is observed at -432.4 ppm attributed to the toluene-solvated ion-pair [Bu$_3$Sn]$^+$[B(C$_6$F$_5$)$_4$]$^-$. CD_2Cl_2 solutions of ion-pair [Bu$_3$Sn]$^+$[B(C$_6$F$_5$)$_4$]$^-$ were prepared by addition of CD_2Cl_2 (approx. 400 mL) at -60 °C to ion-pair [Bu$_3$Sn]$^+$[B(C$_6$F$_5$)$_4$]$^-$ (0.1 mmol) prepared in C$_7$D$_8$: ^{1}H NMR: δ 1.70-1.56 (m, 6H), 1.55-1.41 (m, 6H), 1.39-1.29 (m, 6H), 1.14 (t, 9H, *J* = 7.3 Hz). ^{13}C NMR: 148.2

(d, J = 244 Hz, C-F), 138.4 (d, J = 244 Hz), 136.5 (d, J = 247 Hz), 27.9 ($^3J_{C\text{-}Sn}$ = 11.5 Hz), 27.3 ($^2J_{C\text{-}Sn}$ = 40.6 Hz), 23.6 (br., CH_2SnBu_3), 13.7 (CH_3). ^{119}Sn NMR: δ 422.1.

Preparation of *Mono-* and *Bis-ortho*-Anisaldehyde Adducts of $[Bu_3Sn]^+[B(C_6F_5)_4]^-$, *o*-55 and *o*-56. A solution of *ortho*-anisaldehyde was prepared by dissolving aldehyde (54 mg, 0.4 mmol) in 200 μL of C_7D_8. 100 μL (0.2 mmol of ortho-anisaldehyde) of this solution was added via syringe to an NMR tube containing ion-pair $[Bu_3Sn]^+[B(C_6F_5)_4]^-$ prepared as above. NMR analysis of the bottom layer at -60 °C shows a ^{119}Sn NMR signal at 300.5 ppm. The remainder of the solution (0.4 mmol of *ortho*-anisaldehyde total) was then added and a ^{119}Sn NMR shift of 91.0 ppm was observed. Further NMR characterization by ^{1}H and ^{13}C NMR spectroscopy was carried out at -60 °C on ***o*-55** and ***o*-56** by adding CD_2Cl_2 solutions of *ortho*-anisaldehyde to toluene clathrates of $[Bu_3Sn]^+[B(C_6F_5)_4]^-$ prepared analogously but starting with 0.10 mmol of $[Ph_3C]^+[B(C_6F_5)_4]^-$

***o*-55:** ^{119}Sn NMR: δ 298.6. ^{1}H NMR: δ 10.0 (C*H*O), 8.05 (br. s), 7.94 (br. s), 7.20 (br. s), 7.07 (br. d, J = 6.7 Hz), 4.00 (s, 3H, OCH_3), 1.94-1.45 (m, 18H), 1.20-1.09 (br. m, 9H). ^{13}C NMR: δ 198.3 (*C*HO), 166.8 (br.), 148.2 (d, J = 241 Hz, C-F), 145.4 (br.), 142.0 (br.), 138.4 (d, J = 245 hz, C-F), 136.4 (d, J = 246 Hz), 130.3 (br.), 126.0-122.0 (br., *ipso* Ar_f), 121.8 (br.), 121.3 (br.), 113.0, 56.5, 27.7, 27.4 ($^2J_{C\text{-}Sn}$ = 36.0 Hz), 19.9 (br., CH_2Sn), 13.8 (CH_3).

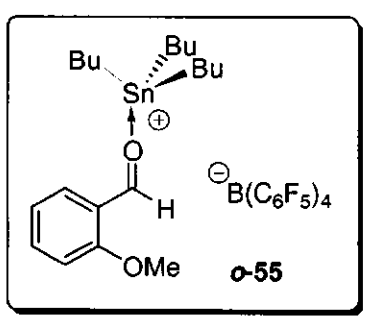

***o*-55**

***o*-56:** ^{119}Sn NMR: δ 91.1. ^{1}H NMR: δ 10.30 (s, 2H, C*H*O), 8.08 (d, 2H, *J* = 7.7 Hz), 7.88

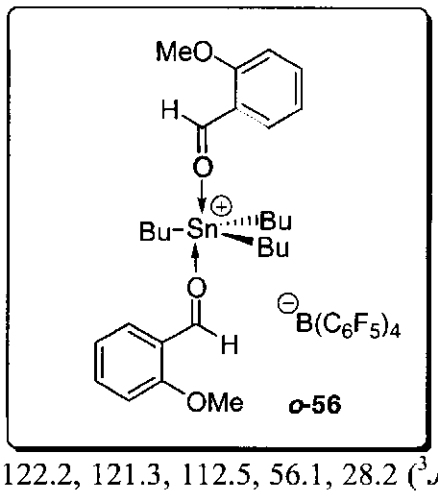

***o*-56**

(app. t, 2H, *J* = 8.0 Hz), 7.23 (app. t, 2H, *J* = 7.2 Hz), 7.10 (d, 2H, *J* = 8.5 Hz), 4.02 (s, 6H), 1.97-1.85 (6H), 1.79-1.69 (6H), 1.69-1.55 (6H), 1.17 (t, 9H, *J* = 7.4 Hz). ^{13}C NMR: δ 195.7 (*C*HO), 164.5, 148.3 (d, *J* = 240 Hz), 141.5, 138.5 (d, *J* = 245 Hz), 136.6 (d, *J* = 245 Hz), 129.5 (br.), 126.0-122.0 (br., *ipso* Ar_f), 122.2, 121.3, 112.5, 56.1, 28.2 ($^{3}J_{C\text{-}Sn}$ = 14.6 Hz), 27.3 ($^{2}J_{C\text{-}Sn}$ = 37.6 Hz), 18.6 ($^{1}J_{C\text{-}Sn(119)}$ = 195.6, $^{1}J_{C\text{-}Sn(117)}$ = 204.0, CH_2Sn), 13.9 (CH_3).

Preparation of *Mono-* and *Bis-para*-Anisaldehyde adducts of $[Bu_3Sn]^+[B(C_6F_5)_4]^-$, *p*-55 and *p*-56. Consecutive additions of *para*-anisaldehyde (24 μL, 0.2 mmol) via syringe to $[Bu_3Sn]^+[B(C_6F_5)_4]^-$ (0.2 mmol) prepared in C_7D_8 led to observation of signals at 291.9 ppm and 81.4 ppm respectively in the ^{119}Sn NMR spectra obtained at -60 °C. Additionally, NMR analysis was carried out on solutions prepared by adding *para*-anisaldehyde (2 x 12 μL) to $[Bu_3Sn]^+[B(C_6F_5)_4]^-$ (approx. 0.10 mmol) dissolved in CD_2Cl_2 at -60 °C.

***p*-55:** ^{119}Sn NMR: δ 291.4. ^{1}H NMR: δ 9.30 (br. s, 1H, C*H*O), 8.27 (d, 1H, *J* = 8.8 Hz),

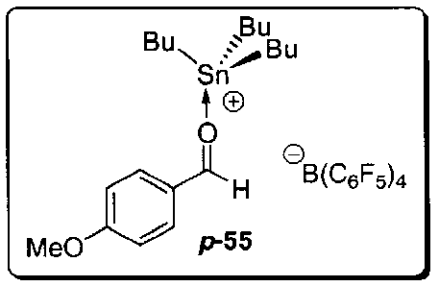

***p*-55**

8.04 (d, 1H, *J* = 8.5 Hz), 7.19 (app. t, 2H, *J* = 7.2 Hz), 4.03 (s, 3H, CH_3), 2.01-1.67 (m, 12 H), 1.66-1.50 (m, 6H), 1.18 (t, 9H, *J* = 7.3 Hz). ^{13}C NMR: δ 198.0 (br., *C*HO), 148.3 (d, *J* = 238 Hz), 143.6, 138.5 (d, *J* = 244 Hz), 136.4 (d, *J* = 247 Hz), 117.9 (br.), 114.5 (br.), 132.6 (br.), 126.0-122.0 (br., *ipso* Ar_f), 56.8 (br., OCH_3), 27.8, 27.5 ($^{2}J_{C\text{-}Sn}$ = 36.0 Hz), 19.7 (br. CH_2Sn).

***p*-56:** ^{119}Sn NMR. δ 83.5. ^{1}H NMR: δ 9.62 (s, 2H, C*H*O), 8.22 (br. s, 2H), 8.05 (br. s, 2H), 7.20 (d, 4H, J = 8.3 Hz), 4.01 (br. s, 6H, OCH_3), 2.07-1.40 (m, 18H), 1.18 (t, 9H, J = 7.0 Hz, CH_3). ^{13}C NMR: δ 196.0 (br., *C*HO), 168.3 (br.), 148.4 (d, J = 240 Hz), 140.6 (br.), 138.4 (d, J = 244 Hz), 136.5 (d, J = 245 Hz), 130.8 (br.), 127.0, 126.0-122.0 (br., ipso Ar$_f$), 116.9, 114.0, 56.3 (O*C*H$_3$), 28.2 ($^{3}J_{C\text{-}Sn}$ = 14.6 Hz), 27.4 ($^{2}J_{C\text{-}Sn}$ = 37.6 Hz), 18.5 ($^{1}J_{C\text{-}Sn(119)}$ = 196.3 Hz, $^{1}J_{C\text{-}Sn(117)}$ = 206.3 Hz, *C*H$_2$Sn), 14.0 (CH$_3$).

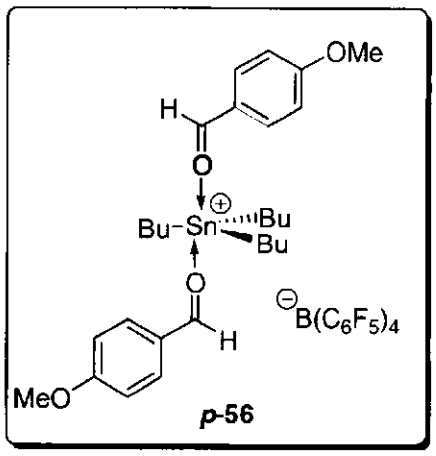

***p*-56**

Preparation of ion-pair *o*-53. An NMR tube was charged with B(C_6F_5)$_3$ (34 mg, 0.067 mmol) and *ortho*-anisaldehyde (27 mg, 0.20 mmol) and CD_2Cl_2 (approx. 500 μL). The sample was cooled to -78 °C and allylSnBu_3 (10 μL, 0.67 mmol) was added via syringe. The reaction mixture was shaken once and placed in the NMR probe precooled to -60 °C. ^{1}H and ^{19}F NMR spectra were obtained. ^{119}Sn, ^{11}B and ^{13}C NMR spectra were obtained at -60 °C on a sample prepared analogously. Very minor resonances can be observed for the stannyl ether, (*ortho*-anisyl)CH(allyl)OSnBu_3, and *ortho*-anisaldehyde:B(C_6F_5)$_3$ but one set of signals attributed to ***o*-53** dominates the spectra. ^{1}H NMR: (cation) δ 10.10 (br. s, 2H, C*H*O), 7.87 (d, 2H, J = 8.0 Hz), 7.78 (app. t, 2H, J = 7.7 Hz), 7.12-7.05 (m, 4H), 3.95 (s, 6H), 1.70-1.20 (m, 18H), 0.87 (t, J = 6.8 Hz); (anion) δ 7.29 (d, 1H, J = 7.3 Hz), 6.91 (app. t,

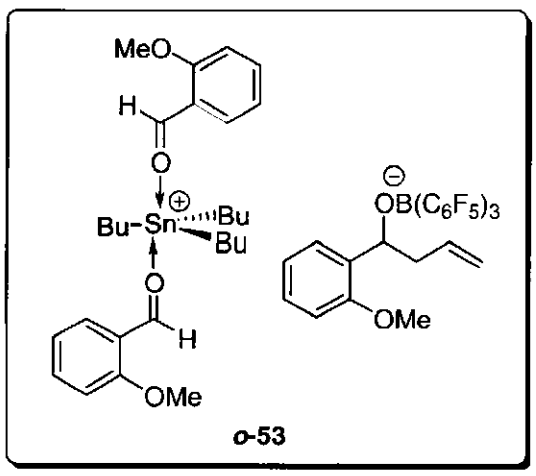

***o*-53**

1H, J = 7.2 Hz), 6.72 (app. t, 1H, J = 7.3 Hz), 6.44 (d, 1H, J = 8.0 Hz), 5.54 (ddd, 1H, J = 7.0, 10.1, 17.0 Hz), 4.87-4.68 (m, 3H), 3.53 (s, 3H), 2.80-2.68 (m ,1H), 2.38-2.25 (m, 1H). ^{19}F NMR: δ -133.0, -164.0, -167.1. ^{13}C NMR: (cation) δ 195.5 (br., *C*HO), 164.2 (br.), 141.5 (br.), 129.3 (br.), 121.7 (br.), 120.9 (br.), 112.3 (br.), 56.1 (br.), 27.7 ($^{3}J_{C\text{-}Sn}$ = 14.6 Hz), 26.9 ($^{2}J_{C\text{-}Sn}$ = 38.3 Hz), 18.2 ($^{1}J_{C\text{-}Sn(119)}$ = 195.5 Hz, $^{1}J_{C\text{-}Sn(117)}$ = 204 Hz, CH_2Sn), 13.6 (CH_3); ^{13}C NMR: (anion) δ 154.7, 147.4 (dm, C-F), 137.5 (dm, C-F), 136.3, 135.7 (dm, C-F), 134.9, 127.6, 126.0-123.5 (br. m, *ipso* Ar_f), 125.7, 119.1, 114.8, 107.7, 67.4, 54.3, 44.7. ^{119}Sn NMR: δ 90.5. ^{11}B NMR: δ -4.5 ppm.

Preparation of ion-pair *p*-53. A similar procedure was used to convert $B(C_6F_5)_3$ (34 mg, 0.067 mmol), *para*-anisaldehyde (24 μL, 0.20 mmol) and allylSnBu_3 (10 μL, 0.67 mmol) in CD_2Cl_2 (approx. 500 μL) to ion-pair ***p*-53** at -60 °C. However, reaction is much slower (60% conversion after 2 hours) with significant formation of stannyl ether byproduct. Signals for ***p*-3** also complicate spectral analysis. The following diagnostic NMR data for the anion of ***p*-53** was obtained (matching that for the Bu_4N^+ salt). ^{1}H NMR: δ 6.84 (d, 2H, J = 8.3 Hz), 6.53 (d, 2H, J = 8.3 Hz), 5.38 (ddd, 1H, J = 6.9, 10.1, 17.1 Hz), 4.83-4.70 (m, 2H), 4.17 (d, 1H, J = 10.1 Hz), 2.86-2.72 (m, 1H), 2.34-2.20 (m, 1H). ^{19}F NMR: δ -133.2, -164.0, -167.1. ^{11}B NMR: δ -4.5 ppm. The nature of the cation was confirmed by ^{119}Sn NMR spectroscopy, δ = 83.6 (*cf.* value of 83.5 for ***p*-56**).

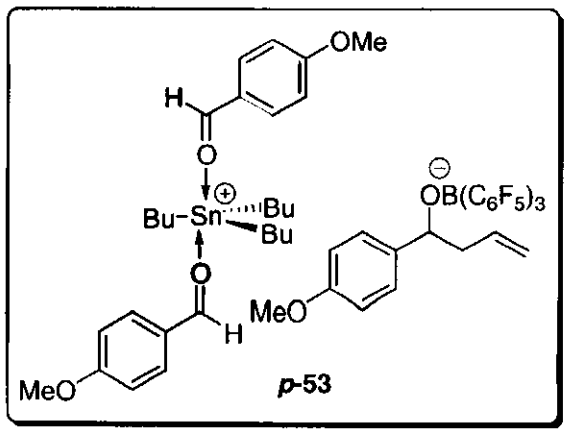

***p*-53**

Preparation of the Stannyl Ether, (*ortho*-anisyl)CH(allyl)OSnBu$_3$, *o*-59. An

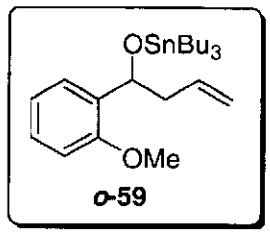

***o*-59**

NMR tube was charged with *ortho*-anisaldehyde (27 mg, 0.20 mmol), $B(C_6F_5)_3$ (approx. 2 mg) and CD_2Cl_2 (approx. 500 μL). AllylSnBu$_3$ was added at -78 °C and then the reaction mixture was warmed to room temperature for a few minutes. NMR spectra were measured at -60 °C. ^{1}H NMR: δ 7.47 (d, 1H, J = 7.6 Hz), 7.18 (app. t, 1H, J = 7.8 Hz), 6.93 (app. t, 1H, J = 7.5 Hz), 6.79 (d, 1H, J = 8.0 Hz), 6.10-5.85 (m, 1H, CH_2=C*H*), 5.10-4.90 (m, 3H, CH_2=CH and C*H*OSnBu$_3$), 3.77 (s, 3H, OC*H*$_3$), 2.45-2.30 (m, 1H, CH_aCH=CH_2), 2.25-2.10 (m, 1H, CH_bCH=CH_2), 1.45-1.28 (m, 6H), 1.25-1.12 (m, 6H), 0.91 (t, 6H, J = 8.0 Hz, C*H*$_2$SnBu$_3$), 0.81 (t, 9H, J = 7.5 Hz, butyl C*H*$_3$'s). ^{13}C NMR: δ 155.2, 137.7, 136.0, 127.3, 126.4, 120.1, 115.3, 109.2, 69.9 (*C*HOSnBu$_3$), 55.0 (O*C*H$_3$), 44.9 (*C*H$_2$CH=CH$_2$), 28.0 ($^3J_{C\text{-}Sn}$ = 10.0 Hz), 27.5 ($^2J_{C\text{-}Sn}$ = 33.0 Hz), 14.3 ($^1J_{C\text{-}Sn(119)}$ = 172.5 Hz, $^1J_{C\text{-}Sn(117)}$ = 181.7 Hz), 13.9. ^{119}Sn NMR: δ 105.3.

Preparation of the Stannyl Ether, (*para*-anisyl)CH(allyl)OSnBu$_3$, *p*-59. The *para*-

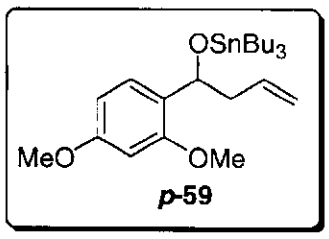

***p*-59**

anisyl derivative was prepared analogously and NMR spectra were recorded at -60 °C in CD_2Cl_2. ^{1}H NMR: δ 7.20 (d, 1H, J = 8.3 Hz), 6.80 (d, J = 8.6 Hz), 5.75 (ddd, 1H, J = 7.2, 10.5, 17.0 Hz, CH_2=C*H*), 4.96 (d, 1H, J = 17.1 Hz, C*Ha*$_2$=CH), 4.91 (d, 1H, J = 10.8 Hz, C*Hb*$_2$=CH), 4.49 (app. t, 1H, J = 6.7 Hz, C*H*OSnBu$_3$), 3.74 (s, 3H, OC*H*$_3$), 2.32 (ABm, 2H, C*H*$_2$CH=CH$_2$), 1.40-1.08 (m, 12H), 0.90-0.83 (m, 6H, C*H*$_2$SnBu$_3$), 0.80 (t, 9H, J = 7.2 Hz, butyl C*H*$_3$'s). ^{13}C NMR: δ 158.1, 139.8, 137.0, 127.2, 115.6, 112.9, 76.9 (*C*HOSnBu$_3$), 55.1 (O*C*H$_3$), 46.8 (*C*H$_2$CH=CH$_2$), 27.9 ($^3J_{C\text{-}Sn}$ =

9.2 Hz), 27.5 ($^2J_{C\text{-}Sn}$ = 33.0 Hz), 14.3 ($^1J_{C\text{-}Sn(119)}$ = 172.5 Hz, $^1J_{C\text{-}Sn(117)}$ = 180.2 Hz), 13.8. ^{119}Sn NMR: δ 104.0.

Relative Rates of Formation of Ion-Pairs *o*-53 and *p*-53. Three NMR tubes were prepared as follows: **NMR tube 1**, $B(C_6F_5)_3$ (10 mg, 0.02 mmol), *ortho*-anisaldehyde (14 mg, 0.1 mmol) and C_7D_8; **NMR tube 2**, $B(C_6F_5)_3$ (10 mg, 0.02 mmol), *para*-anisaldehyde (12 μL, 0.1 mmol) and C_7D_8; **NMR tube 3**, $B(C_6F_5)_3$ (20 mg, 0.04 mmol), *ortho*-anisaldehyde (14 mg, 0.1 mmol), *para*-anisaldehyde (12 μL, 0.1 mmol) and C_7D_8 (approx. 500 μL). $AllylSnBu_3$ (31 μL, 0.1 mmol) was added to each NMR tube at -78 °C. The NMR tubes were then placed in the NMR probe at -60 °C and ^{19}F and ^{1}H NMR spectra were measured at regular intervals to determine % conversion of ***o*-44** and/or ***p*-44** to the ion-pairs ***o*-53**, ***p*-53** and mixed cation derivatives. **Tube 1**: 15 min, -60 °C, 100% ***o*-44** to ***o*-53**; **Tube 2**: 3h, -40 °C, 60% ***p*-44** to ***p*-53**; **Tube 3**: 2h, -60 C, 100% ***o*-44**/ ***p*-44** to ***o*-53**, ***o*-53'**, ***o*–53"** and minor amounts of *para*-analogues. Significant formation of *para*-anisylCH(allyl)$OSnBu_3$ occurs under conditions for Tube 2. In Tube 3, only ^{1}H NMR signals for alkoxyborate derived from allylation of ***o*-44** are apparent. ^{119}Sn NMR at -80 °C for Tube 3 (after reaction for 2 h at -60 °C) shows three cationic species, δ 86.2, 80.9, 76.3 ppm. The first and third species were confirmed to be from ***o*-53** and ***p*-53** respectively by measuring ^{119}Sn NMR spectra of these ion-pairs at -80 °C: ***o*-53**, δ 86.2 and ***p*-53**, 76.3 pmm respectively.

Preparation of Ion-Pair *o*-62. (a) Addition of $B(C_6F_5)_3$ to Stannyl Ether *o*-59.

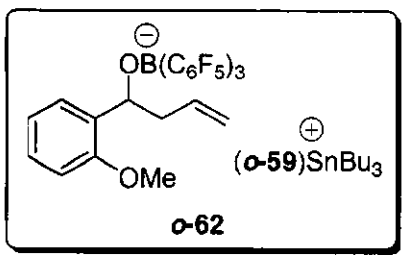

***o*-62**

$B(C_6F_5)_3$ (51 mg, 0.10 mmol) in CD_2Cl_2 was added slowly via syringe to an NMR tube (at -78 °C) containing stannyl ether, ***o*-59**, (0.20 mmol) prepared as described above. The sample was placed in the NMR probe at -60 °C and ^1H and ^{19}F NMR spectra showed that reaction occurred immediately leading to a new ion-pair with the following spectral data measured at -60 °C. ^1H NMR: (cation) δ 7.50 (t, 1H, J = 8.0 Hz), 7.07 (app. t, 1H, J = 7.3 Hz), 6.99 (d, 1H, J = 8.3 Hz), 5.77-5.64 (m, 1H), 5.30-5.20 (m, 3H), 3.88 (s, 3H), 2.82-2.52 (m, 2H), 2.65-2.50 (m, 1H), 2.37-2.22 (m, 1H), 1.50-1.10 (m, 36H, 0.86 (t, 18H, J = 7.2 Hz, CH_3); (anion) δ 7.30 (app. t, 2H, J = 7.0 Hz), 6.91 (app. t, 1H, J = 7.8 Hz), 6.72 (app. t, 1H, J = 7.3 Hz), 6.43 (d, 1H, J = 8.2 Hz), 5.59-5.45 (m, 1H), 4.87-4.68 (m, 3H), 3.52 (s, 3H). ^{19}F NMR: δ -133.2, -163.6, -166.8. ^{13}C NMR: (cation) δ 158.4, 127.7, 124.4, 121.1, 120.6, 111.4, 77.0, 55.7, 38.5, 27.6 ($^3J_{C\text{-}Sn}$ = 5.4 Hz), 27.4 ($^2J_{C\text{-}Sn}$ = 41.4 Hz), 20.1 ($^1J_{C\text{-}Sn(119)}$ = 151.8 Hz, $^1J_{C\text{-}Sn(119)}$ = 158.7 Hz, CH_2SnBu_3), 13.6 (CH_3); (anion) δ 154.9, 147.5 (d, J = 239 Hz), 137.7 (d, J = 240 Hz), 136.4, 135.1, 135.8 (d, J = 245 Hz), 127.5, 126.0-122.0 (br., *ipso* Ar_f), 125.7, 119.2, 114.8, 107.8, 67.5, 54.4, 44.7. ^{119}Sn NMR: δ 266-240 (br.), 229-211 (br.). ^{11}B NMR: δ -4.4.

(b) Addition of allyl$SnBu_3$ to *o*-53. An NMR tube was charged with $B(C_6F_5)_3$ (34 mg, 0.67 mmol) and *ortho*-anisaldehyde (27 mg, 0.20 mmol) and CD_2Cl_2 (approx. 500 μL). The sample was cooled to -78 °C and allyl$SnBu_3$ (31 μL, 0.20 mmol) was added via syringe. The NMR tube was shaken and allowed to warm to room temperature briefly.

The sample was then placed in the NMR probe cooled to -60 °C. ^{1}H, ^{13}C, ^{19}F and ^{11}B NMR analysis at -60 °C all supported the presence of the anion [(*ortho*)-anisylCH(allyl)$OB(C_6F_5)_3]^-$. ^{1}H and ^{13}C NMR spectroscopy for stannyl ether were extremely broad indicating that free and bound stannyl ether are in rapid exchange. ^{1}H NMR: (anion) δ 7.33 (d, 1H, J = 7.3 Hz), 6.93 (app. t, 1H, J = 8.2 Hz), 6.75 (app. t, 1H, J = 7.2 Hz), 6.45 (d, 1H, J = 8.0 Hz), 5.55 (ddd, 1H, J = 7.0, 10.1, 17.1 Hz, C*H*=CH_2), 4.87-4.68 (m, 3H, CH=CH_2, C*H*OB), 3.54 (s, 3H, OCH_3), 2.85-2.73 (m, 1H, C(H_a)H_bCH=CH_2), 2.40-2.26 (m, 1H, C(H_b)H_aCH=CH_2); (cation) δ 7.50-7.25 (br. s, 4H), 7.00 (br. s, 2H), 6.90 (br. s, 2H), 5.85 (br. s, 2H, C*H*=CH_2), 5.12 (br. s, 6H, CH=CH_2, C*H*OSn), 3.83 (br. s, 6H, OCH_3), 2.75-2.30 (br., 4H), 1.60 –1.10 (br., 36H), 0.86 (t, 18H, J = 6.6 Hz). ^{13}C NMR, (cation) δ 156.0, (br.), 126.9 (br.), 120.5 (br.), 110.0 (br.), 55.3 (br.), 27.8, 27.5, 20.0 (br.), 13.7 (4 C's missing); (anion) δ 154.9, 147.5 (dm, J = 240 Hz, C-F), 137.7 (dm, J = 245 Hz, C-F), 136.5, 135.9 (dm, J = 246 Hz, C-F), 135.1, 127.8, 126.0-123.5 (m, *ipso* Ar_f), 125.8, 119.2, 114.9, 107.8, 67.6, 54.4, 44.8. ^{119}Sn NMR: δ 267-244 (br.), 229-210 (br.), 105.3. ^{11}B NMR: δ -4.5.

Preparation of [(*ortho*-Anisaldehyde)$SnMe_3]^+[BF_4]^-$, 63. An NMR tube was charged with $AgBF_4$ (60 mg, 0.3 mmol), Me_3SnCl (40 mg, 0.2 mmol) and CD_2Cl_2. To this reaction mixture was added *ortho*-anisaldehyde (27 mg, 0.2 mmol) at room temperature; NMR spectra were measured at -60 °C. ^{1}H NMR: δ 10.22 (s, 1H), 7.76 (br. d, 1H, J = 7.6 Hz), 7.64 (br., 1H) 7.10-6.95 (br., 2H), 3.89 (s, 3H), 0.64 (s, 9H, $^{2}J_{H\text{-}Sn(119)}$ = 31.0 Hz, $^{2}J_{H\text{-}Sn(117)}$ = 65.9 Hz). ^{19}F NMR, δ -148.7. ^{119}Sn NMR: δ 144.3. Successive additions of *ortho*-anisaldehyde led to a gradual shift in the ^{119}Sn NMR signal from 175.4 ppm (0 eq.) to 144.3 (1 eq) to 122.0 (2 eq.) to 106 ppm (after ten equivalents of aldehyde). Yellow

crystals were grown at -30 °C from a 1:1 mixture of Me_3SnBF_4 and *ortho*-anisaldehyde in toluene. When solvent was removed and the sample was warmed, the crystals "melted" or dissolved in residual solvent. A white solid subsequently was formed from which X-ray quality crystals were obtained leading to the crystal structure of **63** (see attached compact disk for report).

Effect of [*ortho*-Anisaldehyde] on Allylstannation Reaction. A solution of *ortho*-anisaldehyde was prepared by dissolving 136 mg (1.0 mmol) in 1.0 mL of CD_2Cl_2. Three NMR tubes were prepared by addition of 100, 200 and 300 μL of this solution followed by addition of 400, 300 and 200 μL of CD_2Cl_2 respectively to each. A fourth NMR tube was prepared by dissolving *ortho*-anisaldehyde (136 mg, 1.0 mmol) in CD_2Cl_2 (500 μL). A solution of $[Bu_3Sn]^+[B(C_6F_5)_4]^-$ was prepared in C_7D_8 by adding Bu_3SnH (62 μL, 0.2 mmol) to $[Ph_3C]^+[B(C_6F_5)_4]^-$ (182 mg, 0.20 mmol) in C_7D_8. The top layer of the resulting two-phase solution was removed and the bottom layer (approx. 400 μL) was then extracted twice with C_7D_8. Equal aliquots of this solution (20 μL, approx. 0.01 mmol) were then added via syringe to the four NMR tubes prepared above. $AllylSnBu_3$ (15 μL, 0.05 mmol) was added via syringe to each NMR tube cooled to -78 °C. Upon addition, the NMR tube was shaken quickly and placed in the NMR probe at -20 °C. ^1H NMR spectra were recorded at regular intervals for each sample. The progress of each reaction was monitored by integrating the terminal vinylic CH_2 ^1H NMR signals of $allylSnBu_3$ relative to the overlapping terminal vinylic CH_2 and benzylic CH ^1H NMR signals of the stannyl ether product. The results are summarized in Scheme 4.10.

Conversion of *o*-53 to Stannyl Ether *o*-59. (a) No Excess AllylSnBu$_3$. A solution of ion pair ***o*-53** in CD_2Cl_2 was prepared as described above at -60 °C (0.067 mmol). The sample was warmed to -40 °C in the NMR probe and left at this temperature for 60 minutes. ^{1}H NMR analysis revealed that **o-53** is stable under these conditions. The sample was then warmed to -20 °C. ^{1}H NMR analysis revealed that conversion to stannyl ether, ***o*-59**, does occur at this temperature, the rate of which slows down over time (60% after 60 minutes). When the reaction is carried out with a greater excess of *ortho*-anisaldehyde (64 mg, 0.47 mmol), conversion to stannyl ether is much slower (6% after 60 minutes). **(b) Two Equivalents of AllylSnBu$_3$.** A solution of ion pair ***o*-53** was prepared in CD_2Cl_2 at -60 °C from reaction of $B(C_6F_5)_3$ (34 mg, 0.067 mmol), *ortho*-anisaldehyde (27 mg, 0.20 mmol) and allylSnBu$_3$ (62 μL, 0.20 mmol). The sample was warmed in the NMR probe from -60 °C to -40 °C and ^{1}H NMR analysis revealed that conversion of ***o*-53** to stannyl ether occurs facilely.

Allylation of *o*-40/*p*-40 Using $[Bu_4N]^+[allylB(C_6F_5)_3]^-$ Catalyzed by 1.

An NMR tube was charged with $B(C_6F_5)_3$ (45 mg, 0.09 mmol), Bu_4NBr (30 mg, 0.09 mmol) and CD_2Cl_2 (~300 μL). AllylSnBu$_3$ was added (27 μL, 0.09 mmol) and the NMR tube was shaken vigorously. A second NMR tube was charged with *ortho*-anisaldehyde (13.6 mg, 0.10 mmol) and *para*-anisaldehyde (12 μL, 0.10 mmol) and CD_2Cl_2 (~400 μL). The contents of the first NMR tube were then added via syringe to the second NMR tube containing the aldehydes. The solution was shaken and a ^{1}H NMR spectrum was obtained. No reaction had occurred. A solution of $B(C_6F_5)_3$ (2 mg) in CD_2Cl_2 (100 μL) was added to the NMR tube and NMR spectra showed that reaction did occur. After 30 minutes, all allylSnBu$_3$ was converted into alkoxy borate. Comparison to the ^{1}H NMR

spectra of the tetrabutylammonium salts, ***o*-54** and ***p*-54**, showed that allylation was selective (>20:1) for formation of alkoxyborate derived from ***o*-44**.

Preparation of Ion-Pair 65. An NMR tube was charged with $B(C_6F_5)_3$ (10 mg, 0.02 mmol), benzophenone (18 mg, 0.10 mmol), and CD_2Cl_2 (approx. 500 μL). $AllylSnBu_3$ (6 μL, 0.02 mmol) was added at room temperature and ^1H and ^{19}F NMR spectra were measured at various temperatures. Conversion from borane adduct to **65** under these conditions was controlled by a temperature dependent equilibrium (rt, 0%; -20 °C, 48%; -60 °C, 90%). The following spectral data was collected at -60 °C (using $B(C_6F_5)_3$ (30 mg, 0.06 mmol), benzophenone (54 mg, 0.30 mmol), $allylSnBu_3$ (18 μL, 0.06 mmol). ^1H NMR: (anion) δ 5.83 (m, 1H), 4.28 (dd, 1H, J = 3.0, 10.1 Hz), 4.22 (dd, 1H, J = 3.1, 17.1 Hz), 2.02 (d, 2H, J = 7.6 Hz). ^{13}C NMR: (cation) δ 198.2 (br.), 136.5, 133.6, 130.6, 128.6, 27.6 ($^3J_{C\text{-}Sn}$ = 13 Hz), 27.1 ($^2J_{C\text{-}Sn}$ = 46.0 Hz), 21.1 ($^1J_{C\text{-}Sn(119)}$ = 184 Hz, $^1J_{C\text{-}Sn(117)}$ = 192 Hz), 13.5; (anion) δ 144.5 (vinylic C), 109.2 (vinylic C), 30.2 (CH_2B). ^{119}Sn NMR: δ = 148.0. ^{11}B NMR: δ = -14.4. ^{19}F NMR: δ -132.8, -163.7, -166.7.

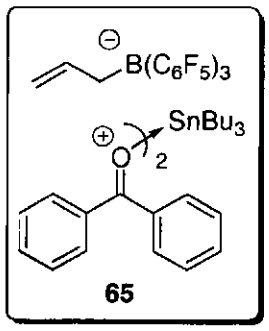

65

---

[1] *The Chemistry of the Carbon-Nitrogen Bond* Patai, S. ed.; Interscience (John Wiley & Sons): Toronto, 1970.

[2] Pangborn, A. B.; Giardello, M. A.; Grubbs, R. H.; Rosen, R. K.; Timmers, F. J. *Organometallics*, **1996**, *15*, 1518.

[3] Keck, G. E.; Andrus, M. B.; Castellino, S. *J. Am. Chem. Soc.* **1989**, *111*, 8136.

[4] Parks, D. J.; Blackwell, J. M.; Piers, W. E. *J. Org. Chem.* **2000**, *65*, 3090.

[5] Chang, S. -Y.; Jiaang, W. -T.; Cherng, C. -D.; Tang, K. -H.; Huang, C. -H.; Tsai, Y. -M. *J. Org. Chem.* **1997**, *62*, 9089.

[6] Barlow, A. P.; Boag, N. M.; Stone, F. G. A. *J. Organomet. Chem.* **1980**, *191*, 39.

[7] Lipshutz, B. H.; Chrisman, W.; Noson, K.; Papa, P.; Sclafani, J. A.; Vivian, R. W.; Keith, J. M.; *Tetrahedron* **2000**. *56*, 2779.

[8] Silverstein, R. M.; Webster, F. X. *Spectrometric Identification of Organic Compounds* 6th ed., John Wiley & Sons: Toronto, 1998, p.186.

[9] Blackwell, J. M.; Foster, K. L.; Beck, V. H.; Piers, W. E. *J. Org. Chem.* **1999**, *64*, 4887.

[10] **Table 3.1: E1-E3**, Chanrasekar, S.; Reddy, M. V.; Chandriah, L. *Synth. Comm.* **1999**, *29*, 3981; **E4-E6**, Frøyen, P.; Juvvik, P. *Tetrahedron Lett.* **1995**, *36*, 9555; **E7-E9**, Nyasse, B.; Grehn, L.; Ragnarsson, U.; Maia, H. L. S.; Monteiro, L. S.; Leito, I.; Koppel, I.; Koppel, J. *J. Chem. Soc. Perkin Trans. 1* **1995**, 2025; **E10-E11**, Mehrotra, K. N.; Giri, B. P. *Synthesis*, **1977**, 489; **E13-14**, Pak, C. S.; Kim, T. H.; Ha, S. J. *J. Org. Chem.* **1998**, *63*, 10006; **E15-E16**, Woodroofe, C. C.; Zhong, B.; Lu, X.; Silverman, R. B. *J. Chem. Soc. Perkin. Trans. 2* **2000**, 55. **Table 3.2: E1-E3**, Ranu, B. C.; Majee, A.; Sarkar, A. *J. Org. Chem.* **1998**, *63*, 370; **E4-E6**, Mehrotra, K. N.; Giri, B. P. *Synthesis*, **1977**, 489; **E7-E8**,^{1}H NMR ($CDCl_3$, 200 MHz): 7.67-7.59 (m, 2H), 7.43-7.20 (m, 3H), 3.94 (d, 1H), 3.68 (d, 1H), 2.31 (q, 1H), 0.91 (s, 9H); **E9**, Tomaszewski, M. J.; Warkentin, J.; Werstiuk, N. H. *Aust. J. Chem.* **1995**, *48*, 291. **Table 3.3: E1-E2**, Suwa, T.; Sugiyama, E.; Shibata, I.; Baba, A. *Synthesis* **2000**, 789; **E3**, Frimer, A. A.; Aljadeff, G.; Ziv, J.; *J.Org.Chem.* **1983**, *48*, 1700; **E4**, Schepartz, A.; Breslow, R *J.Am. Chem.Soc* **1987**, *109*, 1814; **E5**, Cooper, B. E.; Owen, W. J. *J. Organomet. Chem.* **1971**, *29*, 33; **E6**, Rische, T.; Eilbracht, P *Tetrahedron* **1998**, *54*, 8441.

[11] Sandström, J. *Dynamic NMR Spectroscopy* Academic Press: Toronto, 1982.

[12] All of the homoallylic alcohols have previously been made except the TBS derivatives. ***ortho*-methoxy**: see, Yasuda, M.; Fujibayashi, T.; Baba, A. *J.Org.Chem.* **1998**, *63*; 6401. ***ortho*- and *para*-methyl**: see, Yi, X. -H.; Haberman, J. X.; Li, C. -J. *Synth.Commun.* **1998**, *28*, 2999. ***ortho*-chloro and *ortho*- and *para*-fluoro**: see, Yamataka, H.; Nishikawa, K.; Hanafusa, T. *Bull.Chem.Soc. Jpn*, **1992**, *65*, 2145. ***para*-chloro**: see, Furstner, A.; Voigtlaender, D. *Synthesis* **2000**, 959. ***para*-methoxy**: see, Batey, R. A.; Thadani, A. N.; Smil, D. V.; Lough, A. J. *Synthesis* **2000**, 990.

Appendix – X-ray Structural Data

A1 X-ray Structural Data for Adduct 33 (M.Parvez).

Table A1.1 Crystal Data, Measurements and Refinement

Empirical formula	$C_{38}H_{17}BF_{15}N + 0.5\ C_7H_8$	
Formula weight	829.42	
Temperature	170(2) K	
Wavelength	0.71069 Å	
Crystal system	Triclinic	
Space group	P1 (#2)	
Unit cell dimensions	a = 12.706(5) Å	α= 113.10(4)°.
	b = 13.574(7) Å	β= 101.03(5)°.
	c = 11.860(8) Å	γ = 96.88(5)°.
Volume	1803.3(20) $Å^3$	
Z	2	
Density (calculated)	1.527 Mg/m^3	
Absorption coefficient	1.43 cm^{-1}	
F(000)	834.00	
Crystal size	0.40 x 0.34 x 0.22 mm^3	
Diffractometer	Rigaku AFC6S	
Radiation	MoKα (λ = 0.71069 Å) monochromatised with Zr- filter	
Scan Type	ω-2θ	
Scan Rate	8.0°/min (in ω) (up to 4 scans)	
Scan Width	(1.21 + 0.34 tan θ)°	
$2\theta_{max}$	50.1°	
No. of Reflections Measured	Total: 6699	
	Unique: 6387 (R_{int} = 0.047)	
Corrections	Lorentz-polarization	
	Absorption	
	(trans. factors: 0.9659 – 1.0000)	
	Decay (1.63%)	
Structure Solution	Direct Methods (SIR92)	
Refinement	Full-matrix least-squares	
Function Minimized	$\Sigma w(\|F_o\| - \|F_c\|)^2$	
p-factor	0.140	
No. Observations (I>3.00σ(I))	2201	
No. Variables	541	
Reflection/Parameter Ratio	4.07	
Residuals: R; R_w	0.040; 0.040	
Goodness of Fit Indicator	1.40	
Max. Shift/Error in Final Cycle	0.06	
Maximum peak in Final Diff. Map	0.22 $e^-/ Å^3$	
Minimum peak in Final Diff. Map	-0.18 $e^-/ Å^3$	

Table A1.2 Atomic Coordinates and B_{iso}/B_{eq} and occupancy

atom	x	y	z	B_{eq}	occ
F1	0.9591(3)	0.2963(3)	0.9188(3)	3.68(10)	
F2	1.1150(30	0.4308(3)	1.1227(3)	5.18(11)	
F3	1.1377(3)	0.4075(3)	1.3426(3)	5.95(12)	
F4	0.9979(3)	0.2453(3)	1.3519(3)	5.22(12)	
F5	0.395(3)	0.1117(3)	1.1518(3)	3.84(10)	
F6	0.8751	-0.0516(3)	0.9345(3)	3.46(10)	
F7	0.7652(3)	-0.2314(3)	0.9355(4)	4.97(12)	
F8	0.5433(3)	-0.2680(3)	0.8951(4)	4.88(12)	
F9	0.4335(3)	-0.1206(3)	0.8524(3)	3.44(9)	
F10	0.5403(3)	0.0599(3)	0.8564(3)	2.68(8)	
F11	1.0228(3)	0.1044(3)	0.8505(3)	3.95(10)	
F12	1.0654(3)	-0.0239(3)	0.6416(4)	4.74(12)	
F13	0.9019(3)	-0.1514(3)	0.4301(4)	5.53(12)	
F14	0.6888(3)	-0.1446(3)	0.4355(4)	5.41(11)	
F15	0.6420(3)	-0.0201(3)	0.6472(3)	3.11(9)	
N1	0.7172(4)	0.2099(4)	0.8887(4)	1.76(12)	
C1	0.6379(5)	0.2379(4)	0.8006(6)	2.23(15)	
C2	0.5924(5)	0.3094(5)	0.8127(5)	2.29(15)	
C3	0.6179(6)	0.4064(6)	0.8001(6)	3.75(19)	
C4	0.5424(8)	0.4724(6)	0.8051(7)	5.6(2)	
C5	0.4406(7)	0.4419(7)	0.8213(7)	5.3(2)	
C6	0.4128(6)	0.3440(7)	0.8280(6)	4.2(2)	
C7	0.4890(5)	0.2787(5)	0.8250(6)	3.09(18)	
C8	0.7003(5)	0.2045(5)	0.6750(5)	2.16(15)	
C9	0.6142(5)	0.1490(5)	0.5659(6)	2.95(17)	
C10	0.6355(6)	0.1178(6)	0.4470(6)	4.1(2)	
C11	0.7359(6)	0.1462(6)	0.4345(6)	4.3(2)	
C12	0.8198(5)	0.2062(6)	0.5411(7)	4.0(2)	
C13	0.8024(5)	0.2350(5)	0.6614(6)	3.13(18)	
C14	0.6891(4)	0.2606(4)	1.1036(5)	1.87(14)	
C15	0.7621(5)	0.3682(5)	1.1101(5)	2.04(15)	
C16	0.8097(5)	0.4488(5)	1.0805(6)	3.23(17)	
C17	0.8685(6)	0.5493(6)	1.1763(8)	4.7(2)	
C18	0.8823(6)	0.5684(6)	1.3004(8)	5.2(2)	
C19	0.8359(6)	0.4890(6)	1.3306(6)	4.8(2)	
C20	0.7768(5)	0.3896(5)	1.2355(6)	3.55(18)	
C21	0.8928(5)	0.1911(5)	1.0186(5)	2.04(15)	
C22	0.9671(5)	0.2766(5)	1.0239(6)	2.43(16)	
C23	1.0479(5)	0.3497(5)	1.1286(6)	3.23(18)	
C24	1.0587(5)	0.3370(6)	1.2384(6)	3.45(18)	
C25	0.9894(5)	0.2584(6)	1.2423(6)	3.19(18)	
C26	0.9089(5)	0.1863(5)	1.1356(6)	2.69(17)	

C27	0.7159(5)	0.0176(5)	0.9017(5)	2.13(15)	
C28	0.7646(5)	-0.0636(5)	0.9179(6)	2.61(17)	
C29	0.7105(6)	-0.1568(5)	0.9178(6)	3.33(19)	
C30	0.5986(6)	-0.1762(5)	0.8968(6)	3.15(19)	
C31	0.5450(5)	-0.1016(5)	0.8771(6)	2.49(16)	
C32	0.6033(5)	-0.0077(5)	0.8795(5)	2.12(16)	
C33	0.8293(5)	0.0563(5)	0.7603(5)	2.00(15)	
C34	0.9346(5)	0.0473(5)	0.7505(6)	2.72(17)	
C35	0.9608(6)	-0.0194(5)	0.6430(7)	3.24(19)	
C36	0.8797(6)	-0.0833(5)	0.5370(7)	3.6(2)	
C37	0.7725(6)	-0.0821(5)	0.5389(6)	3.53(18)	
C38	0.7512(5)	-0.0145(5)	0.6508(6)	2.89(18)	
C39	0.532(5)	0.561(4)	0.514(2)	11.5(13)	1/2
C40	0.5913(14)	0.4919(17)	0.4919(12)	9.5(5)	
C41	0.552(3)	0.374(2)	0.455(2)	8.8(8)	1/2
C42	0.448(2)	0.3260(14)	0.4492(13)	12.1(6)	
C43	0.368(3)	0.372(6)	0.448(4)	15.6(17)	1/2
B1	0.7917(5)	0.1196(6)	0.8914(6)	2.02(17)	

Table A1.3 Selected Interatomic Distances (Å)

F(1)—C(22)	1.362(14)	C(27)—B(1)	1.649(42)		
F(2)—C(23)	1.342(36)	C(28)—C(29)	1.365(33)		
F(3)—C(24)	1.348(66)	C(29)—C(30)	1.370(21)		
F(4)—C(25)	1.341(11)	C(30)—C(31)	1.354(29)		
F(5)—C(26)	1.358(35)	C(31)—C(32)	1.383(35)		
F(6)—C(28)	1.360(15)	C(33)—C(34)	1.381(12)		
F(7)—C(29)	1.354(28)	C(33)—C(38)	1.376(67)		
F(8)—C(30)	1.346(33)	C(33)—B(1)	1.649(40)		
F(9)—C(31)	1.362(21)	C(34)—C(35)	1.373(37)		
F(10)—C(32)	1.359(30)	C(35)—C(36)	1.352(65)		
F(11)—C(34)	1.351(63)	C(36)—C(37)	1.369(11)		
F(12)—C(35)	1.341(9)	C(37)—C(38)	1.385(37)		
F(13)—C(36)	1.350(37)	C(39)—C(39)	1.630(86)		
F(14)—C(37)	1.350(65)	C(39)—C(40)	1.252(72)		
F(15)—C(38)	1.372(9)	C(39)—C(40)	1.620(72)		
N(1)—C(1)	1.296(27)	C(39)—C(41)	1.474(80)		
N(1)—C(14)	1.502(32)	C(39)—C(42)	1.395(60)		
N(1)—B(1)	1.642(36)	C(39)—C(43)	1.352(87)		
C(1)—C(2)	1.491(35)	C(40)—C(41)	1.476(47)		
C(1)—C(8)	1.495(26)	C(40)—C(43)	1.669(87)		
C(2)—C(3)	1.39(2)	C(41)—C(42)	1.378(53)		
C(2)—C(7)	1.382(23)	C(42)—C(43)	1.256(69)		
C(3)—C(4)	1.383(34)	F(1)—C(17)	3.488(79)		
C(3)—H(1)	0.950(17)	F(2)—F(7)	3.169(70)		
C(4)—C(5)	1.382(25)	F(2)—C(3)	3.559(115)		

C(4)—H(2)	0.949(15)	F(3)—C(43) 3.125(80)
C(5)—C(6)	1.370(22)	F(3)—C(40) 3.429(123)
C(5)—H(3)	0.950(24)	F(3)—C(19) 3.496(61)
C(6)—C(7)	1.385(33)	F(4)—F(12) 3.051(40)
C(6)—H(4)	0.950(17)	F(4)—C(35) 3.194(27)
C(7)—H(5)	0.950(14)	F(4)—C(36) 3.361(67)
C(8)—C(9)	1.391(64)	F(4)—F(13) 3.413(64)
C(8)—C(13)	1.373(23)	F(5)—F(12) 3.223(61)
C(9)—C(10)	1.384(23)	F(5)—F(9) 3.477(9)
C(9)—H(6)	0.950(13)	F(5)—F(11) 3.585(71)
C(10)—C(11)	1.365(23)	F(6)—F(11) 3.015(61)
C(10)—H(7)	0.949(45)	F(6)—F(6) 3.129(108)
C(11)—C(12)	1.366(65)	F(6)—C(26) 3.528(79)
C(11)—H(8)	0.950(16)	F(6)—C(25) 3.599(101)
C(12)—C(13)	1.393(22)	F(7)—C(23) 3.073(70)
C(12)—H(9)	0.950(17)	F(7)—F(11) 3.083(142)
C(13)—H(10)	0.951(45)	F(7)—C(24) 3.395(88)
C(14)—C(15)	1.504(70)	F(7)—C(22) 3.505(38)
C(14)—H(11)	0.950(13)	F(8)—C(4) 3.254(43)
C(14)—H(12)	0.949(13)	F(8)—C(14) 3.333(48)
C(15)—C(16)	1.382(29)	F(8)—C(7) 3.478(22)
C(15)—C(20)	1.369(18)	F(9)—C(32) 3.127(71)
C(16)—C(17)	1.387(63)	F(9)—F(10) 3.159(38)
C(16)—H(13)	0.951(11)	F(9)—C(14) 3.342(67)
C(17)—C(18)	1.362(19)	F(9)—C(31) 3.367(107)
C(17)—H(14)	0.951(20)	F(9)—C(10) 3.506(43)
C(18)—C(19)	1.367(29)	F(9)—C(11) 3.524(104)
C(18)—H(15)	0.950(44)	F(10)—C(31) 3.397(55)
C(19)—C(20)	1.377(63)	F(10)—C(10) 3.538(161)
C(19)—H(16)	0.949(12)	F(12)—F(13) 2.836(33)
C(20)—H(17)	0.95(2)	F(12)—C(36) 3.136(47)
C(21)—C(22)	1.378(41)	F(12)—C(11) 3.263(75)
C(21)—C(26)	1.392(14)	F(12)—C(12) 3.288(94)
C(21)—B(1)	1.637(77)	F(13)—C(35) 3.218(71)
C(22)—C(23)	1.372(68)	F(13)—C(18) 3.454(65)
C(23)—C(24)	1.363(14)	F(14)—C(6) 3.121(131)
C(24)—C(25)	1.358(38)	F(14)—C(7) 3.145(143)
C(25)—C(26)	1.366(66)	F(15)—C(10) 3.39(9)
C(27)—C(28)	1.385(27)	F(15)—C(9) 3.473(150)
C(27)—C(32)	1.379(24)	C(4)—C(39) 3.550(61)

Table A1.4 Selected Interatomic Angles (deg)

C(1)—N(1)—C(14)	116.94(46)	F(4)—C(25)—C(24)	119.59(65)
C(1)—N(1)—B(1)	133.25(54)	F(4)—C(25)—C(26)	121.18(56)
C(14)—N(1)—B(1)	109.59(43)	C(24)—C(25)—C(26)	119.16(67)
N(1)—C(1)—C(2)	124.12(58)	F(5)—C(26)—C(21)	120.28(59)
N(1)—C(1)—C(8)	124.62(55)	F(5)—C(26)—C(25)	114.51(60)
C(2)—C(1)—C(8)	111.25(53)	C(21)—C(26)—C(25)	125.17(59)
C(1)—C(2)—C(3)	118.56(64)	C(28)—C(27)—C(32)	112.31(60)
C(1)—C(2)—C(7)	122.61(59)	C(28)—C(27)—B(1)	119.00(63)
C(3)—C(2)—C(7)	118.58(66)	C(32)—C(27)—B(1)	128.10(59)
C(2)—C(3)—C(4)	120.22(77)	F(6)—C(28)—C(27)	118.47(58)
C(2)—C(3)—H(1)	119.90(78)	F(6)—C(28)—C(29)	116.25(61)
C(4)—C(3)—H(1)	119.88(82)	C(27)—C(28)—C(29)	125.28(70)
C(3)—C(4)—C(5)	120.31(89)	F(7)—C(29)—C(28)	121.18(65)
C(3)—C(4)—H(2)	119.85(88)	F(7)—C(29)—C(30)	119.44(67)
C(5)—C(4)—H(2)	119.84(92)	C(28)—C(29)—C(30)	119.36(70)
C(4)—C(5)—C(6)	119.91(87)	F(8)—C(30)—C(29)	120.47(67)
C(4)—C(5)—H(3)	120.15(91)	F(8)—C(30)—C(31)	120.87(66)
C(6)—C(5)—H(3)	119.94(97)	C(29)—C(30)—C(31)	118.66(70)
C(5)—C(6)—C(7)	119.74(86)	F(9)—C(31)—C(30)	119.72(61)
C(5)—C(6)—H(4)	120.11(89)	F(9)—C(31)—C(32)	120.26(59)
C(7)—C(6)—H(4)	120.15(75)	C(30)—C(31)—C(32)	120.00(69)
C(2)—C(7)—C(6)	121.14(64)	F(10)—C(32)—C(27)	121.14(58)
C(2)—C(7)—H(5)	119.43(69)	F(10)—C(32)—C(31)	114.51(62)
C(6)—C(7)—H(5)	119.43(76)	C(27)—C(32)—C(31)	124.34(64)
C(1)—C(8)—C(9)	117.92(51)	C(34)—C(33)—C(38)	112.12(58)
C(1)—C(8)—C(13)	123.58(57)	C(34)—C(33)—B(1)	126.83(55)
C(9)—C(8)—C(13)	118.17(59)	C(38)—C(33)—B(1)	119.67(50)
C(8)—C(9)—C(10)	120.45(57)	F(11)—C(34)—C(33)	121.43(57)
C(8)—C(9)—H(6)	119.79(64)	F(11)—C(34)—C(35)	113.62(57)
C(10)—C(9)—H(6)	119.76(66)	C(33)—C(34)—C(35)	124.94(63)
C(9)—C(10)—C(11)	120.76(66)	F(12)—C(35)—C(34)	121.23(66)
C(9)—C(10)—H(7)	119.62(62)	F(12)—C(35)—C(36)	119.20(68)
C(11)—C(10)—H(7)	119.62(74)	C(34)—C(35)—C(36)	119.57(68)
C(10)—C(11)—C(12)	119.19(69)	F(13)—C(36)—C(35)	121.39(66)
C(10)—C(11)—H(8)	120.46(72)	F(13)—C(36)—C(37)	118.97(66)
C(12)—C(11)—H(8)	120.36(65)	C(35)—C(36)—C(37)	119.60(72)
C(11)—C(12)—C(13)	120.67(65)	F(14)—C(37)—C(36)	121.71(66)
C(11)—C(12)—H(9)	119.65(70)	F(14)—C(37)—C(38)	120.14(57)
C(13)—C(12)—H(9)	119.68(68)	C(36)—C(37)—C(38)	118.15(67)
C(8)—C(13)—C(12)	120.58(60)	F(15)—C(38)—C(33)	119.47(56)
C(8)—C(13)—H(10)	119.73(64)	F(15)—C(38)—C(37)	115.04(58)
C(12)—C(13)—H(10)	119.69(64)	C(33)—C(38)—C(37)	125.48(59)
N(1)—C(14)—C(15)	116.64(44)	C(39)^{i}—C(39)—C(40)	66.91(335)
N(1)—C(14)—H(11)	107.62(47)	C(39)^{i}—C(39)—C(40)^{i}	45.33(257)
N(1)—C(14)—H(12)	107.62(48)	C(39)^{i}—C(39)—C(41)^{i}	101.96(341)
C(15)—C(14)—H(11)	107.67(50)	C(39)^{i}—C(39)—C(42)^{i}	159.10(405)
C(15)—C(14)—H(12)	107.66(55)	C(39)^{i}—C(39)—C(43)^{i}	144.17(463)
H(11)—C(14)—H(12)	109.51(56)	C(40)—C(39)—C(40)^{i}	112.24(434)
C(14)—C(15)—C(16)	124.25(61)	C(40)—C(39)—C(41)^{i}	168.32(471)
C(14)—C(15)—C(20)	117.41(50)	C(40)—C(39)—C(42)^{i}	133.53(401)
C(16)—C(15)—C(20)	118.23(59)	C(40)—C(39)—C(43)^{i}	79.62(311)
C(15)—C(16)—C(17)	120.31(69)	C(40)^{i}—C(39)—C(41)^{i}	56.73(236)
C(15)—C(16)—H(13)	119.90(65)	C(40)^{i}—C(39)—C(42)^{i}	114.05(354)
C(17)—C(16)—H(13)	119.79(67)	C(40)^{i}—C(39)—C(43)^{i}	162.76(473)
C(16)—C(17)—C(18)	120.30(76)	C(41)^{i}—C(39)—C(42)^{i}	57.32(278)

C(16)—C(17)—H(14)	119.84(83)	$C(41)^{i}$—C(39)—$C(43)^{i}$	110.27(480)
C(18)—C(17)—H(14)	119.87(85)	$C(42)^{i}$—C(39)—$C(43)^{i}$	54.38(370)
C(17)—C(18)—C(19)	119.79(78)	C(39)—C(40)—$C(39)^{i}$	67.76(369)
C(17)—C(18)—H(15)	120.12(84)	C(39)—C(40)—C(41)	124.26(289)
C(19)—C(18)—H(15)	120.08(85)	C(39)—C(40)—$C(43)^{i}$	52.81(292)
C(18)—C(19)—C(20)	119.88(76)	$C(39)^{i}$—C(40)—C(41)	56.66(227)
C(18)—C(19)—H(16)	120.02(75)	$C(39)^{i}$—C(40)—$C(43)^{i}$	119.31(263)
C(20)—C(19)—H(16)	120.10(63)	C(41)—C(40)—$C(43)^{i}$	172.39(309)
C(15)—C(20)—C(19)	121.47(58)	$C(39)^{i}$—C(41)—C(40)	66.61(245)
C(15)—C(20)—H(17)	119.33(66)	$C(39)^{i}$—C(41)—C(42)	58.45(288)
C(19)—C(20)—H(17)	119.21(72)	C(40)—C(41)—C(42)	125.06(248)
C(22)—C(21)—C(26)	111.39(60)	$C(39)^{i}$—C(42)—C(41)	64.23(277)
C(22)—C(21)—B(1)	120.55(56)	$C(39)^{i}$—C(42)—C(43)	61.04(400)
C(26)—C(21)—B(1)	127.58(51)	C(41)—C(42)—C(43)	123.42(313)
F(1)—C(22)—C(21)	118.90(59)	$C(39)^{i}$—C(43)—$C(40)^{i}$	47.57(288)
F(1)—C(22)—C(23)	114.80(54)	$C(39)^{i}$—C(43)—C(42)	64.58(446)
C(21)—C(22)—C(23)	126.23(64)	$C(40)^{i}$—C(43)—C(42)	111.84(432)
F(2)—C(23)—C(22)	120.92(60)	N(1)—B(1)—C(21)	102.58(46)
F(2)—C(23)—C(24)	120.99(63)	N(1)—B(1)—C(27)	108.63(58)
C(22)—C(23)—C(24)	118.09(59)	N(1)—B(1)—C(33)	115.48(50)
F(3)—C(24)—C(23)	119.30(55)	C(21)—B(1)—C(27)	112.92(52)
F(3)—C(24)—C(25)	120.77(63)	C(21)—B(1)—C(33)	115.09(46)
C(23)—C(24)—C(25)	119.93(70)	C(27)—B(1)—C(33)	102.35(48)

A2 X-ray Structural Data for Adduct 34-k (Bob McDonald).

Table A2.1 Crystal Data, Measurements and Refinement

formula	$C_{36.5}H_{19}BF_{15}N$
formula weight	767.34
crystal dimensions (mm)	0.43 × 0.26 × 0.04
crystal system	monoclinic
space group	$P2_1/c$ (No. 14)
unit cell parameters:	
a (Å) 22.0355 (16)	α (deg) 90.0
b (Å) 15.8326 (11)	β (deg) 115.5817 (13)
c (Å) 20.3764 (14)	γ (deg) 90.0
V (Å^3) 6412.0 (8)	Z 8
ρ_{calcd} (g cm^{-3})	1.590
μ (mm^{-1})	0.154
Data Collection and Refinement Conditions	
diffractometer	Bruker PLATFORM/SMART 1000 CCD[b]
radiation (λ [Å])	graphite-monochromated Mo Kα (0.71073)
temperature (°C)	–80
scan type	ω scans (0.2°) (25 s exposures)
data collection 2θ limit (deg)	52.78
total data collected	32358 (-27 ≤ h ≤ 26, -19 ≤ k ≤ 19, -25 ≤ l ≤ 25)
independent reflections	12952

number of observed reflections (*NO*)	5007 [$F_o^2 \geq 2\sigma(F_o^2)$]
structure solution method	direct methods (*SHELXS–86*[c])
refinement method	full-matrix least-squares on F^2 (*SHELXL–93*[d])
absorption correction method	empirical (*SADABS*)
range of transmission factors	0.9939–0.9369
data/restraints/parameters	12952 [$F_o^2 \geq -3\sigma(F_o^2)$] / 0 / 957
goodness-of-fit (*S*)[e]	0.939 [$F_o^2 \geq -3\sigma(F_o^2)$]
final *R* indices[f]	
R_1 [$F_o^2 \geq 2\sigma(F_o^2)$]	0.0765
wR_2 [$F_o^2 \geq -3\sigma(F_o^2)$]	0.1457
largest difference peak and hole	0.262 and –0.341 e Å^{-3}

Table A2.2 Atomic Coordinates and Equivalent Isotropic Displacement Parameters

(a) Me(Ph)C=N(CH$_2$Ph)B(C$_6$F$_5$)$_3$, molecule A

Atom	*x*	*y*	*z*	U_{eq}, Å^2
F32	-0.06381(14)	0.12519(17)	0.26855(14)	0.0423(7)*
F33	-0.05733(17)	0.14780(19)	0.39959(15)	0.0603(9)*
F34	0.05241(16)	0.2206(2)	0.50649(13)	0.0673(10)*
F35	0.15508(15)	0.27465(19)	0.47628(15)	0.0611(9)*
F36	0.14948(14)	0.25700(18)	0.34603(13)	0.0471(8)*
F42	-0.08789(13)	0.26726(16)	0.19786(12)	0.0386(7)*
F43	-0.18240(13)	0.31764(17)	0.07320(14)	0.0442(8)*
F44	-0.17916(14)	0.27599(18)	-0.05521(14)	0.0505(8)*
F45	-0.07666(13)	0.17761(17)	-0.05275(12)	0.0391(7)*
F46	0.02067(12)	0.12812(15)	0.07197(12)	0.0295(6)*
F52	0.05463(15)	0.34466(16)	0.21795(15)	0.0490(8)*
F53	0.13598(16)	0.43408(19)	0.17852(17)	0.0689(10)*
F54	0.22717(16)	0.3544(2)	0.14183(16)	0.0719(11)*
F55	0.23205(15)	0.1827(2)	0.14386(15)	0.0607(9)*
F56	0.15022(12)	0.09303(17)	0.17884(13)	0.0362(7)*
N1	0.05618(17)	0.0656(2)	0.22906(18)	0.0218(9)*
C1	0.0282(2)	-0.0002(3)	0.1893(2)	0.0256(11)*
C2	0.0630(3)	-0.0851(3)	0.2039(3)	0.0431(14)*
C11	-0.0392(2)	-0.0014(3)	0.1262(2)	0.0249(11)*
C12	-0.0975(2)	0.0180(3)	0.1326(3)	0.0355(13)*
C13	-0.1589(3)	0.0109(3)	0.0735(3)	0.0485(15)*
C14	-0.1637(3)	-0.0146(3)	0.0078(3)	0.0484(15)*
C15	-0.1062(3)	-0.0359(3)	0.0006(3)	0.0386(13)*
C16	-0.0443(2)	-0.0310(3)	0.0594(2)	0.0326(12)*
C20	0.1214(2)	0.0514(3)	0.2952(2)	0.0273(11)*
C21	0.1140(2)	0.0248(3)	0.3628(2)	0.0303(12)*
C22	0.0582(3)	-0.0155(3)	0.3622(2)	0.0341(13)*
C23	0.0556(3)	-0.0378(3)	0.4270(3)	0.0443(14)*

C24	0.1100(3)	-0.0226(3)	0.4927(3)	0.0525(16)*
C25	0.1667(3)	0.0153(3)	0.4931(3)	0.0520(16)*
C26	0.1687(3)	0.0388(3)	0.4292(2)	0.0421(14)*
C31	0.0407(2)	0.1945(3)	0.2970(2)	0.0283(12)*
C32	-0.0095(3)	0.1684(3)	0.3172(2)	0.0334(13)*
C33	-0.0071(3)	0.1784(3)	0.3852(3)	0.0437(15)*
C34	0.0487(3)	0.2144(4)	0.4394(3)	0.0444(15)*
C35	0.0989(3)	0.2415(3)	0.4233(3)	0.0437(14)*
C36	0.0943(3)	0.2323(3)	0.3535(2)	0.0337(13)*
C41	-0.0284(2)	0.1909(3)	0.1432(2)	0.0238(11)*
C42	-0.0823(2)	0.2404(3)	0.1375(2)	0.0253(11)*
C43	-0.1323(2)	0.2685(3)	0.0730(3)	0.0320(12)*
C44	-0.1308(2)	0.2483(3)	0.0084(2)	0.0332(12)*
C45	-0.0793(2)	0.1989(3)	0.0098(2)	0.0253(11)*
C46	-0.0303(2)	0.1737(3)	0.0752(2)	0.0238(11)*
C51	0.0988(2)	0.2145(3)	0.2024(2)	0.0243(11)*
C52	0.0988(3)	0.3011(3)	0.2000(2)	0.0368(13)*
C53	0.1390(3)	0.3494(3)	0.1796(3)	0.0457(15)*
C54	0.1852(3)	0.3098(4)	0.1612(3)	0.0496(16)*
C55	0.1886(3)	0.2239(4)	0.1629(3)	0.0422(14)*
C56	0.1450(2)	0.1786(3)	0.1823(2)	0.0317(12)*
B1	0.0385(3)	0.1660(3)	0.2174(3)	0.0253(13)

(b) Me(Ph)C=N(CH$_2$Ph)B(C$_6$F$_5$)$_3$, molecule B

Atom	*x*	*y*	*z*	U_{eq}, Å^2
F32	-0.45704(13)	-0.14336(16)	-0.28478(13)	0.0398(7)*
F33	-0.46413(14)	-0.12584(19)	-0.41677(14)	0.0527(9)*
F34	-0.56756(15)	-0.0407(2)	-0.52169(14)	0.0608(9)*
F35	-0.66442(15)	0.0282(2)	-0.48867(15)	0.0598(9)*
F36	-0.66156(14)	0.00913(18)	-0.36044(14)	0.0488(8)*
F42	-0.42527(13)	0.00337(17)	-0.21989(13)	0.0398(7)*
F43	-0.32441(13)	0.04985(18)	-0.09769(14)	0.0462(8)*
F44	-0.32402(14)	0.0173(2)	0.03276(14)	0.0584(9)*
F45	-0.43223(14)	-0.06219(19)	0.03739(13)	0.0483(8)*
F46	-0.53521(13)	-0.10916(17)	-0.08392(13)	0.0367(7)*
F52	-0.56785(15)	0.09032(17)	-0.23293(14)	0.0471(8)*
F53	-0.65322(17)	0.1824(2)	-0.20244(16)	0.0700(10)*
F54	-0.74947(16)	0.1064(2)	-0.17253(16)	0.0772(11)*
F55	-0.75799(15)	-0.0651(2)	-0.17472(15)	0.0665(10)*
F56	-0.66846(14)	-0.15845(18)	-0.19521(14)	0.0485(8)*
N1	-0.56825(19)	-0.1905(2)	-0.2349(2)	0.0299(10)*
C1	-0.5392(3)	-0.2520(3)	-0.1890(3)	0.0349(13)*
C2	-0.5736(3)	-0.3358(3)	-0.1967(3)	0.0598(18)*
C11	-0.4711(3)	-0.2472(3)	-0.1277(3)	0.0348(13)*
C12	-0.4133(3)	-0.2335(3)	-0.1385(3)	0.0463(15)*
C13	-0.3505(3)	-0.2362(4)	-0.0804(3)	0.0608(17)*

C14	-0.3437(3)	-0.2506(4)	-0.0111(3)	0.0621(18)*
C15	-0.3995(3)	-0.2667(3)	0.0002(3)	0.0523(16)*
C16	-0.4628(3)	-0.2676(3)	-0.0573(3)	0.0445(14)*
C20	-0.6310(2)	-0.2103(3)	-0.3019(2)	0.0359(13)*
C21	-0.6175(2)	-0.2417(3)	-0.3651(2)	0.0309(12)*
C22	-0.5613(3)	-0.2868(3)	-0.3575(3)	0.0391(13)*
C23	-0.5529(3)	-0.3123(3)	-0.4176(3)	0.0431(14)*
C24	-0.6014(3)	-0.2942(4)	-0.4864(3)	0.0502(15)*
C25	-0.6581(3)	-0.2500(3)	-0.4952(3)	0.0488(15)*
C26	-0.6657(3)	-0.2234(3)	-0.4344(3)	0.0440(14)*
C31	-0.5569(2)	-0.0647(3)	-0.3119(2)	0.0302(12)*
C32	-0.5091(3)	-0.0971(3)	-0.3329(3)	0.0337(13)*
C33	-0.5112(3)	-0.0897(3)	-0.4009(3)	0.0360(13)*
C34	-0.5635(3)	-0.0457(3)	-0.4537(2)	0.0380(14)*
C35	-0.6112(3)	-0.0125(3)	-0.4368(3)	0.0405(14)*
C36	-0.6077(3)	-0.0226(3)	-0.3679(3)	0.0344(13)*
C41	-0.4858(2)	-0.0602(3)	-0.1592(2)	0.0262(11)*
C42	-0.4300(2)	-0.0174(3)	-0.1577(2)	0.0295(12)*
C43	-0.3765(2)	0.0071(3)	-0.0949(3)	0.0339(12)*
C44	-0.3761(3)	-0.0076(3)	-0.0289(3)	0.0403(14)*
C45	-0.4303(2)	-0.0469(3)	-0.0267(2)	0.0316(12)*
C46	-0.4824(2)	-0.0708(3)	-0.0905(3)	0.0296(12)*
C51	-0.6147(2)	-0.0393(3)	-0.2186(2)	0.0309(12)*
C52	-0.6143(3)	0.0478(3)	-0.2176(2)	0.0351(13)*
C53	-0.6580(3)	0.0979(4)	-0.2027(3)	0.0441(15)*
C54	-0.7068(3)	0.0592(4)	-0.1885(3)	0.0503(16)*
C55	-0.7100(3)	-0.0263(4)	-0.1884(3)	0.0426(14)*
C56	-0.6643(3)	-0.0737(3)	-0.2018(2)	0.0356(13)*
B1	-0.5537(3)	-0.0874(3)	-0.2310(3)	0.0305(14)

Anisotropically-refined atoms are marked with an asterisk (*). The form of the anisotropic displacement parameter is: $\exp[-2\pi^2(h^2a^{*2}U_{11} + k^2b^{*2}U_{22} + l^2c^{*2}U_{33} + 2klb^*c^*U_{23} + 2hla^*c^*U_{13} + 2hka^*b^*U_{12})]$.

Table A2.3 Selected Interatomic Distances (Å)

(a) $Me(Ph)C{=}N(CH_2Ph)B(C_6F_5)_3$

Molecule A			*Molecule B*		
Atom1	Atom2	Distance	Atom1	Atom2	Distance
F32	C32	1.363(5)	F32	C32	1.358(5)
F33	C33	1.351(6)	F33	C33	1.340(5)
F34	C34	1.337(5)	F34	C34	1.352(5)
F35	C35	1.348(6)	F35	C35	1.355(5)
F36	C36	1.347(5)	F36	C36	1.357(5)
F42	C42	1.356(4)	F42	C42	1.356(5)
F43	C43	1.352(5)	F43	C43	1.355(5)
F44	C44	1.347(5)	F44	C44	1.343(5)
F45	C45	1.344(4)	F45	C45	1.347(5)
F46	C46	1.360(5)	F46	C46	1.370(5)
F52	C52	1.365(5)	F52	C52	1.370(5)
F53	C53	1.342(5)	F53	C53	1.342(6)
F54	C54	1.352(5)	F54	C54	1.345(6)
F55	C55	1.347(6)	F55	C55	1.353(6)
F56	C56	1.363(5)	F56	C56	1.355(5)
N1	C1	1.300(5)	N1	C1	1.310(5)
N1	C20	1.504(5)	N1	C20	1.498(5)
N1	B1	1.630(6)	N1	B1	1.658(6)
C1	C2	1.512(6)	C1	C2	1.503(6)
C1	C11	1.486(6)	C1	C11	1.484(6)
C11	C12	1.380(6)	C11	C12	1.400(6)
C11	C16	1.397(6)	C11	C16	1.401(6)
C12	C13	1.374(6)	C12	C13	1.381(7)
C13	C14	1.358(6)	C13	C14	1.373(7)
C14	C15	1.378(7)	C14	C15	1.369(7)
C15	C16	1.374(6)	C15	C16	1.381(7)
C20	C21	1.514(6)	C20	C21	1.524(6)
C21	C22	1.380(6)	C21	C22	1.380(6)
C21	C26	1.387(6)	C21	C26	1.382(6)
C22	C23	1.393(6)	C22	C23	1.374(6)
C23	C24	1.379(7)	C23	C24	1.377(7)
C24	C25	1.382(7)	C24	C25	1.374(7)
C25	C26	1.373(6)	C25	C26	1.387(6)
C31	C32	1.398(6)	C31	C32	1.393(6)
C31	C36	1.381(6)	C31	C36	1.376(6)
C31	B1	1.664(6)	C31	B1	1.661(7)
C32	C33	1.374(6)	C32	C33	1.370(6)

Molecule A			*Molecule B*		
Atom1	Atom2	Distance	Atom1	Atom2	Distance
C33	C34	1.371(7	C33	C34	1.380(6
C34	C35	1.354(7	C34	C35	1.346(7
C35	C36	1.388(6	C35	C36	1.381(6
C41	C42	1.384(6	C41	C42	1.393(6
C41	C46	1.395(6	C41	C46	1.378(6
C41	B1	1.641(7	C41	B1	1.636(7
C42	C43	1.375(6	C42	C43	1.369(6
C43	C44	1.370(6	C43	C44	1.361(6
C44	C45	1.369(6	C44	C45	1.365(6
C45	C46	1.362(6	C45	C46	1.366(6
C51	C52	1.373(6	C51	C52	1.380(6
C51	C56	1.376(6	C51	C56	1.389(6
C51	B1	1.673(7	C51	B1	1.656(7
C52	C53	1.364(7	C52	C53	1.378(7
C53	C54	1.378(7	C53	C54	1.374(7
C54	C55	1.362(7	C54	C55	1.355(7
C55	C56	1.386(6	C55	C56	1.374(7

Table A2.4. Selected Interatomic Angles (deg)

Molecule A				*Molecule B*			
Atom1	Atom2	Atom3	Angle	Atom1	Atom2	Atom3	Angle
C1	N1	C20	116.8(4	C1	N1	C20	118.0(4
C1	N1	B1	132.2(4	C1	N1	B1	132.2(4
C20	N1	B1	110.6(3	C20	N1	B1	109.5(4
N1	C1	C2	121.7(4	N1	C1	C2	120.9(5
N1	C1	C11	125.3(4	N1	C1	C11	124.7(4
C2	C1	C11	113.0(4	C2	C1	C11	114.4(4
C1	C11	C12	122.6(4	C1	C11	C12	122.2(4
C1	C11	C16	118.5(4	C1	C11	C16	119.2(5
C12	C11	C16	118.6(4	C12	C11	C16	118.1(5
C11	C12	C13	120.3(4	C11	C12	C13	120.2(5
C12	C13	C14	121.1(5	C12	C13	C14	120.8(6
C13	C14	C15	119.5(5	C13	C14	C15	119.7(6
C14	C15	C16	120.4(5	C14	C15	C16	120.7(5
C11	C16	C15	120.0(4	C11	C16	C15	120.3(5
N1	C20	C21	114.9(4	N1	C20	C21	113.5(4
C20	C21	C22	124.4(4	C20	C21	C22	124.6(4
C20	C21	C26	116.9(4	C20	C21	C26	116.8(4
C22	C21	C26	118.6(4	C22	C21	C26	118.6(4
C21	C22	C23	120.7(5	C21	C22	C23	120.8(5
C22	C23	C24	120.1(5	C22	C23	C24	120.1(5
C23	C24	C25	119.1(5	C23	C24	C25	120.1(5
C24	C25	C26	120.7(5	C24	C25	C26	119.4(5
C21	C26	C25	120.7(5	C21	C26	C25	120.9(5
C32	C31	C36	112.6(4	C32	C31	C36	112.0(4
C32	C31	B1	120.8(4	C32	C31	B1	120.8(4
C36	C31	B1	125.8(4	C36	C31	B1	126.7(4
F32	C32	C31	119.5(4	F32	C32	C31	119.4(4

A3 X-Ray Structural Data for Adduct 34-t (Masood Parvez).

Table A3.1 Crystal Data, Measurements and Refinement

Empirical formula	$C_{33}H_{15}BF_{15}N$
Formula weight	721.27
Temperature	170(2) K
Wavelength	0.71073 Å
Crystal system	Triclinic
Space group	P -1
Unit cell dimensions	a = 9.6120(3) Å α= 79.983(2)°. b = 11.4664(4) Å β= 88.101(2)°. c = 13.4295(4) Å γ = 1.8331(11)°.
Volume	1442.73(8) $Å^3$
Z	2
Density (calculated)	1.660 Mg/m^3
Absorption coefficient	0.17 mm^{-1}
F(000)	720
Crystal size	0.25 x 0.15 x 0.08 mm^3
Theta range for data collection	2.0 to 27.5°.
Index ranges	-12<=h<=12, -14<=k<=14, -16<=l<=17
Reflections collected	11944
Independent reflections	6465 [R(int) = 0.033]
Observed data [I>2sigma(I)]	4972
Completeness to theta = 27.5°	98.6 %
Absorption correction	Multi-scan method
Max. and min. transmission	0.988 and 0.960
Refinement method	Full-matrix least-squares on F^2
Data / restraints / parameters	6465 / 0 / 451
Goodness-of-fit on F^2	1.02
Final R indices [I>2sigma(I)]	R1 = 0.046, wR2 = 0.118
R indices (all data)	R1 = 0.068, wR2 = 0.133
Weighting scheme	$w = 1/[\sigma^2(Fo^2) + (0.0750P)^2 + 0.238P]$ where $P = (Fo^2 + 2Fc^2)/3$
(Δ/θ)max	0.000
Largest diff. peak and hole	0.35 and -0.28 $e.Å^{-3}$

Table A3.2. Atomic coordinates (x 10^4) and equivalent isotropic displacement parameters ($Å^2$x 10^3) for $C_{33}H_{15}BF_{15}N$. U(eq) is defined as one third of the trace of the orthogonalized U^{ij} tensor.

Atom	x	y	z	U(eq)
B(1)	2798(2)	256(2)	7683(1)	26(1)
F(32)	3680(1)	934(1)	9540(1)	36(1)
F(33)	2140(1)	2256(1)	10726(1)	48(1)
F(34)	-542(1)	3257(1)	10204(1)	47(1)
F(35)	-1677(1)	2778(1)	8518(1)	40(1)
F(36)	-268(1)	1337(1)	7411(1)	34(1)
F(42)	2731(1)	-1158(1)	9848(1)	38(1)
F(43)	4299(1)	-3208(1)	10522(1)	50(1)
F(44)	6128(1)	-4304(1)	9274(1)	55(1)
F(45)	6455(1)	-3204(1)	7320(1)	49(1)
F(46)	5019(1)	-1056(1)	6654(1)	38(1)
F(52)	559(1)	-1109(1)	8271(1)	36(1)
F(53)	-895(1)	-2191(1)	7142(1)	43(1)
F(54)	-246(1)	-2153(1)	5149(1)	48(1)
F(55)	1739(1)	-814(1)	4273(1)	42(1)
F(56)	3124(1)	361(1)	5352(1)	35(1)
N(1)	3612(2)	1324(1)	7056(1)	25(1)
C(1)	4914(2)	1494(2)	7050(1)	27(1)
C(2)	5991(2)	781(2)	7777(1)	34(1)
C(11)	5474(2)	2450(2)	6302(1)	30(1)
C(12)	5440(2)	2397(2)	5274(1)	32(1)
C(13)	6053(2)	3219(2)	4573(2)	41(1)
C(14)	6685(2)	4093(2)	4897(2)	46(1)
C(15)	6725(2)	4149(2)	5910(2)	45(1)
C(16)	6140(2)	3323(2)	6621(2)	37(1)
C(20)	2582(2)	2275(2)	6457(1)	26(1)
C(21)	2112(2)	3348(2)	6970(1)	28(1)
C(22)	2854(2)	3674(2)	7721(1)	33(1)
C(23)	2347(2)	4684(2)	8137(1)	42(1)
C(24)	1100(3)	5370(2)	7805(2)	45(1)
C(25)	349(2)	5057(2)	7054(2)	43(1)
C(26)	854(2)	4047(2)	6635(1)	34(1)
C(31)	1777(2)	979(2)	8446(1)	26(1)
C(32)	2311(2)	1299(2)	9294(1)	28(1)
C(33)	1551(2)	2017(2)	9905(1)	33(1)
C(34)	199(2)	2511(2)	9653(1)	33(1)
C(35)	-375(2)	2260(2)	8807(1)	30(1)

C(36)	399(2)	1495(2)	8240(1)	27(1)
C(41)	3813(2)	-961(2)	8212(1)	28(1)
C(42)	3668(2)	-1595(2)	9187(1)	31(1)
C(43)	4436(2)	-2688(2)	9551(1)	36(1)
C(44)	5361(2)	-3246(2)	8930(2)	39(1)
C(45)	5536(2)	-2681(2)	7945(2)	36(1)
C(46)	4784(2)	-1576(2)	7623(1)	31(1)
C(51)	1915(2)	-304(2)	6881(1)	27(1)
C(52)	890(2)	-1002(2)	7274(1)	29(1)
C(53)	141(2)	-1597(2)	6716(1)	33(1)
C(54)	452(2)	-1562(2)	5705(1)	35(1)
C(55)	1459(2)	-890(2)	5267(1)	32(1)
C(56)	2160(2)	-284(2)	5853(1)	29(1)

Table A3.3 Bond lengths [Å] and angles [°] for $C_{33}H_{15}BF_{15}N$.

B(1)-N(1)	1.640(2)	C(1)-C(11)	1.500(2)
B(1)-C(31)	1.642(2)	C(11)-C(12)	1.393(2)
B(1)-C(41)	1.649(3)	C(11)-C(16)	1.395(3)
B(1)-C(51)	1.658(2)	C(12)-C(13)	1.391(3)
F(32)-C(32)	1.343(2)	C(13)-C(14)	1.380(3)
F(34)-C(34)	1.342(2)	C(14)-C(15)	1.376(3)
F(35)-C(35)	1.345(2)	C(15)-C(16)	1.388(3)
F(36)-C(36)	1.3545(19)	C(20)-C(21)	1.520(2)
F(42)-C(42)	1.351(2)	C(21)-C(22)	1.384(2)
F(43)-C(43)	1.347(2)	C(21)-C(26)	1.394(3)
F(44)-C(44)	1.343(2)	C(22)-C(23)	1.393(3)
F(45)-C(45)	1.348(2)	C(23)-C(24)	1.378(3)
F(46)-C(46)	1.359(2)	C(24)-C(25)	1.384(3)
F(52)-C(52)	1.354(2)	C(25)-C(26)	1.393(3)
F(53)-C(53)	1.342(2)	C(31)-C(36)	1.387(3)
F(54)-C(54)	1.344(2)	C(31)-C(32)	1.390(2)
F(55)-C(55)	1.343(2)	C(32)-C(33)	1.382(3)
F(56)-C(56)	1.356(2)	C(33)-C(34)	1.370(3)
N(1)-C(1)	1.293(2)	C(34)-C(35)	1.370(3)
N(1)-C(20)	1.502(2)	C(35)-C(36)	1.383(2)
C(1)-C(2)	1.497(2)	C(41)-C(42)	1.395(2)
C(41)-C(46)	1.398(3)	C(42)-C(43)	1.379(3)
C(43)-C(44)	1.368(3)	C(44)-C(45)	1.385(3)
C(45)-C(46)	1.373(3)	C(51)-C(56)	1.389(2)
C(51)-C(52)	1.390(2)	C(52)-C(53)	1.378(2)
C(53)-C(54)	1.375(3)	C(54)-C(55)	1.376(3)

N(1)-B(1)-C(31)	101.62(13)	C(22)-C(21)-C(26)	119.13(16)
N(1)-B(1)-C(41)	115.94(14)	C(26)-C(21)-C(20)	116.30(15)
C(31)-B(1)-C(41)	116.64(14)	C(21)-C(22)-C(23)	120.44(18)
C(41)-B(1)-C(51)	100.34(13)	C(24)-C(23)-C(22)	120.16(18)
C(1)-N(1)-C(20)	118.11(14)	C(23)-C(24)-C(25)	120.05(19)
C(1)-N(1)-B(1)	131.23(15)	C(24)-C(25)-C(26)	119.9(2)
C(20)-N(1)-B(1)	110.51(13)	C(21)-C(26)-C(25)	120.30(18)
N(1)-C(1)-C(2)	124.14(15)	N(1)-C(20)-C(21)	114.31(13)
N(1)-C(1)-C(11)	121.99(16)	C(15)-C(16)-C(11)	119.64(18)
C(2)-C(1)-C(11)	113.87(15)	C(14)-C(15)-C(16)	120.50(19)
C(16)-C(11)-C(1)	121.07(16)	C(15)-C(14)-C(13)	120.36(18)
C(13)-C(12)-C(11)	120.08(18)	C(14)-C(13)-C(12)	119.86(19)
C(36)-C(31)-C(32)	113.18(15)	C(36)-C(31)-B(1)	124.73(14)
C(32)-C(31)-B(1)	121.29(15)		

A4 X-ray Structural Data for Adduct 35-t (B. McDonald).

Table A4.1 Crystal Data, Measurements and Refinement

formula	$C_{32}H_{13}BF_{15}N$
formula weight	707.24
crystal dimensions (mm)	$0.46 \times 0.14 \times 0.18$
crystal system	monoclinic
space group	$P2_1/n$ (a nonstandard setting of $P2_1/c$ [No. 14])
unit cell parameters[a]	
a (Å)	14.144 (4)
b (Å)	13.679 (4)
c (Å)	15.863 (5)
β (deg)	115.267 (6)
V (Å^3)	2775.2 (14)
Z	4
ρ_{calcd} (g cm^{-3})	1.693
μ (mm^{-1})	0.169
Data Collection and Refinement Conditions	
diffractometer	Bruker P4/RA/SMART 1000 CCD[b]
radiation (λ [Å])	graphite-monochromated Mo Kα (0.71073)
temperature (°C)	–80
scan type	ϕ rotations (0.3°) / ω scans (0.3°) (20 s exposures)
data collection 2θ limit (deg)	53.10
total data collected	13490 ($-11 \le h \le 17$, $-17 \le k \le 12$, $-19 \le l \le$

16)

independent reflections	5714
number of observations (*NO*)	3624 [$F_o^2 \geq 2\sigma(F_o^2)$]
structure solution method	direct methods (*SHELXS–86*[c])
refinement method	full-matrix least-squares on F^2 (*SHELXL–93*[d])
absorption correction method	*SADABS*
range of transmission factors	0.9804–0.7279
data/restraints/parameters	5714 [$F_o^2 \geq -3\sigma(F_o^2)$] / 0 / 442
goodness-of-fit (*S*)[e]	0.904 [$F_o^2 \geq -3\sigma(F_o^2)$]
final *R* indices[f]	
R_1 [$F_o^2 \geq 2\sigma(F_o^2)$]	0.0371
wR_2 [$F_o^2 \geq -3\sigma(F_o^2)$]	0.0870
largest difference peak and hole	0.238 and –0.233 e Å^{-3}

Table A4.2 Atomic Coordinates and Equivalent Isotropic Displacement Parameters

Atom	*x*	*y*	*z*	U_{eq}, Å^2
F32	0.48171(8)	0.27199(8)	0.21101(7)	0.0347(3)*
F33	0.45876(10)	0.29518(9)	0.36574(8)	0.0476(3)*
F34	0.26528(10)	0.30398(9)	0.36304(8)	0.0492(3)*
F35	0.09341(9)	0.29523(9)	0.19719(9)	0.0466(3)*
F36	0.11346(8)	0.27475(8)	0.03868(8)	0.0367(3)*
F42	0.43273(8)	0.42303(7)	0.08314(8)	0.0320(3)*
F43	0.61368(9)	0.46154(8)	0.07597(8)	0.0398(3)*
F44	0.69535(9)	0.33303(9)	-0.00610(9)	0.0491(3)*
F45	0.59818(9)	0.15743(9)	-0.06815(9)	0.0466(3)*
F46	0.42630(9)	0.11215(8)	-0.05002(8)	0.0380(3)*
F52	0.19617(9)	0.44812(8)	0.01984(8)	0.0388(3)*
F53	0.10096(10)	0.56711(8)	-0.12085(9)	0.0514(4)*
F54	0.08306(10)	0.52334(10)	-0.29375(9)	0.0603(4)*
F55	0.16518(10)	0.35299(10)	-0.32171(8)	0.0521(4)*
F56	0.26589(9)	0.23228(8)	-0.18069(8)	0.0381(3)*
N	0.26400(11)	0.14255(11)	-0.00520(10)	0.0238(4)*
C1	0.19001(14)	0.11139(14)	-0.08107(13)	0.0256(4)*
C2	0.32561(14)	0.07436(13)	0.07104(13)	0.0267(4)*
C11	0.15674(14)	0.01180(13)	-0.11619(13)	0.0261(4)*
C12	0.11173(15)	0.00522(15)	-0.21325(14)	0.0315(5)*
C13	0.08071(16)	-0.08407(15)	-0.25750(15)	0.0361(5)*
C14	0.09125(16)	-0.16754(15)	-0.20585(15)	0.0366(5)*
C15	0.13220(16)	-0.16201(14)	-0.10987(15)	0.0351(5)*
C16	0.16621(15)	-0.07377(14)	-0.06460(14)	0.0323(5)*
C21	0.27903(15)	0.05859(13)	0.14071(13)	0.0270(4)*
C22	0.17229(15)	0.05653(14)	0.11583(14)	0.0310(5)*

C23	0.13500(16)	0.04449(14)	0.18268(15)	0.0360(5)*
C24	0.20292(18)	0.03468(15)	0.27516(16)	0.0402(5)*
C25	0.30927(18)	0.03599(16)	0.30082(16)	0.0425(6)*
C26	0.34675(16)	0.04717(15)	0.23398(14)	0.0347(5)*
C31	0.29791(14)	0.27836(13)	0.11453(13)	0.0242(4)*
C32	0.38190(14)	0.28288(13)	0.20137(13)	0.0264(4)*
C33	0.37285(16)	0.29209(14)	0.28394(13)	0.0300(5)*
C34	0.27591(17)	0.29619(14)	0.28329(14)	0.0330(5)*
C35	0.18920(16)	0.29183(14)	0.19938(15)	0.0312(5)*
C36	0.20192(15)	0.28268(13)	0.11885(13)	0.0274(4)*
C41	0.41989(14)	0.26549(13)	0.01743(12)	0.0247(4)*
C42	0.47293(15)	0.35315(13)	0.04714(13)	0.0262(4)*
C43	0.56516(15)	0.37600(14)	0.04239(13)	0.0289(5)*
C44	0.60749(15)	0.31071(15)	0.00246(14)	0.0321(5)*
C45	0.55795(15)	0.22281(15)	-0.02899(14)	0.0317(5)*
C46	0.46782(15)	0.20160(14)	-0.01943(13)	0.0287(5)*
C51	0.23172(14)	0.32907(13)	-0.07217(13)	0.0255(4)*
C52	0.18912(14)	0.41815(14)	-0.06352(13)	0.0279(4)*
C53	0.14041(15)	0.48268(15)	-0.13547(15)	0.0347(5)*
C54	0.13214(16)	0.46151(16)	-0.22248(15)	0.0385(5)*
C55	0.17379(16)	0.37520(16)	-0.23630(14)	0.0349(5)*
C56	0.22321(15)	0.31369(14)	-0.16196(14)	0.0289(5)*
B	0.30236(16)	0.25581(15)	0.01456(15)	0.0241(5)*

Table A4.3 Selected Interatomic Distances (Å)

Atom1	Atom2	Distance	Atom1	Atom2	Distance
F32	C32	1.362(2)	C11	C12	1.395(3)
F33	C33	1.348(2)	C11	C16	1.401(3)
F34	C34	1.340(2)	C12	C13	1.384(3)
F35	C35	1.341(2)	C13	C14	1.376(3)
F36	C36	1.355(2)	C14	C15	1.381(3)
F42	C42	1.356(2)	C15	C16	1.382(3)
F43	C43	1.346(2)	C21	C22	1.388(3)
F44	C44	1.342(2)	C21	C26	1.386(3)
F45	C45	1.346(2)	C22	C23	1.381(3)
F46	C46	1.354(2)	C23	C24	1.375(3)
F52	C52	1.347(2)	C24	C25	1.380(3)
F53	C53	1.345(2)	C25	C26	1.382(3)
F54	C54	1.344(2)	C31	C32	1.384(3)
F55	C55	1.342(2)	C31	C36	1.390(3)
F56	C56	1.358(2)	C31	B	1.643(3)
N	C1	1.285(2)	C32	C33	1.375(3)
N	C2	1.481(2)	C33	C34	1.368(3)
N	B	1.627(3)	C34	C35	1.373(3)
C1	C11	1.471(3)	C35	C36	1.370(3)
C2	C21	1.524(3)	C41	C42	1.386(3)

C41	C46	1.380(2)
C41	B	1.649(3)
C42	C43	1.374(2)
C43	C44	1.371(3)
C44	C45	1.374(3)
C45	C46	1.377(3)
C51	C52	1.392(3)
C51	C56	1.393(3)
C51	B	1.650(3)
C52	C53	1.373(3)
C53	C54	1.366(3)
C54	C55	1.378(3)
C55	C56	1.372(3)

Table A4.4 Selected Interatomic Angles (deg)

Atom1	Atom2	Atom3	Angle	Atom1	Atom2	Atom3	Angle
Cl	N	C2	121.08(16)	C46	C41	B	127.55(17)
Cl	N	B	124.59(16)	F42	C42	C41	119.31(16)
C2	N	B	114.26(14)	F42	C42	C43	116.17(16)
N	C1	C11	131.54(18)	C41	C42	C43	124.52(17)
N	C2	C21	113.29(14)	F43	C43	C42	120.76(17)
Cl	C11	C12	113.52(17)	F43	C43	C44	119.98(17)
Cl	C11	C16	128.09(18)	C42	C43	C44	119.26(18)
C12	C11	C16	118.38(18)	F44	C44	C43	120.28(18)
C11	C12	C13	120.88(19)	F44	C44	C45	120.89(17)
C12	C13	C14	120.0(2)	C43	C44	C45	118.83(17)
C13	C14	C15	119.93(19)	F45	C45	C44	119.91(17)
C14	C15	C16	120.7(2)	F45	C45	C46	120.29(18)
C11	C16	C15	120.05(19)	C44	C45	C46	119.80(17)
C2	C21	C22	123.43(17)	F46	C46	C41	120.51(16)
C2	C21	C26	118.31(17)	F46	C46	C45	115.53(16)
C22	C21	C26	118.26(18)	C41	C46	C45	123.95(18)
C21	C22	C23	120.63(19)	C52	C51	C56	112.38(17)
C22	C23	C24	120.6(2)	C52	C51	B	125.68(17)
C23	C24	C25	119.4(2)	C56	C51	B	121.20(17)
C24	C25	C26	120.1(2)	F52	C52	C51	120.63(17)
C21	C26	C25	121.0(2)	F52	C52	C53	114.89(17)
C32	C31	C36	112.99(17)	C51	C52	C53	124.45(18)
C32	C31	B	126.79(17)	F53	C53	C52	120.44(19)
C36	C31	B	119.76(17)	F53	C53	C54	119.57(19)
F32	C32	C31	121.01(17)	C52	C53	C54	119.99(19)
F32	C32	C33	114.62(17)	F54	C54	C53	120.5(2)
C31	C32	C33	124.25(18)	F54	C54	C55	120.5(2)
F33	C33	C32	120.52(18)	C53	C54	C55	118.98(19)
F33	C33	C34	119.66(18)	F55	C55	C54	119.58(19)
C32	C33	C34	119.81(18)	F55	C55	C56	121.46(19)
F34	C34	C33	120.80(19)	C54	C55	C56	118.95(19)
F34	C34	C35	120.31(18)	F56	C56	C51	119.65(17)
C33	C34	C35	118.89(18)	F56	C56	C55	115.19(17)
F35	C35	C34	119.87(18)	C51	C56	C55	125.16(19)
F35	C35	C36	120.82(18)	N	B	C31	102.57(14)
C34	C35	C36	119.30(18)	N	B	C41	109.34(14)
F36	C36	C31	118.72(17)	N	B	C51	112.60(15)
F36	C36	C35	116.51(17)	C31	B	C41	114.32(15)
C31	C36	C35	124.74(18)	C31	B	C51	115.58(15)
C42	C41	C46	113.55(17)	C41	B	C51	102.64(14)
C42	C41	B	118.15(16)				

A5 X-ray Structural Data for Zwitterion 37 (Bob McDonald).

Table A5.1 Crystal Data, Measurements and Refinement

A. Crystal Data

formula	$C_{31}H_{19}BF_{15}N$
formula weight	701.28
crystal dimensions (mm)	$0.61 \times 0.34 \times H$
crystal system	monoclinic
space group	$P2_1/n$ (an alternate setting of $P2_1/c$ [No. 14])
unit cell parameters[a]	
a (Å)	16.5297 (15)
b (Å)	9.8869 (9)
c (Å)	18.0700 (16)
β (deg)	104.1531 (17)
V (Å^3)	2863.5 (4)
Z	4
ρ_{calcd} (g cm^{-3})	1.627
μ (mm^{-1})	0.163

B. Data Collection and Refinement Conditions

diffractometer	Bruker P4/RA/SMART 1000 CCD[b]
radiation (λ [Å])	graphite-monochromated Mo Kα (0.71073)
temperature (°C)	–80
scan type	ϕ rotations (0.3°) / ω scans (0.3°) (30 s exposures)
data collection 2θ limit (deg)	52.82
total data collected	14351 ($-19 \le h \le 20$, $-12 \le k \le 9$, $-20 \le l \le 22$)
independent reflections	5877
number of observed reflections (*NO*)	4822 [$F_o^2 \ge 2\sigma(F_o^2)$]
structure solution method	direct methods (*SHELXS–86*[c])
refinement method	full-matrix least-squares on F^2 (*SHELXL–93*[d])
absorption correction method	*SADABS*
range of transmission factors	0.9482–0.9071
data/restraints/parameters	5877 [$F_o^2 \ge -3\sigma(F_o^2)$] / 0 / 433
goodness-of-fit (S)[e]	1.031 [$F_o^2 \ge -3\sigma(F_o^2)$]
final R indices[f]	
R_1 [$F_o^2 \ge 2\sigma(F_o^2)$]	0.0340
wR_2 [$F_o^2 \ge -3\sigma(F_o^2)$]	0.0908
largest difference peak and hole	0.231 and –0.211 e Å^{-3}

Table A5.2 Atomic Coordinates and Equivalent Isotropic Displacement Parameters

Atom	*x*	*y*	*z*	U_{eq}, Å^2
F22	-0.07608(5)	0.03444(9)	0.16164(5)	0.0384(2)*
F23	-0.04907(6)	0.16281(9)	0.04217(5)	0.0423(2)*
F24	0.10259(6)	0.15212(10)	0.00762(5)	0.0458(2)*
F25	0.22709(6)	0.00009(10)	0.09679(6)	0.0417(2)*
F26	0.20129(5)	-0.13766(9)	0.21433(5)	0.0339(2)*
F32	-0.00449(6)	-0.02840(10)	0.41622(5)	0.0442(2)*
F33	-0.15859(7)	-0.04145(12)	0.43252(7)	0.0627(3)*
F34	-0.28250(6)	-0.15738(13)	0.32397(8)	0.0700(4)*
F35	-0.24577(6)	-0.26870(13)	0.19802(6)	0.0573(3)*
F36	-0.09330(5)	-0.24464(9)	0.17518(5)	0.0370(2)*
F42	0.23128(5)	-0.20774(9)	0.38172(5)	0.0340(2)*
F43	0.32802(5)	-0.04139(10)	0.47623(5)	0.0419(2)*
F44	0.28580(6)	0.22442(11)	0.48515(6)	0.0524(3)*
F45	0.13674(6)	0.31535(10)	0.39619(6)	0.0478(3)*
F46	0.03347(5)	0.14686(9)	0.30473(5)	0.0357(2)*
N	-0.01314(7)	-0.47085(12)	0.29578(7)	0.0295(3)*
C1	0.03133(8)	-0.41394(14)	0.25388(8)	0.0253(3)*
C2	0.08795(8)	-0.30162(14)	0.28563(8)	0.0254(3)*
C3	0.03077(8)	-0.48091(14)	0.17741(8)	0.0276(3)*
C4	0.10484(10)	-0.58171(16)	0.19615(9)	0.0374(3)*
C5	0.04552(10)	-0.38014(16)	0.11766(9)	0.0347(3)*
C6	-0.05026(10)	-0.56026(18)	0.14460(9)	0.0383(4)*
C10	-0.00775(10)	-0.44417(16)	0.37794(8)	0.0338(3)*
C11	-0.07300(9)	-0.52263(15)	0.40586(8)	0.0311(3)*
C12	-0.14732(11)	-0.46205(19)	0.40968(11)	0.0464(4)*
C13	-0.20628(12)	-0.5314(2)	0.43795(11)	0.0530(5)*
C14	-0.19102(11)	-0.6619(2)	0.46307(10)	0.0460(4)*
C15	-0.11690(11)	-0.72376(18)	0.46025(10)	0.0445(4)*
C16	-0.05799(10)	-0.65458(16)	0.43149(9)	0.0367(3)*
C21	0.06010(8)	-0.06476(14)	0.19489(8)	0.0251(3)*
C22	0.00020(8)	0.01712(14)	0.14782(8)	0.0278(3)*
C23	0.01316(9)	0.08837(14)	0.08568(8)	0.0305(3)*
C24	0.08933(10)	0.08376(15)	0.06781(8)	0.0320(3)*
C25	0.15157(9)	0.00618(15)	0.11242(8)	0.0300(3)*
C26	0.13577(8)	-0.06492(14)	0.17298(8)	0.0267(3)*
C31	-0.03944(8)	-0.13201(14)	0.29284(8)	0.0271(3)*
C32	-0.06177(9)	-0.08317(15)	0.35738(9)	0.0329(3)*
C33	-0.14242(11)	-0.08828(17)	0.36761(10)	0.0416(4)*
C34	-0.20482(10)	-0.14740(18)	0.31329(11)	0.0441(4)*
C35	-0.18671(9)	-0.20221(17)	0.24949(10)	0.0386(4)*
C36	-0.10629(8)	-0.19129(15)	0.24053(8)	0.0304(3)*
C41	0.12346(8)	-0.04278(14)	0.33920(8)	0.0257(3)*
C42	0.20135(8)	-0.08057(14)	0.38389(8)	0.0268(3)*

C43	0.25530(8)	0.00630(16)	0.43290(8)	0.0310(3)*
C44	0.23438(9)	0.13978(16)	0.43748(9)	0.0346(3)*
C45	0.15926(9)	0.18490(15)	0.39268(9)	0.0335(3)*
C46	0.10699(8)	0.09454(15)	0.34583(8)	0.0288(3)*
B	0.05511(9)	-0.13650(16)	0.27700(9)	0.0244(3)*

Anisotropically-refined atoms are marked with an asterisk (*). The form of the anisotropic displacement parameter is: $\exp[-2\pi^2(h^2a^{*2}U_{11} + k^2b^{*2}U_{22} + l^2c^{*2}U_{33} + 2klb^*c^*U_{23} + 2hla^*c^*U_{13} + 2hka^*b^*U_{12})]$.

Table A5.3 Selected Interatomic Distances (Å)

Atom1	Atom2	Distance	Atom1	Atom2	Distance
F22	C22	1.3548(16)	C12	C13	1.387(3)
F23	C23	1.3499(16)	C13	C14	1.371(3)
F24	C24	1.3433(17)	C14	C15	1.381(3)
F25	C25	1.3469(16)	C15	C16	1.391(2)
F26	C26	1.3612(15)	C21	C22	1.3953(19)
F32	C32	1.3520(18)	C21	C26	1.4013(19)
F33	C33	1.3470(19)	C21	B	1.665(2)
F34	C34	1.3479(17)	C22	C23	1.386(2)
F35	C35	1.3440(19)	C23	C24	1.375(2)
F36	C36	1.3575(17)	C24	C25	1.375(2)
F42	C42	1.3552(17)	C25	C26	1.378(2)
F43	C43	1.3491(16)	C31	C32	1.393(2)
F44	C44	1.3440(17)	C31	C36	1.395(2)
F45	C45	1.3481(18)	C31	B	1.6569(19)
F46	C46	1.3618(16)	C32	C33	1.391(2)
N	C1	1.3048(18)	C33	C34	1.369(3)
N	C10	1.4888(18)	C34	C35	1.372(3)
C1	C2	1.4750(19)	C35	C36	1.382(2)
C1	C3	1.5302(19)	C41	C42	1.3931(19)
C2	B	1.715(2)	C41	C46	1.396(2)
C3	C4	1.551(2)	C41	B	1.667(2)
C3	C5	1.532(2)	C42	C43	1.390(2)
C3	C6	1.5404(19)	C43	C44	1.372(2)
C10	C11	1.512(2)	C44	C45	1.380(2)
C11	C12	1.384(2)	C45	C46	1.380(2)
C11	C16	1.386(2)			

Table A5.4 Selected Interatomic Angles (deg)

Atom	Atom	Atom	Angle	Atom	Atom	Atom	Angle
C1	N	C10	126.69(12)	C22	C21	B	127.45(12)
N	C1	C2	119.53(12)	C26	C21	B	119.57(12)
N	C1	C3	117.23(12)	F22	C22	C21	120.98(13)
C2	C1	C3	122.69(12)	F22	C22	C23	114.85(12)
C1	C2	B	121.64(11)	C21	C22	C23	124.16(13)
C1	C3	C4	104.53(11)	F23	C23	C22	120.15(13)
C1	C3	C5	112.84(12)	F23	C23	C24	119.50(13)
C1	C3	C6	112.38(12)	C22	C23	C24	120.35(13)
C4	C3	C5	108.58(12)	F24	C24	C23	120.90(13)
C4	C3	C6	108.82(13)	F24	C24	C25	120.57(14)
C5	C3	C6	109.46(12)	C23	C24	C25	118.53(13)
N	C10	C11	111.61(12)	F25	C25	C24	120.06(13)
C10	C11	C12	120.60(15)	F25	C25	C26	120.59(13)
C10	C11	C16	120.69(14)	C24	C25	C26	119.35(13)
C11	C12	C13	121.11(17)	F26	C26	C21	119.40(12)
C12	C13	C14	119.89(17)	F26	C26	C25	115.18(12)
C13	C14	C15	119.85(16)	C21	C26	C25	125.40(13)
C14	C15	C16	120.30(16)	C32	C31	C36	112.62(12)
C11	C16	C15	120.22(15)	C32	C31	B	127.47(12)
C22	C21	C26	112.20(13)				

A6 X-ray Structural Data for Adduct *o*-44 (M.Parvez).

Table A6.1 Crystal Data, Measurements and Refinement

Formula sum	$C_{29.50}$ H_{12} B F_{15} O_2
Formula weight	694.20
Crystal system	triclinic
Space group	*P* -1 (no. 2)
Unit cell dimensions	*a* = 11.814(2) Å *b* = 13.051(3) Å *c* = 9.819(3) Å α = 110.27(2) ° β = 107.23(2) ° γ = 80.22(2) °
Cell volume	1352.62(50) $Å^3$
Z	2
Density, calculated	1.704 g/cm^3
RAll	0.036
RObs	0.036
Pearson code	aP124
Formula type	N2O4P24Q30R59

Table A6.2 Atomic coordinates and isotropic displacement parameters (in Å ^{2})

Atom	Wyck.	Occ.	x	y	z	U
F(1)	2*i*		0.2082(2)	-0.0849(2)		0.5535(3)
F(2)	2*i*		0.3030(2)	-0.1395(2)		0.3243(3)
F(3)	2*i*		0.4161(2)	0.0091(2)	0.2833(3)	
F(4)	2*i*		0.4341(3)	0.2129(2)	0.4841(3)	
F(5)	2*i*		0.3363(2)	0.2719(2)	0.7136(3)	
F(6)	2*i*		0.0510(2)	0.1596(2)	0.4942(3)	
F(7)	2*i*		-0.1432(2)	0.2921(2)	0.4560(3)	
F(8)	2*i*		-0.2193(2)	0.4315(2)	0.6957(3)	
F(9)	2*i*		-0.0967(2)	0.4326(2)	0.9775(3)	
F(10)	2*i*		0.0968(2)	0.2967(2)	1.0194(3)	
F(11)	2*i*		-0.0360(2)	0.0598(2)	0.7485(3)	
F(12)	2*i*		-0.0692(2)	-0.1063(2)		0.8244(3)
F(13)	2*i*		0.1187(2)	-0.2229(2)	0.9540(3)	
F(14)	2*i*		0.3430(2)	-0.1717(2)	0.9987(3)	
F(15)	2*i*		0.3794(2)	-0.0104(2)	0.9129(3)	
O(1)	2*i*		0.2999(2)	0.1954(2)	0.9306(3)	
O(2)	2*i*		0.3665(2)	0.5036(2)	1.0596(3)	
C(1)	2*i*		0.3163(3)	0.2963(3)	0.9833(4)	
C(2)	2*i*		0.4092(3)	0.3385(3)	1.1123(5)	
C(3)	2*i*		0.4325(4)	0.4484(4)	1.1528(5)	
C(4)	2*i*		0.5211(4)	0.4911(4)	1.2792(5)	
C(5)	2*i*		0.5865(4)	0.4248(4)	1.3611(5)	
C(6)	2*i*		0.5649(4)	0.3155(4)	1.3219(5)	
C(7)	2*i*		0.4773(4)	0.2724(3)	1.1976(5)	
C(8)	2*i*		0.3774(4)	0.6194(4)	1.1021(6)	
C(9)	2*i*		0.2679(3)	0.0958(3)	0.6505(5)	
C(10)	2*i*		0.2648(4)	-0.0069(4)	0.5439(5)	
C(11)	2*i*		0.3123(4)	-0.0379(4)	0.4234(5)	
C(12)	2*i*		0.3686(4)	0.0365(4)	0.4007(5)	
C(13)	2*i*		0.3776(4)	0.1393(4)	0.5026(6)	
C(14)	2*i*		0.3272(4)	0.1657(4)	0.6209(5)	
C(15)	2*i*		0.0878(3)	0.2242(3)	0.7602(5)	
C(16)	2*i*		0.0198(4)	0.2272(3)	0.6192(5)	
C(17)	2*i*		-0.0816(4)	0.2954(4)	0.5971(5)	
C(18)	2*i*		-0.1206(4)	0.3640(4)	0.7165(5)	
C(19)	2*i*		-0.0580(4)	0.3642(3)	0.8581(5)	
C(20)	2*i*		0.0414(4)	0.2948(3)	0.8753(5)	
C(21)	2*i*		0.1744(4)	0.0371(3)	0.8327(4)	
C(22)	2*i*		0.0628(4)	0.0060(3)	0.8122(5)	
C(23)	2*i*		0.0427(4)	-0.0804(4)	0.8499(5)	
C(24)	2*i*		0.1359(5)	-0.1393(4)	0.9143(5)	
C(25)	2*i*		0.2488(4)	-0.1127(4)	0.9371(5)	
C(26)	2*i*		0.2658(4)	-0.0279(3)	0.8953(5)	

C(27)	2*i*	0.5	0.173(1)	0.363(1)	0.429(2)	
C(28)	2*i*		0.090(1)	0.4272(7)	0.459(2)	
C(29)	2*i*		-0.012(2)	0.445(1)	0.353(1)	
C(30)	2*i*		-0.104(1)	0.514(1)	0.384(2)	
B(1)	2*i*		0.2015(4)	0.1368(4)	0.7859(5)	
H(1)	2*i*		0.26500	0.34520	0.93550	0.0340
H(2)	2*i*		0.53670	0.56590	1.30940	0.0540
H(3)	2*i*		0.64850	0.45430	1.44710	0.0700
H(4)	2*i*		0.61080	0.27150	1.38110	0.0640
H(5)	2*i*		0.46240	0.19760	1.16880	0.0470
H(6)	2*i*		0.45730	0.63180	1.11430	0.0740
H(7)	2*i*		0.32630	0.64740	1.02620	0.0740
H(8)	2*i*		0.35600	0.65530	1.19420	0.0740
H(9)	2*i*	0.5	0.14760	0.29040	0.38260	0.1280
H(10)	2*i*	0.5	0.20360	0.38090	0.36070	0.1280
H(11)	2*i*	0.5	0.23400	0.36580	0.51780	0.1280
H(12)	2*i*		-0.01700	0.40540	0.25000	0.1650
H(13)	2*i*		-0.17400	0.52370	0.30990	0.1790
H(14)	2*i*	0.5	-0.15330	0.62620	0.57460	0.1470

A7 X-ray Structural Data for Adduct *p*-44 (M.Parvez).

Table A7.1 Crystal Data, Measurements and Refinement

Empirical formula	$C_{26}H_8BF_{15}O_2 \bullet 0.5\ C_7H_8$	
Formula weight	694.20	
Temperature	173(2) K	
Wavelength	0.71069 Å	
Crystal system	Monoclinic	
Space group	C2/c	
Unit cell dimensions	a = 31.9967(5) Å	α= 90°.
	b = 12.1517(2) Å	β= 108.8000(10)°.
	c = 14.5995(2) Å	γ = 90°.
Volume	5373.65(14) $Å^3$	
Z	8	
Density (calculated)	1.716 Mg/m^3	
Absorption coefficient	0.18 mm^{-1}	
F(000)	2760	
Crystal size	0.31 x 0.26 x 0.19 mm^3	
Theta range for data collection	2.0 to 30.0°.	
Index ranges	-44<=h<=45, -16<=k<=17, -20<=l<=20	
Reflections collected	14239	
Independent reflections	7790 [R(int) = 0.018]	
Observed data [I>2sigma(I)]	5708	
Completeness to theta = 30.0°	99.0 %	

Absorption correction	Multi-scan method
Max. and min. transmission	0.967 and 0.947
Refinement method	Full-matrix least-squares on F^2
Data / restraints / parameters	7790 / 0 / 450
Goodness-of-fit on F^2	1.02
Final R indices [I>2sigma(I)]	R1 = 0.042, wR2 = 0.107
R indices (all data)	R1 = 0.064, wR2 = 0.121
Weighting scheme	$w = 1/[\sigma^2(Fo^2) + (0.0558P)^2 + 2.99P]$ where $P = (Fo^2 + 2Fc^2)/3$
(Δ/θ)max	0.001
Largest diff. peak and hole	0.27 and -0.32 e.Å^{-3}

Table A7.2 Atomic coordinates (x 10^4) and equivalent isotropic displacement parameters (Å^{2}x 10^3) for $C_{26}H_8BF_{15}O_2 \bullet 0.5\ C_7H_8$. U(eq) is defined as one third of the trace of the orthogonalized U^{ij} tensor.

Atom	x	y	z	U(eq)
F(1)	4165(1)	1623(1)	1565(1)	53(1)
F(2)	4908(1)	1224(1)	1204(1)	71(1)
F(3)	5139(1)	-856(1)	895(1)	69(1)
F(4)	4598(1)	-2558(1)	951(1)	64(1)
F(5)	3836(1)	-2185(1)	1287(1)	52(1)
F(6)	4025(1)	830(1)	3488(1)	44(1)
F(7)	3941(1)	2812(1)	4199(1)	57(1)
F(8)	3329(1)	4269(1)	3128(1)	57(1)
F(9)	2761(1)	3627(1)	1382(1)	51(1)
F(10)	2828(1)	1663(1)	671(1)	41(1)
F(11)	3412(1)	-158(1)	-439(1)	52(1)
F(12)	2723(1)	-872(1)	-1883(1)	58(1)
F(13)	1982(1)	-1593(1)	-1557(1)	48(1)
F(14)	1947(1)	-1600(1)	281(1)	44(1)
F(15)	2618(1)	-866(1)	1740(1)	47(1)
O(1)	3471(1)	-909(1)	2486(1)	35(1)
O(2)	3502(1)	-4502(1)	5601(1)	45(1)
C(1)	3782(1)	-1409(1)	3088(1)	36(1)
C(2)	3711(1)	-2191(1)	3739(1)	34(1)
C(3)	4073(1)	-2742(1)	4370(1)	42(1)
C(4)	4019(1)	-3533(1)	4999(1)	42(1)
C(5)	3595(1)	-3769(1)	5007(1)	35(1)
C(6)	3228(1)	-3224(1)	4377(1)	41(1)
C(7)	3284(1)	-2446(1)	3753(1)	39(1)
C(8)	3859(1)	-5102(2)	6255(2)	62(1)
C(9)	3959(1)	-268(1)	1458(1)	33(1)

C(10)	4250(1)	565(1)	1421(1)	38(1)
C(11)	4642(1)	384(2)	1229(1)	47(1)
C(12)	4758(1)	-668(2)	1073(1)	49(1)
C(13)	4483(1)	-1528(1)	1095(1)	44(1)
C(14)	4094(1)	-1311(1)	1281(1)	38(1)
C(15)	3424(1)	1123(1)	2055(1)	31(1)
C(16)	3695(1)	1493(1)	2949(1)	35(1)
C(17)	3664(1)	2514(1)	3324(1)	41(1)
C(18)	3353(1)	3251(1)	2792(1)	42(1)
C(19)	3072(1)	2933(1)	1906(1)	38(1)
C(20)	3113(1)	1894(1)	1556(1)	33(1)
C(21)	3064(1)	-511(1)	746(1)	31(1)
C(22)	3058(1)	-522(1)	-211(1)	34(1)
C(23)	2705(1)	-876(1)	-982(1)	37(1)
C(24)	2327(1)	-1237(1)	-820(1)	35(1)
C(25)	2311(1)	-1234(1)	111(1)	33(1)
C(26)	2670(1)	-869(1)	860(1)	32(1)
B(1)	3485(1)	-98(1)	1655(1)	31(1)
C(27)	50(1)	556(3)	7219(2)	68(1)
C(28)	-24(1)	-465(2)	7568(3)	92(2)
C(29)	-213(2)	-530(3)	8300(4)	97(2)
C(30)	-328(1)	427(4)	8683(3)	91(3)
C(31)	-254(1)	1448(3)	8334(3)	78(2)
C(32)	-65(1)	1512(2)	7602(3)	70(2)
C(33)	260(3)	734(9)	6475(6)	118(4)

Table A7.3 Bond lengths [Å] and angles [°] for $C_{26}H_8BF_{15}O_2 \bullet 0.5\ C_7H_8$.

F(1)-C(10)	1.3447(18)	C(11)-C(12)	1.370(3)
F(2)-C(11)	1.338(2)	C(12)-C(13)	1.373(3)
F(3)-C(12)	1.3468(17)	C(13)-C(14)	1.382(2)
F(4)-C(13)	1.3401(18)	C(15)-C(16)	1.3886(19)
F(5)-C(14)	1.3466(18)	C(15)-C(20)	1.3898(18)
F(6)-C(16)	1.3581(16)	C(15)-B(1)	1.630(2)
F(7)-C(17)	1.3488(17)	C(16)-C(17)	1.373(2)
F(8)-C(18)	1.3409(18)	C(17)-C(18)	1.379(2)
F(9)-C(19)	1.3404(17)	C(18)-C(19)	1.371(2)
F(10)-C(20)	1.3493(16)	C(19)-C(20)	1.384(2)
F(11)-C(22)	1.3520(15)	C(21)-C(22)	1.3903(19)
F(12)-C(23)	1.3357(16)	C(21)-C(26)	1.3942(18)
F(13)-C(24)	1.3415(16)	C(21)-B(1)	1.636(2)
F(14)-C(25)	1.3410(15)	C(22)-C(23)	1.383(2)
F(15)-C(26)	1.3493(15)	C(23)-C(24)	1.374(2)
O(1)-C(1)	1.2523(16)	C(24)-C(25)	1.377(2)

O(1)-B(1)	1.5743(17)	C(27)-C(27)#1	0.972(5)
O(2)-C(5)	1.3420(17)	C(27)-C(32)#1	1.1885(18)
O(2)-C(8)	1.430(2)	C(27)-C(28)#1	1.288(2)
C(1)-C(2)	1.413(2)	C(27)-C(28)	1.3900
C(2)-C(3)	1.3971(19)	C(27)-C(32)	1.3900
C(2)-C(7)	1.4083(19)	C(27)-C(33)	1.465(9)
C(3)-C(4)	1.378(2)	C(27)-C(31)#1	1.611(5)
C(4)-C(5)	1.393(2)	C(27)-C(29)#1	1.686(5)
C(5)-C(6)	1.402(2)	C(27)-C(30)#1	1.819(5)
C(6)-C(7)	1.365(2)	C(28)-C(29)	1.3900
C(9)-C(10)	1.388(2)	C(29)-C(30)	1.3900
C(9)-C(14)	1.390(2)	C(30)-C(31)	1.3900
C(9)-B(1)	1.6443(19)	C(31)-C(32)	1.3900
C(10)-C(11)	1.389(2)		

C(1)-O(1)-B(1)	129.04(11)	C(16)-C(17)-C(18)	119.67(14)
C(5)-O(2)-C(8)	118.35(12)	F(8)-C(18)-C(19)	120.51(14)
O(1)-C(1)-C(2)	122.38(12)	F(8)-C(18)-C(17)	120.61(15)
C(3)-C(2)-C(7)	119.20(13)	C(19)-C(18)-C(17)	118.87(14)
C(3)-C(2)-C(1)	119.18(12)	F(9)-C(19)-C(18)	120.06(13)
C(7)-C(2)-C(1)	121.60(12)	F(9)-C(19)-C(20)	120.30(14)
C(4)-C(3)-C(2)	121.22(13)	C(18)-C(19)-C(20)	119.64(13)
C(3)-C(4)-C(5)	118.74(13)	F(10)-C(20)-C(19)	115.36(12)
O(2)-C(5)-C(4)	124.16(13)	F(10)-C(20)-C(15)	120.70(12)
O(2)-C(5)-C(6)	115.13(12)	C(19)-C(20)-C(15)	123.93(13)
C(4)-C(5)-C(6)	120.71(13)	C(22)-C(21)-C(26)	113.42(12)
C(7)-C(6)-C(5)	120.16(13)	C(22)-C(21)-B(1)	123.99(11)
C(6)-C(7)-C(2)	119.96(13)	C(26)-C(21)-B(1)	122.58(11)
C(10)-C(9)-C(14)	113.94(12)	F(11)-C(22)-C(23)	115.56(12)
C(10)-C(9)-B(1)	125.65(12)	F(11)-C(22)-C(21)	120.17(12)
C(14)-C(9)-B(1)	120.39(12)	C(23)-C(22)-C(21)	124.26(12)
F(1)-C(10)-C(9)	121.31(12)	F(12)-C(23)-C(24)	119.36(13)
F(1)-C(10)-C(11)	115.13(14)	F(12)-C(23)-C(22)	121.12(13)
C(9)-C(10)-C(11)	123.55(14)	C(24)-C(23)-C(22)	119.52(13)
F(2)-C(11)-C(12)	119.94(14)	F(13)-C(24)-C(23)	120.38(13)
F(2)-C(11)-C(10)	120.56(16)	F(13)-C(24)-C(25)	120.59(13)
C(12)-C(11)-C(10)	119.50(15)	C(23)-C(24)-C(25)	119.02(13)
F(3)-C(12)-C(11)	120.08(16)	F(14)-C(25)-C(24)	119.57(12)
F(3)-C(12)-C(13)	120.15(16)	F(14)-C(25)-C(26)	120.75(12)
C(11)-C(12)-C(13)	119.77(13)	C(24)-C(25)-C(26)	119.67(12)
F(4)-C(13)-C(12)	119.84(14)	F(15)-C(26)-C(25)	115.34(11)
F(4)-C(13)-C(14)	121.22(16)	F(15)-C(26)-C(21)	120.58(12)
C(12)-C(13)-C(14)	118.93(15)	C(25)-C(26)-C(21)	124.08(12)
F(5)-C(14)-C(13)	116.34(14)	O(1)-B(1)-C(15)	104.90(10)

F(5)-C(14)-C(9)	119.35(12)	O(1)-B(1)-C(21)	102.25(10)
C(13)-C(14)-C(9)	124.30(15)	C(15)-B(1)-C(21)	114.04(11)
C(16)-C(15)-C(20)	113.59(13)	O(1)-B(1)-C(9)	108.32(10)
C(16)-C(15)-B(1)	121.31(12)	C(15)-B(1)-C(9)	113.63(11)
C(20)-C(15)-B(1)	125.09(12)	C(21)-B(1)-C(9)	112.57(11)
F(6)-C(16)-C(17)	116.51(13)	C(27)#1-C(27)-C(32)#1	79.4(3)
F(6)-C(16)-C(15)	119.16(13)	C(27)#1-C(27)-C(28)#1	74.4(3)
C(17)-C(16)-C(15)	124.29(13)	C(32)#1-C(27)-C(28)#1	152.9(5)
F(7)-C(17)-C(16)	120.75(14)	C(27)#1-C(27)-C(28)	63.21(14)
F(7)-C(17)-C(18)	119.57(14)		

Symmetry transformations used to generate equivalent atoms:
#1 -x,y,-z+3/2

A8 X-ray Structural Data for Adduct 45 (Bob McDonald).

Table A8.1 Crystal Data, Measurements and Refinement

A. Crystal Data	
formula	$C_{32}H_{13}BF_{16}O$
formula weight	728.23
crystal dimensions (mm)	0.23 × 0.15 × 0.04
crystal system	triclinic
space group	$P\bar{1}$ (No. 2)
unit cell parameters[a]	
a (Å)	9.4511 (9)
b (Å)	12.3822 (12)
c (Å)	12.6845 (11)
α (deg)	93.1029 (18)
β (deg)	93.2127 (18)
γ (deg)	97.2902 (16)
V (Å^3)	1467.3 (2)
Z	2
ρ_{calcd} (g cm^{-3})	1.648
μ (mm^{-1})	0.169
B. Data Collection and Refinement Conditions	
diffractometer	Bruker P4/RA/SMART 1000 CCD[b]
radiation (λ [Å])	graphite-monochromated Mo Kα (0.71073)
temperature (°C)	–80
scan type	ϕ rotations (0.3°) / ω scans (0.3°) (30 s exposures)
data collection 2θ limit (deg)	52.90
total data collected	7336 (-11 ≤ h ≤ 11, -15 ≤ k ≤ 15, -5 ≤ l ≤ 15)
independent reflections	5956
number of observations (NO)	2675 [$F_o^2 \geq 2\sigma(F_o^2)$]

structure solution method	direct methods (*SHELXS–86*[c])
refinement method	full-matrix least-squares on F^2 (*SHELXL–93*[d])
absorption correction method	Gaussian integration (face-indexed)
range of transmission factors	0.9898–0.9688
data/restraints/parameters	5956 [$F_o^2 \geq -3\sigma(F_o^2)$] / 0 / 462
goodness-of-fit (S)[i]	0.833 [$F_o^2 \geq -3\sigma(F_o^2)$]
final R indices[j]	
R_1 [$F_o^2 \geq 2\sigma(F_o^2)$]	0.0527
wR_2 [$F_o^2 \geq -3\sigma(F_o^2)$]	0.1210
largest difference peak and hole	0.250 and –0.309 e Å^{-3}

Table A8.2 Atomic Coordinates and Equivalent Isotropic Displacement Parameters

Atom	x	y	z	U_{eq}, Å^2
F1	-0.0615(2)	0.50268(18)	-0.36042(15)	0.0613(7)*
F12	0.0960(2)	0.14007(16)	0.07741(14)	0.0466(6)*
F13	0.0880(2)	0.14651(16)	0.28561(14)	0.0488(6)*
F14	-0.1165(2)	0.24512(18)	0.38320(13)	0.0603(7)*
F15	-0.3131(2)	0.33590(17)	0.26437(14)	0.0558(6)*
F16	-0.3132(2)	0.32535(17)	0.05567(13)	0.0472(6)*
F22	-0.2633(2)	0.03482(16)	0.02671(14)	0.0496(6)*
F23	-0.4508(2)	-0.11810(17)	-0.07258(19)	0.0677(7)*
F24	-0.5135(2)	-0.11751(18)	-0.28403(19)	0.0687(7)*
F25	-0.3746(3)	0.04063(18)	-0.39611(15)	0.0684(7)*
F26	-0.1807(2)	0.19448(17)	-0.29864(14)	0.0512(6)*
F32	0.11311(19)	0.41443(15)	-0.04031(14)	0.0423(5)*
F33	0.3892(2)	0.42712(18)	-0.08026(15)	0.0542(6)*
F34	0.4938(2)	0.25243(18)	-0.17219(15)	0.0541(6)*
F35	0.3132(2)	0.06579(16)	-0.22733(15)	0.0513(6)*
F36	0.0393(2)	0.05190(16)	-0.18895(15)	0.0471(5)*
O	-0.1673(2)	0.33067(17)	-0.11190(15)	0.0297(5)*
C1	-0.2024(3)	0.4764(3)	-0.2149(2)	0.0272(8)*
C2	-0.1672(4)	0.5333(3)	-0.3035(2)	0.0364(9)*
C3	-0.2361(4)	0.6181(3)	-0.3357(3)	0.0406(9)*
C4	-0.3431(4)	0.6494(3)	-0.2756(3)	0.0433(10)*
C5	-0.3816(4)	0.5951(3)	-0.1862(2)	0.0374(9)*
C6	-0.3133(3)	0.5093(3)	-0.1564(2)	0.0321(8)*
C7	-0.1286(3)	0.3875(3)	-0.1859(2)	0.0287(8)*
C11	-0.1040(3)	0.2363(3)	0.0539(2)	0.0281(8)*
C12	-0.0067(4)	0.1923(3)	0.1196(2)	0.0325(8)*
C13	-0.0091(4)	0.1935(3)	0.2281(2)	0.0351(9)*

C14	-0.1130(4)	0.2417(3)	0.2766(2)	0.0400(9)*
C15	-0.2104(4)	0.2874(3)	0.2170(3)	0.0369(9)*
C16	-0.2063(4)	0.2836(3)	0.1084(2)	0.0328(8)*
C21	-0.2141(3)	0.1258(3)	-0.1296(2)	0.0286(8)*
C22	-0.2881(4)	0.0422(3)	-0.0786(3)	0.0357(9)*
C23	-0.3852(4)	-0.0386(3)	-0.1287(3)	0.0427(9)*
C24	-0.4161(4)	-0.0392(3)	-0.2346(3)	0.0472(10)*
C25	-0.3467(4)	0.0407(3)	-0.2902(3)	0.0454(10)*
C26	-0.2491(4)	0.1187(3)	-0.2382(3)	0.0358(9)*
C31	0.0618(3)	0.2327(3)	-0.1117(2)	0.0279(8)*
C32	0.1591(4)	0.3251(3)	-0.0867(2)	0.0306(8)*
C33	0.3012(4)	0.3337(3)	-0.1066(2)	0.0375(9)*
C34	0.3544(4)	0.2462(3)	-0.1532(3)	0.0372(9)*
C35	0.2634(4)	0.1525(3)	-0.1809(2)	0.0361(9)*
C36	0.1209(4)	0.1474(3)	-0.1602(2)	0.0326(8)*
B	-0.1006(4)	0.2251(3)	-0.0749(3)	0.0294(9)*

Anisotropically-refined atoms are marked with an asterisk (*). The form of the anisotropic displacement parameter is: $\exp[-2\pi^2(h^2a^{*2}U_{11} + k^2b^{*2}U_{22} + l^2c^{*2}U_{33} + 2klb^*c^*U_{23} + 2hla^*c^*U_{13} + 2hka^*b^*U_{12})]$. [a]The toluene methyl carbon was found to be distributed over two equally-abundant positions (C10S and C17S); each was refined with an occupancy factor of 0.5.

Table A8.3 Selected Interatomic Distances (Å)

Atom1	Atom2	Distance	Atom1	Atom2	Distance
F1	C2	1.346(4)	C2	C3	1.372(4)
F12	C12	1.352(3)	C3	C4	1.381(5)
F13	C13	1.349(4)	C4	C5	1.392(4)
F14	C14	1.353(3)	C5	C6	1.371(4)
F15	C15	1.356(3)	C11	C12	1.388(4)
F16	C16	1.353(3)	C11	C16	1.390(4)
F22	C22	1.353(4)	C11	B	1.635(5)
F23	C23	1.353(4)	C12	C13	1.377(4)
F24	C24	1.350(4)	C13	C14	1.369(5)
F25	C25	1.354(4)	C14	C15	1.357(5)
F26	C26	1.365(4)	C15	C16	1.378(4)
F32	C32	1.356(3)	C21	C22	1.386(4)
F33	C33	1.351(4)	C21	C26	1.394(4)
F34	C34	1.346(4)	C21	B	1.622(5)
F35	C35	1.346(4)	C22	C23	1.371(5)
F36	C36	1.347(4)	C23	C24	1.358(5)
O	C7	1.247(3)	C24	C25	1.368(5)
O	B	1.603(4)	C25	C26	1.362(5)
C1	C2	1.392(4)	C31	C32	1.385(4)
C1	C6	1.406(4)	C31	C36	1.387(4)
C1	C7	1.430(4)	C31	B	1.623(5)

Table A8.4 Selected Interatomic Angles (deg)

Atom1	Atom2	Atom3	Angle	Atom1	Atom2	Atom3	Angle
C7	O	B	126.4(3	F23	C23	C22	120.0(3
C2	C1	C6	117.4(3	F23	C23	C24	119.8(4
C2	C1	C7	120.7(3	C22	C23	C24	120.3(4
C6	C1	C7	121.8(3	F24	C24	C23	120.5(4
F1	C2	C1	118.2(3	F24	C24	C25	120.7(4
F1	C2	C3	118.8(3	C23	C24	C25	118.8(4
C1	C2	C3	123.0(3	F25	C25	C24	119.7(4
C2	C3	C4	118.1(3	F25	C25	C26	120.9(4
C3	C4	C5	120.9(3	C24	C25	C26	119.4(3
C4	C5	C6	120.2(3	F26	C26	C21	118.5(3
C1	C6	C5	120.4(3	F26	C26	C25	116.5(3
O	C7	C1	120.9(3	C21	C26	C25	125.0(3
C12	C11	C16	113.3(3	C32	C31	C36	113.7(3
C12	C11	B	121.9(3	C32	C31	B	121.1(3
C16	C11	B	124.7(3	C36	C31	B	124.9(3
F12	C12	C11	119.9(3	F32	C32	C31	118.9(3
F12	C12	C13	115.4(3	F32	C32	C33	116.7(3
C11	C12	C13	124.6(3	C31	C32	C33	124.3(3
F13	C13	C12	120.5(3	F33	C33	C32	120.8(3
F13	C13	C14	120.5(3	F33	C33	C34	119.7(3
C12	C13	C14	119.0(3	C32	C33	C34	119.5(4
F14	C14	C13	120.1(3	F34	C34	C33	120.5(3
F14	C14	C15	120.5(3	F34	C34	C35	120.4(3
C13	C14	C15	119.4(3	C33	C34	C35	119.1(3
F15	C15	C14	119.8(3	F35	C35	C34	120.1(3
F15	C15	C16	119.9(3	F35	C35	C36	120.3(3
C14	C15	C16	120.3(3	C34	C35	C36	119.7(3
F16	C16	C11	120.7(3	F36	C36	C31	120.5(3
F16	C16	C15	115.7(3	F36	C36	C35	115.8(3
C11	C16	C15	123.5(3	C31	C36	C35	123.7(3
C22	C21	C26	112.4(3	O	B	C11	103.3(2
C22	C21	B	126.6(3	O	B	C21	102.4(2
C26	C21	B	121.0(3	O	B	C31	108.2(3
F22	C22	C21	120.1(3	C11	B	C21	113.2(3
F22	C22	C23	115.8(3	C11	B	C31	111.5(3
C21	C22	C23	124.1(3	C21	B	C31	116.7(3

A9 X-ray Structural Data for Ion-Pair 63 (Bob McDonald).

Table A9.1 Crystal Data, Measurements and Refinement

A *Crystal Data*	
formula	$C_{11}H_{17}BF_4O_2Sn$
formula weight	386.75
crystal dimensions (mm)	0.34 × 0.12 × 0.04
crystal system	monoclinic
space group	*C*2/*c* (No. 15)
unit cell parameters[a]	
a (Å)	32.3199 (19)
b (Å)	7.3722 (4)
c (Å)	28.0359 (17)
β (deg)	113.5282 (11)
V (Å^3)	6124.7 (6)
Z	16
ρ_{calcd} (g cm^{-3})	1.678
μ (mm^{-1})	1.704
B. Data Collection and Refinement Conditions	
diffractometer	Bruker PLATFORM/SMART 1000 CCD[b]
radiation (λ [Å])	graphite-monochromated Mo Kα (0.71073)
temperature (°C)	–80
scan type	ω scans (0.2°) (30 s exposures)
data collection 2θ limit (deg)	52.82
total data collected	14122 (-40 ≤ h ≤ 33, -9 ≤ k ≤ 7, -29 ≤ l ≤ 35)
independent reflections	6271
number of observed reflections (*NO*)	4308 [$F_o^2 \geq 2\sigma(F_o^2)$]
structure solution method	direct methods/fragment search (*DIRDIF–96*[c])
refinement method	full-matrix least-squares on F^2 (*SHELXL–93*[d])
absorption correction method	*SADABS*
range of transmission factors	0.9349–0.5949
data/restraints/parameters	6271 [$F_o^2 \geq -3\sigma(F_o^2)$] / 0 / 349
goodness-of-fit (S)[e]	0.993 [$F_o^2 \geq -3\sigma(F_o^2)$]
final R indices[f]	
R_1 [$F_o^2 \geq 2\sigma(F_o^2)$]	0.0402
wR_2 [$F_o^2 \geq -3\sigma(F_o^2)$]	0.0928
largest difference peak and hole	0.809 and –0.561 e Å^{-3}

Table A9.2. Atomic Coordinates and Equivalent Isotropic Displacement Parameters

(a) Molecule A

Atom	*x*	*y*	*z*	U_{eq}, Å^2
Sn	0.125628(10)	0.04351(4)	0.318704(10)	0.03171(10)*
F1	0.09030(10)	0.0603(4)	0.22604(9)	0.0519(7)*
F2	0.08349(14)	0.1602(4)	0.14736(11)	0.0827(12)*
F3	0.10617(14)	-0.1240(4)	0.17163(12)	0.0841(12)*
F4	0.15245(14)	0.1058(6)	0.21010(16)	0.0980(13)*
O10	0.16407(10)	0.0237(4)	0.40461(10)	0.0356(7)*
O11	0.11370(12)	0.0006(4)	0.51136(12)	0.0451(8)*
C1	0.06038(18)	0.0261(8)	0.3182(2)	0.0661(16)*
C2	0.15225(19)	0.3025(6)	0.31702(18)	0.0494(13)*
C3	0.15720(17)	-0.1927(6)	0.30741(17)	0.0452(12)*
C10	0.14942(16)	0.0101(5)	0.43887(16)	0.0321(10)*
C11	0.17793(15)	-0.0147(5)	0.49288(16)	0.0322(10)*
C12	0.15841(16)	-0.0258(6)	0.52958(16)	0.0361(10)*
C13	0.1859(2)	-0.0618(6)	0.58137(18)	0.0500(13)*
C14	0.2313(2)	-0.0833(7)	0.59526(19)	0.0572(15)*
C15	0.25154(19)	-0.0682(7)	0.56012(19)	0.0579(15)*
C16	0.22456(16)	-0.0335(6)	0.50913(18)	0.0460(12)*
C17	0.0924(2)	-0.0224(7)	0.5468(2)	0.0568(14)*
B	0.1089(2)	0.0493(8)	0.1876(2)	0.0492(15)*

(b) Molecule B

Atom	*x*	*y*	*z*	U_{eq}, Å^2
Sn	0.010003(11)	-0.46588(4)	0.112854(12)	0.03954(11)*
F1	-0.06049(11)	-0.4777(5)	0.12146(13)	0.0769(10)*
F2	-0.12758(13)	-0.3496(5)	0.10228(15)	0.0930(12)*
F3	-0.12402(15)	-0.6284(5)	0.07665(17)	0.1085(14)*
F4	-0.10242(13)	-0.3995(5)	0.03954(13)	0.0860(11)*
O10	0.07615(11)	-0.4616(4)	0.10399(12)	0.0430(8)*
O11	0.19931(13)	-0.4656(5)	0.21652(13)	0.0587(10)*
C1	0.0364(2)	-0.5045(8)	0.1939(2)	0.0633(16)*
C2	-0.00385(19)	-0.1997(7)	0.0849(2)	0.0600(15)*
C3	-0.01271(18)	-0.6809(7)	0.0588(2)	0.0576(15)*
C10	0.11476(16)	-0.4687(6)	0.13891(19)	0.0386(10)*
C11	0.15432(16)	-0.4543(6)	0.12721(18)	0.0402(11)*
C12	0.19767(17)	-0.4514(6)	0.16792(19)	0.0426(11)*
C13	0.23511(18)	-0.4329(7)	0.1563(2)	0.0519(13)*
C14	0.23021(19)	-0.4198(7)	0.1053(2)	0.0556(14)*
C15	0.18792(18)	-0.4273(7)	0.0648(2)	0.0508(13)*
C16	0.15029(17)	-0.4431(6)	0.07558(18)	0.0424(11)*
Atom	*x*	*y*	*z*	U_{eq}, Å^2
C17	0.2424(2)	-0.4863(8)	0.2587(2)	0.0682(17)*
B	-0.1051(2)	-0.4666(8)	0.0851(3)	0.0509(15)*

Anisotropically-refined atoms are marked with an asterisk (*). The form of the anisotropic displacement parameter is: $\exp[-2\pi^2(h^2a^{*2}U_{11} + k^2b^{*2}U_{22} + l^2c^{*2}U_{33} + 2klb^*c^*U_{23} + 2hla^*c^*U_{13} + 2hka^*b^*U_{12})]$.

Table A9.3 Selected Interatomic Distances (Å)

(a) Molecule A			*(b) Molecule B*		
Atom1	Atom2	Distance	Atom1	Atom2	Distance
Sn	F1	2.387(2)	Sn	F1	2.386(3)
Sn	O10	2.231(3)	Sn	O10	2.249(3)
Sn	C1	2.107(6)	Sn	C1	2.104(5)
Sn	C2	2.103(5)	Sn	C2	2.094(5)
Sn	C3	2.105(4)	Sn	C3	2.112(5)
F1	B	1.431(7)	F1	B	1.396(7)
F2	B	1.370(6)	F2	B	1.335(7)
F3	B	1.345(6)	F3	B	1.318(7)
F4	B	1.357(7)	F4	B	1.405(7)
O10	C10	1.233(5)	O10	C10	1.242(5)
O11	C12	1.341(5)	O11	C12	1.347(6)
O11	C17	1.427(6)	O11	C17	1.430(6)
C10	C11	1.436(5)	C10	C11	1.445(7)
C11	C12	1.408(6)	C11	C12	1.411(7)
C11	C16	1.396(6)	C11	C16	1.403(6)
C12	C13	1.392(6)	C12	C13	1.379(7)
C13	C14	1.369(8)	C13	C14	1.379(7)
C14	C15	1.387(8)	C14	C15	1.386(7)
C15	C16	1.369(6)	C15	C16	1.371(7)

Table A9.4 Selected Interatomic Angles (deg)

(a) Molecule A				*(b) Molecule B*			
Atom1	Atom2	Atom3	Angle	Atom1	Atom2	Atom3	Angle
F1	Sn	O10	175.21(11)	F1	Sn	O10	178.61(12)
F1	Sn	C1	87.30(17)	F1	Sn	C1	82.99(18)
F1	Sn	C2	87.17(14)	F1	Sn	C2	90.11(18)
F1	Sn	C3	85.94(14)	F1	Sn	C3	88.45(18)
O10	Sn	C1	97.36(17)	O10	Sn	C1	97.33(18)
O10	Sn	C2	91.56(15)	O10	Sn	C2	90.93(18)
O10	Sn	C3	90.78(14)	O10	Sn	C3	90.25(18)
C1	Sn	C2	118.2(2	C1	Sn	C2	117.7(2
C1	Sn	C3	119.5(2	C1	Sn	C3	123.3(2
C2	Sn	C3	121.4(2	C2	Sn	C3	118.3(2
Sn	F1	B	130.9(3	Sn	F1	B	132.3(4
Sn	O10	C10	128.7(3	Sn	O10	C10	127.8(3
C12	O11	C17	117.6(4	C12	O11	C17	118.4(4
O10	C10	C11	123.2(4	O10	C10	C11	121.3(4
C10	C11	C12	119.5(4	C10	C11	C12	120.0(4
C10	C11	C16	120.8(4	C10	C11	C16	120.8(4
C12	C11	C16	119.7(4	C12	C11	C16	119.2(5
O11	C12	C11	116.3(4	O11	C12	C11	116.3(5
O11	C12	C13	124.6(5	O11	C12	C13	124.2(5
C11	C12	C13	119.1(5	C11	C12	C13	119.5(5
C12	C13	C14	119.0(5	C12	C13	C14	120.2(5
C13	C14	C15	122.9(5	C13	C14	C15	121.0(5
C14	C15	C16	118.2(5	C14	C15	C16	119.6(5
C11	C16	C15	120.9(5	C11	C16	C15	120.5(5
F1	B	F2	107.0(5	F1	B	F2	109.1(5
F1	B	F3	108.2(5	F1	B	F3	110.4(5
F1	B	F4	107.6(4	F1	B	F4	105.3(5
F2	B	F3	110.8(4	F2	B	F3	111.7(6
F2	B	F4	111.7(5	F2	B	F4	109.9(5
F3	B	F4	111.4(5	F3	B	F4	110.3(5

[a]Obtained from least-squares refinement of 5229 centered reflections.

[b]Programs for diffractometer operation, data collection, data reduction and absorption correction were those supplied by Bruker.

[c]Sheldrick, G. M. *Acta Crystallogr.* **1990**, *A46*, 467–473.

[d]Sheldrick, G. M. *SHELXL-93*. Program for crystal structure determination. University of Göttingen, Germany, 1993. Refinement on F_o^2 for all reflections (all of these having $F_o^2 \geq -3\sigma(F_o^2)$). Weighted *R*-factors wR_2 and all goodnesses of fit *S* are based on F_o^2; conventional *R*-factors R_1 are based on F_o, with F_o set to zero for negative F_o^2. The observed criterion of $F_o^2 > 2\sigma(F_o^2)$ is used only for calculating R_1, and is not relevant to the choice of reflections for refinement. *R*-factors based on F_o^2 are statistically about twice as large as those based on F_o, and *R*-factors based on ALL data will be even larger.

[e]$S = [\Sigma w(F_o^2 - F_c^2)^2/(n-p)]^{1/2}$ (n = number of data; p = number of parameters varied; $w = [\sigma^2(F_o^2) + (0.0389P)^2]^{-1}$ where $P = [\mathrm{Max}(F_o^2, 0) + 2F_c^2]/3$).

[f]$R_1 = \Sigma||F_o| - |F_c||/\Sigma|F_o|$; $wR_2 = [\Sigma w(F_o^2 - F_c^2)^2/\Sigma w(F_o^4)]^{1/2}$.